REPORT DOCUMENTATION PAGE

Form Approved
OMB NO. 0704-0188

1. AGENCY USE ONLY (Leave Blank)	2. REPORT DATE 5-1-01	3. REPORT TYPE AND DATES COVERED Final: 5/1/99 - 8/31/00

4. TITLE AND SUBTITLE
Tunable Optical Polymer Systems

5. FUNDING NUMBERS
DADD19-99-1-0206

6. AUTHOR(S)
Samson Jenekhe

7. PERFORMING ORGANIZATION NAME(S) AND ADDRESS(ES)

University of Rochester
Rochester, NY 14627

8. PERFORMING ORGANIZATION REPORT NUMBER

9. SPONSORING / MONITORING AGENCY NAME(S) AND ADDRESS(ES)

U. S. Army Research Office
P.O. Box 12211
Research Triangle Park, NC 27709-2211

10. SPONSORING / MONITORING AGENCY REPORT NUMBER
39836-CH-MUR
.15

11. SUPPLEMENTARY NOTES
The views, opinions and/or findings contained in this report are those of the author(s) and should not be construed as an official Department of the Army position, policy or decision, unless so designated by other documentation.

12 a. DISTRIBUTION / AVAILABILITY STATEMENT	12 b. DISTRIBUTION CODE
Approved for public release; distribution unlimited.	

13. ABSTRACT (Maximum 200 words)

The research program focused on new polymeric materials for use in reflective displays and other optoelectronic applications. It was carried out by a consortium of seven researchers from four universities (University of Rochester, Massachusetts Institute of Technology, University of Texas at Austin, and Utah State University). The cornerstone of the planned research was to design, synthesize, and characterize polymeric materials having environmentally responsive optical properties, which allows them to be switched efficiently. In recognition of the importance of studying these materials in the context of their intended application, the team included expertise in modeling, fabricating, and evaluating display devices and systems.

14. SUBJECT TERMS	15. NUMBER OF PAGES 244
	16. PRICE CODE

17. SECURITY CLASSIFICATION OR REPORT	18. SECURITY CLASSIFICATION ON THIS PAGE	19. SECURITY CLASSIFICATION OF ABSTRACT	20. LIMITATION OF ABSTRACT
UNCLASSIFIED	UNCLASSIFIED	UNCLASSIFIED	UL

Enclosure 2

MASTER COPY: PLEASE KEEP THIS "MEMORANDUM OF TRANSMITTAL" BLANK FOR REPRODUCTION PURPOSES. WHEN REPORTS ARE GENERATED UNDER THE ARO SPONSORSHIP, FORWARD A COMPLETED COPY OF THIS FORM WITH EACH REPORT SHIPMENT TO THE ARO. THIS WILL ASSURE PROPER IDENTIFICATION. NOT TO BE USED FOR INTERIM PROGRESS REPORTS; SEE PAGE 2 FOR INTERIM PROGRESS REPORT INSTRUCTIONS.

MEMORANDUM OF TRANSMITTAL

U.S. Army Research Office
ATTN: AMSRL-RO-BI (TR)
P.O. Box 12211
Research Triangle Park, NC 27709-2211

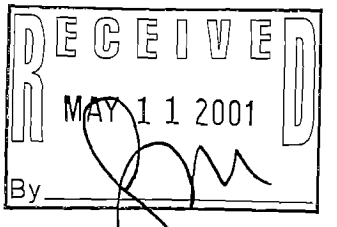

☐ Reprint (Orig + 2 copies)

☐ Technical Report (Orig + 2 copies)

☐ Manuscript (1 copy)

☒ Final Progress Report (Orig + 2 copies)

☐ Related Materials, Abstracts, Theses (1 copy)

CONTRACT/GRANT NUMBER: DAAD19-99-1-0206

REPORT TITLE: Tunable Optical Polymer Systems

is forwarded for your information.

SUBMITTED FOR PUBLICATION TO (applicable only if report is manuscript):

Sincerely,

Samson Jenekhe

TUNABLE OPTICAL POLYMER SYSTEMS (TOPS)
MURI CENTER PERSONNEL

Douglas J. Kiserow – ARO Program Manager
Army Research Office
PO Box 12211
Research Triangle Park, NC 27709-2211
E-mail: kiserow@aro-emh1.army.mil
Phone: 919-549-4213
Fax: 919-549-4310 or 4399

Professor Samson A. Jenekhe
Department of Chemical Engineering
University of Washington,
Benson Hall Room 106, Box 351750
Seattle, WA 98195
E-mail: jenekhe@cheme.washington.edu
Phone: (206) 685-5525
Fax: (206) 685-3451

Professor Allen J. Bard
University of Texas at Austin
Department of Chemistry & Biochemistry
Speedway at 24th Street
Austin, TX 78712
E-mail: ajbard@mail.utexas.edu
Phone: (512) 471-3761
Fax: (512) 471-0088

Professor Shaw H. Chen
Laboratory for Laser Energetics,
Univ. of Rochester
250 E River Road
Rochester, NY 14627
E-mail: shch@lle.rochester.edu
Phone: (716) 275-0909
Fax: (716) 275-5960

Professor Paula T. Hammond
Massachusetts Institute of Technology
Department of Chemical Engineering
25 Ames Street, 66-350
Cambridge, MA 02139-4307
E-mail: hammond@mit.edu
Phone: (617) 258-7577
Fax: (617) 258-5766

Professor Steve Scheiner
Department of Chemistry & Biochemistry
Utah State University
Logan, UT 84322-0300
E-mail: scheiner@cc.usu.edu
Phone: (435) 797-7419
Fax: (435) 797-3390

Professor Timothy M. Swager
Massachusetts Institute of Technology
Department of Chemistry
77 Massachusetts Avenue, 18-390
Cambridge, MA 02139
E-mail: tswager@mit.edu
Phone: (617) 253-4423
Fax: (617) 253-7929

Professor Lewis J. Rothberg
Department of Chemistry
University of Rochester
Rochester, NY 14627
E-mail: ljr@chem.chem.rochester.edu
Phone: (716) 275-8286
Fax: (716) 242-9485

TUNABLE OPTICAL POLYMER SYSTEMS (TOPS)

An extensive research program to investigate new polymeric materials for use in reflective displays and other optoelectronic applications is proposed by a consortium of seven researchers from four universities (University of Rochester, Massachusetts Institute of Technology, University of Texas at Austin, and Southern Illinois University). The cornerstone of the planned research is to design, synthesize, and characterize polymeric materials having environmentally responsive optical properties which allow them to be switched efficiently. In recognition of the importance of studying these materials in the context of their intended application, the team includes expertise in modeling, fabricating, and evaluating display devices and systems.

The MURI program on Tunable Optical Polymer Systems (TOPS) consists of the following coordinated activities: (1) Development of new synthetic methodology and new chromogenic materials: Three synthetic polymer chemists (**Chen**, **Jenekhe** and **Swager**) have designed novel approaches to incorporation of optically and electrically active chromogenic chromophores into processable polymers suitable for conformal coatings of large areas. New classes of electrochromic conjugated polymers, photoelectrochromic polymer/organometallic nanocomposites, liquid crystalline conjugated polymers and block copolymers, electroluminescent polymers, and self-organizing polymers will be synthesized. (2) Experimental and theoretical characterization of color switching phenomena: Extensive material characterization is planned, including studies of the multifunctional optical polymers during operation in model devices. Various types of color change phenomena will be exploited including those which rely on electrochemical reaction (**Bard**), photoelectrochromic effects, photochromism and electroluminescence. Molecular modeling (**Scheiner**) of electron and proton transfer processes will accompany these studies to guide synthetic work towards more durable materials with larger chromogenic effects. (3) New paradigms for self-assembly of organized sub-wavelength and wavelength-sized supramolecular structures and nanostructures: Perhaps the most important property of organic polymers is their ability to be processed conveniently. Recently, much activity has extended this further by taking advantage of their thermodynamic or intermolecular forces driven propensity to self-organize via microphase separation. Three of the leading practitioners in this area (**Chen, Hammond, Jenekhe**) are among the team members and propose several ideas for making sub-wavelength and wavelength-dimension structures which will be useful in enhancement of optical switching phenomena in polymers. (4) Design and modeling of device structures to enhance color-change phenomena: Our team includes a device physicist experienced in utilizing microcavity effects to tailor and improve the properties of optical display devices (**Rothberg**). Construction and characterization of microcavity geometries which enhance switching is planned, and modeling software to assist team members in designing devices which optimally take advantage of material properties will be developed. (5) Development of patterning technologies to organize these polymeric materials and devices into large arrays: Exciting new work on microcontact printing promises to revolutionize the way pixelation of displays is done. One team member has combined this work with self-assembling layers so that it is possible to make three-dimensional structures with micron dimensions and incorporate a wide variety of functional materials (**Hammond**). The potential for construction of large area color switchable arrays avoiding expensive and cumbersome processes such as lithography and evaporation is enormous. (6) Fabrication and testing of devices to deduce mechanism and robustness: Spectroscopic characterization of materials during device operation is planned to determine properties such as switching efficiency, speed and degradation rate (**Bard**). Standard measurements such as electroabsorption and electroreflectance (**Rothberg**) will be available. These will help to determine operation mechanism of these devices so that appropriate materials properties can be incorporated in the polymers. (7) Colorimetric evaluation of devices and assemblies from a display perspective. Finally, we plan a common facility for testing optical properties at a systems level. This will include colorimetric and contrast measurements as performed in the display industry.

The primary goal of this MURI research program is to identify promising new classes of chromogenic polymers and device structures into which they can be incorporated to produce large-area, addressable color tunable devices which are low cost and rugged. We also plan to intimately involve many graduate, undergraduate, and postdoctoral students as well as industrial and DoD collaborators in this highly interdisciplinary research with important commercial and military applications. In addition, the infrastructure for research in the areas of materials chemistry, polymer science, computational chemistry and organic devices in the participating universities will be augmented.

TOPS MURI AGENDA
Annual Review Meeting, 15-16 August 2000
Army Natick RD&E Center: Natick, MA

15 August 2000

			PAGE
08:40 - Introductory Remarks	(10 min.)	Doug Kiserow	
08:50 Overview of NRDEC	(25 min)	Ed Crivello	
09:15 - Overview of TOPS MURI Center	(25 min.)	Sam Jenekhe	**1**
09:40 - Break	(20 min.)		
10:00 - Tunable Reflection Systems			
10:00 - Liquid Crystalline Polymers with Tunable Optical Properties	(25 min.)	Shaw Chen	**11**
10:25 - Liquid Crystalline Conjugated Polymers as Multifunctional Optical Materials	(30 min.)	Dimitris Katsis	**15**
10:55 -Chromogenic Block Copolymer Assemblies	(25 min.)	Paula Hammond	**42**
11:20 - TOPS Test Beds	(25 min.)	Lewis Rothberg	**65**
11:45 - Additional Questions and Discussions			
12:00 - Lunch Break			
13:00 - Posters and Device Demonstrations			
14:45 - Break			
15:00 - Tunable Emission Systems			
15:00 - Tunable Light Emitting Polymers and Devices: Polymer/Polymer Interfaces	(25 min.)	Sam Jenekhe	**83**
15:25 - Tunable Electroluminescence in Conjugated Polymers	(25 min.)	Katie Meeker	**102**
15:50 - Aggregation Quenching in EL Polymers	(25 min.)	Pei Wang	**122**
16:15 - ECL and Light Emitting Devices	(25 min.)	Al Bard	**133**
16:40 - Additional Questions and Discussions			
17:00 - TOPS TAB/EAB Executive Session			

16 August 2000

08:40 - Tunable Absorption Systems

08:40	- Thin Film Electrochromic Devices	(25 min.) D. DeLongchamp	**159**
09:05	- Electrochromic Ladder Polymers	(25 min.) Maurizio Quinto	**NA**
09:30:	- Highly Stable Polycyclic Aromatic Conjugated Polymers Polymers	(25 min.) JD Tovar	**179**
09:55	**- Break**	**(20 min)**	
10:15	- Computational Modeling of Chromogenic Effects	(25 min.) Steve Scheiner	**193**
10:40	- Synthesis of New Electrochromic Polymers	(25 min.) Tim Swager	**225**
11:05	- Discussions and Concluding Remarks	(15 min.) Sam Jenekhe	
11:20	TOPS TAB/EAB Executive Session (Lunch Break for MURI Center Team)		
13:30	- Feedback of TAB/EAB to MURI PIs	(30 min.) Doug Kiserow	

14:00 - TOPS MURI Annual Review Meeting Adjourned

***Each Speaker should plan to leave 5 minutes of allotted time for questions and change of speakers.**

U. S. ARMY RESEARCH OFFICE
MURI GRANT #DAAD19-99-1-0206
TUNABLE OPTICAL POLYMER SYSTEMS (TOPS)

PUBLICATIONS

1. F. G. Gao and A. J. Bard "Solid-State Organic Light-Emitting Diodes Based on Tris(2,2'-bipyridine)ruthenium(II) Complexes" *J. Am. Chem. Soc.*, **122**, 7426-7427(2000).

2. X. Zhang and S. A. Jenekhe "Electroluminescence of Multicomponent Conjugated Polymers. 1. Roles of Polymer/Polymer Interfaces in Emission Enhancement and Voltage-Tunable Multicolor Emission in Semiconducting Polymer/Polymer Heterojunctions" *Macromolecules*, **33**, 2069-2082 (2000).

3. D. DeLongchamp and P. Hammond "Ion Conductive Polymer Multilayers for Electrochromic Applications" *ACS Polymer Preprints*, August (2000).

4. K. Meeker, L.Lu, S.A. Jenekhe, "Multicolor Emission and Tunable Electroluminescence from Blends of Conjugated Polymers" *ACS Polymer Preprints*, August (2000).

5. S. A. Jenekhe and S. Yi "Highly Photoconductive Nanocomposites of Metallophthalocyanines and Conjugated Polymers" *Adv. Mater.*, in press.

6. D. Katsis, H.-M. P. Chen, J. C. Mastrangelo, and S. H. Chen "Thermotropic Chiral-Nematic Poly(p-phenylene)s as Novel Multifunctional Optical Materials" *Adv. Mater.*, in press.

7. H. P. Chen, D. Katsis, J. C. Mastrangelo, K. L. Marshall, S. H. Chen, and T. H. Mourey, "Thermotropic Chiral-Nematic Poly(p-phenylene)s as a Paradigm of Helically Stacked π-Conjugated Systems" *Chem. Mater.*, in press.

8. H. P. Chen, D. Katsis, J. C. Mastrangelo, S. H. Chen, S. D. Jacobs, and P. J. Hood, "Glassy Liquid-Crystal Films with Opposite Chirality as High Performance Reflectors and Optical Notch Filters" *Adv. Mater.*, in press.

9. M. Quinto and A. J. Bard "Polymer Films on Electrodes. 29. Electropolymirized Poly(7,14-Diphenylacenaptho[1,2-k]fluoranthene): Electrochemistry and Conductance of a Novel electrochromic Hydrocarbon Ladder Polymer Film" *J. Electroanalytical Chem.*, submitted.

10. D. Katsis, H. P. Chen, L. J. Rothberg, S. H. Chen, and T. Tsutsui, "Polarized Photoluminescence from Solid Films of Nematic and Chiral-Nematic Poly(p-phenylene)s" *Appl. Phys. Lett.*, submitted.

11. C. J. Collison, V. Tremaneekarn, W. Oldham, and L. J. Rothberg "Aggregation Effect on the Structure and Optical Properties of a Model PV Oligomer" *Synthetic Metals*, submitted.

12. A. E. Pullen and T. M. Swager "Regiospecific Copolyanilines from Substituted Oligoanilines: Electrochemical Comparisons with Random Copolyanilines", *Macromolecules*, submitted.

13. T. Kar and S. Scheiner "Substituent Effect on the Protonation-Induced Red Shift of PPV-PyV Models", in preparation.

14. P. Wang, C. J. Collison, and L. J. Rothberg "Interchain Effects on Conjugated Polymer Photophysics", in preparation.

15. J. H. Hsu, W. S. Fann, L. J. Rothberg, K. R. Chuang, and S. A. Chen "Correlation Between Electronic Properties and Chain Length in a Phenylene Vinylene Conjugated Polymer", in preparation.

16. L. Marshall and L. J. Rothberg "Absolute Quantum Yield Determination in Thin Films Using Photoacoustic Calorimetry", in preparation.

17. J. D. Tovar and T. M. Swager "Napthodithiophenes as a new class of functional electroactive materials: chemical and electrochemical investigations", in preparation for *J. Am. Chem. Soc.*

18. D. T. McQuade, A. H. Hegedus, and T. M. Swager "Signal Amplification of a Turn-On Sensor: Harvesting the Light Captured by a Conjugated Polymer," in preparation.

19. K. Meeker and S.A.Jenekhe " Effects of Inter- and Intrachain Emission Mechanisms and Selective Hole Injections on Tunable Luminescence of Polymer Blends," in preparation.

20. K. Meeker, S.A. Jenekhe, and A.J. Bard "Voltage-Tunable Multicolor Light-Emitting Diodes From Bilayers of Poly(p-phenylene vinylene)/Tris (2,2'-Bipyridine) Ruthenium Complexes" in preparation.

21. M. Quinto, S.A. Jenekhe, and A.J. Bard "Polymer Films on Electrodes. 30. Electrochemistry and SECM Characterization of Benzimidazole-Benzophenanthroline-Type Ladder (BBL) and Semiladder (BBB) Polymer Films" in preparation.

22. Alam, M.A. and S.A. Jenekhe, "Nanolayered Heterojunctions of Donor and Acceptor Conjugated Polymers of Interest in Light Emitting and Photovoltaic Devices: Photoinduced Electron Transfer at Polythiophene/Polyquinoline Interfaces" in preparation.

CHROMOGENIC PHENOMENA IN POLYMERS

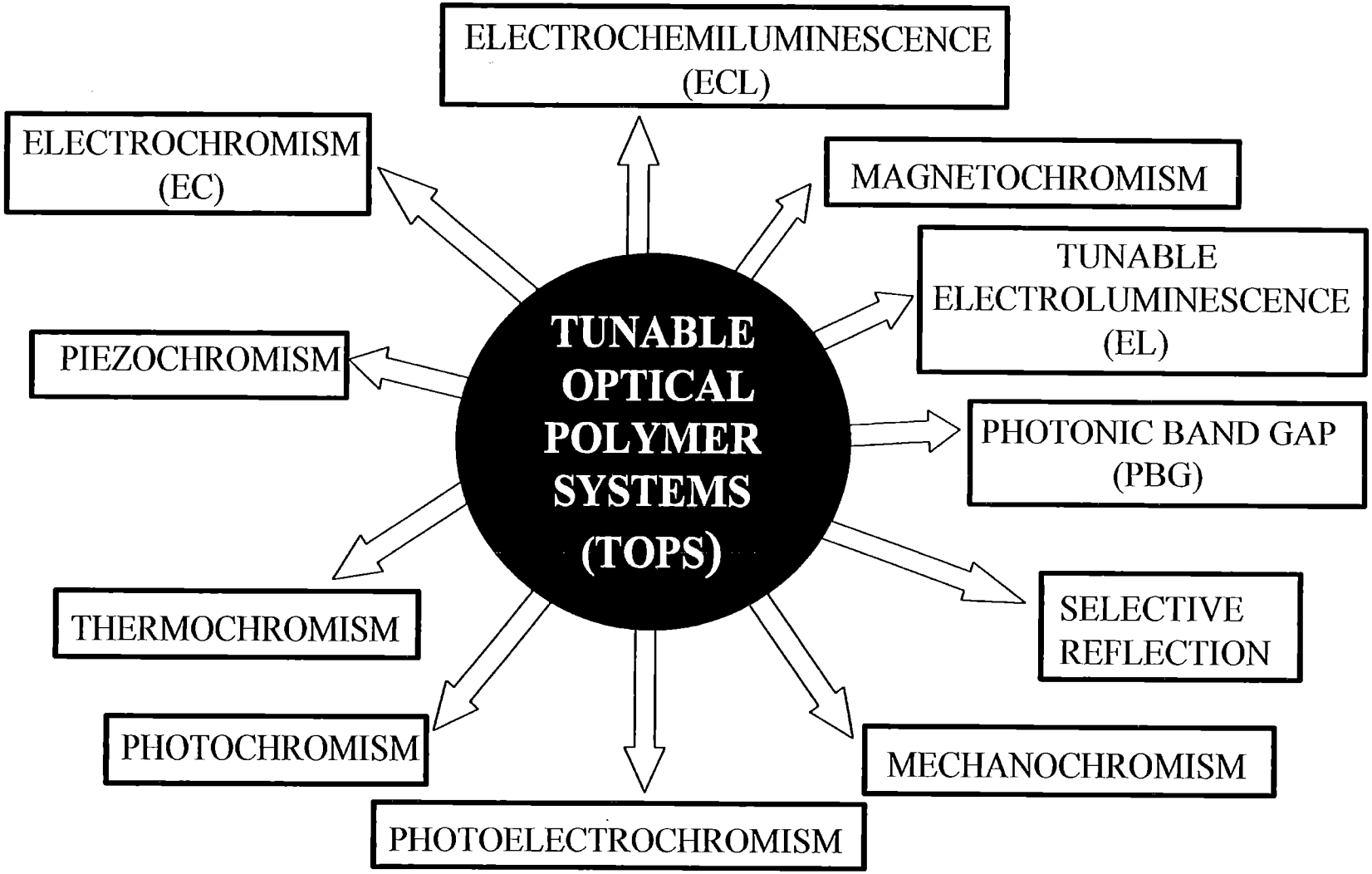

TUNABLE OPTICAL POLYMER SYSTEMS

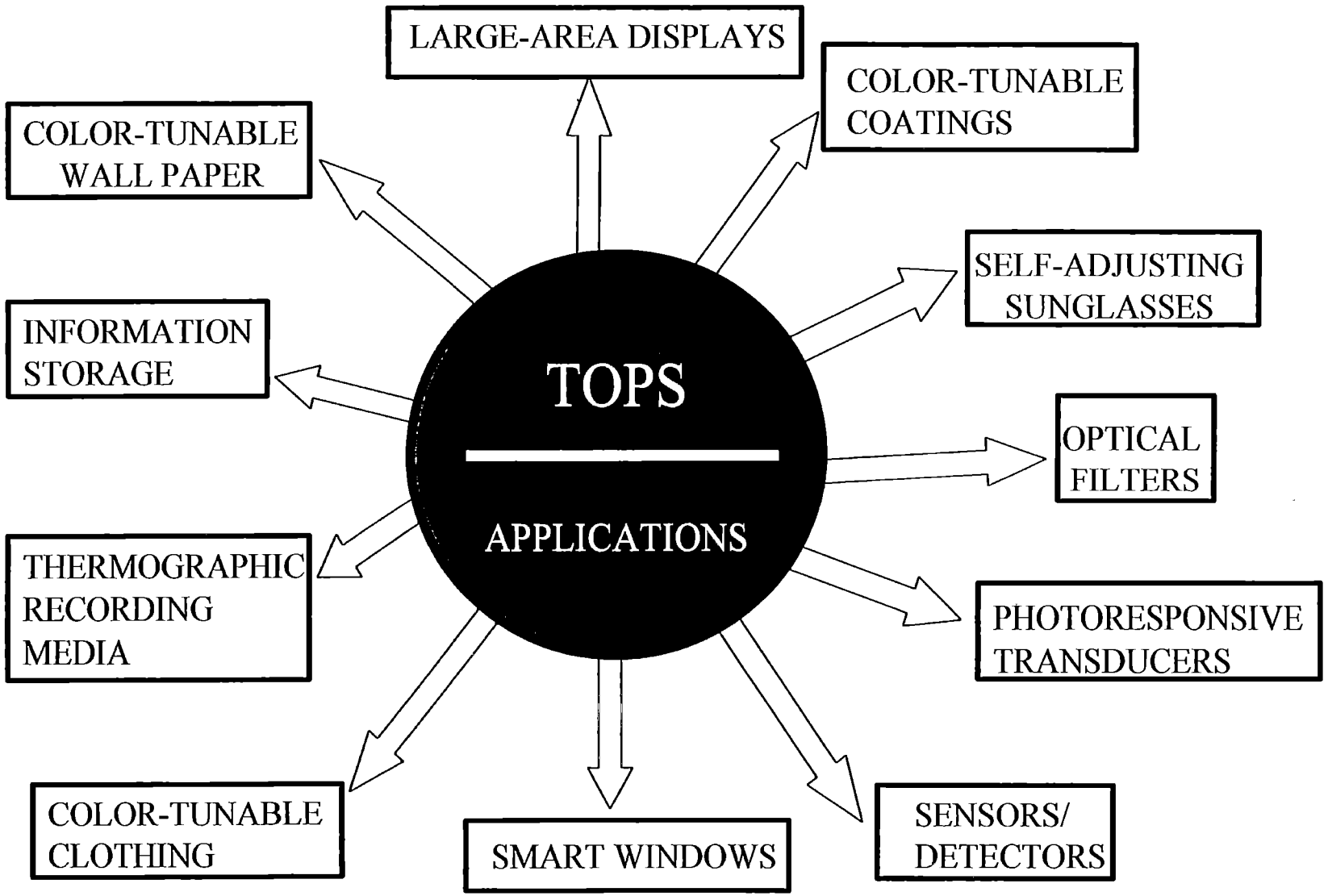

CHAMELEONS AND THE FUTURE OF TOPS

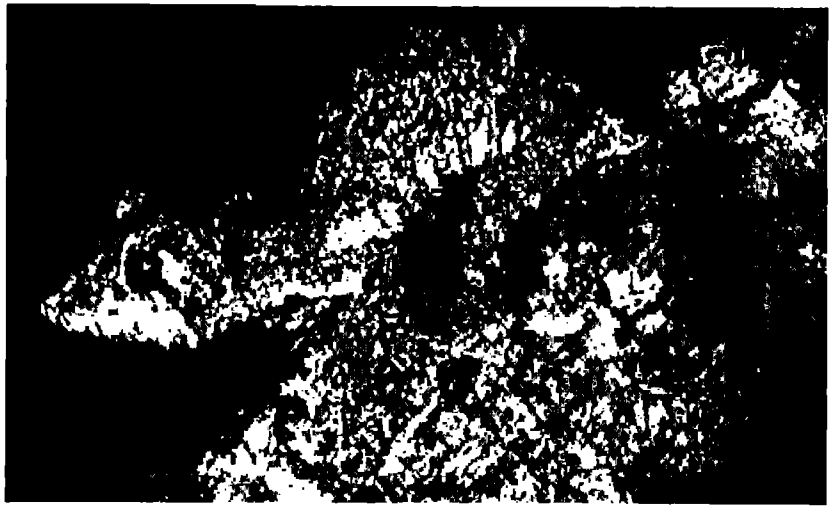

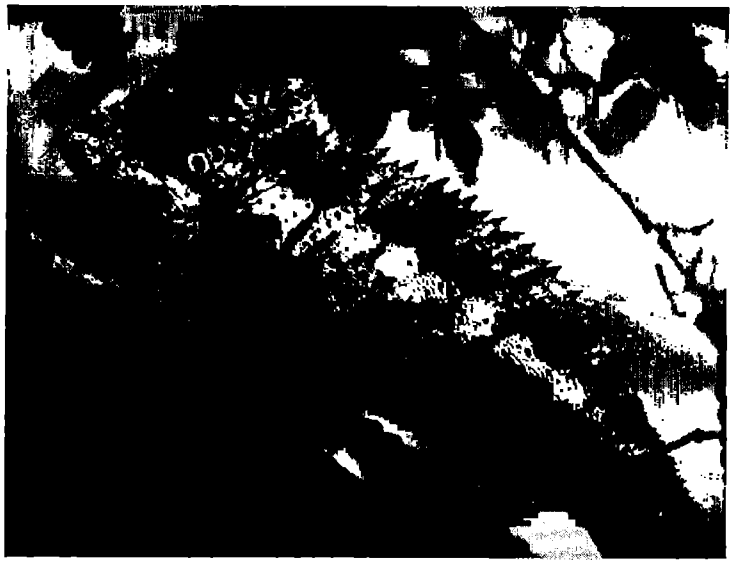

- Learning From Nature
- Chameleon Optoelectronics
- Chameleon Nanophotonics
- Novel Reflective Displays
- Color Switchable Wall Paper

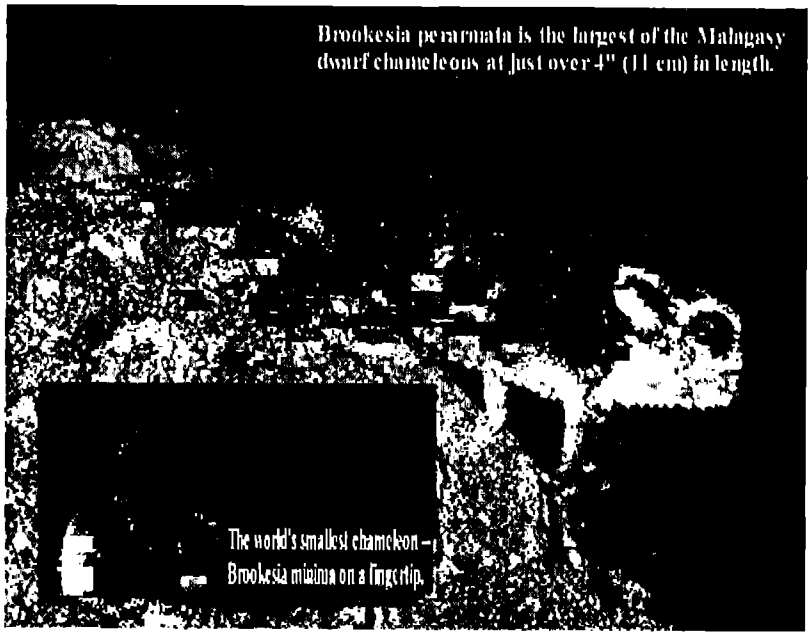

ARO TOPS MURI

S. A. JENEKHE

ACADEMIC RESEARCH PERSONNEL

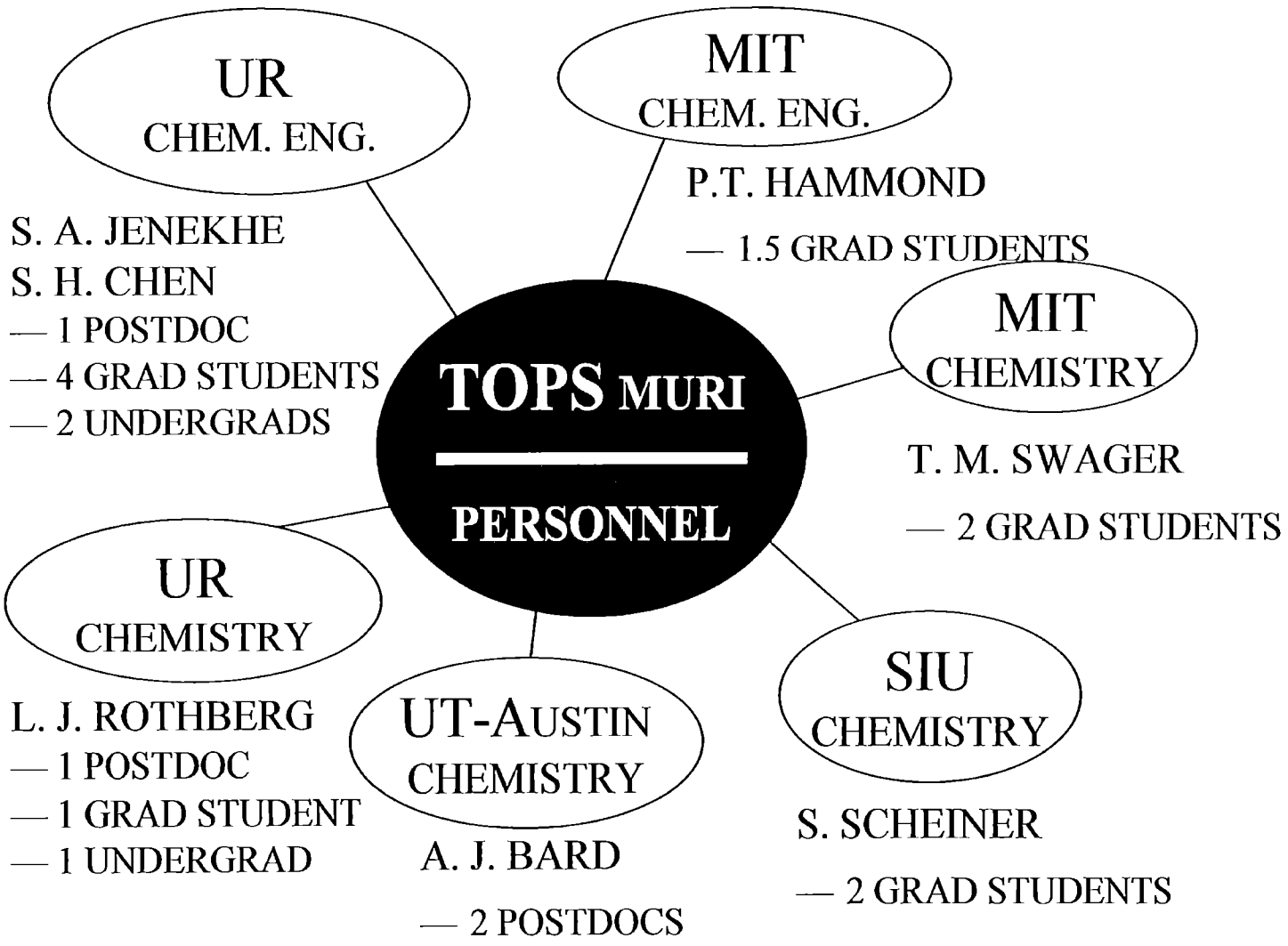

INSTITUTIONAL COLLABORATIONS

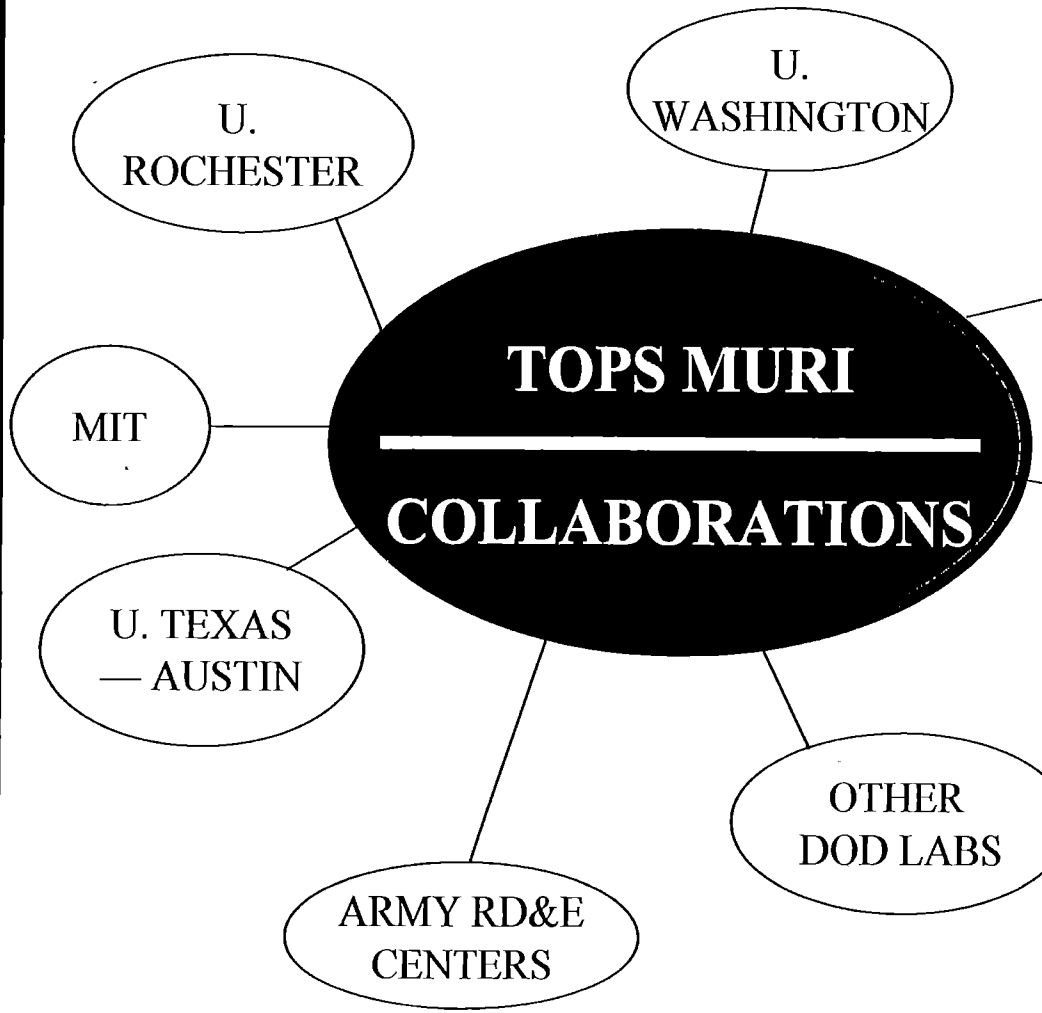

- CORNERSTONE RESEARCH
- EASTMAN KODAK
- 3M
- BAUSCH & LOMB
- PPG
- HONEYWELL
- TEXAS INSTRUMENTS
- ROHM & HAAS?
- HEWLETT-PACKARD?
- LUCENT

SCIENTIFIC GOALS OF TOPS MURI

I. Design, synthesis, characterization and processing of new generation of chromogenic polymers for optoelectronic and photonic applications

–Structural design at the electronic, molecular, supramolecular, nanostructure and macroscopic levels
–New synthetic methodologies
–New paradigms for self-assembly of nanostructures and for polymer processing
–Enhanced chromogenic effects
–Lower switching energies
–Improved durability and switching speeds

II. Fundamental understanding of the physical/chemical mechanisms of chromogenic phenomena in polymers

–Chemistry and photophysics of color switching
–Dynamics of color-switching processes
–What factors influence lifetime (# of cycles)
–Learn from chromogenic phenomena in nature (biology)

III. Construction and evaluation of model devices/displays using the new chromogenic polymers

TOPS MURI RESEARCH GROUPS

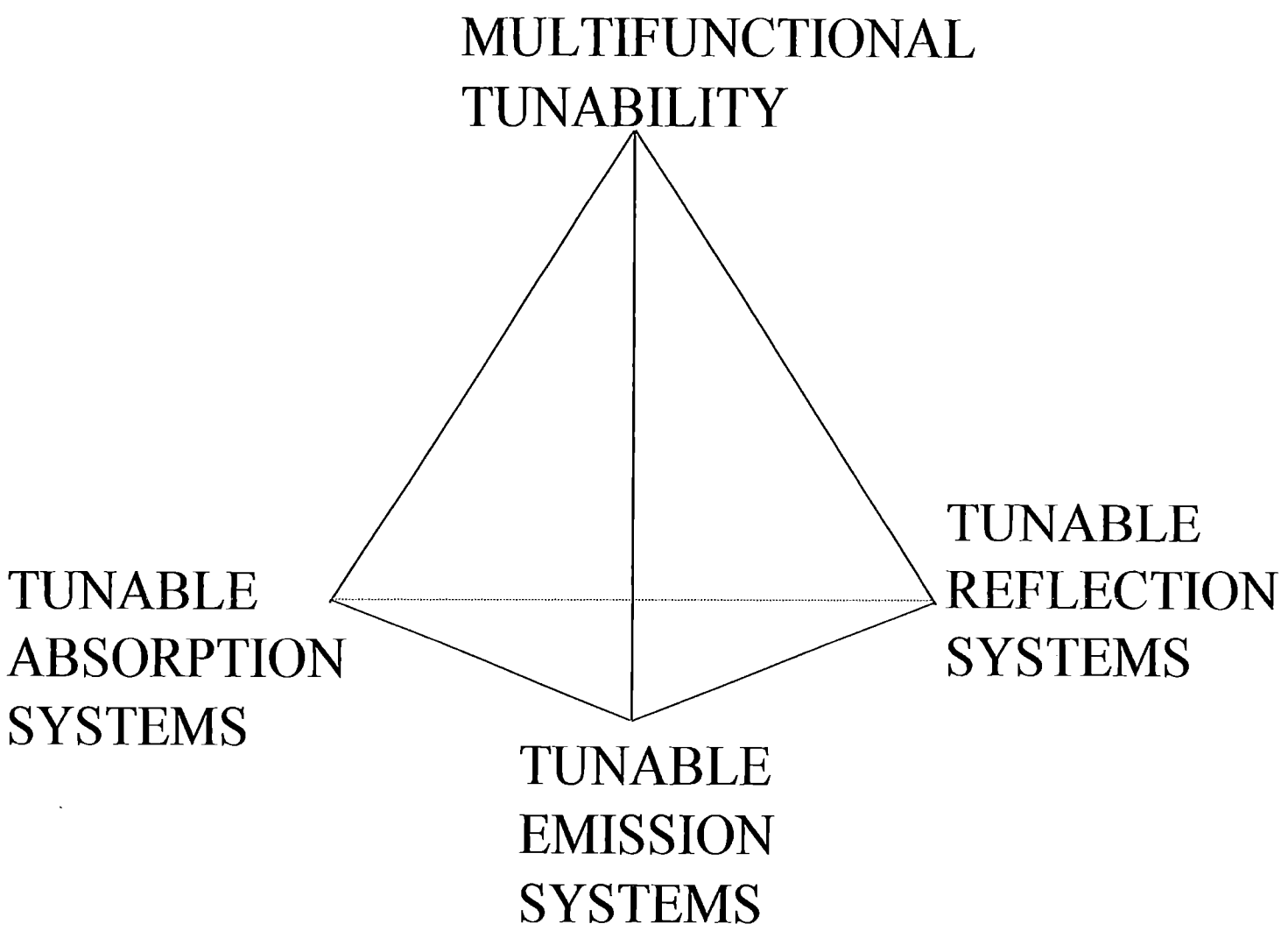

TUNABLE REFLECTION SYSTEMS

Research Team

- Shaw Chen - LC Polymers with Tunable Optical Properties
- Paula Hammond - Chromogenic Block Copolymer Assemblies
- Sam Jenekhe - Self-Organizing Photonic Band Gap Materials
- Lewis Rothberg - TOPS Test Beds

Relationship to DoD

Reflective Displays; Self-Aseembly for Nanotechnology; Intelligent Sensors/ Detectors; Materials for Photonics; Optical Filters; Photoresponsive Transducers

Interactions with Army

- CRADA with ARDEC, Picatinny Arsenal
- Many Planned

MURI Funding Level: $350 K/yr.

Personnel

- Graduate Students: 3
- Postdocs: 1
- Undergraduate Students: 1

TUNABLE EMISSION SYSTEMS

Research Team

- Al Bard - Electrochemiluminescent Systems
- Paula Hammond - 3-D Array Patterning by Self-Assembly
- Sam Jenekhe - Tunable Electroluminescent Polymers and Devices
- Lewis Rothberg - Microcavity Design for Emissive Displays

Relationship to DoD

Addressable Color Tunable Devices; Large Area Displays; Nanofunctional Devices; Smart/Interactive Clothing; Low Cost Rugged Flexible Displays.

Interactions with Army

- Many Planned

MURI Funding Level: $270 K/yr.

Personnel

- Graduate Students: 1
- Postdocs: 2.5
- Undergraduate Students: 1

yi5099s3rep

TUNABLE ABSORPTION SYSTEMS

Research Team
- Al Bard - Electrochromic Ladder Polymers
- Paula Hammond - Electrochromic Thin Film Devices
- Steve Scheiner - Computational Modeling of Chromogenic Effects
- Tim Swager - Synthesis of New Electrochromic Polymers
- Lewis Rothberg - Electrochromic Test Beds

Relationship to DoD

Large Area Displays; Color-Tunable Clothing/Wall Papers/Coatings; Environmentally Responsive Materials; Smart Materials

Interactions with Army
- Many Planned

MURI Funding Level: $380 K/yr.

Personnel
- Graduate Students: 6
- Postdocs: 1
- Undergraduate Students: 1

yi5099s3rep

FIRST YEAR HIGHLIGHTS

TUNABLE REFLECTION

- Developed Chiral-Nematic Poly(p-phenylene)s Having Tunable Selective Reflection (IR to UV) (Dimitris Katsis)
- High Degree of Circular Polarization Demonstrated (Dimitris Katsis)
- Micropatterning of Chromogenic Polymers Demonstrated (Paula Hammond)

TUNABLE EMISSION

- Tris(bipyridine)ruthenium (II) Complexes (Al Bard)
  - –Efficient Bright Red LEDs Developed (Al Bard)
  - –Tunable Multicolor PPV/$Ru(bpy)_3^{2+}$ LEDs (Katie Meeker)
- Understanding of Polymer/Polymer Interfaces in Optoelectronic Devices (Sam Jenekhe)
- Developed a New Calorimetric Instrument for Measuring Absolute Fluorescence Quantum Yields (Lewis Rothberg)

TUNABLE ABSORPTION

- New Approaches to Electrochromic Thin Film Devices (Dean DeLongchamp)
- Electrochromic BBL and BBB Ladder Polymers Demonstrated (Maurizio Quinto)
- New Electroactive Conjugated Polymers Synthesized (Tim Swager)

S.A. JENEKHE **ARO TOPS MURI**

TUNABLE REFLECTION SYSTEMS

Research Team

- **Shaw Chen — LC Polymers and glasses with Tunable Optical Properties**
- **Paula Hammond — Chromogenic Block Copolymer Assemblies**
- **Sam Jenekhe — Self-Organizing Photonic Band Gap Materials**
- **Lewis Rothberg — Reflective Display Devices and TOPS Test Beds**

Personnel

- **Graduate Students: 3**
- **Postdocs: 1**
- **Undergraduate Students: 3**

Relationship to DoD

- **Reflective Displays; Optical Notch Filters; Self-Assembly for Nanotechnology; Intelligent Sensors and Detectors; Materials for Photonics; Photoresponsive Transducers**

Interactions with Army

- **CRADA with ARDEC, Picatinny Arsenal**
- **Others Planned**

Background and Introduction

- **Nature of coloration**
  - pigmentary colors due to absorption
  - structural colors due to interference, diffraction or scattering
  - emissive colors due to photo- or electroluminescence
  - structural colors tend to be brilliant, iridescent, and long lasting
- **Stimuli to induce color change**
  - thermal, electric, magnetic
  - photochemical, electrochemical
  - proton transfer, pH
- **Mechanisms of color crypsis**
  - spontaneous response to external stimuli $\Rightarrow$ "smart skins"
  - nervous control of color change $\Rightarrow$ "intelligent skins"
- **Bio-inspired synthetic materials as an ultimate goal**

Research Overview: Shaw H. Chen, U. Rochester

- **Research Projects**
  - Multifunctional liquid crystalline conjugated polymers (presentation by Dr. Katsis)
  - Poly(fluorene)s for electroluminescence: stability, efficiency, color tunability, morphology and polarization control
  - Tuning reflective, emissive, and absorptive colors in fluid, gel, melt, and solid films
- **Objectives**
  - Conjugated polymers for coloration by selective reflection, emission and absorption
  - Helically stacked or coiled conjugated systems for efficient emission of polarized light
  - Color tunability by external stimuli: photochemical, thermal, electric, magnetic, etc.
- **MURI Collaborators**
  - Lewis Rothberg, Samson Jenekhe, Paula Hammond
- **Publications**
  - H. P. Chen, D. Katsis, J. C. Mastrangelo, K. L. Marshall, S. H. Chen, and T. H. Mourey, "Thermotropic Chiral-Nematic Poly(*p*-phenylene)s as a Paradigm of Helically Stacked π-Conjugated Systems," *Chem. Mater.* (in press).
  - H. P. Chen, D. Katsis, J. C. Mastrangelo, S. H. Chen, S. D. Jacobs, and P. J. Hood, "Glassy Liquid-Crystal Films with Opposite Chirality as High Performance Reflectors and Optical Notch Filters," *Adv. Mater.* (in press).
  - D. Katsis, H. P. Chen, L. J. Rothberg, S. H. Chen, and T. Tsutsui, "Polarized Photoluminescence from Solid Films of Nematic and Chiral-Nematic Poly(*p*-phenylene)s," *Appl. Phys. Lett.* (submitted).

Liquid Crystalline Conjugated Polymers as Multifunctional Optical Materials

D. Katsis, H. P. Chen, J. C. Mastrangelo*, and S. H. Chen

Department of Chemical Engineering, Materials Science Program
Laboratory for Laser Energetics, Room 1210, COI, University of Rochester

*Now at Naval Research Laboratory, Washington, D.C.

TOPS MURI Review Meeting, 15-16 August 2000, Natick, MA

Four Types of Liquid Crystalline Order

Nematic

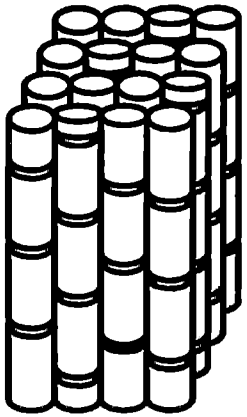

Smectic

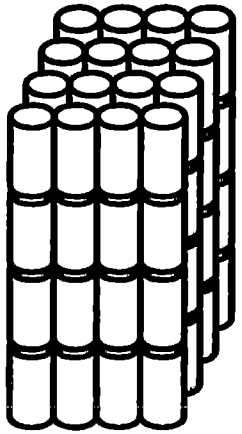

Cholesteric

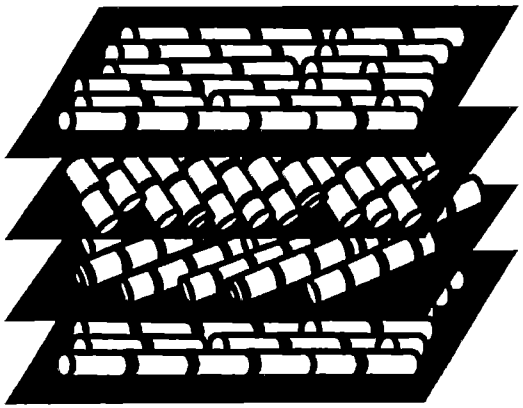

Columnar

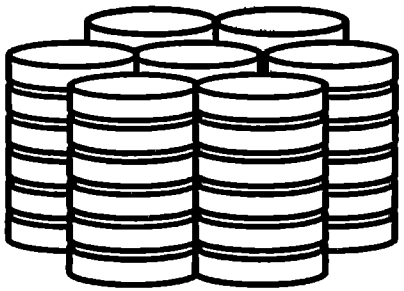

Characteric Textures of Liquid Crystals Observed with Polarizing Optical Microscopy

Nematic

Smectic

Cholesteric

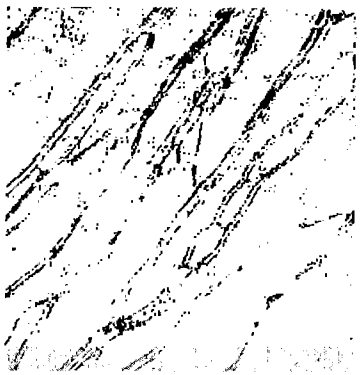

Columnar

Four Types of Liquid Crystalline Order

Nematic

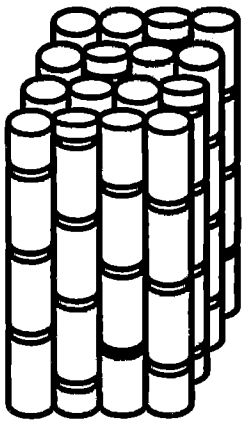

Smectic

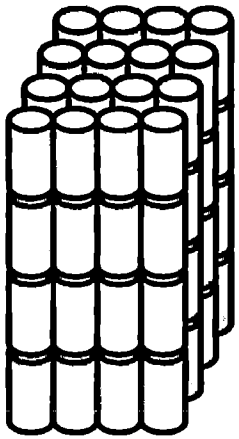

Cholesteric

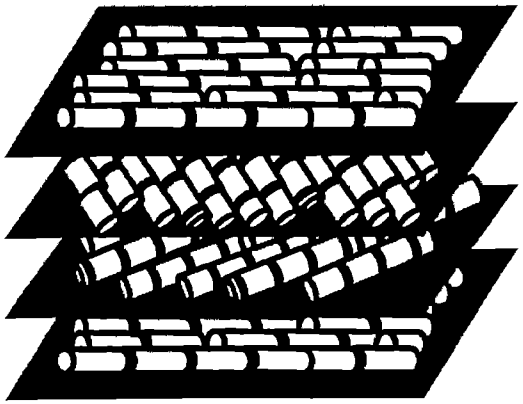

Columnar

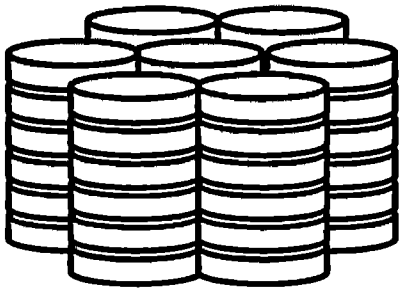

Characteric Textures of Liquid Crystals Observed with Polarizing Optical Microscopy

Nematic

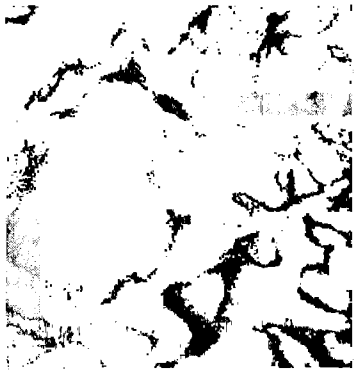

Smectic

Cholesteric

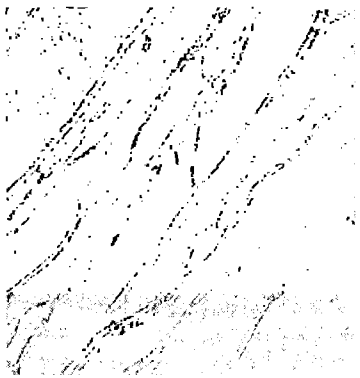

Columnar

Coloration via Selective Reflection

- **Chiral-nematic liquid crystalline film as a helical stack of quasinematic layers, illustrated below with a LH structure:**

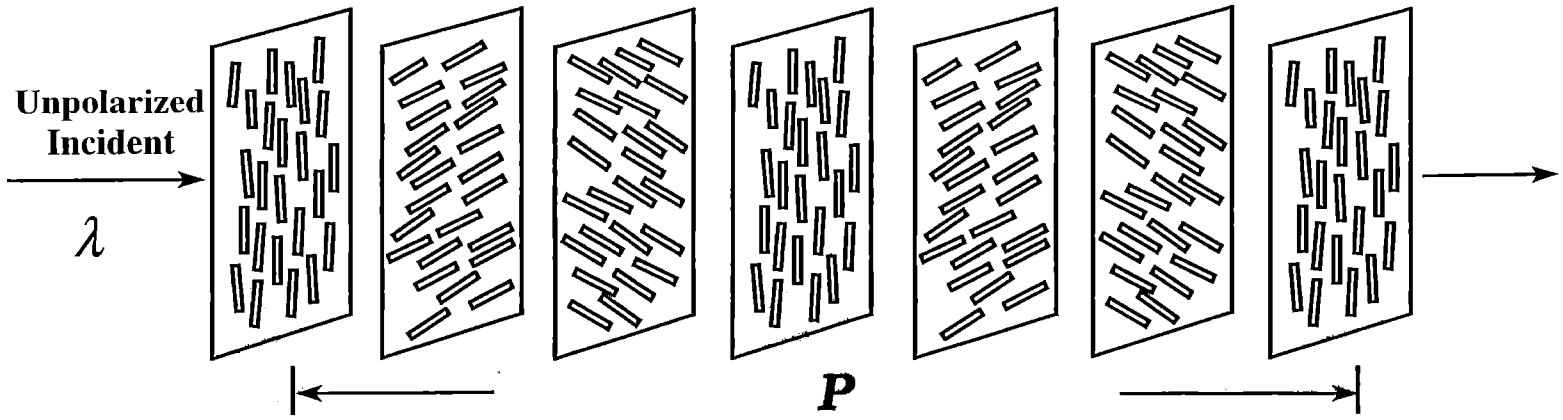

Case 1: $\lambda \neq \lambda_R = p\bar{n}$**, complete transmission**

Case 2: $\lambda = \lambda_R$**, LHCP reflected and RHCP transmitted**

A Concept of Tunable Reflection via Electrochemical Doping with Chiral Salts

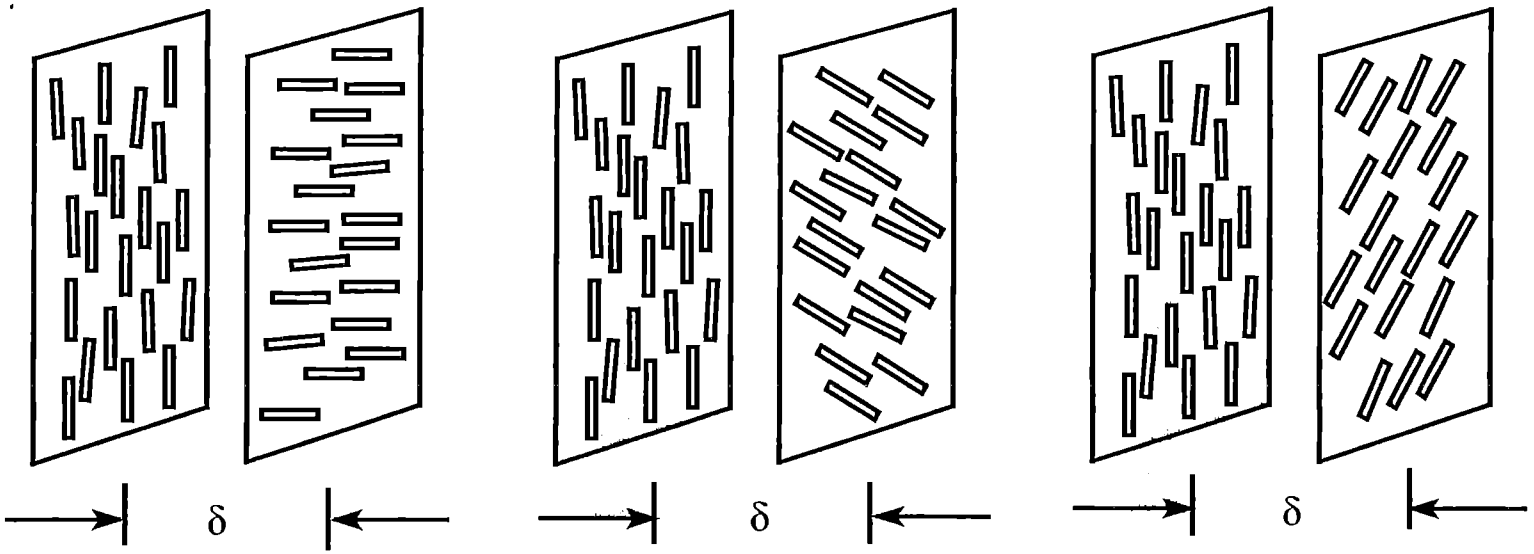

Undoped

Doped with C_R^*
Pitch Tightening

Doped with C_S^*
Pitch Loosening

Existing Chiral-Nematic Materials

- **Low viscosity fluids, polymer melts**
- **Lyotropic polymers, 'chaotropic effect'**
- **Polymer/LC composites, anisotropic gels**
- **Thermotropic polymers**
- **Low-molar-mass vitrifiable LCs**

All these are nonconjugated systems with tunable reflection color by various means

Multifunctional LC Polymers

- Amorphous or crystalline conjugated polymers capable of tunable absorption and emission
- Chiral-nematic nonconjugated polymers capable of tunable reflection
- A new challenge: chiral-nematic conjugated polymers for multiple modes of tunability

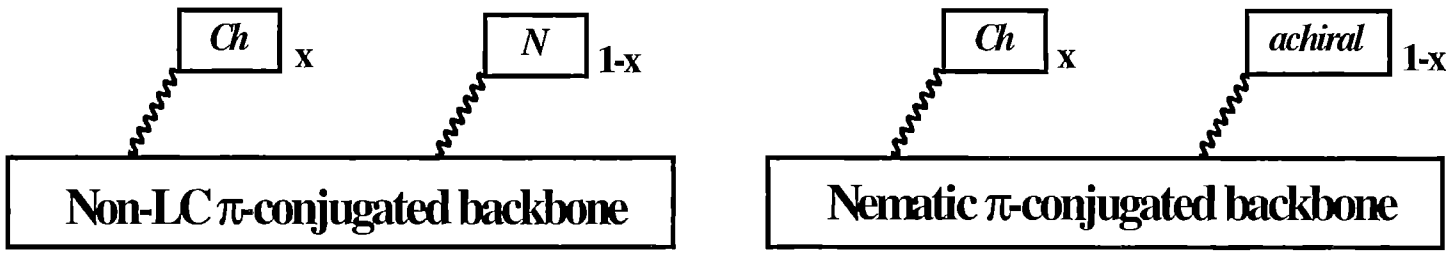

Synthetic Scheme for Chiral-Nematic Poly(*p*-phenylene)s

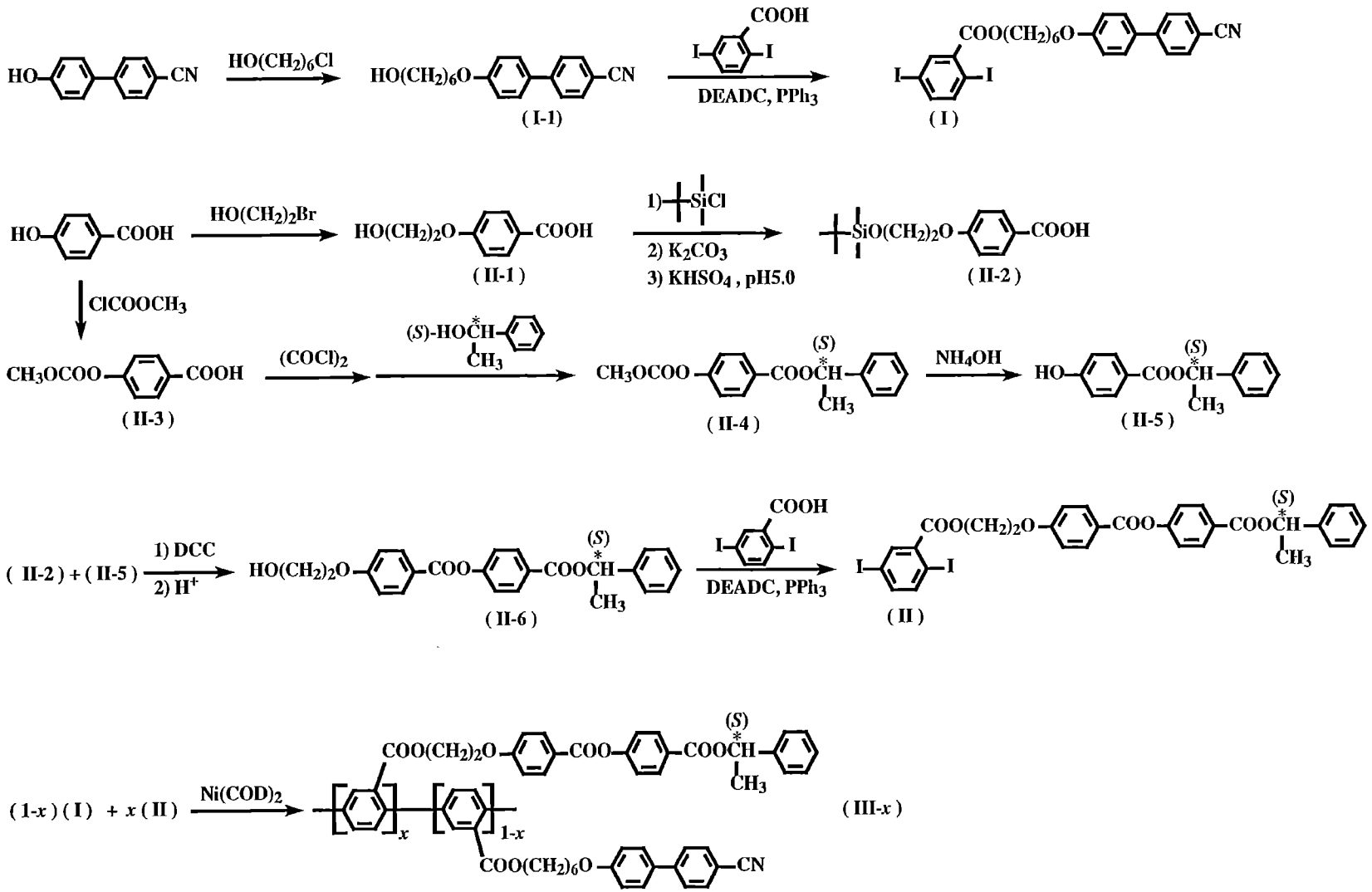

Absorption and Emission Spectra in Dilute Solution

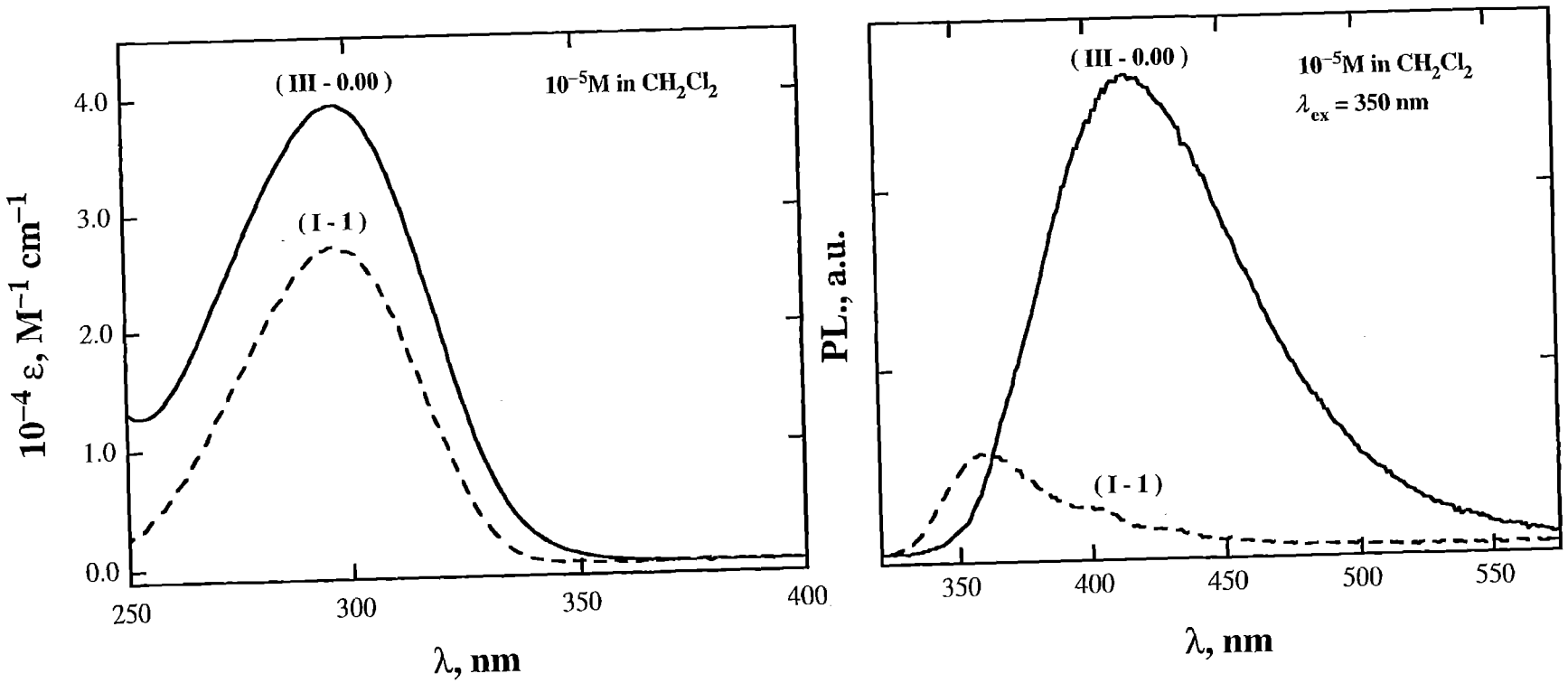

Optical Set-Up for Characterization of LPPL

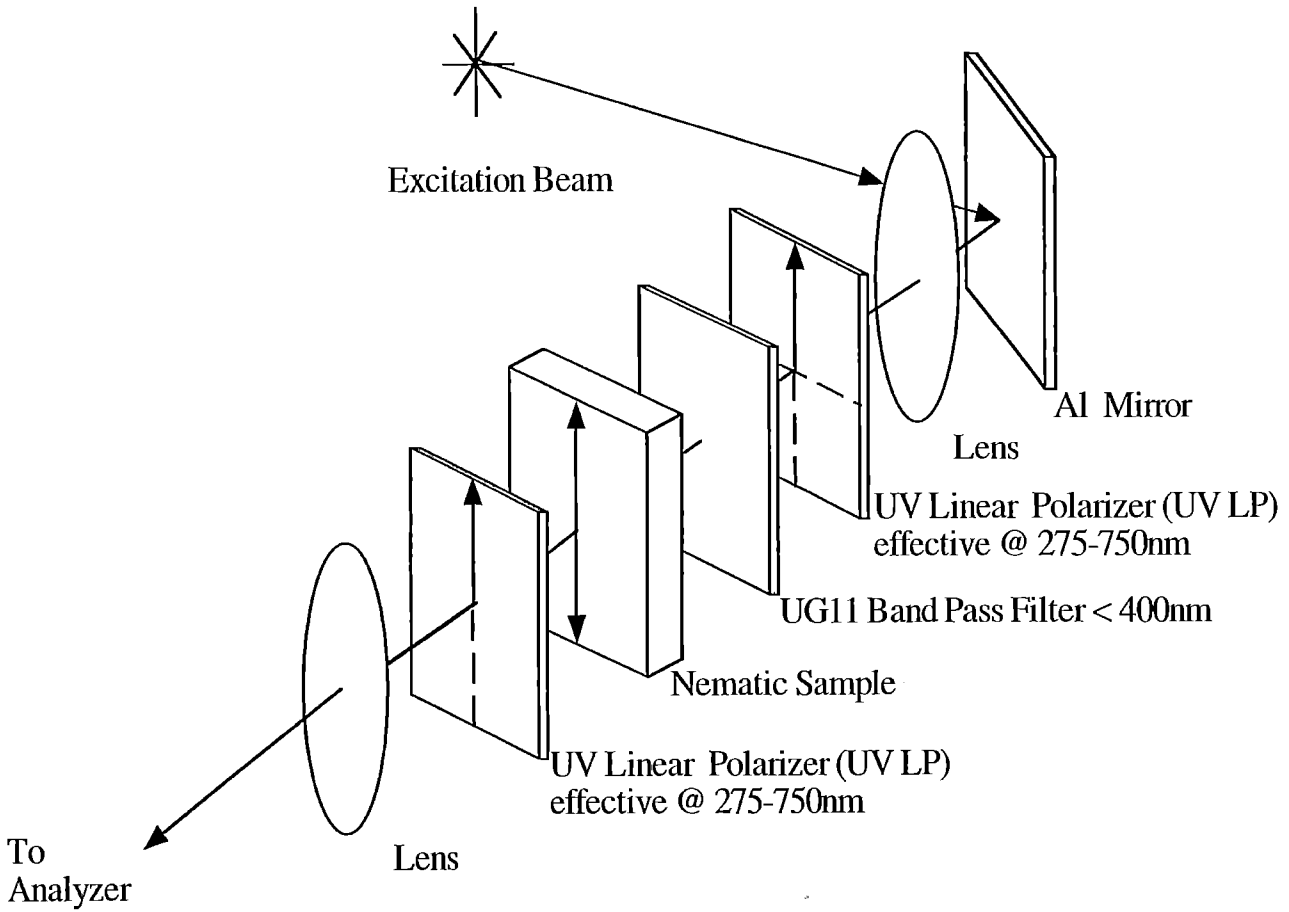

Characterization of the Alignment of Conjugated Backbones and Nematic Pendants

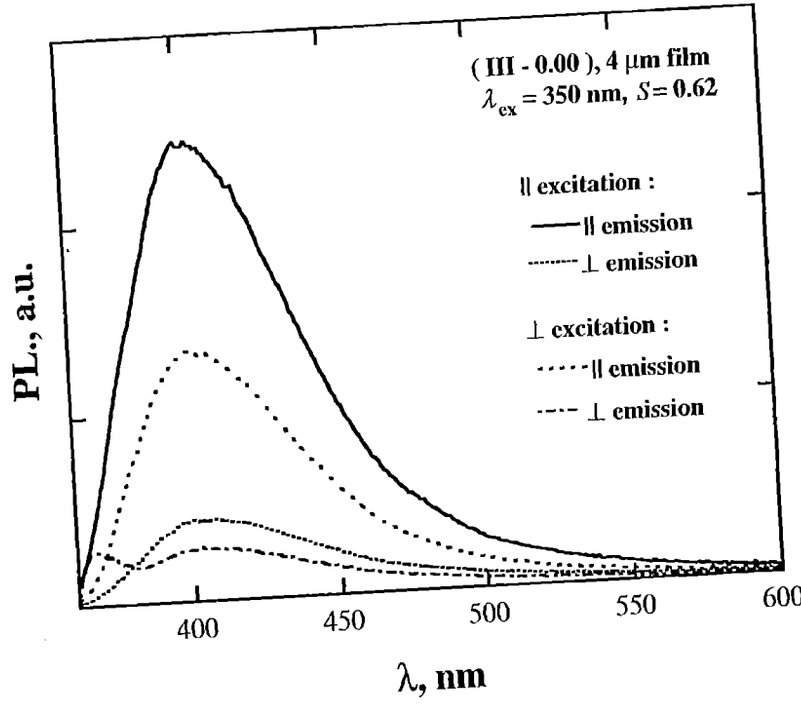

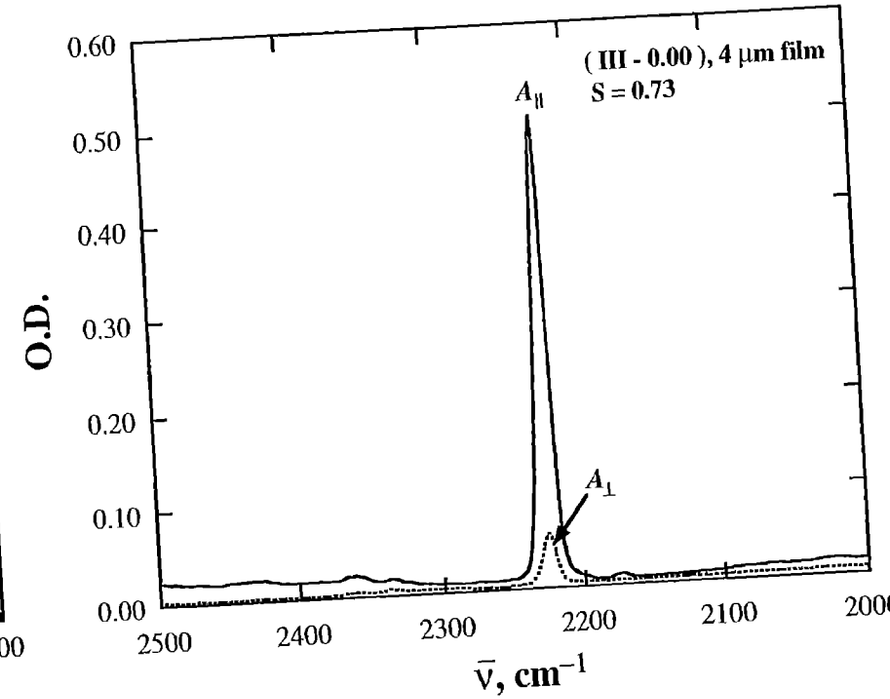

Supramolecular Structure of Chiral-Nematic Poly(*p*-phenylene)s

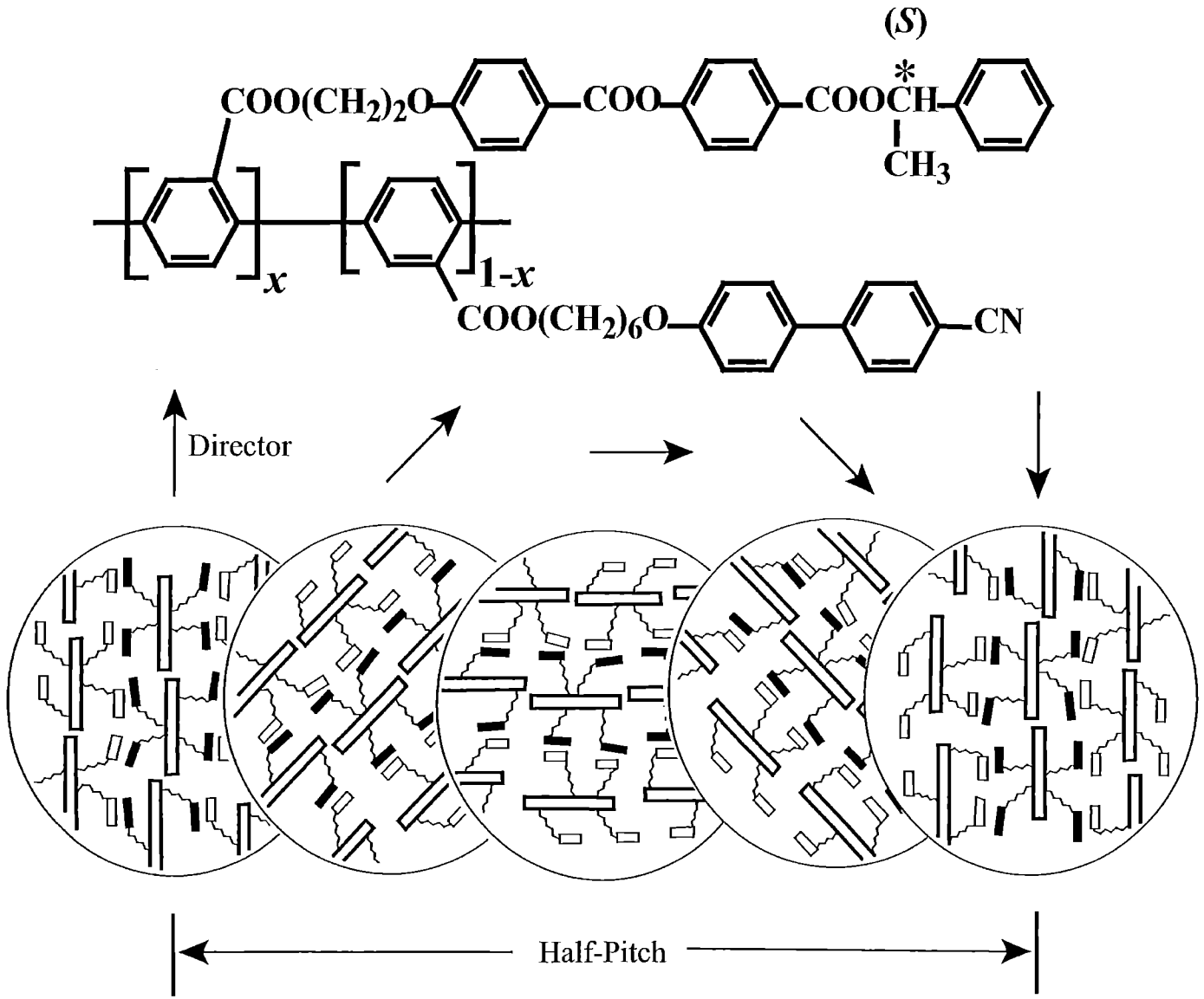

Absorption and Selective Reflection of Thin Films

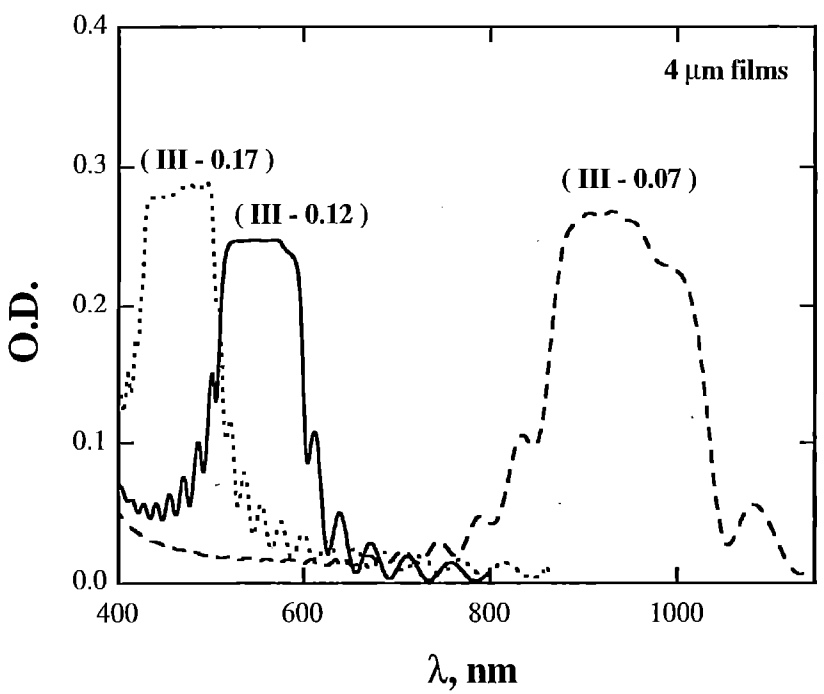

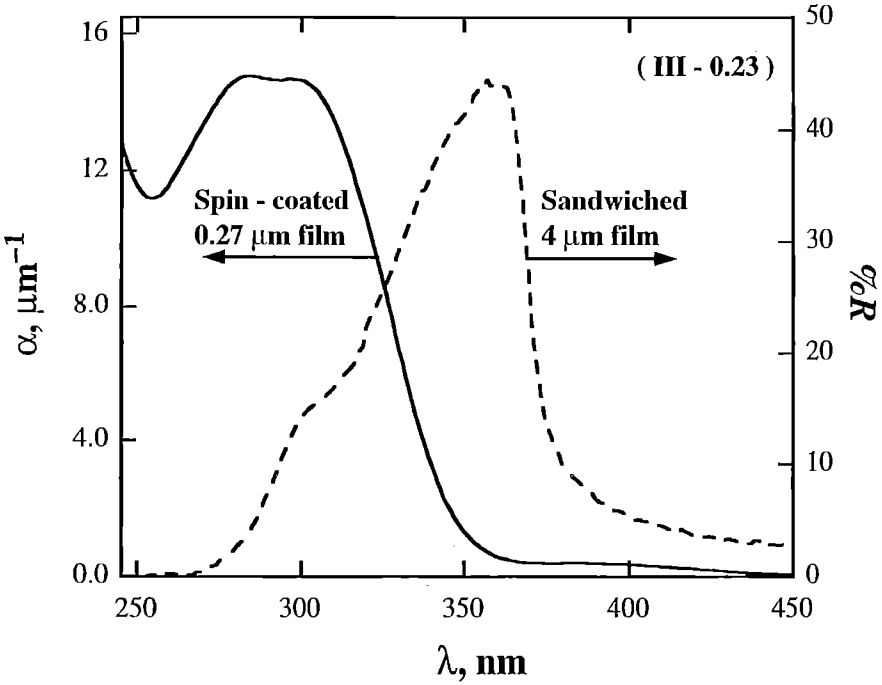

Transmission of Circularly Polarized Light

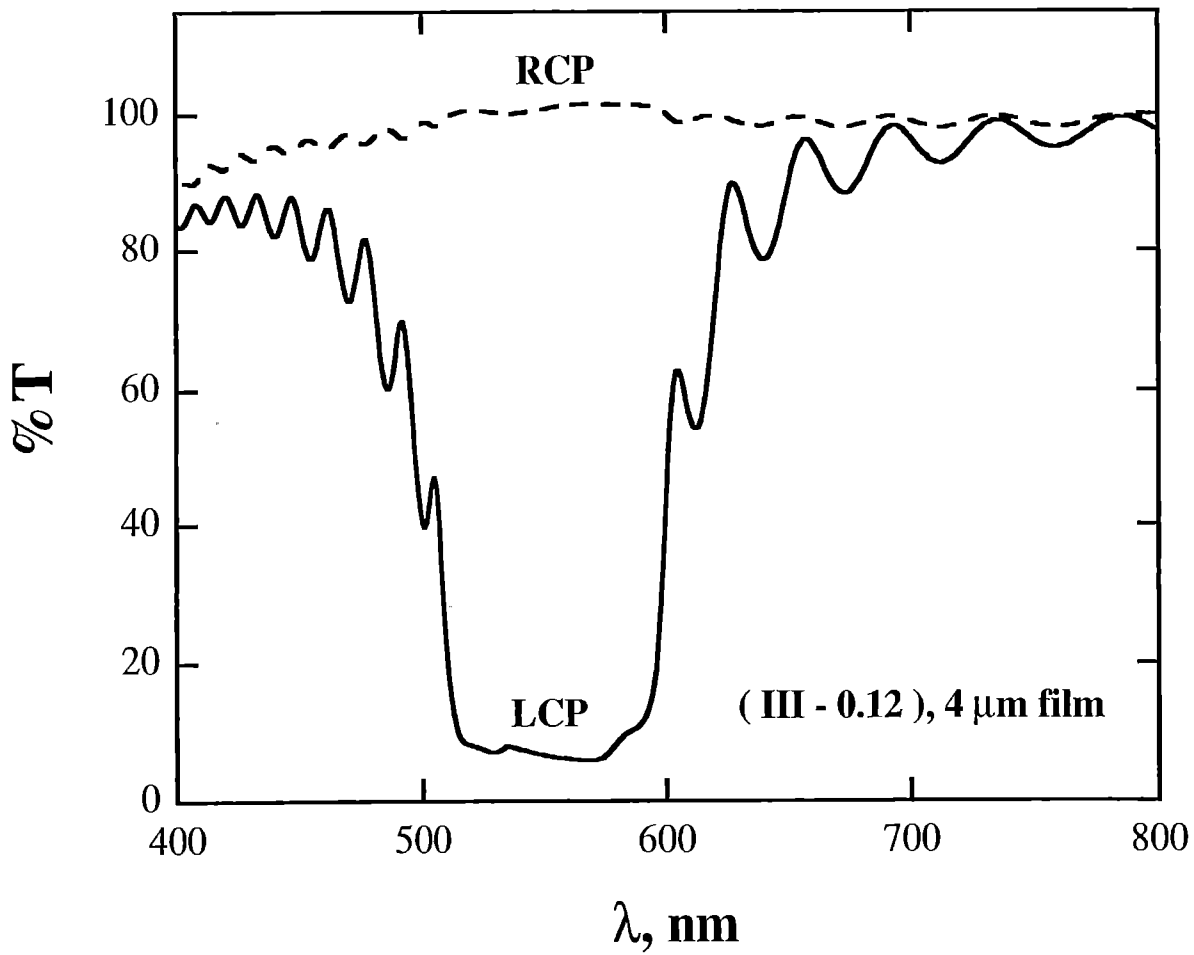

Optical Set-Up for Characterization of CPPL

$$g_e = 2\frac{I_L - I_R}{I_L + I_R}$$

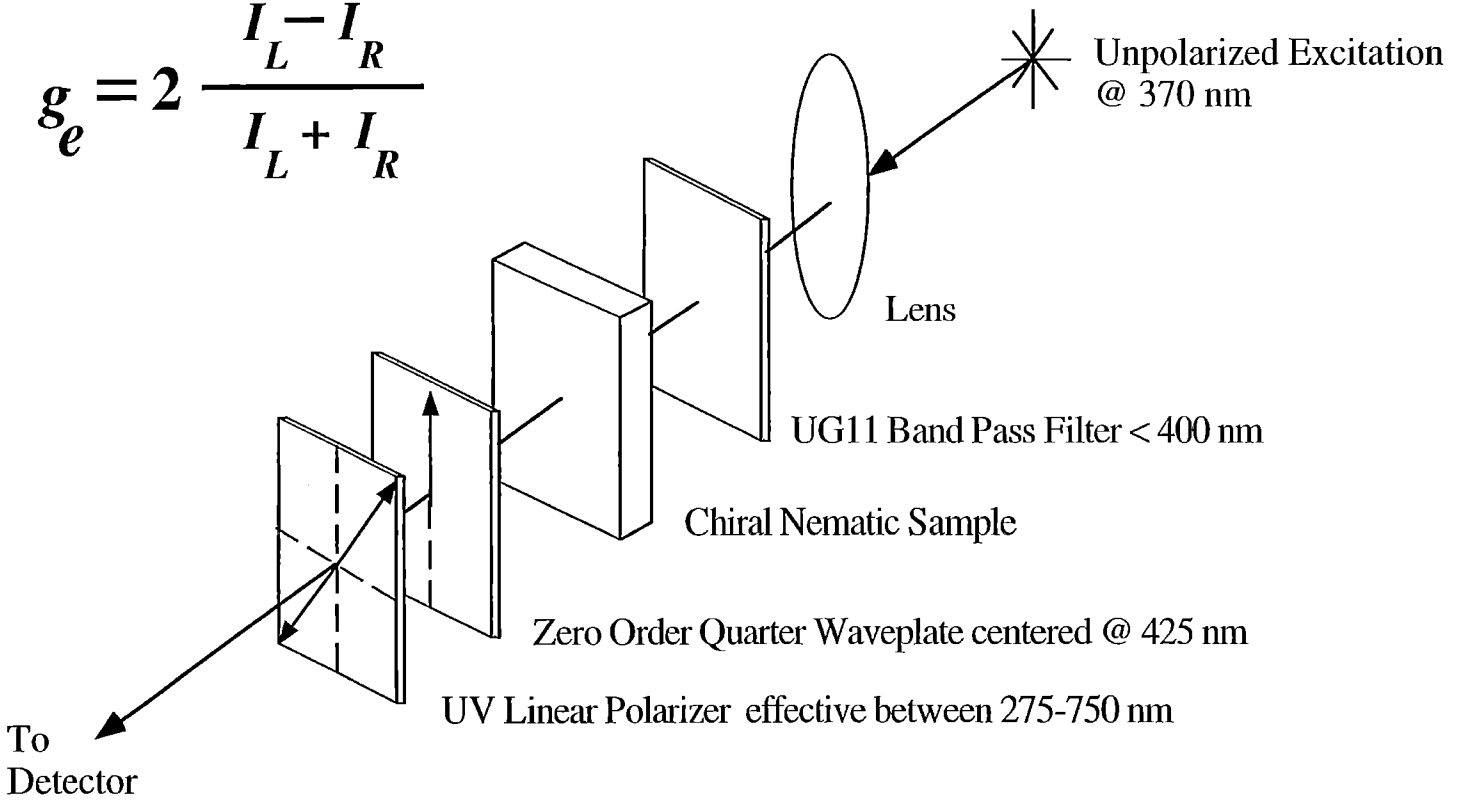

Spectra of Circularly Polarized Photoluminescence from Thin Films

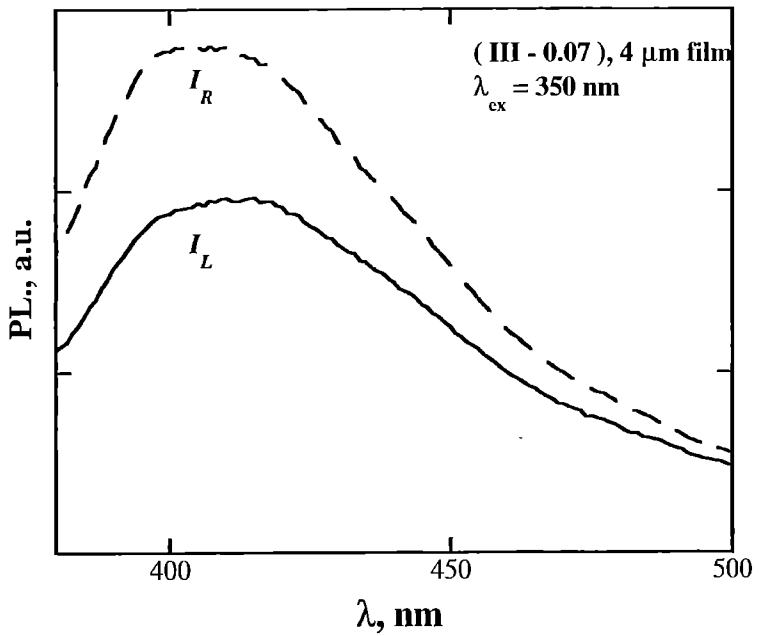

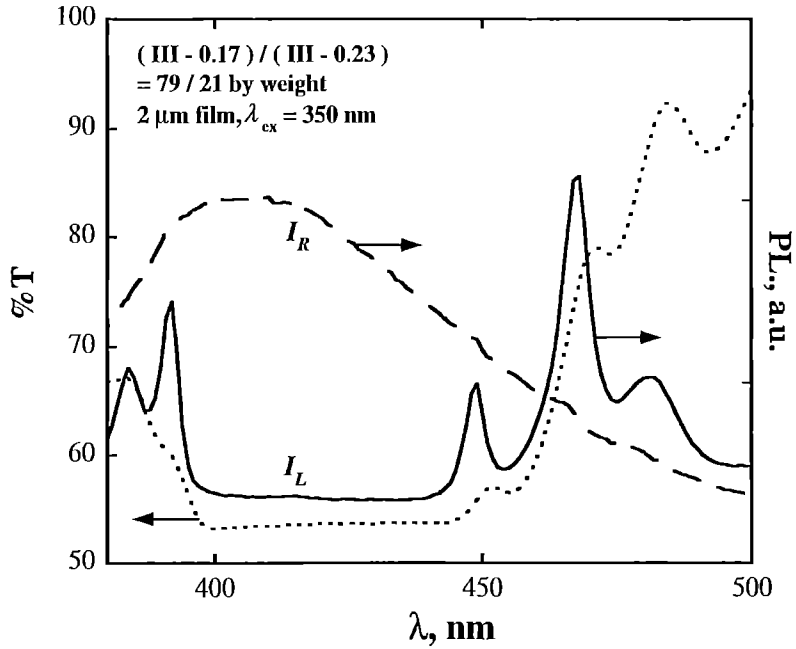

Effect of Film Thickness on Degree of Circular Polarization

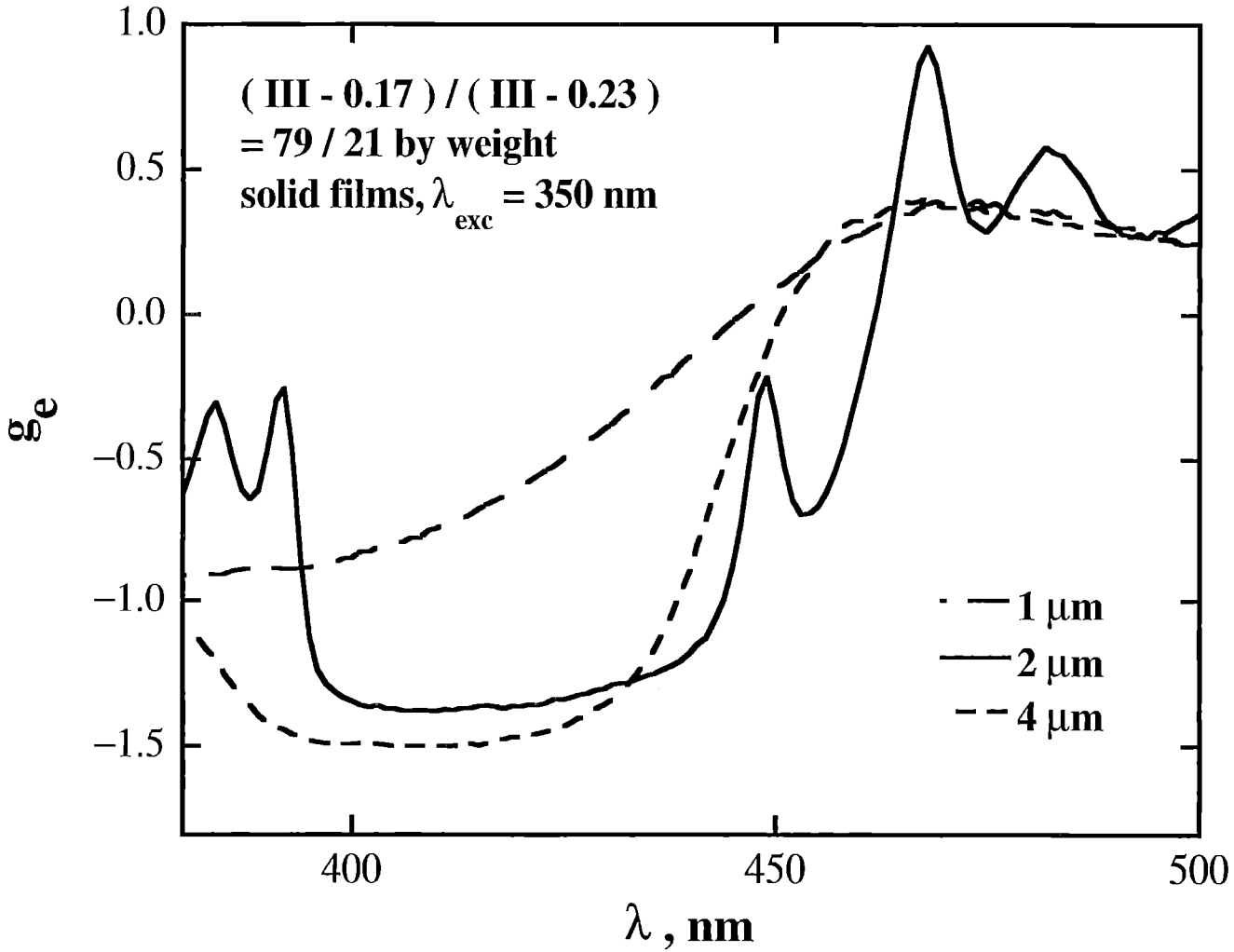

Optical Set-Up for Characterization of Viewing Angle Dependence

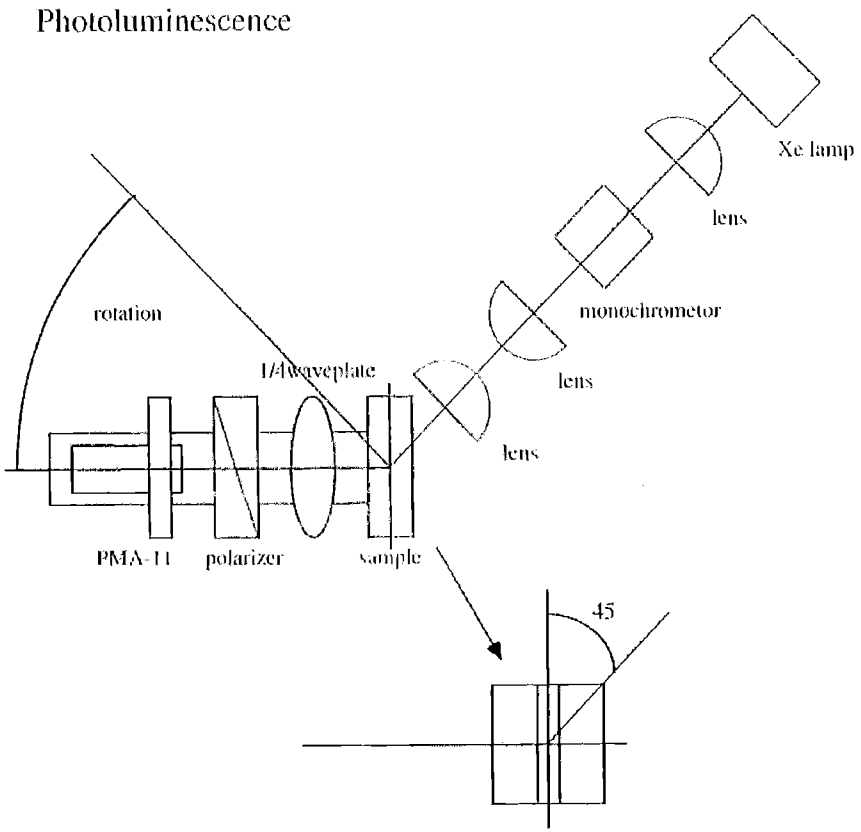

Viewing Angle Dependence Of CPPL

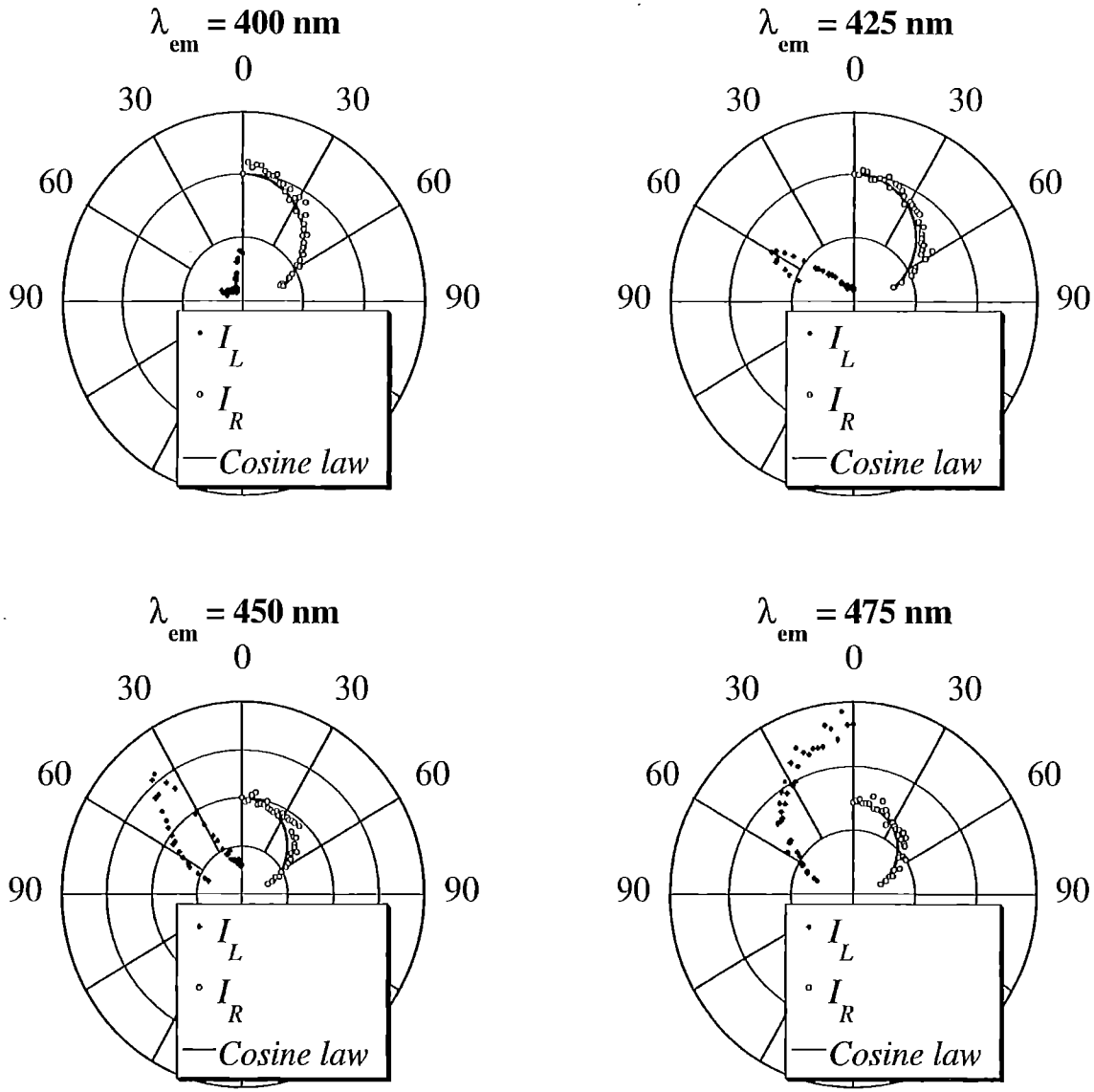

Glass-Forming Chiral-Nematic Liquid Crystals

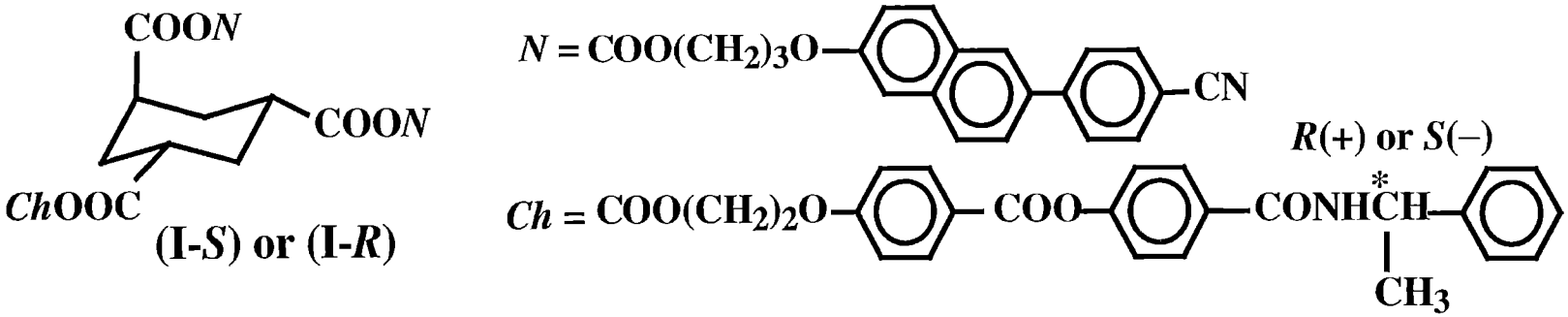

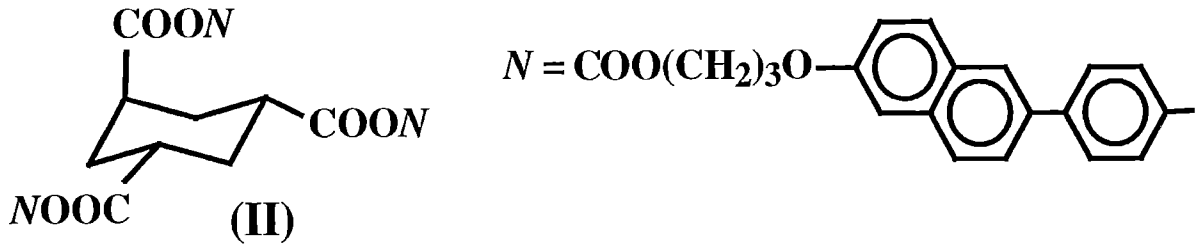

- Ease of processing into large area, monodomain, vitrified films
- Environmental durability
- Availability of both enantiomers
- Selective reflection tunable from UV to IR depending on ratio (I)/(II)

Material Synthesis

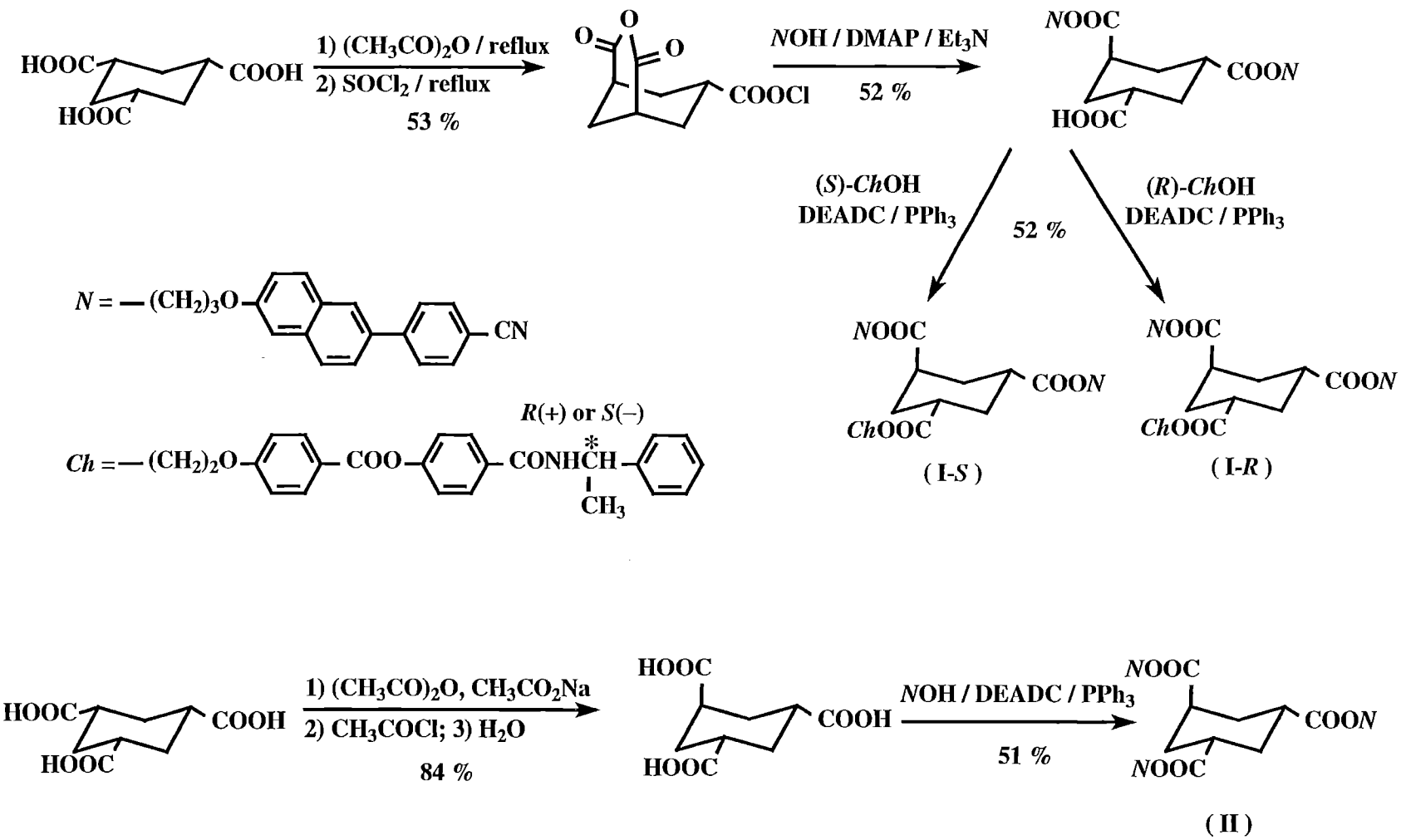

DMAP: 4-(dimethylamino)pyridine; DEADC: diethyl azodicarboxylate; PPh_3: triphenylphosphine

Transmission of Circularly Polarized Light through Glassy Chiral-Nematic Films

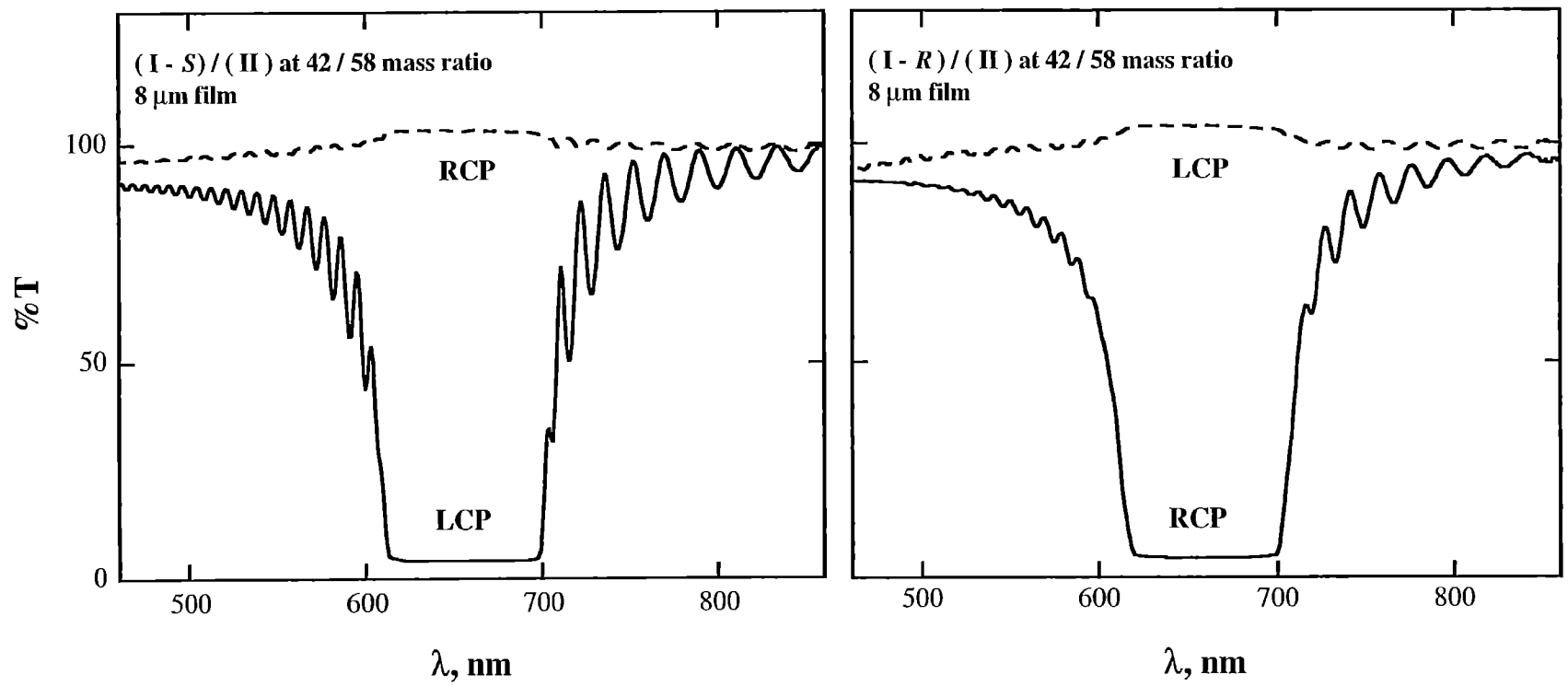

High-Performance Reflector and Notch Filter

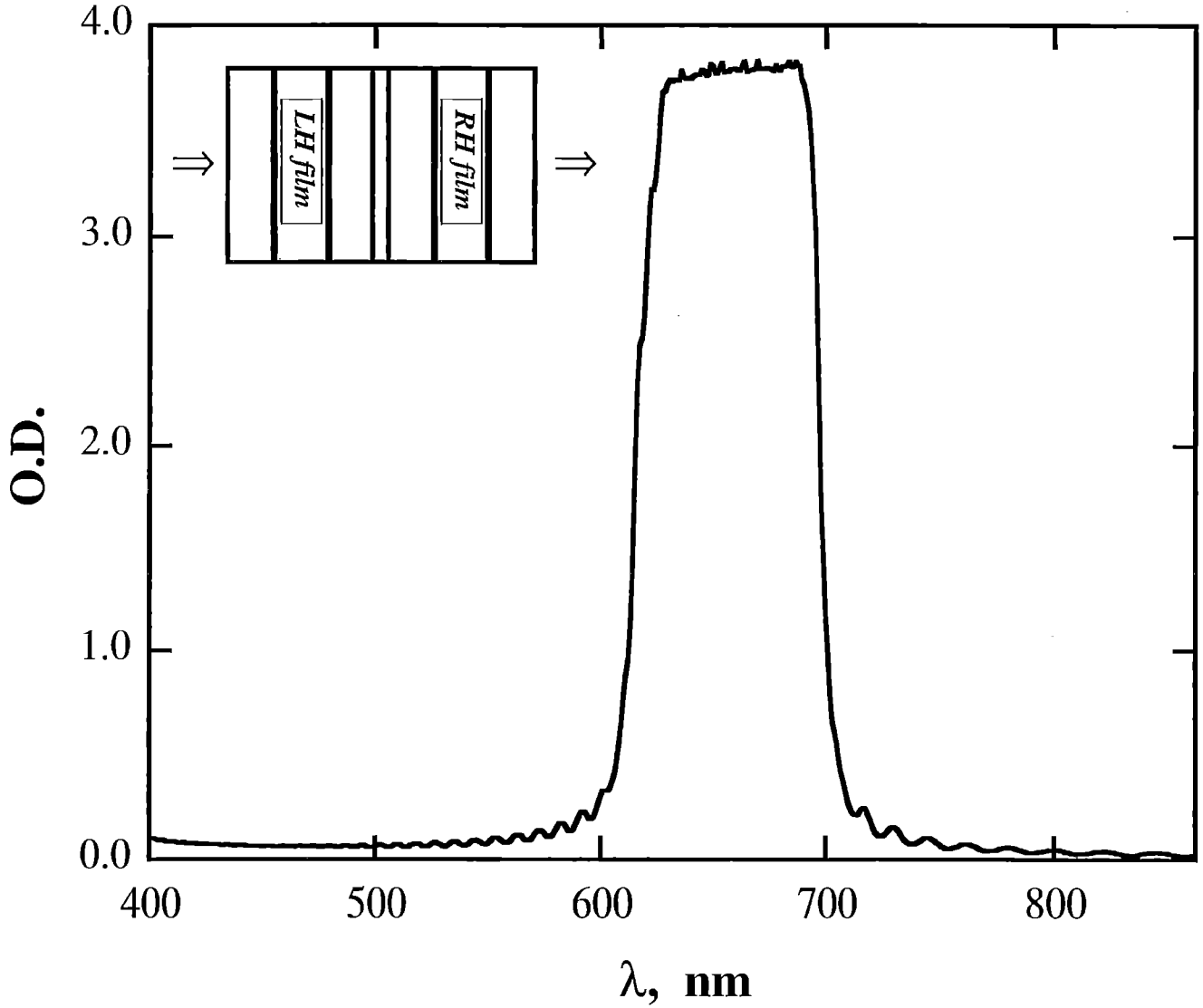

Conclusions

- Chiral-nematic poly(*p*-phenylene)s were shown to self-assemble into helically stacked π-conjugated systems
- With increasing chiral content, selective reflection of neat films was tunable from the infrared, through the visible, and down to the ultraviolet region
- Unpolarized excitation at 350 nm was found to induce emission predominantly from the polymer backbone with no evidence of excimer formation
- A high degree of circular polarization was observed with chiral-nematic films when emission occurred in the resonance region
- High-performance reflectors were prepared with glass-forming LCs having identical chemical structure except opposite chirality

Current and Future Research

- Tuning reflection colors via reversible isomerization of photoresponsive dopants in vitrified chiral-nematic films
- Design, synthesis, characterization and molecular dynamics simulation of helically coiled conjugated polymers in addition to helically stacked systems
- Electroluminescent poly(fluorene)s: optimized structure for efficient and stable electroluminescence, color tunability via copolymerization or blending, and polarization control
- Potential of helically arranged conjugated polymers for tunable absorption and reflection colors via electrochemical doping with chiral salts
- Synergy between two or three modes of color tunability
- Color patterning via spatially modulated thermal and photochemical film processing

Tunable Optical Polymer Systems: Mesostructured Chromogenic Polymer Assemblies

ARO MURI - TOPS

Co-PI: Paula T. Hammond

Dept. of Chemical Engineering, MIT

1) Layer-by-Layer Polydye Microstructures
2) Block Copolymer Chromogenic Materials

3D Array Patterning by Self Assembly

Research Team

- Paula T. Hammond Patterned Deposition Techniques/Chromic Thin Films
- Alan Bard Electrochemical Analysis/ Adsorption Studies
- Lewis Rothberg Electrochemically Assisted Microfabrication

Goals

- New Solid State Medium for Electro and Photochromic Systems
- Opportunity for Device Fabrication

Interactions with Army

- Potential Contact with Natick Labs on Thin Films

MURI Funding Level: $50 K/yr.

Personnel

- P.T. Hammond
- Dean Delongchamp

TOPS Objectives - Mesostructured Polymers
Layer-by-Layer Films

- Use ionic layer-by-layer technique to develop new electro- and photochromic, reversible, polymer-dye layered composite films (with **Swager/Jenekhe** lab).
- Create functional microstructures for chromogenic display applications based on expertise in selective deposition.
- Characterize electron transfer processes of complex multilayered systems using spectroelectochemistry and spectroscopy (with **Bard** and **Rothberg** labs).

Layer-by-Layer Ionic Assembly

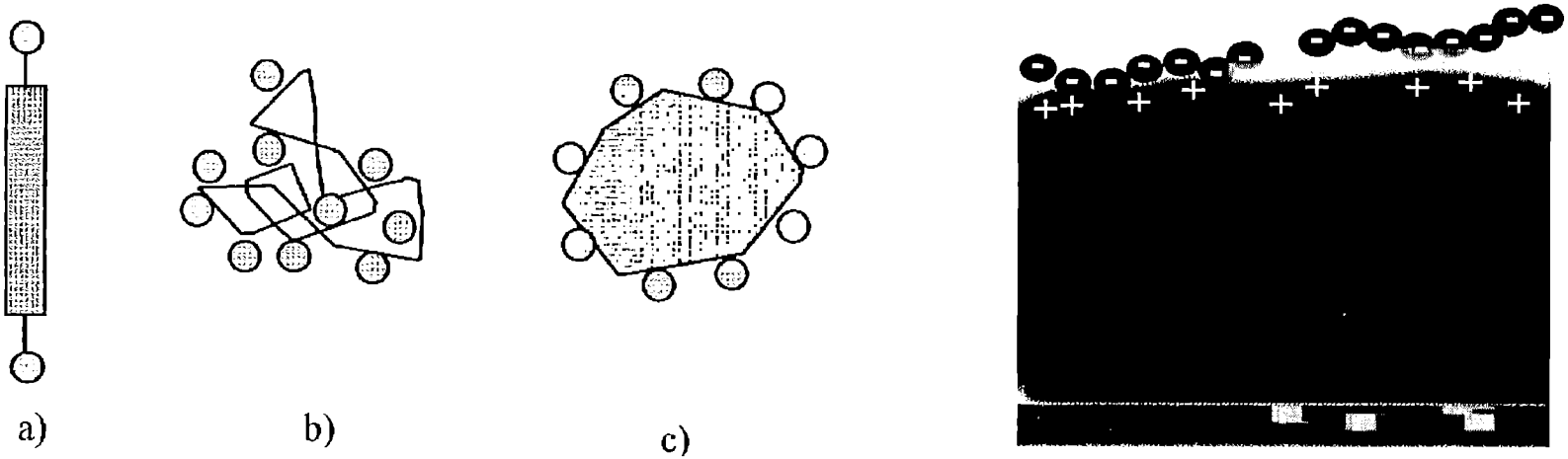

- Step-wise deposition of molecular scale layers
- Can incorporate a number of functional dyes
- Use layer-by-layer to tailor redox properties
- Vary electron transfer to different regions with layer position

Comparison of Photolithography to Chemistry-templated Multilayer Assembly

Photolithography

- expensive both in capital and operating cost
- not suitable for patterning non-planar surface
- ineffective in generating 3-D structures
- difficult for introducing specific chemical functionality

Chemistry-templated assembly

- little capital investment, procedurally simple
- access to new types of surfaces, optical structures, sensors and prototype devices etc.
- not subject to the limitations set by optical diffraction and optical transparency

Self-Assembled Monolayers(SAMs) and Micro-contact Printing(μCP)

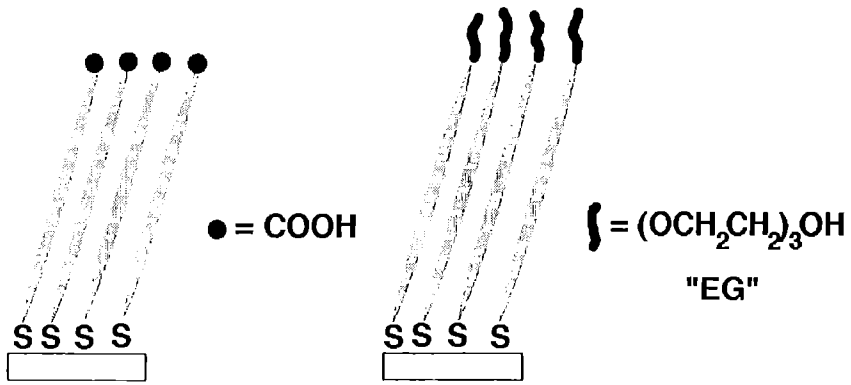

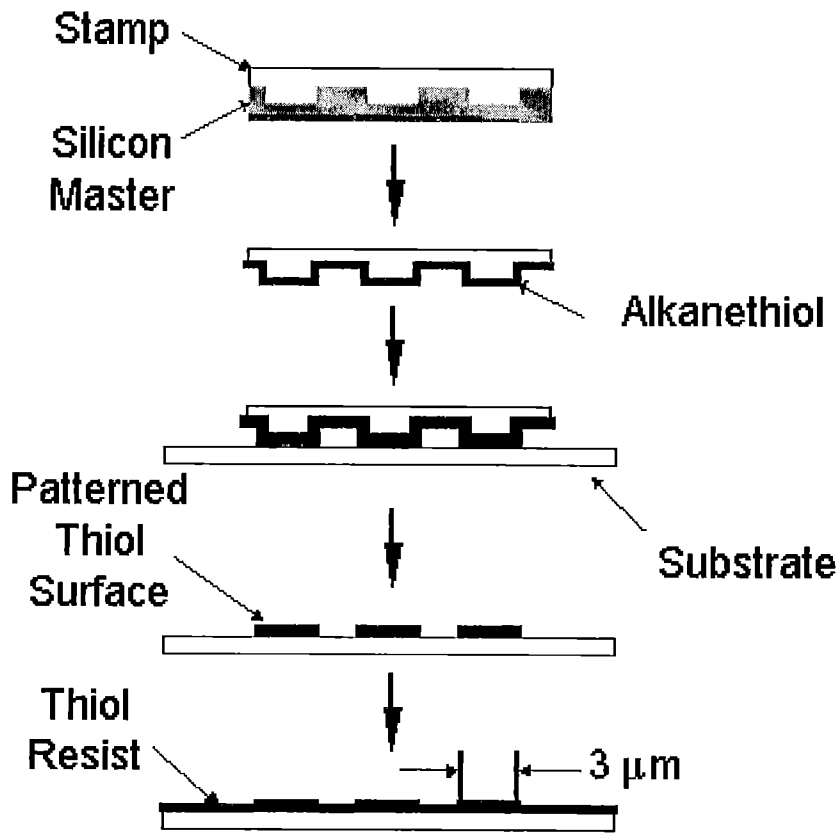

- **COOH SAM promotes adsorption**
- **Oligoethylene glycol (EG) SAM resists adsorption of polyions.**

Luminescent dyes

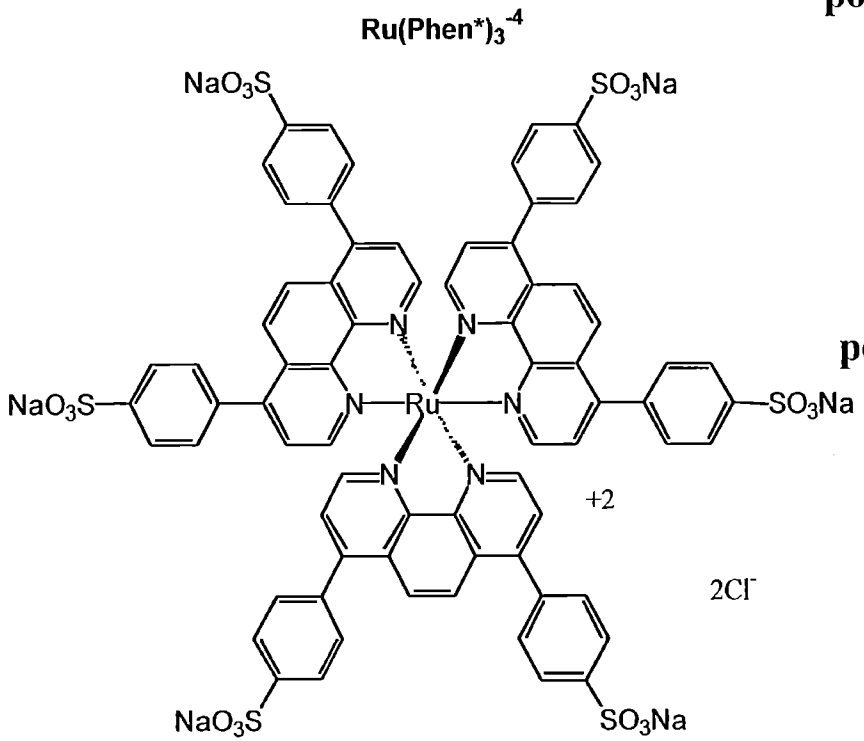

absorbance max. 470nm
emission max. 628nm (red)

(supplied by Rubner group at MIT)

poly(p-phenylene) anion

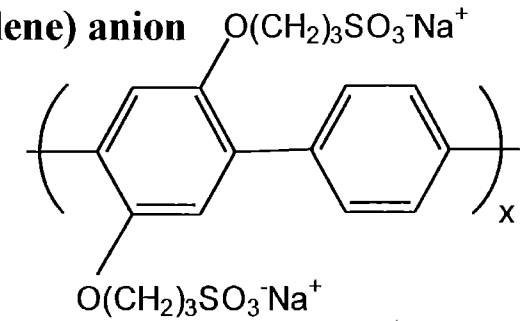

poly(p-phenylene) cation

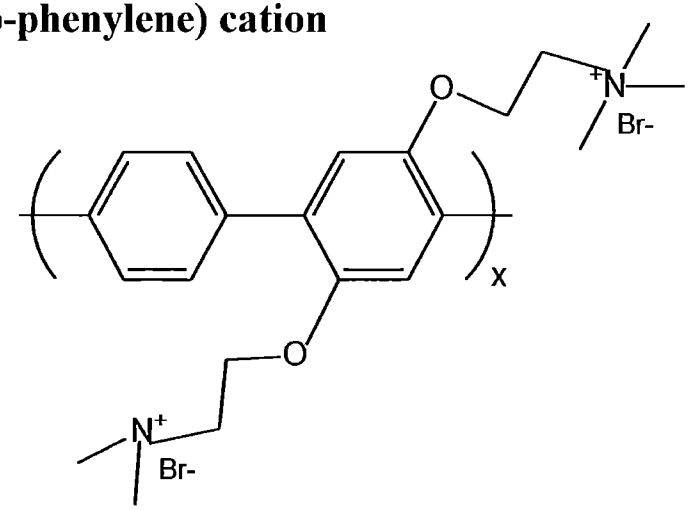

absorbance max. 350nm
emission max. 420nm (blue)

Microscopy of Patterned Ru Dye Multilayers

Optical Microscopy

Fluorescence Microscopy

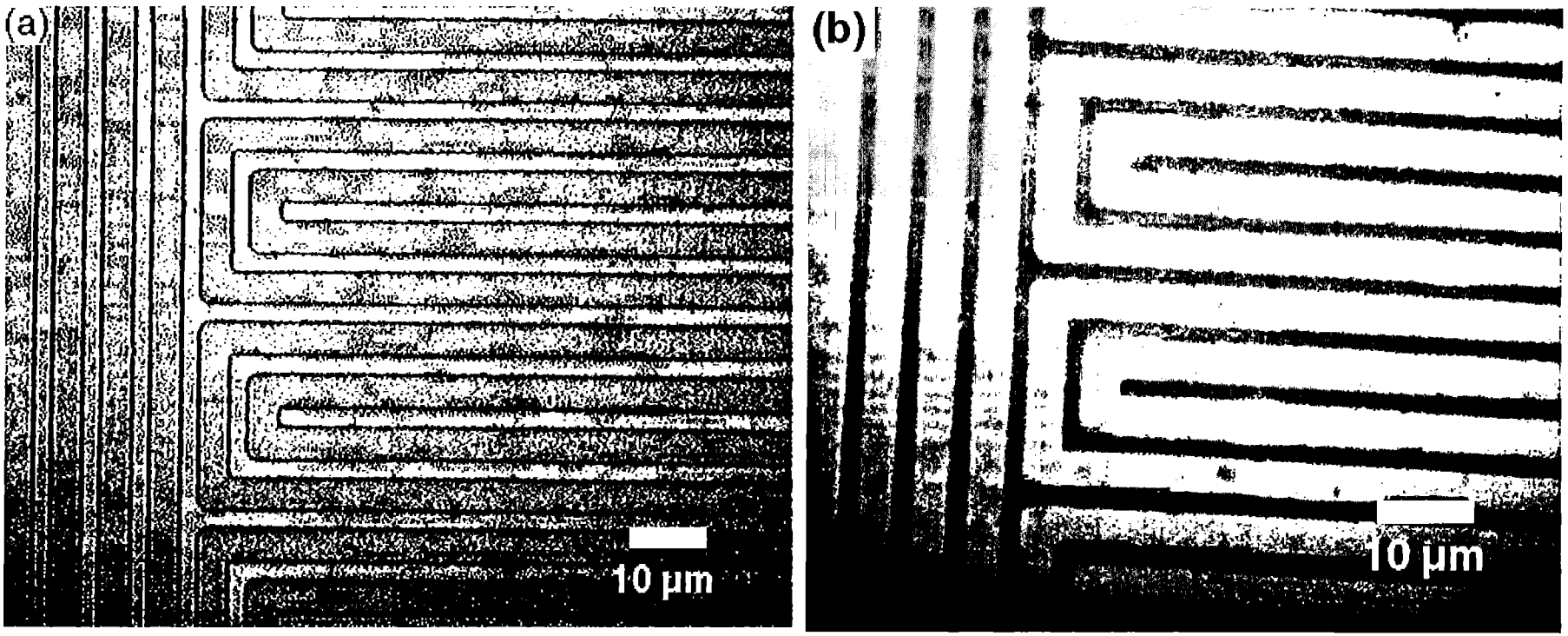

Ten bilayers of Ru/LPEI on five bilayers of PAA/LPEI adsorbed at pH 4.8.

Patterning Ru dye with different polyamine ---- fluorescence micrographs

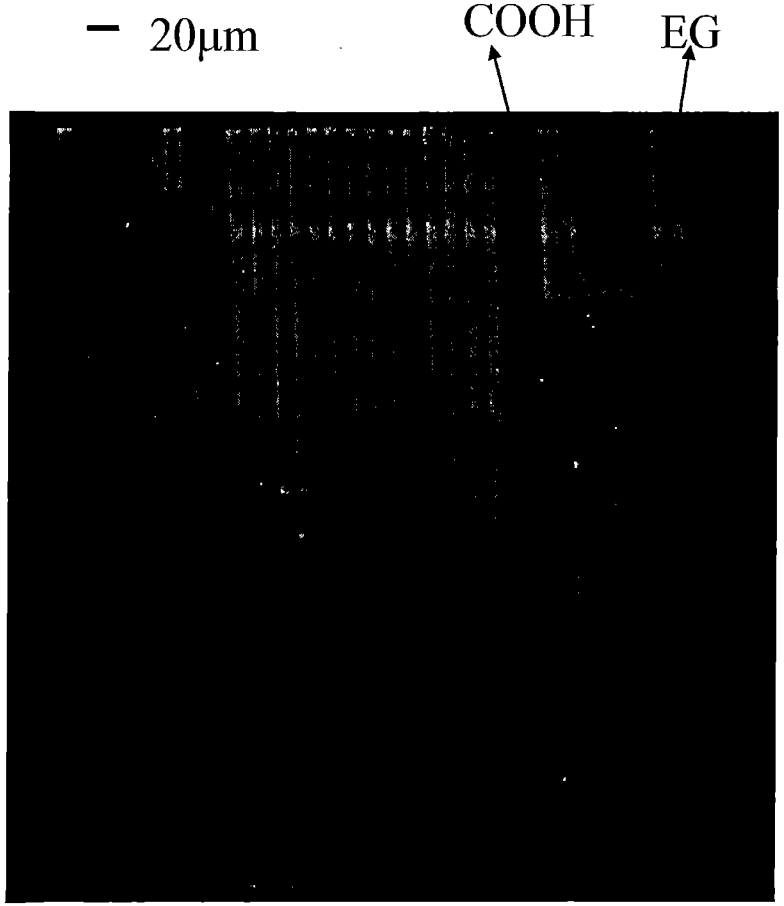

(PAH/PAA)5(PAH/Ru)10, pH4.8

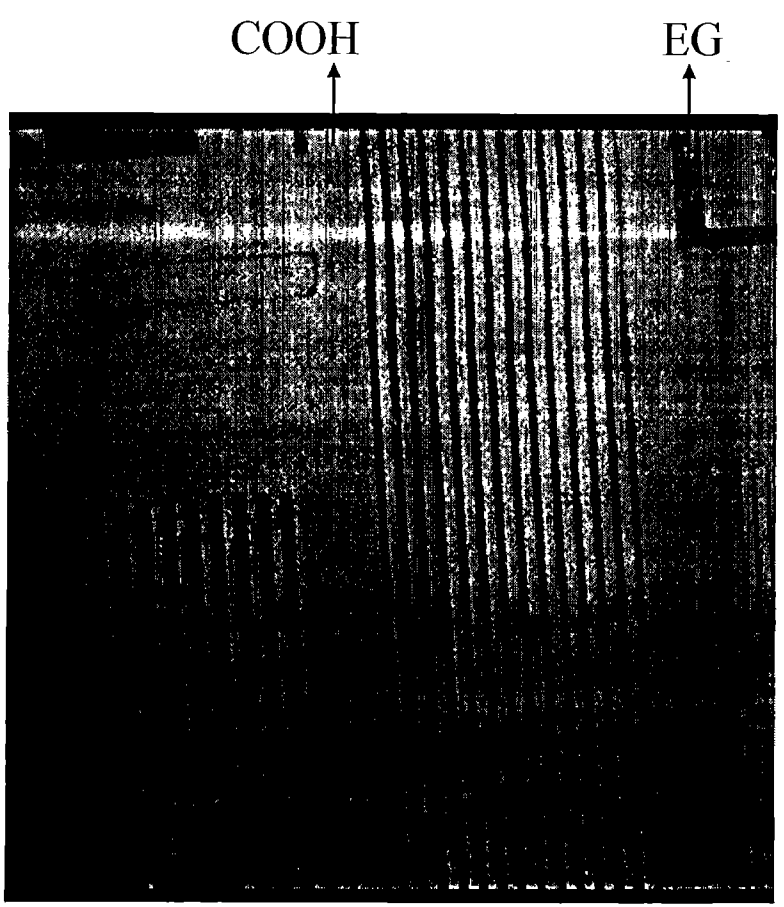

(LPEI/PAA)5(LPEI/Ru)10, pH4.8

Combination of two dyes into patterned thin film

EG $(PAH/Ru)_{10}$

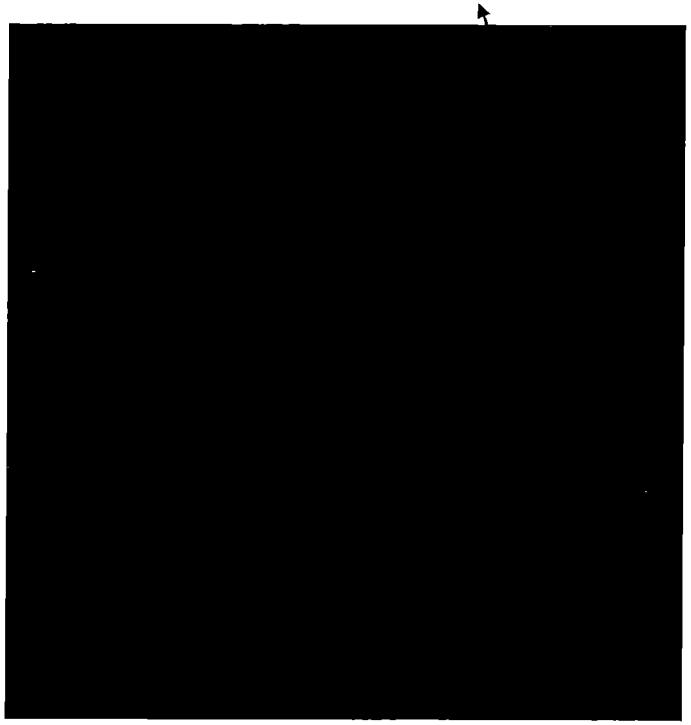

$(PAH/Ru)_{10}$ under Fluorescence Microscope using red filter

COOH $(PDAC/PPP(-))_{10}$

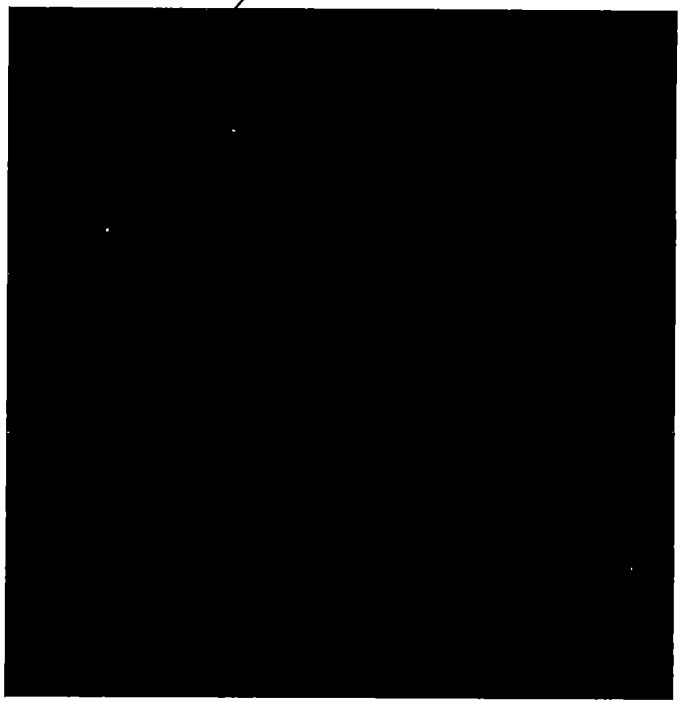

$(PDAC/PPP(-))_{10}$ under Fluorescence Microscope using DAPI filter

Hammond et al., 2000

Motivation
---Multicolor Flat Panel Display

Advantages of using fluorescent dyes in organic electroluminescent devices:

- an emission in wide visible spectral range
- large area flat panel displays driven at low voltage

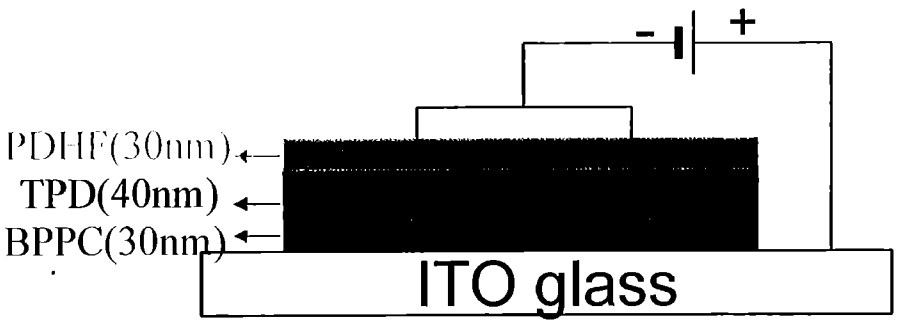

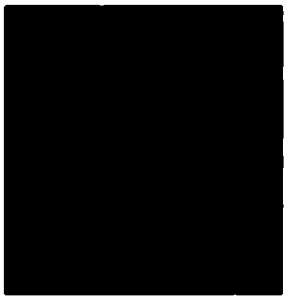

Old:

- vapor deposition, spin coating
- color variability is controlled by polarity and strength of E field based on stacking multilayer of fluorescent dyes

New:

- layer by layer assembly
- color image is controlled by site addressing and E field variation based on multicolor pixel array

Multilevel Patterning

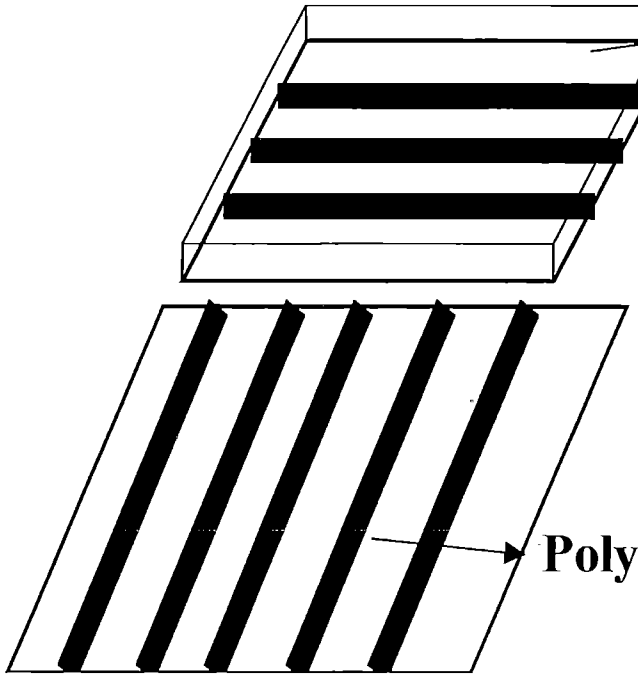

- **Pattern with COOH/EG**
- **polyion multilayers**
- **stamping functional resist**
- **polyion multilayers**

- **Idea: stamping resist on underneath multilayer**
- **Model resist:**

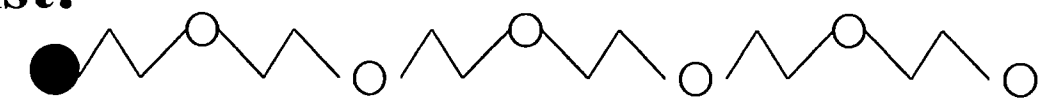

Multilevel pattern containing Ru dye -AFM

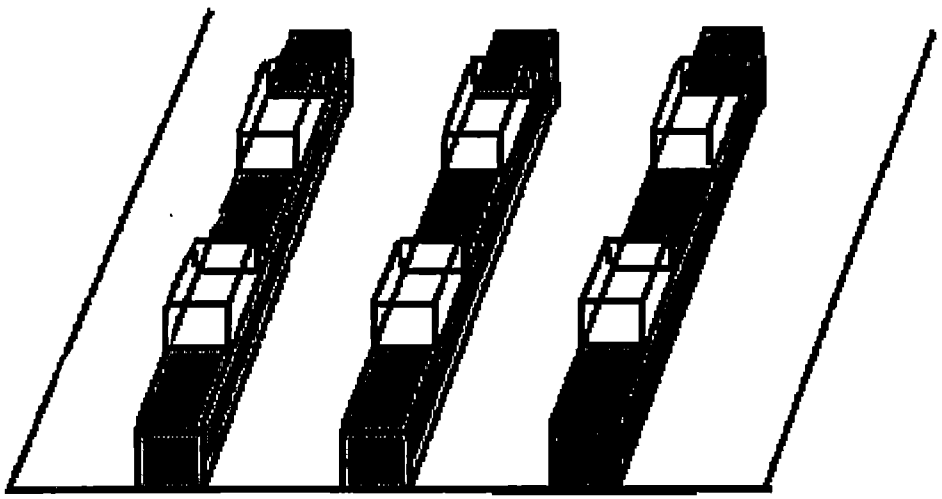

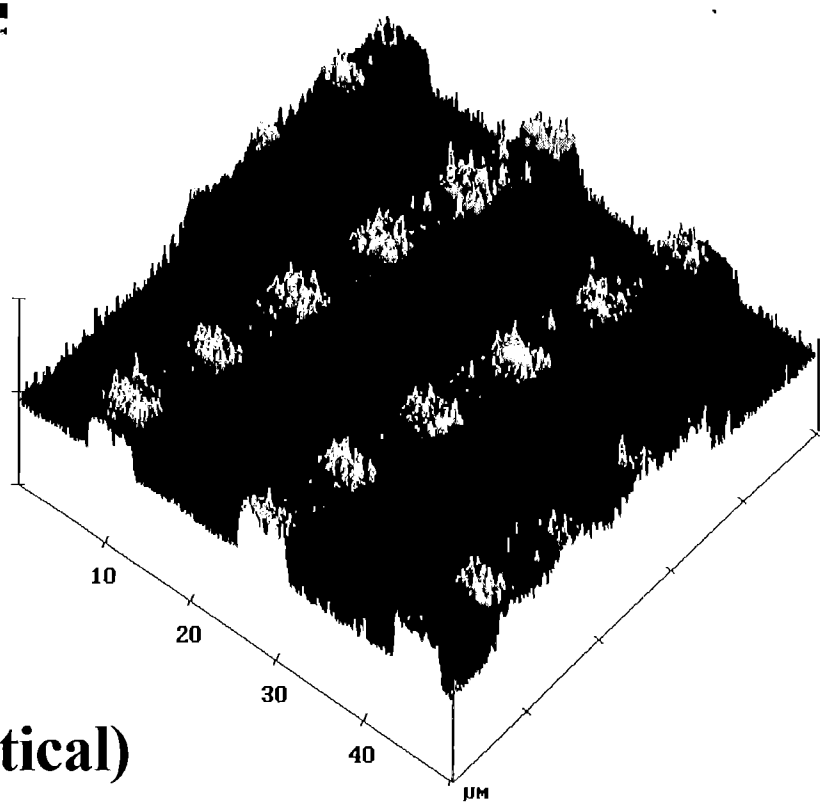

1. Adsorb multilayer system A (vertical)
2. EO-MAL stamp(horizontal)
3.Adsorb multilayer system B

EO-MAL patterning on Polystyrene Substrate (dot stamp)

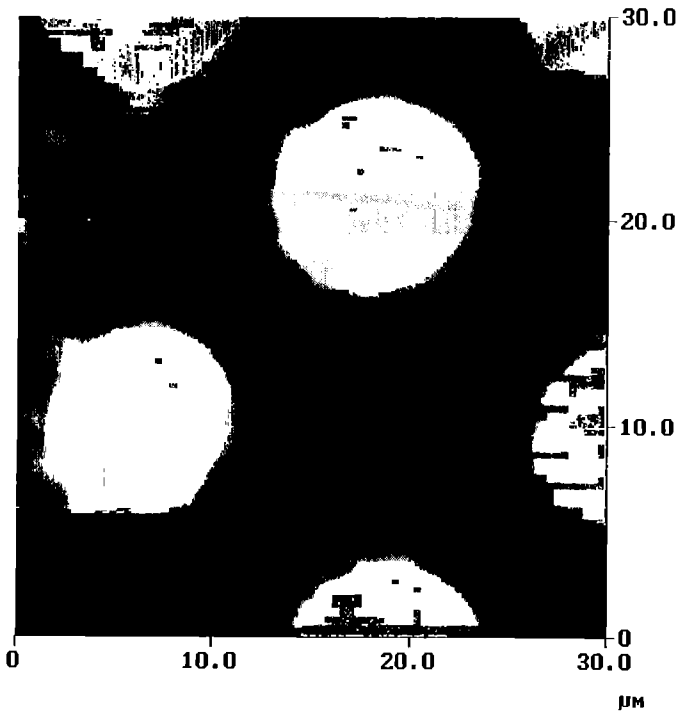

1. (BPEI/PAA)4BPEI at pH5
2. Stamp EO-MAL 1hr (EO-MAL is stamped outside dots)
3. (PAA/LPEI)12 at pH5

Chromogenic Block Copolymer Assemblies

Research Team

- Paula T. Hammond Block Copolymer Synthesis and Characterization
- Shaw Chen Collaborative design of chiral nematic copolymer systems
- Lewis Rothberg Characterization of chromic and spectroscopic prop.
- Sam Jenekhe Synthesis of Chromogenic Dyes for Functionalization

Goals

- New reflective and absorptive displays utilizing Block Copolymer Morphology

Interactions with Army

- Possible interaction with LC/Displays groups

MURI Funding Level: $50 K/yr.

Personnel

- P.T. Hammond
- Aaron Moment

LC Side Chain Block Copolymers

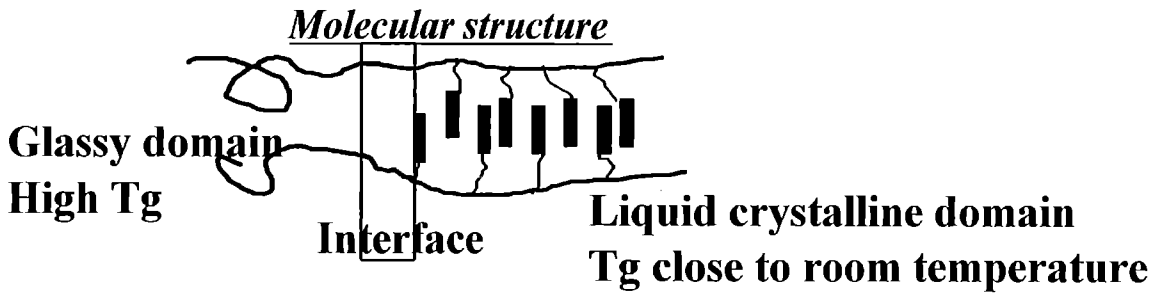

Design:

- **Flexible "soft" block - chromophore attached as side group**
- **Spacer unit - decouples chromophore from main chain**
- **Glassy rigid block - mechanical properties, transparent medium**

Most rigid chromophores would act as LC systems:

- can orient block copolymer continuous morphologies for anisotropic chromic behavior

Advantages of Block Copolymers

- Ability to use thermoplastic processing, obtain uniform films
- Nanoscale morphology presents potential
- Films with high mechanical integrity
- Can utilize a low Tg block to obtain "fluid" matrix

  Increased kinetics for coloration, switching

TOPS Objectives - Mesostructured Polymers: Side Chain LC Block Copolymers

- Attach known LC's/chromophores of interest to polystyrene-vinyl siloxane backbone
  - Cholesteric LC's (reflective)
  - Merocyanine dyes
  - Salicylidenes
  - Substituted azobenzenes
- Examine chromic and spectroscopic behavior in oriented block copolymers as function of structure(**Rothberg**)
- Explore potential for reflective systems via layered photonic arrays or chiral nematics(**Shen**)

Investigating Interplay between LC order and Morphological Order

- Discovered BlockCopolymer Order-Disorder as well as Order-Order transitions can be induced by liquid crystal phase changes.

- Established LC orientation w/in blocks can be controlled by molecular structure.

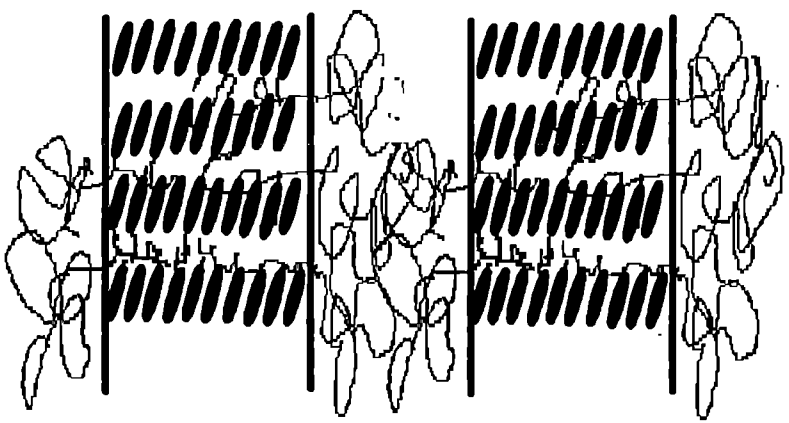

Spacer length = 6

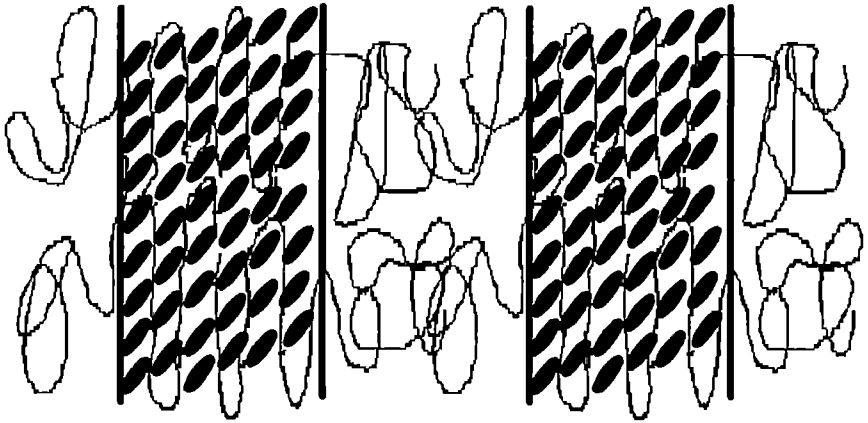

Spacer length = 10

Can use oriented blocks to obtain highly ordered, switchable chromophores

TEM images of Mesogen B polymers

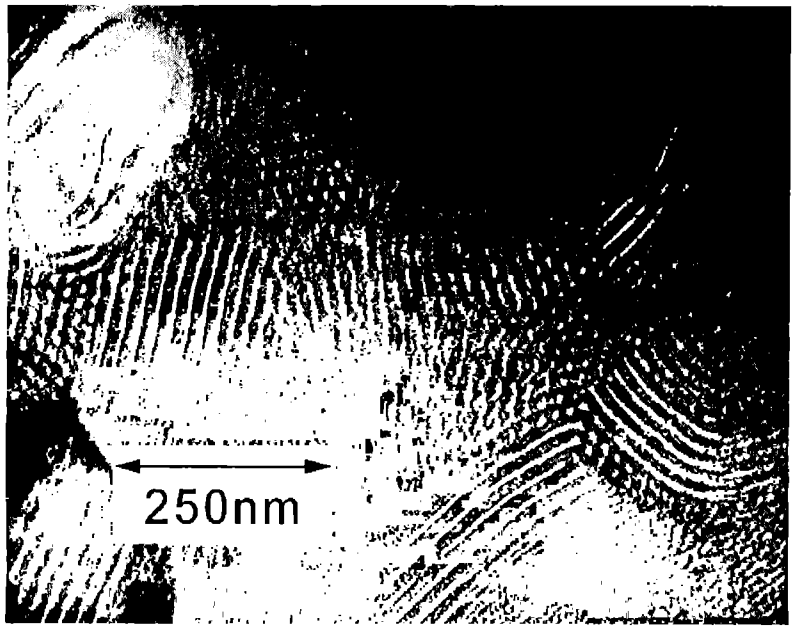

PS 12 - LCPB 8
TEM 155Å, SAXS 186Å

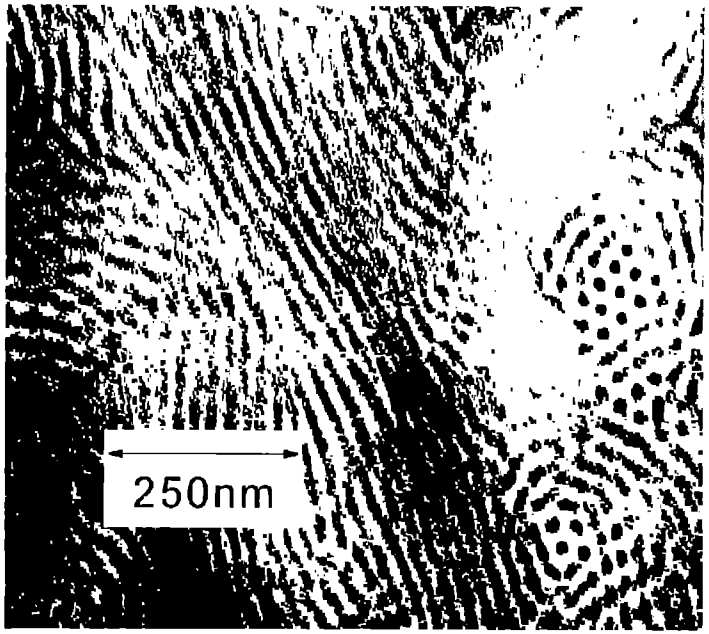

PS 14 - LCPB 94
TEM 257Å, SAXS 294Å

OM images of PS14K-LCP57K (A) elastomeric material on stretching

Mesogen A:

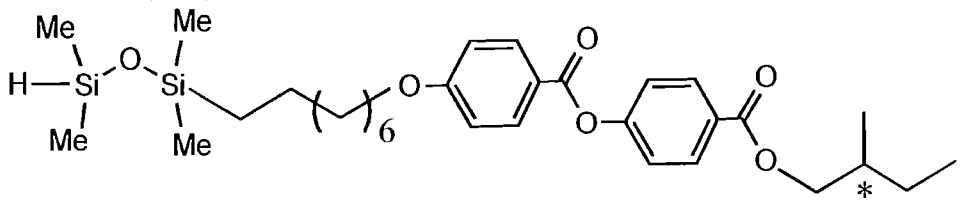

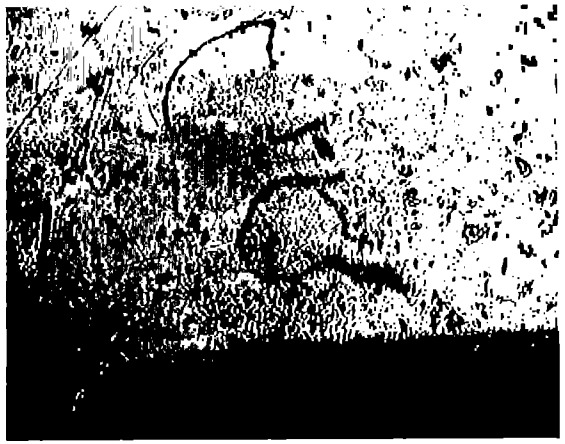

stretch

release

500um

Free standing film, 25 C

~ 8% strain,
1mm stretch

Summary of liquid crystalline transitions and SAXS data for block copolymers

Mesogen A:

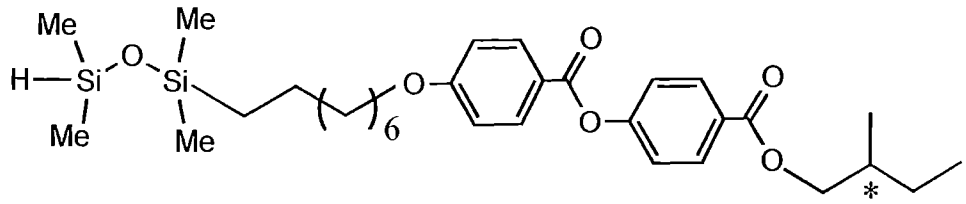

Wt% PS	Mn PS Block	Mn LC Block	S-I C	SAXS Smectic d, Å	SAXS Morphology d, Å
0	- -	34,000	89.6	37	none
43	12,000	16,000	none	none	weak
26	13,000	38,000	66.3	36	PS cylinders
20	14,000	57,057	79.4	36	PS cylinders
66	40,000	21,000	42.6	36	327/lamellar

Summary of liquid crystalline transitions and SAXS data for block copolymers

Mesogen A:

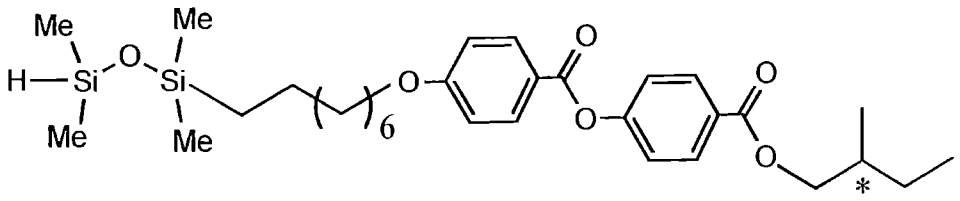

Wt% PS	Mn PS Block	Mn LC Block	S-I C	SAXS Smectic d, Å	SAXS Morphology d, Å
0	- -	34,000	89.6	37	none
43	12,000	16,000	none	none	none
26	13,000	38,000	66.3	36	none
20	14,000	57,057	79.4	36	none
66	40,000	21,000	42.6	36	327/ weak

TOPS MURI Review

August 2000

Natick Meeting

Lewis Rothberg

Overview

- Absolute luminescence quantum yields in films: Development and applications of a new calorimetric technique (Lisa Marshall)
- Origin of luminescence quenching in the solid state: dynamical studies that implicate interchain excitation (Pei Wang)
- Molecular weight dependence of conjugated polymer optical properties (Jui-Hung Hsu)
- Aggregation studies of MEH-PPV trimers (Jui-Hung Hsu)
- Patterned electrostatic self-assembly (with Hammond)
- Devices based on conjugated polymers in vitrified liquid crystal (with Chen)
- Testbeds

Overview

» Absolute luminescence quantum yields in films: Development and applications of a new calorimetric technique (Lisa Marshall)

- Origin of luminescence quenching in the solid state: dynamical studies that implicate interchain excitation (Pei Wang)
- Molecular weight dependence of conjugated polymer optical properties (Jui-Hung Hsu)
- Aggregation studies of MEH-PPV trimers (Jui-Hung Hsu)
- Patterned electrostatic self-assembly (with Hammond)
- Devices based on conjugated polymers in vitrified liquid crystal (with Chen)
- Testbeds

Motivation

- Luminescence efficiency is an important factor in organic light-emitting diodes
  - theory predicts that EL proportional to PL
- Direct measurement of emitted light out per absorbed energy is difficult due to surface roughness, self-absorption and waveguiding
  - no reliable standards available
  - many calibrations required for integrating sphere measurements

Idea: calorimetric measurement

- Measure the heat in and assume that what does not come out as heat must come out as light
  - premises:
    - No photochemistry
    - No "irreversible" charge generation
- KEY TRICK: No standard required. Use internal calibration of the amount of heat based on Kasha's Rule

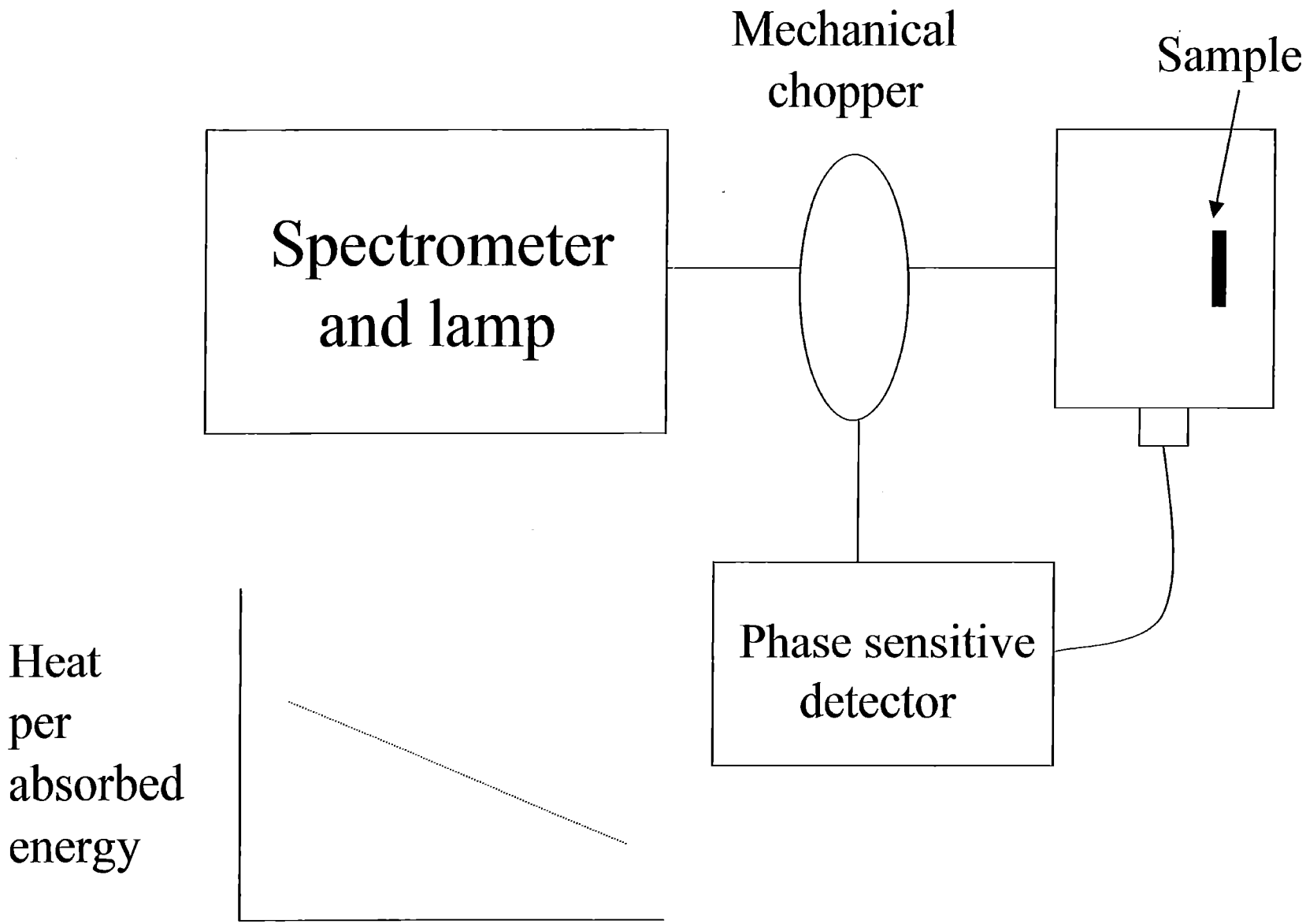
Mechanical
chopper
Sample
Spectrometer
and lamp
Phase sensitive
detector
Heat
per
absorbed
energy
Wavelength

Procedure

Heat will be proportional not only to the fraction of energy going into heat but also to the total energy deposited. This depends on the lamp intensity at the given wavelength and the absorption of the sample at that wavelength. Therefore, the first things we do are:

1) Measure the absorption spectrum of the sample
   (standard UV-vis)
2) Measure the emission spectrum of the lamp and spectrometer
   (by using a black absorber in the heat deposition setup)

These are used to correct the observed signal and turn it into heat yield. Obtaining quantum yield from that is described on the next viewgraph. It also involves knowing the PL spectrum.

Analysis

We assume that luminescence quantum yield is excitation wavelength independent (Kasha's rule)

Energy out as heat = Total energy - Energy out as light

where the latter term is not dependent on excitation wavelength

known

$$\text{Heat per absorbed photon} = hc/\lambda_{exc} - \phi_{PL}(hc/\lambda_{em})$$

measured

Predicted Behavior

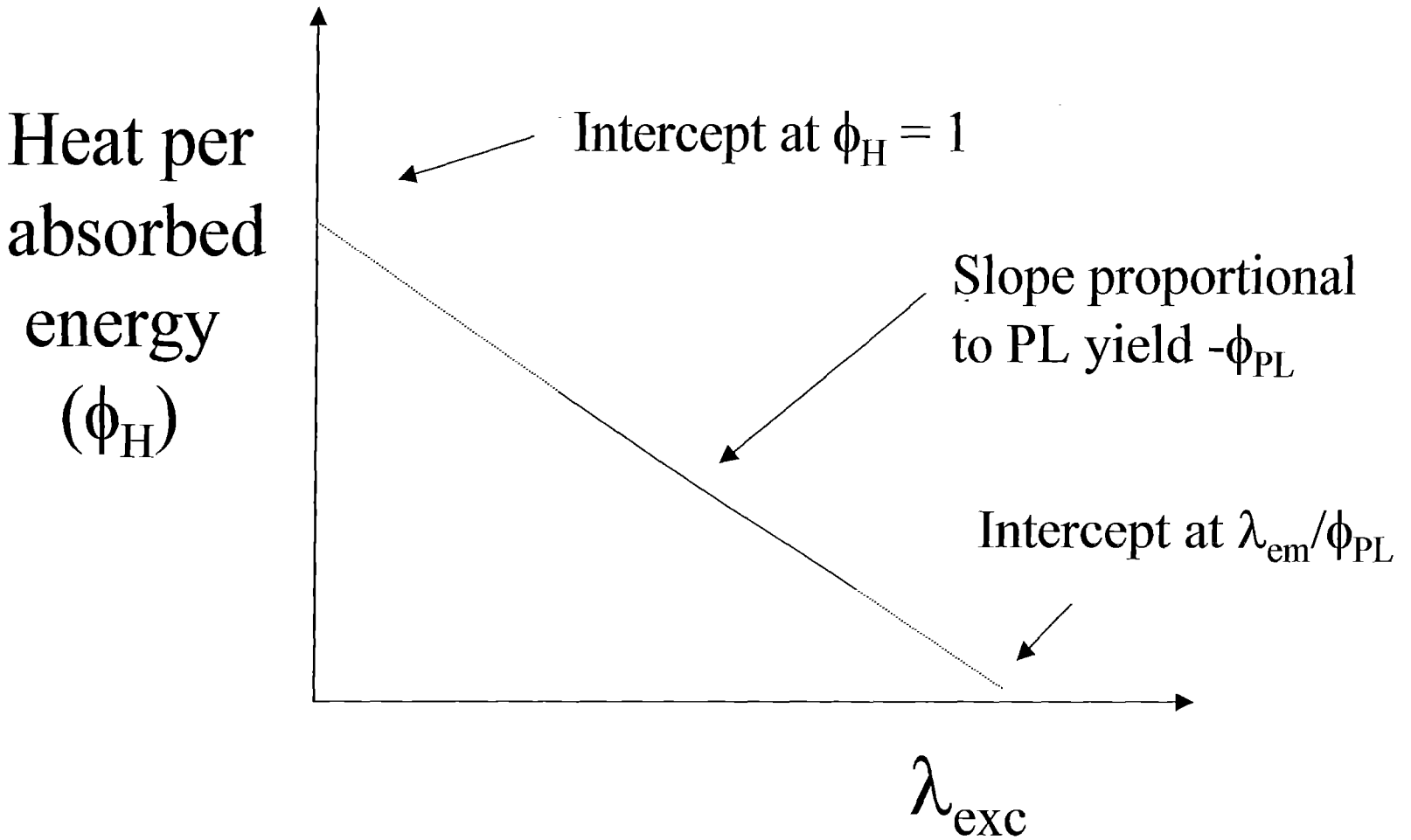

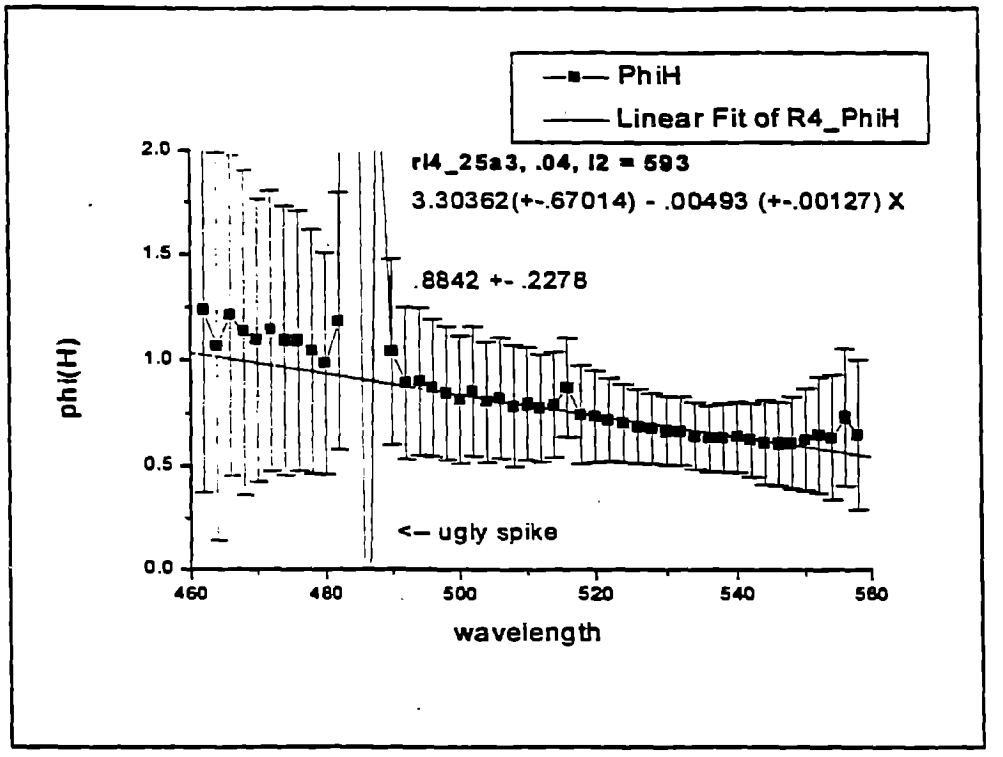
PhiH
Linear Fit of R4_PhiH
rl4_25a3, .04, l2 = 593
3.30362(+-.67014) - .00493 (+-.00127) X
.8842 +- .2278
<-- ugly spike
phi(H)
wavelength
2.0
1.5
1.0
0.5
0.0
460
480
500
520
540
560

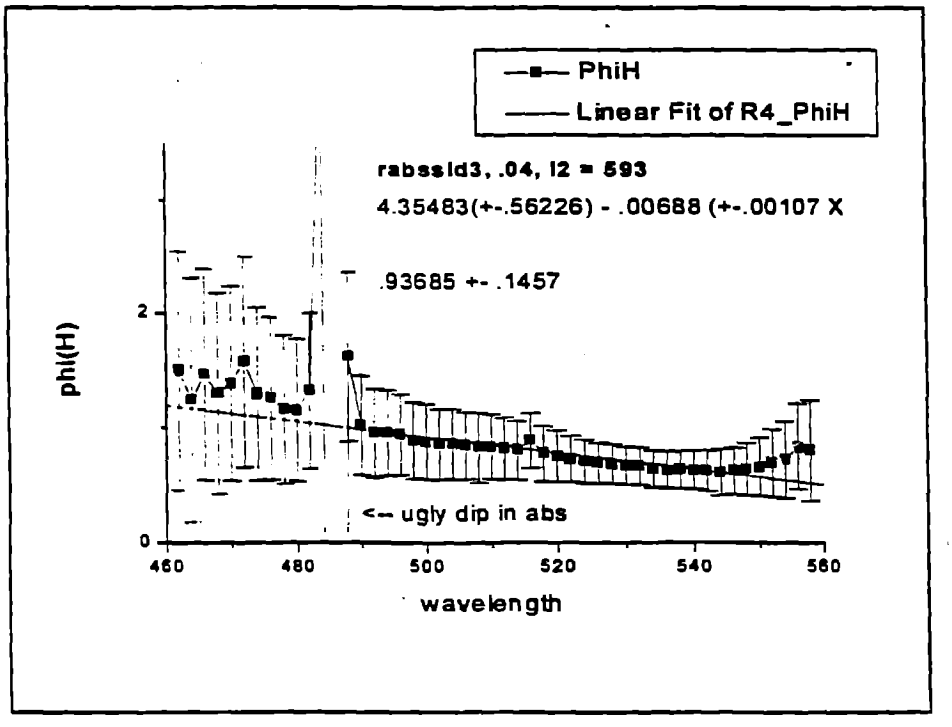
PhiH
Linear Fit of R4_PhiH
rabssld3, .04, l2 = 593
4.35483(+-.56226) - .00688 (+-.00107 X
.93685 +- .1457
<-- ugly dip in abs
phi(H)
wavelength
2
0
460
480
500
520
540
560

$\varphi_H \approx .63$ 19 12 - O M_c

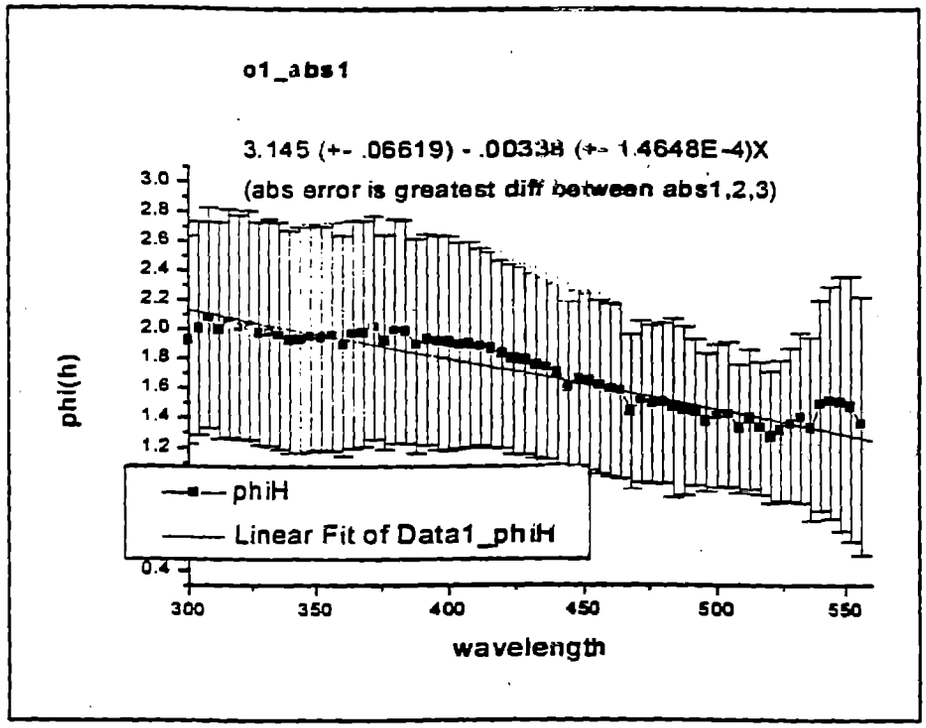

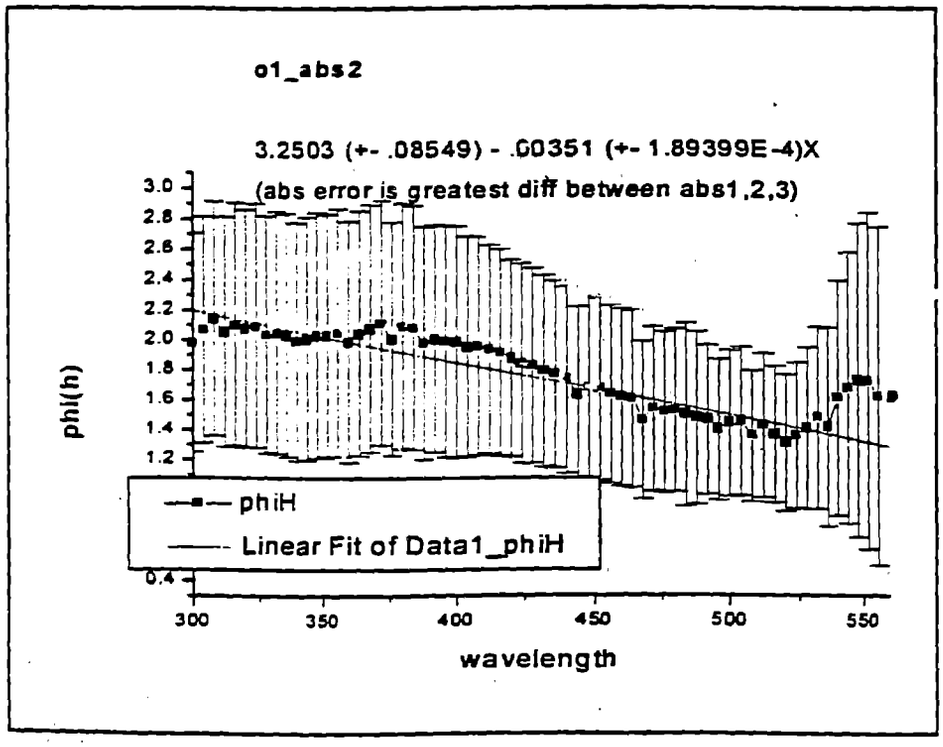

Overview

- Absolute luminescence quantum yields in films: Development and applications of a new calorimetric technique (Lisa Marshall)
- Origin of luminescence quenching in the solid state: dynamical studies that implicate interchain excitation (Pei Wang)
- » Molecular weight dependence of conjugated polymer optical properties (Jui-Hung Hsu)
- Aggregation studies of MEH-PPV trimers (Jui-Hung Hsu)
- Patterned electrostatic self-assembly (with Hammond)
- Devices based on conjugated polymers in vitrified liquid crystal (with Chen)
- Testbeds

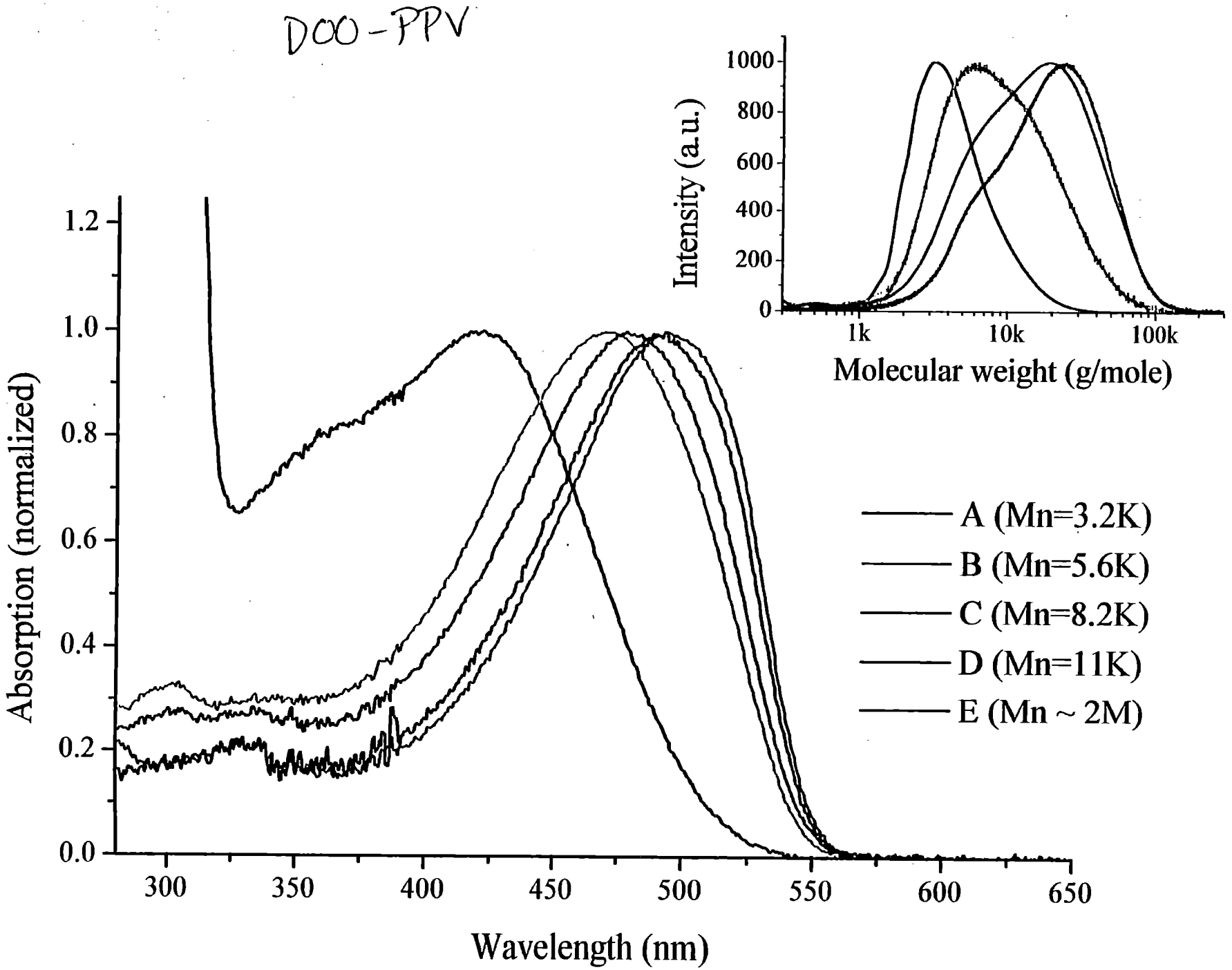
DOO-PPV
Intensity (a.u.)
1000
800
600
400
200
0
1k
10k
100k
Molecular weight (g/mole)
Absorption (normalized)
1.2
1.0
0.8
0.6
0.4
0.2
0.0
300
350
400
450
500
550
600
650
Wavelength (nm)
A (Mn=3.2K)
B (Mn=5.6K)
C (Mn=8.2K)
D (Mn=11K)
E (Mn ~ 2M)

77

Fig 1

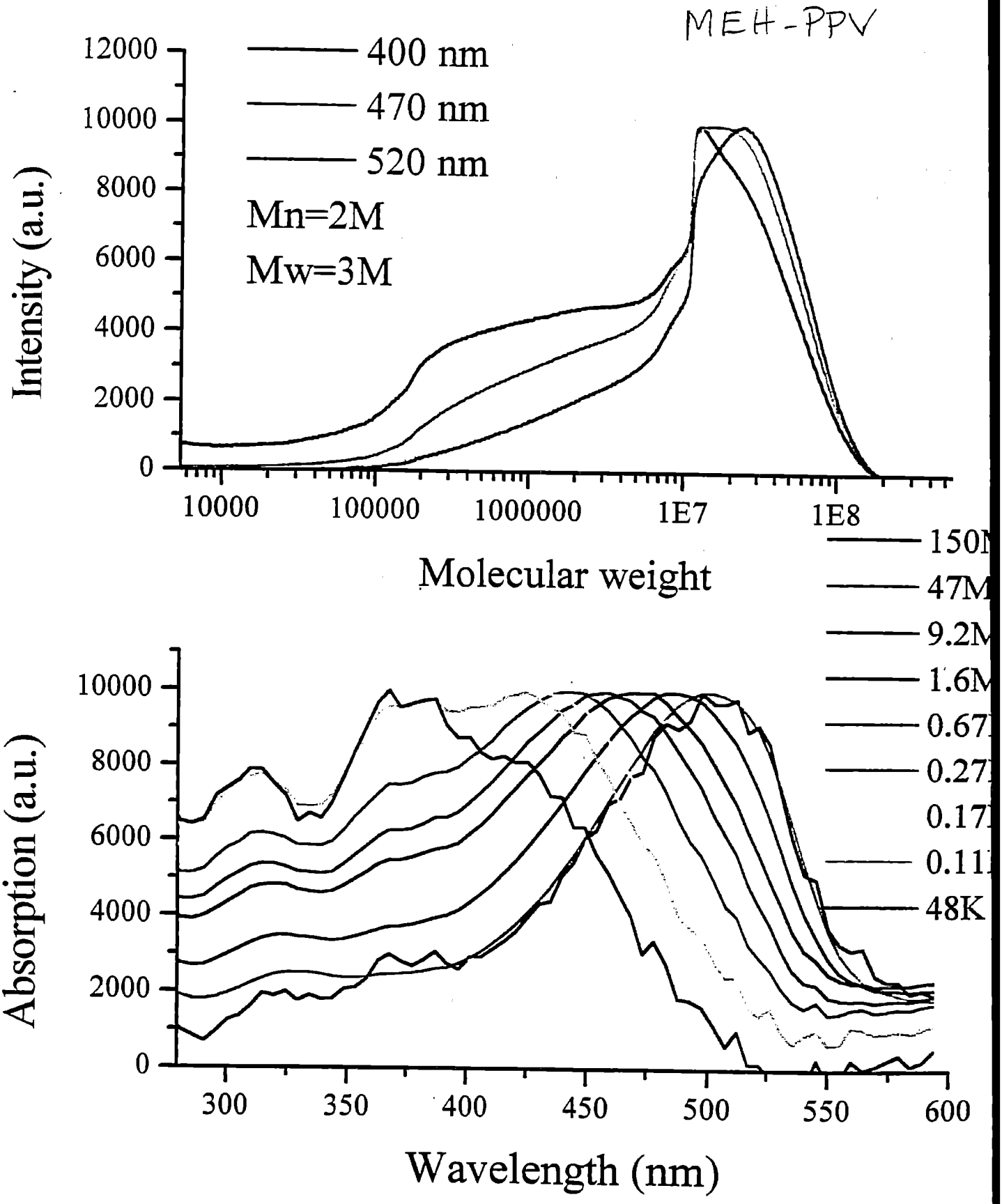
MEH-PPV
400 nm
470 nm
520 nm
Mn=2M
Mw=3M
Intensity (a.u.)
12000
10000
8000
6000
4000
2000
0
10000
100000
1000000
1E7
1E8
Molecular weight
150
47M
9.2M
1.6M
0.67
0.27
0.17
0.11
48K
Absorption (a.u.)
10000
8000
6000
4000
2000
0
300
350
400
450
500
550
600
Wavelength (nm)

Overview

- Absolute luminescence quantum yields in films: Development and applications of a new calorimetric technique (Lisa Marshall)
- Origin of luminescence quenching in the solid state: dynamical studies that implicate interchain excitation (Pei Wang)
- Molecular weight dependence of conjugated polymer optical properties (Jui-Hung Hsu)

» Aggregation studies of MEH-PPV trimers (Jui-Hung Hsu)

- Patterned electrostatic self-assembly (with Hammond)
- Devices based on conjugated polymers in vitrified liquid crystal (with Chen)
- Testbeds

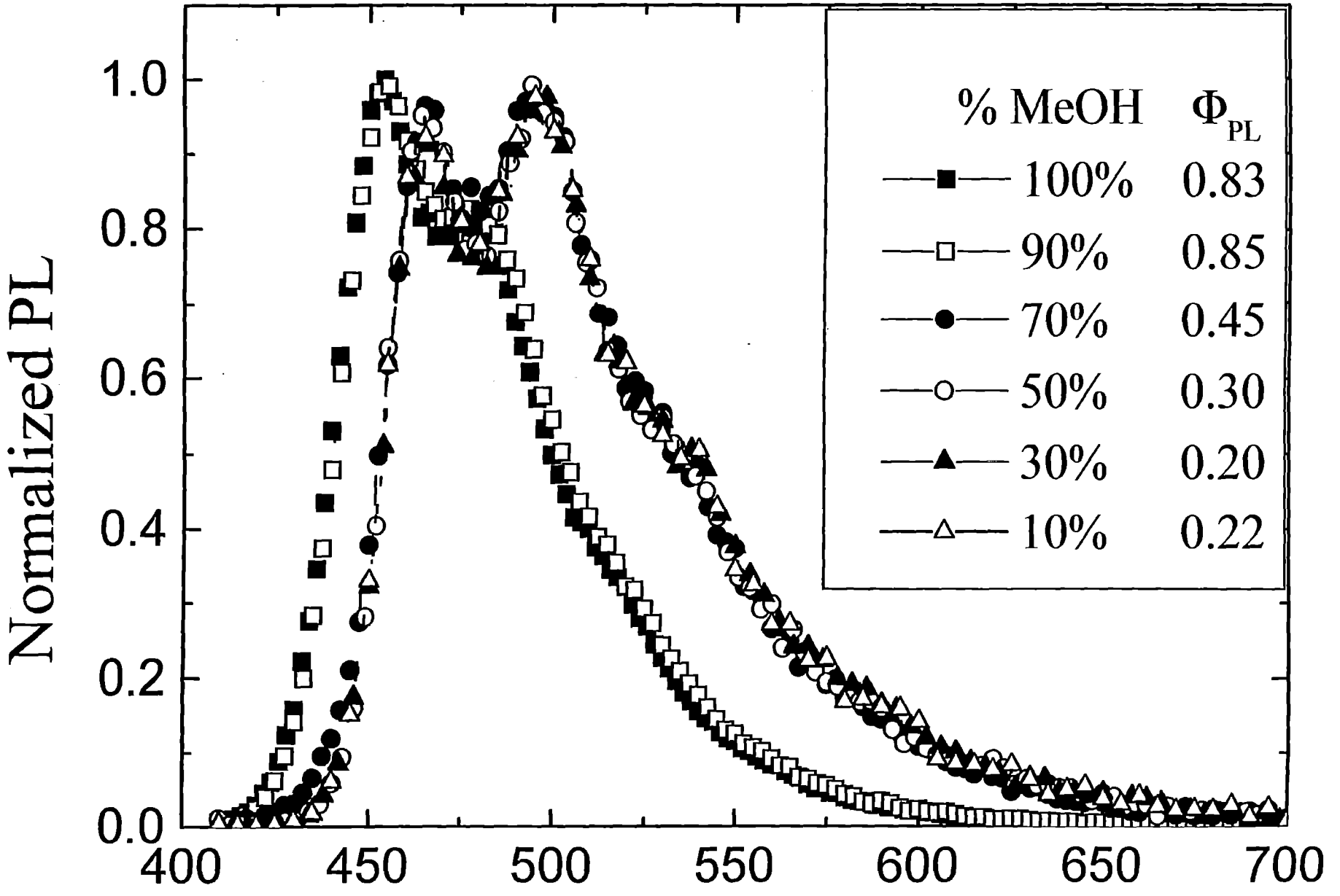
Normalized PL
1.0
0.8
0.6
0.4
0.2
0.0
400
450
500
550
600
650
700
% MeOH
Φ_{PL}
100% 0.83
90% 0.85
70% 0.45
50% 0.30
30% 0.20
10% 0.22

Solvent Effect Studies in the ^{1}H-NMR Spectroscopy

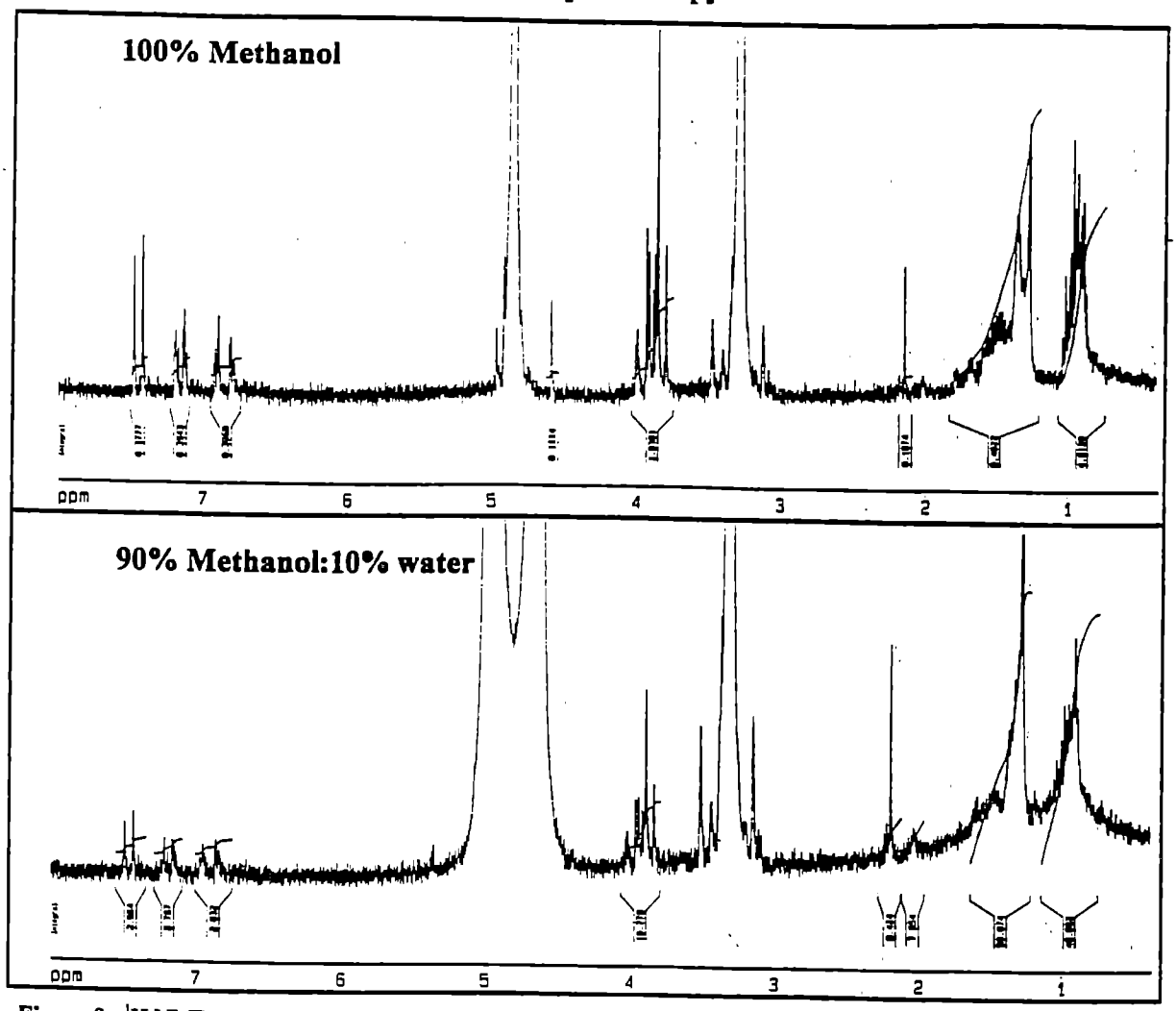

Figure 9: ^{1}H-NMR spectra of the Trimer of MEH-PPV in 100% methanol and 90% methanol-10%water.

Table 2: ^{1}H-NMR assignment of the Trimer of MEH-PPV and its intensity in both mixtures.

Chemical shift (ppm)	Assignments	Integral(100%MeOH)	Integral(90%MeOH)
6.7-7.5	ring, vinylene ^{1}H	0.15	0.075
3.6-4.0	O-C-H ^{1}H	0.18	0.09
2.3-0.8	ethylhexoxy ^{1}H	1	1

Status

- **Luminescence yield**
  - ready for ARO MURI use
  - publish and apply to conjugated polymer processing methods
  - AC thin-film EL materials with Dave Morton
- **Aggregation quenching**
  - preparing manuscripts for MEH-PPV and trimer
  - study trimer dynamics
- **Molecular weight dependence of optical properties**
  - working to understand the issues
- **Patterned electrostatic self-assembly**
  - dipping instrument working, Swager materials available soon
  - ellipsometer purchased
  - sending student to Hammond lab to learn printing and assembly
- **Testbeds**
  - I-V setup, PL yield complete
  - TSC with ARL (Forsythe and Morton) for charge mobility

TUNABLE EMISSION SYSTEMS

Research Team

- Al Bard - Electrochemiluminescent Systems
- Paula Hammond - 3-D Array Patterning by Self-Assembly
- Sam Jenekhe - Tunable Electroluminescent Polymers and Devices
- Lewis Rothberg - Microcavity Design for Emissive Displays

Relationship to DoD

Addressable Color Tunable Devices; Large Area Displays; Nanofunctional Devices; Smart/Interactive Clothing; Low Cost Rugged Flexible Displays.

Interactions with Army

- Many Planned

MURI Funding Level: $270 K/yr.

Personnel

- Graduate Students: 1
- Postdocs: 2.5
- Undergraduate Students: 1

yi5099s3rep

TUNABLE MULTICOLOR EL POLYMERS AND DEVICES

CONCEPT

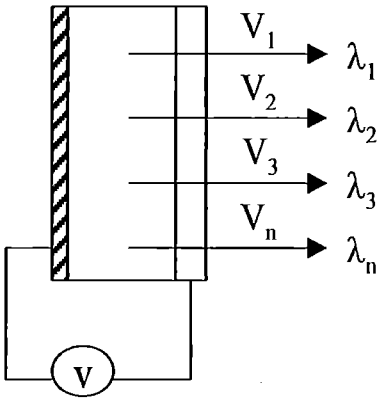

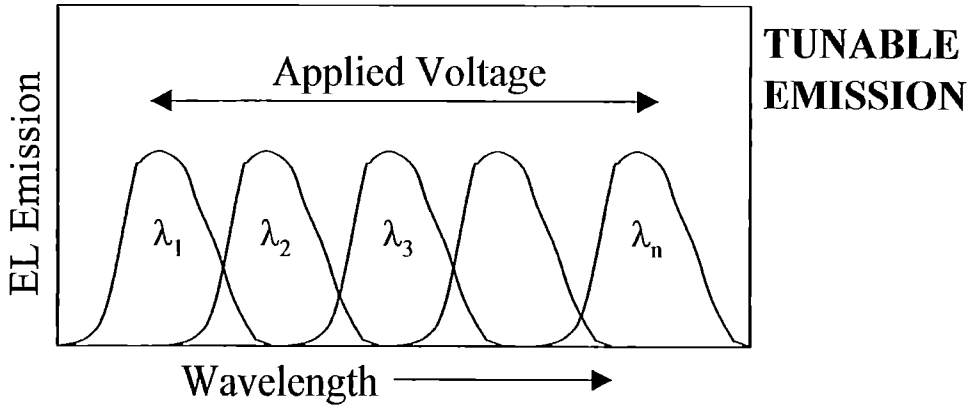

TUNABLE EMISSION

POSSIBLE APPROACHES

A. Bilayer/Multilayer EL polymers

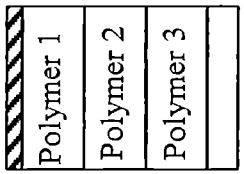

B. Phase-Separated EL Polymer Blends

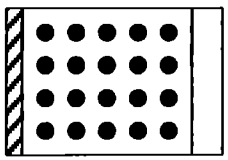

C. Microphase-Separated Block Copolymers

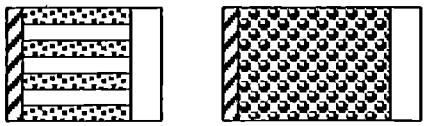

CHALLENGES

- Design of Multicomponent EL Polymers
  - — Availability of R, G, B EL Polymers
  - — Energy Transfer
  - — Exciplex Formation
  - — Photoinduced Electron Transfer
- Processing and Control of Nanophase Multicomponent EL Polymer Systems
  - — Insolubility in Common Solvents
  - — Solubility in Common Solvents
  - — Control of Scale of Phase Separation
- Synthesis of Emissive n-Type Polymers
  - — Red, Blue, Green EL

VOLTAGE-TUNABLE MULTICOLOR POLYMER LEDs

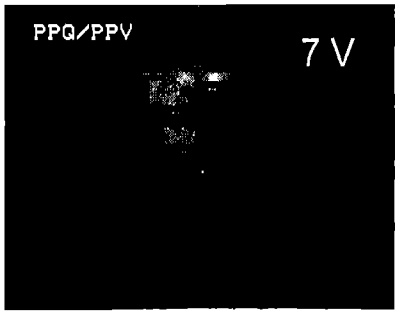

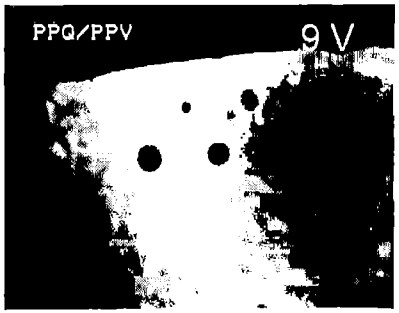

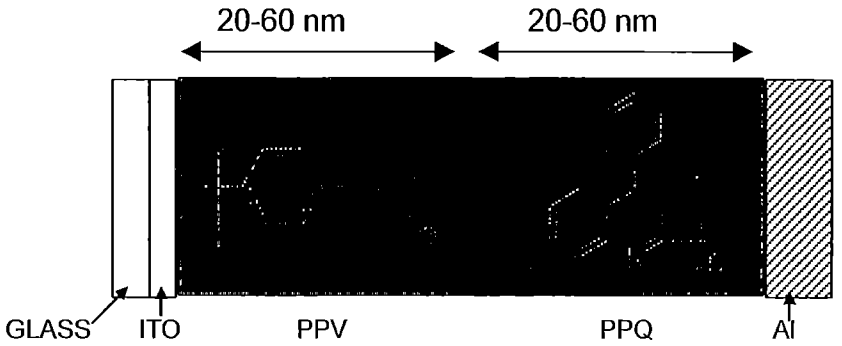

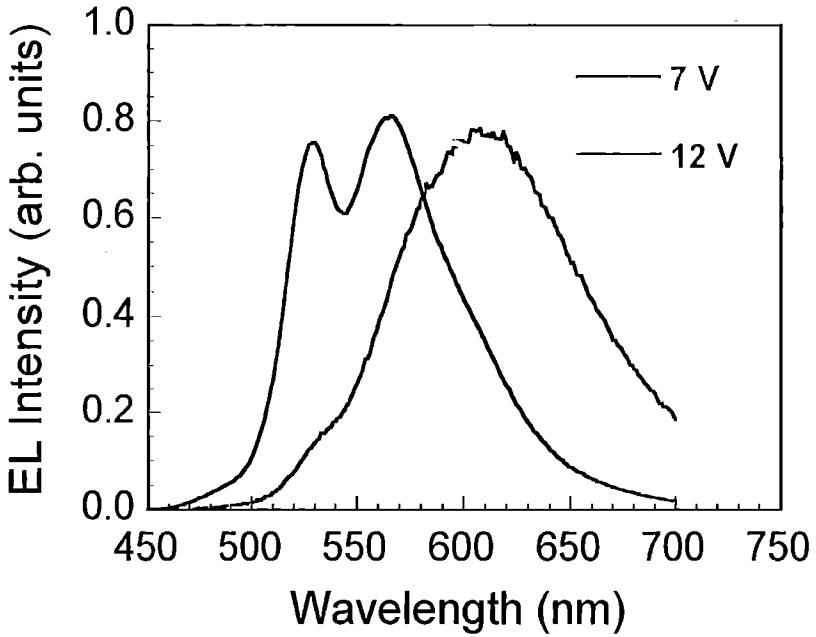

Jenekhe et al., *Chem. Mater.* **1997**, *9*, 409.
Zhang & Jenekhe, *Macromolecules* **2000**, *33*, 2069.

kms0811s1

New n-Type Light-emitting Polymers

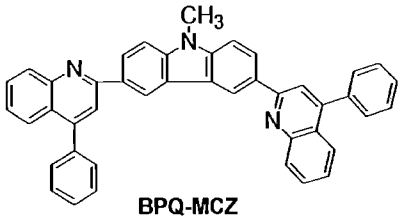

BPQ-MCZ

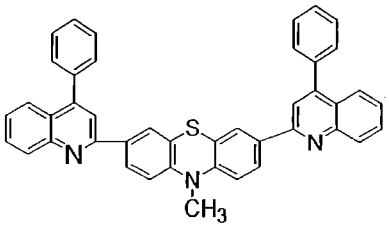

BPQ-PTZ

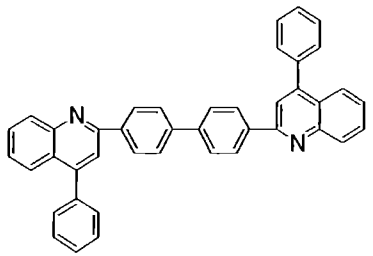

BPQ-P

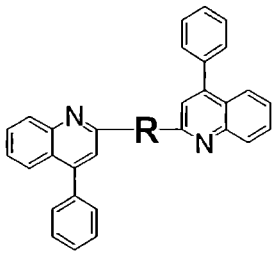

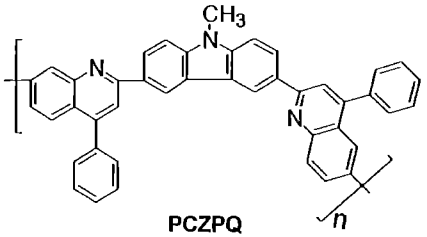

PCZPQ

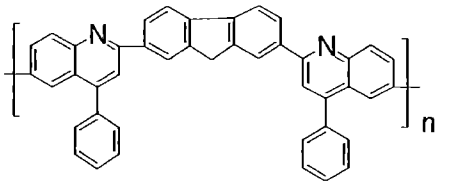

PFPQ

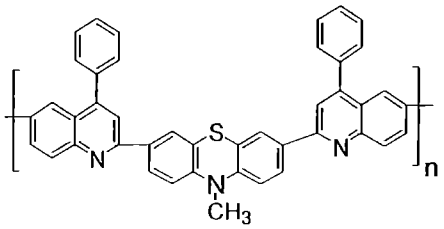

PPTZPQ

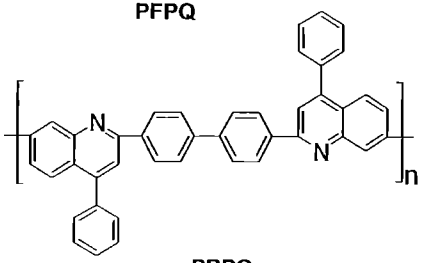

PBPQ

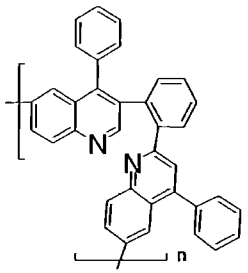

1,2-PPPQ

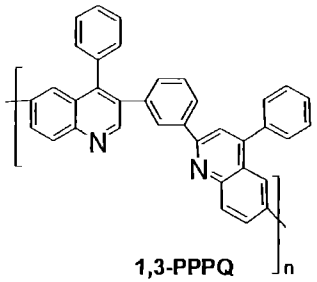

1,3-PPPQ

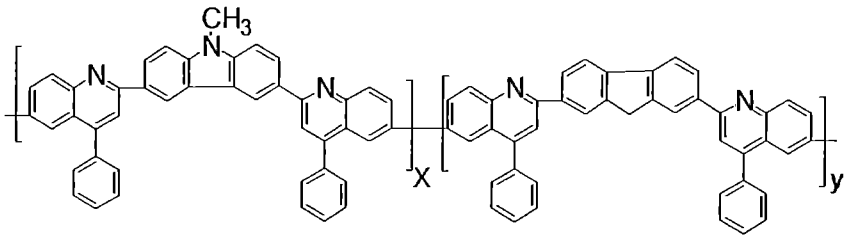

PCZPQ-co-PFPQ

ARO TOPS MURI

S A IENEKHE

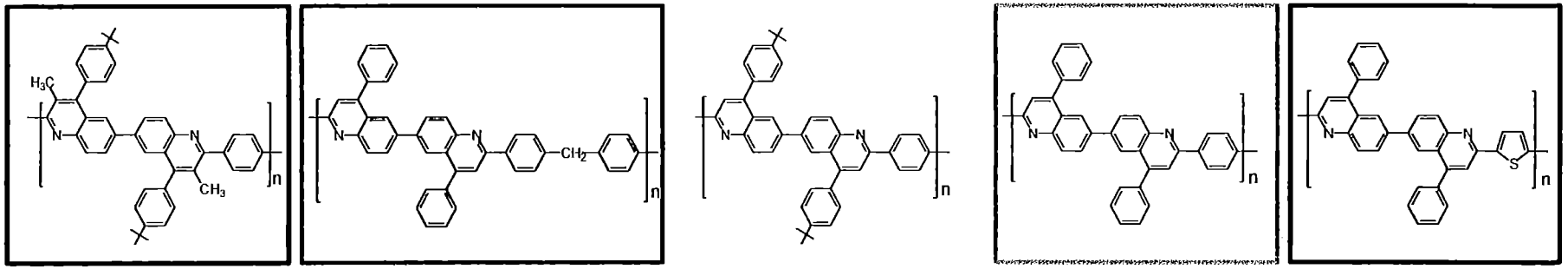

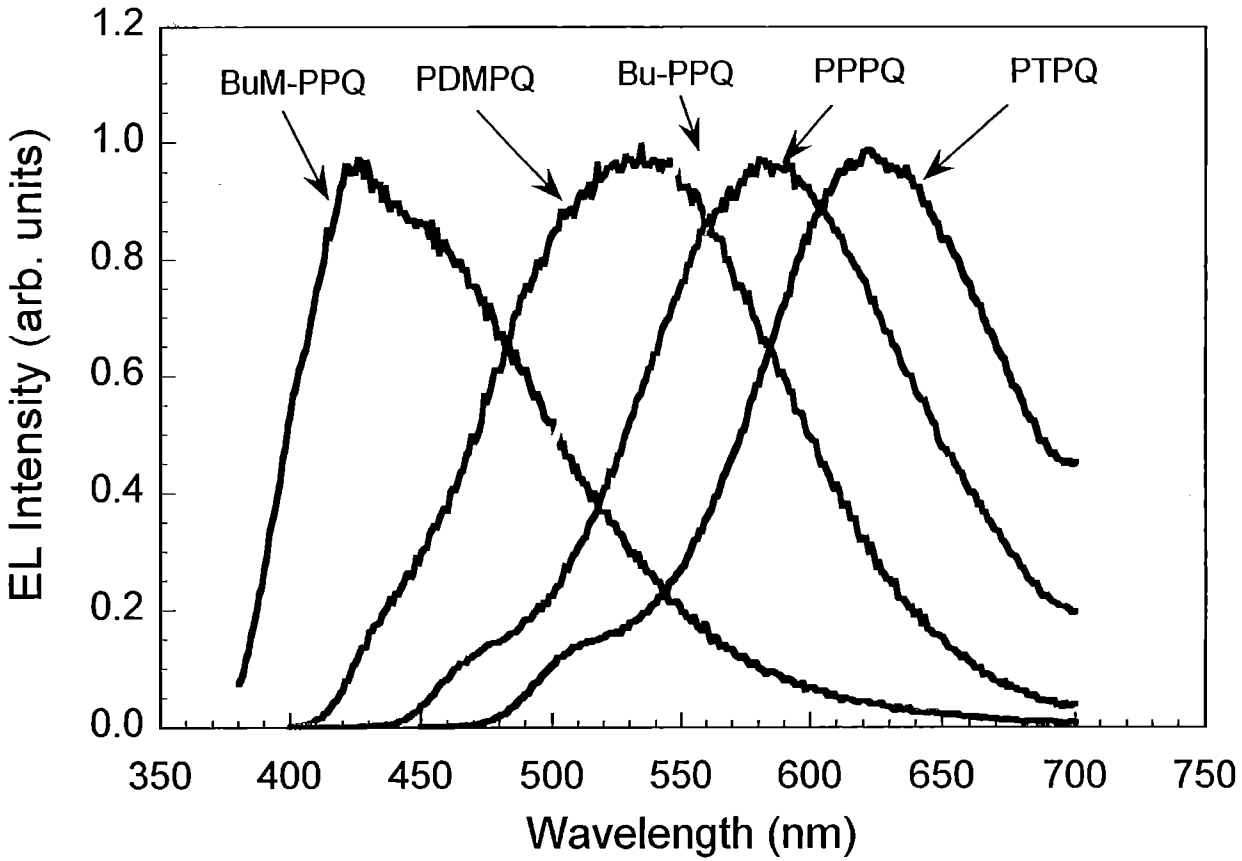

Al
Polyquinoline
TAPC/PS
ITO

POLYMER/POLYMER INTERFACES IN DEVICES

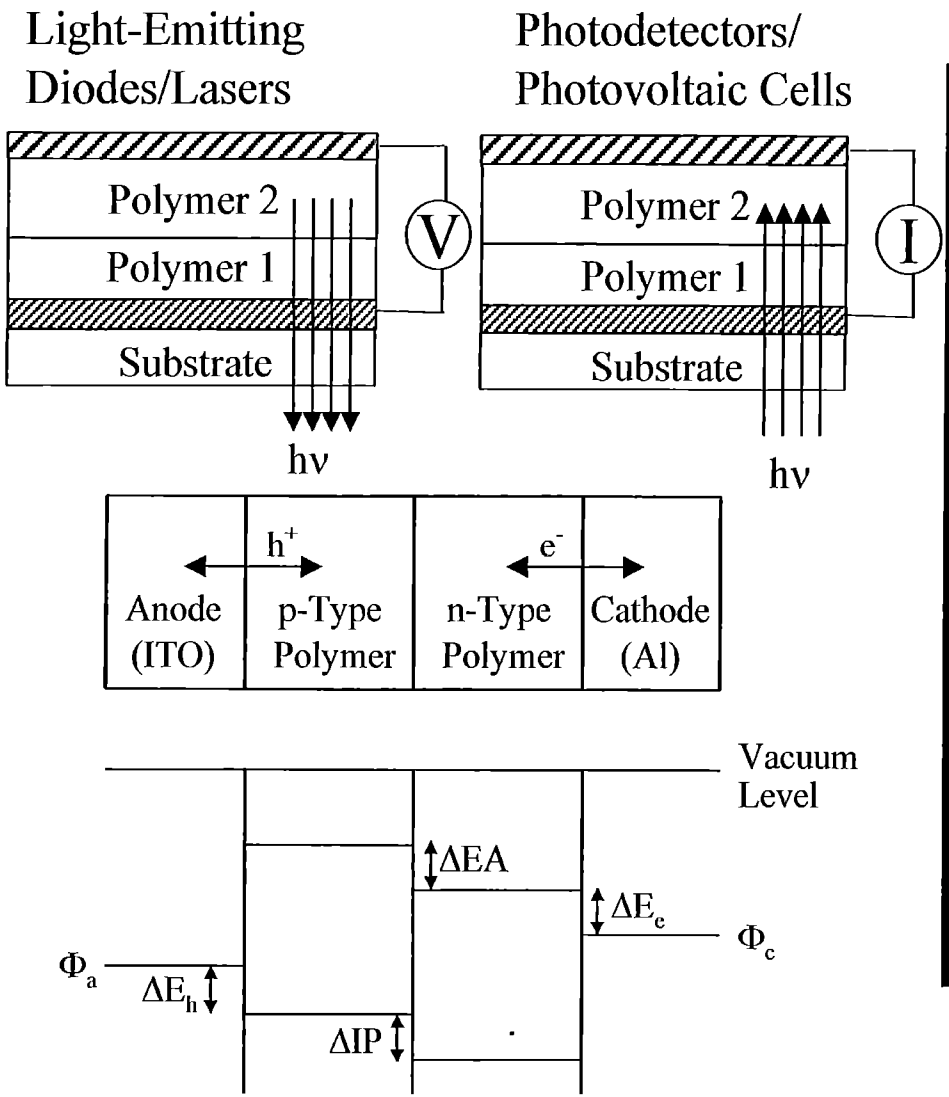

- Role of Polymer/Polymer Interface
  - –(ΔIP, ΔEA)
  - –Charge Depletion (Space Charge) Region?
  - –Built-In Potential (Field)
  - –Energy Transfer
  - –Exciplex Formation
  - –Photoinduced Charge Transfer
    - IP = Ionization Potential (eV)
    - EA = Electron Affinity (eV)
- Finite Size Effects
- Electrode/Polymer Interfaces
  - –Charge Injection Barriers (EA, IP Values)

kms0807s1

Polymer/Polymer Heterojunction LEDs

p-Type (Hole Transport)

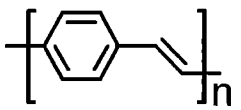

1

n-Type (Electron Transport)

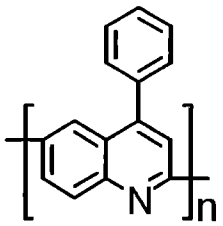

2

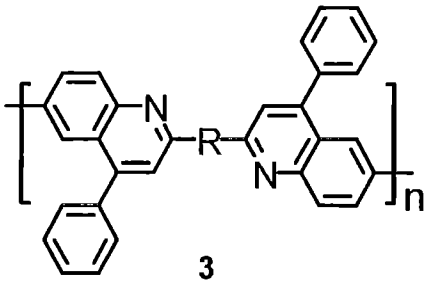

3

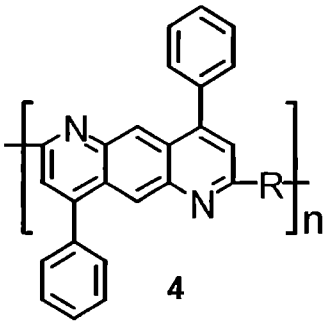

4

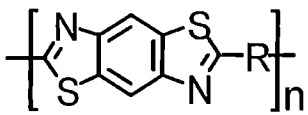

5

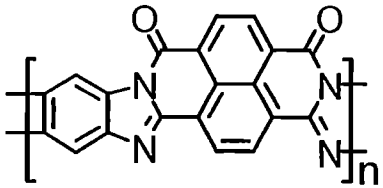

6

R

a 

b 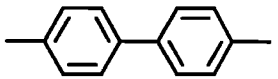

c 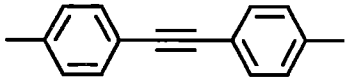

d 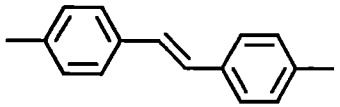

e 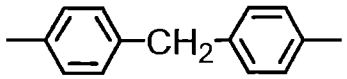

f 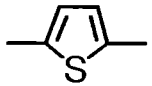

g 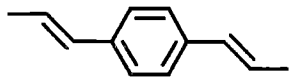

h 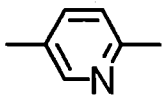

1. PPV
2. PPQ
3a. PPPQ
3b. PBPQ
3c. PBAPQ
3d. PSPQ
3e. PDMPQ
3f. PTPQ

4a. PPDA
4b. PBDA
4c. PBADA
4d. PSDA
4e. PDMDA
4f. PTDA
5g. PBTPV
5h. PPyBT
6. BBL

YI081899S3

POLYMER/POLYMER INTERFACES IN HETEROJUNCTION LEDS

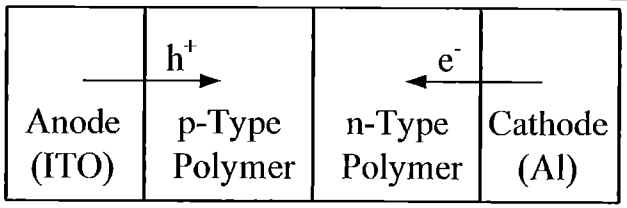

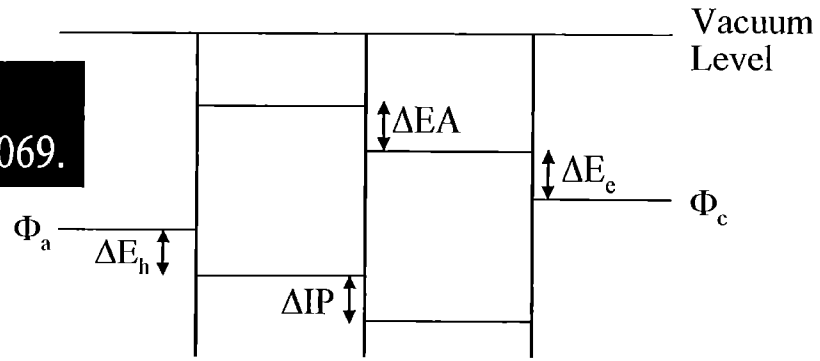

Zhang and Jenekhe,
Macromolecules **2000**, *33*, 2069.

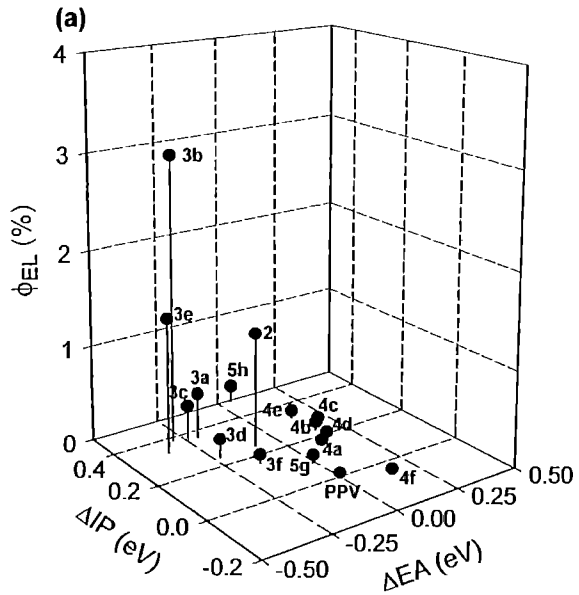

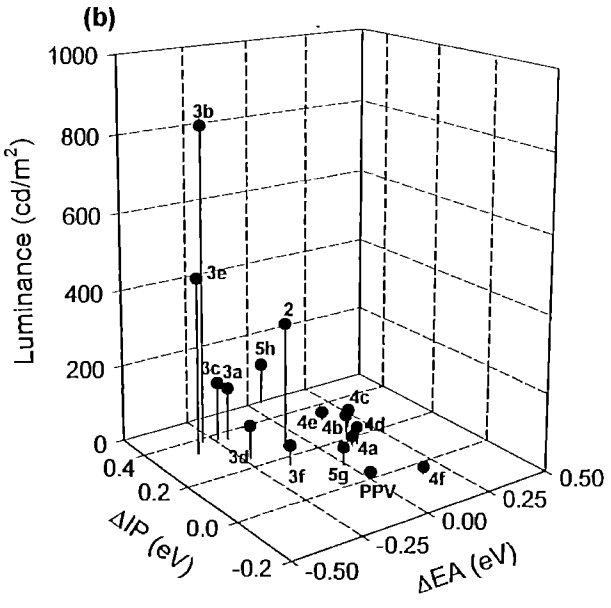

Efficient LEDs From Polymer/Polymer Heterojuctions

POLYMER/POLYMER INTERFACES IN DEVICES

- Can Be More Important than Injection Barriers at Electrodes
- ΔEA and ΔIP Control EL Efficiency and Luminance
- Charge Transfer at Interface Coupled to Finite Size Effects
- Single–Color versus Multicolor LEDs
- Insights for Design and Synthesis of Next Generation EL Polymers (ϕ_{PL}, ΔEA, ΔIP)

VOLTAGE TUNABLE MULTICOLOR LEDs

- Simple Polymer Heterojunction Diodes
- Continuous Tunability in CIE Color Space
- Easy Pixelation for Full Color Displays
- Efficient (1-3%) and Bright (820 cd/m^2) Devices
- Mechanism: Mixing of p-Type and n-Type EL Spectra
- Polyquinolines — Excellent n-Type EL Polymers

PROBING POLYMER/POLYMER INTERFACES

Investigate the Photophysical and Charge transfer Processes of Novel Donor/Acceptor Heterojunctions of π-conjugated Polymers

- **Photophysical and Charge Transfer Processes at Polymer/Polymer Interfaces play a Critical Role in the Efficiency and Performance of LEDs.**
- **Charge Transfer and Separation at Polymer/Polymer Interfaces are Key to Efficient Photovoltaic Devices.**

Probe of Polymer/Polymer Interfaces using both Steady-State Photoluminescence (PL) Spectroscopy and Picosecond Time-Resolved PL Decay Dynamics:

- **Photoinduced Electron Transfer**
- **Exciplex Formation**
- **Energy Transfer**

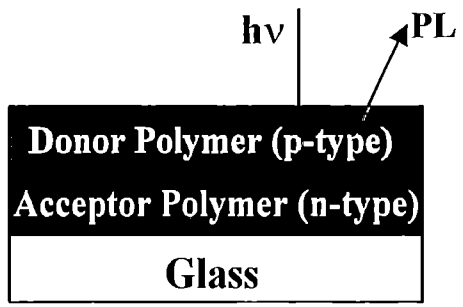

1) Front Face Geometry

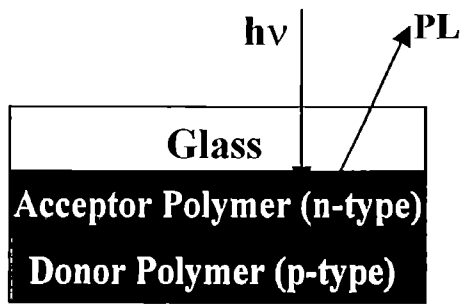

2) Inverted Face Geometry

Electroluminescent Conjugated Polymers

Acceptor Polymers

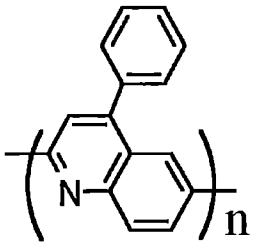

PPQ: poly(2,6-(4-phenylquinoline)

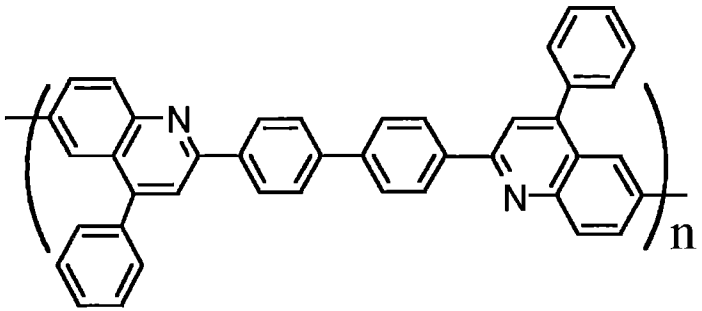

PBPQ: poly(2,2'-(*p,p'*-biphenylene)-6,6'-bis(4-phenylquinoline))

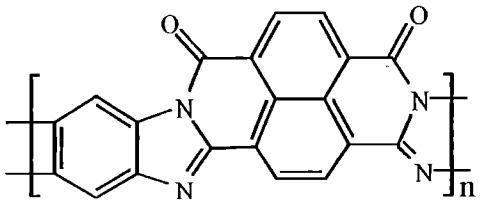

BBL: poly(benzimidazobenzo phenanthroline ladder)

Donor Polymers

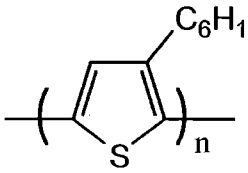

PHT: poly(3-hexylthiophene)

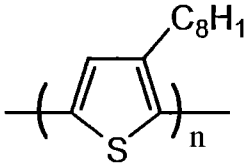

POT: poly(3-octylthiophene)

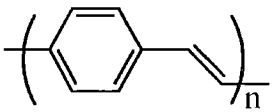

PPV: poly(p-phenylene vinylene)

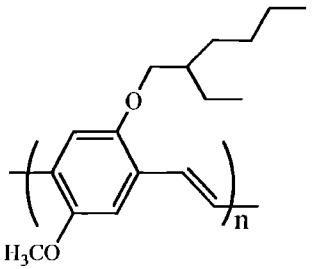

MEH-PPV: poly(2-methoxy-5-(2'ethylhexyloxy) -1,4-phenylene vinylene)

Photoinduced Charge Transfer in Polyquinoline/Polythiophene Heterojunctions

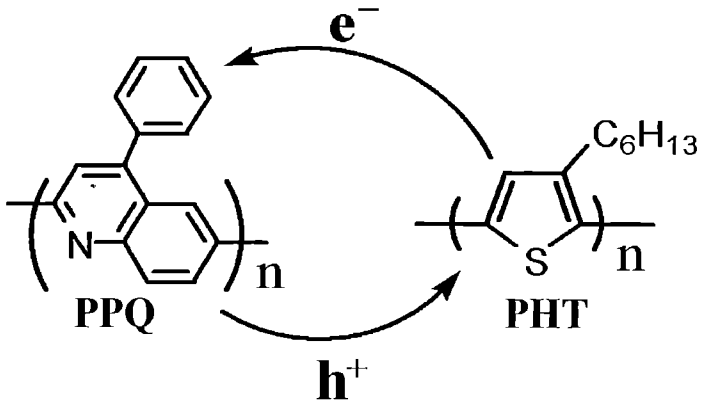

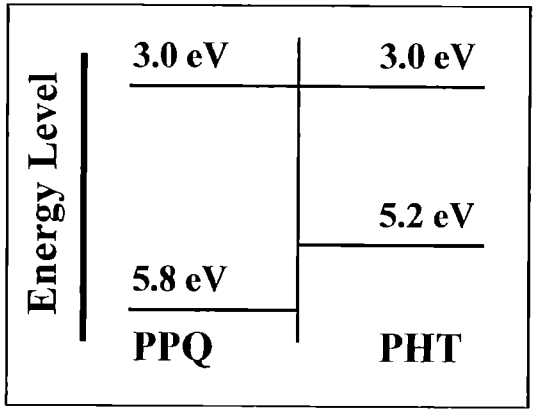

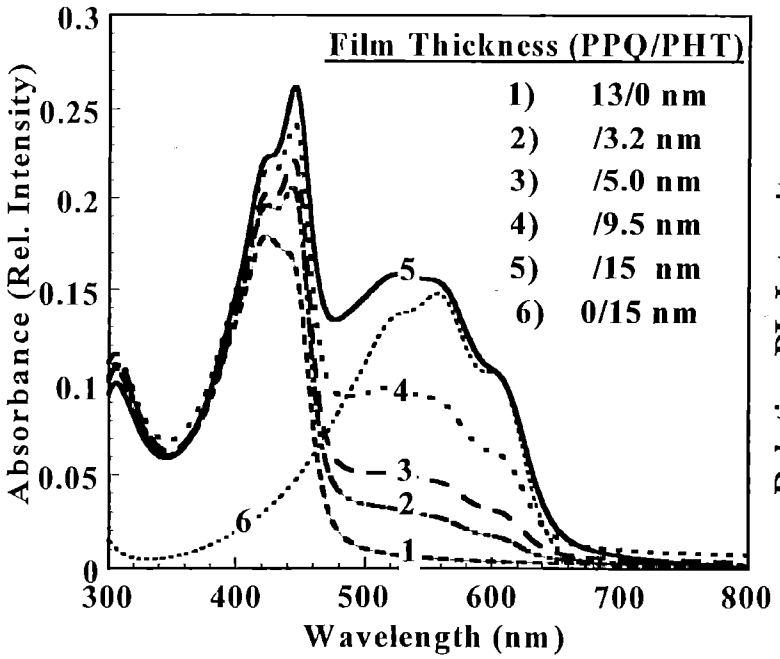

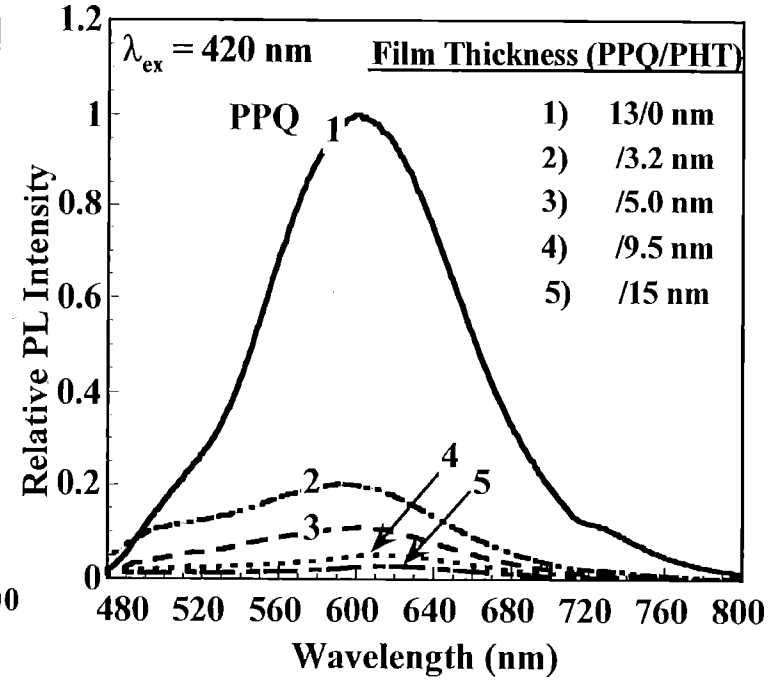

PL Quenching in Polyquinoline/Polythiophene Heterojunctions

— *Effect of Film Thickness*

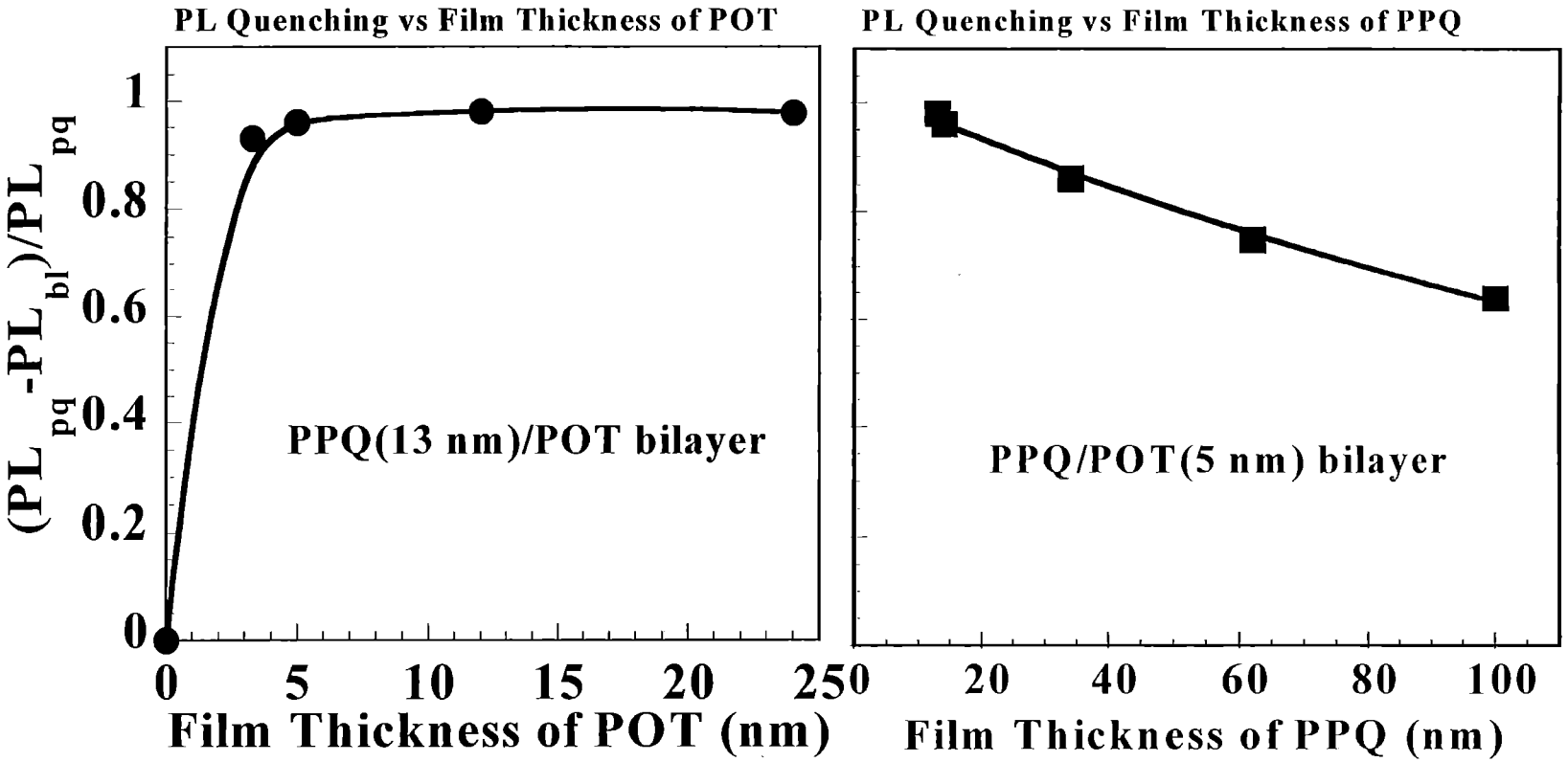

- Exciton Diffusion Length estimated to be 15 - 20 nm for Polyquinolines

ARO TOPS MURI S. A. JENEKHE

Photoinduced Charge Transfer in Polyquinoline/Polythiophene Heterojunctions

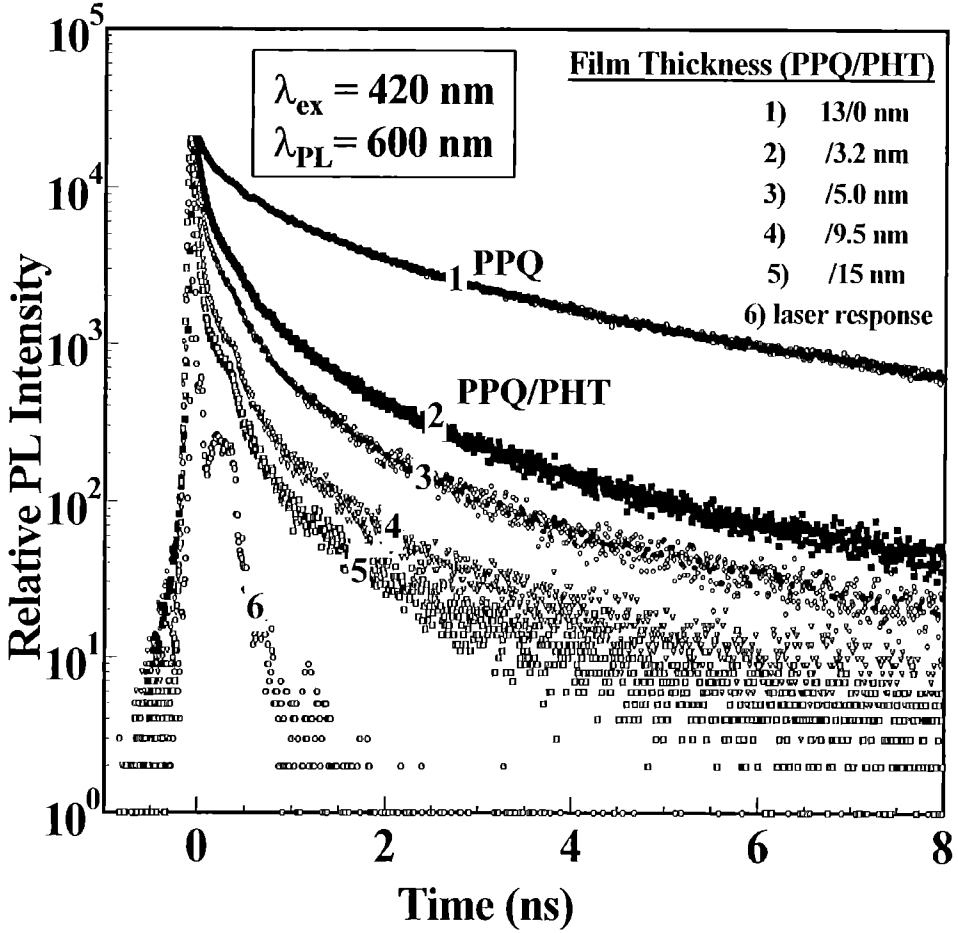

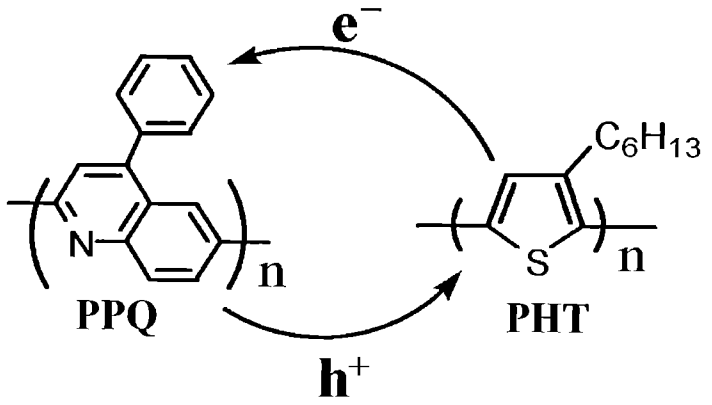

- PPQ Thin Film
  PL Lifetime , τ = 4.4 ns
- PPQ/PHT(13/15 nm) bilayer
  PL lifetime , τ = 29 ps.
- A factor of 150 reduction in PL lifetime.

Photoinduced Charge Transfer at PPV/BBL Heterojunctions

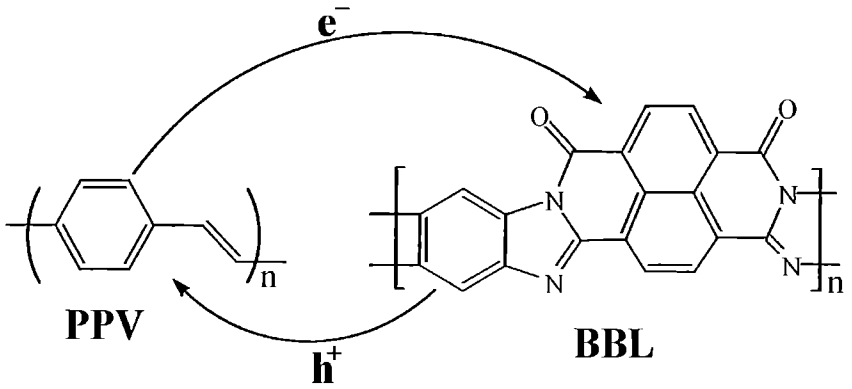

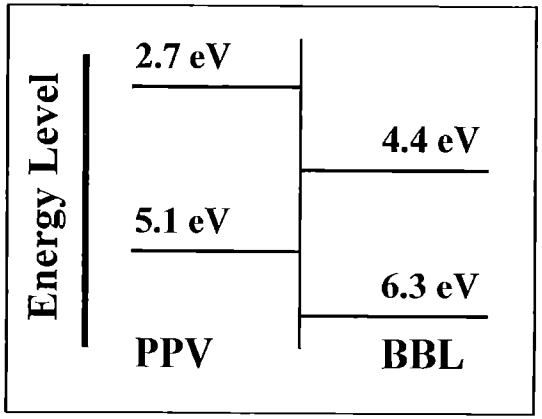

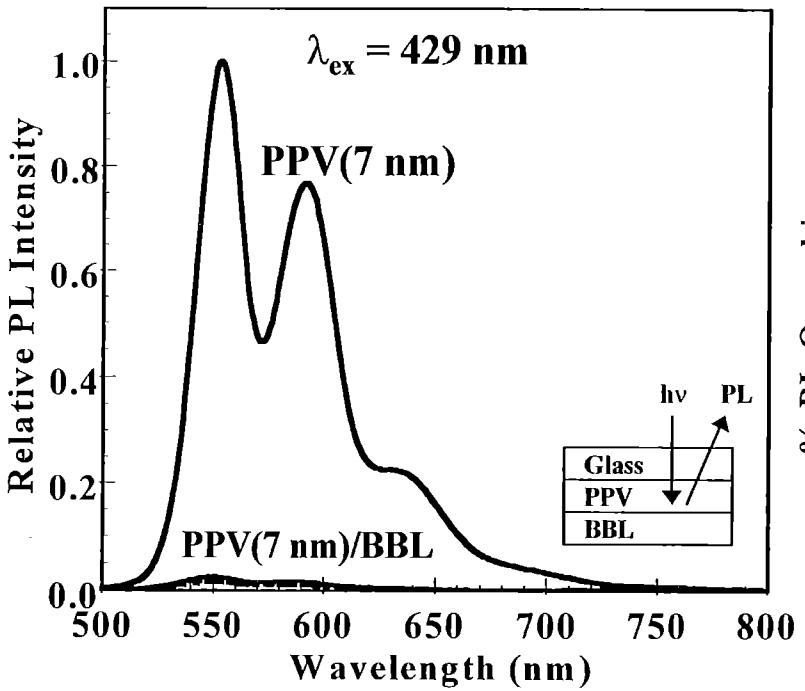

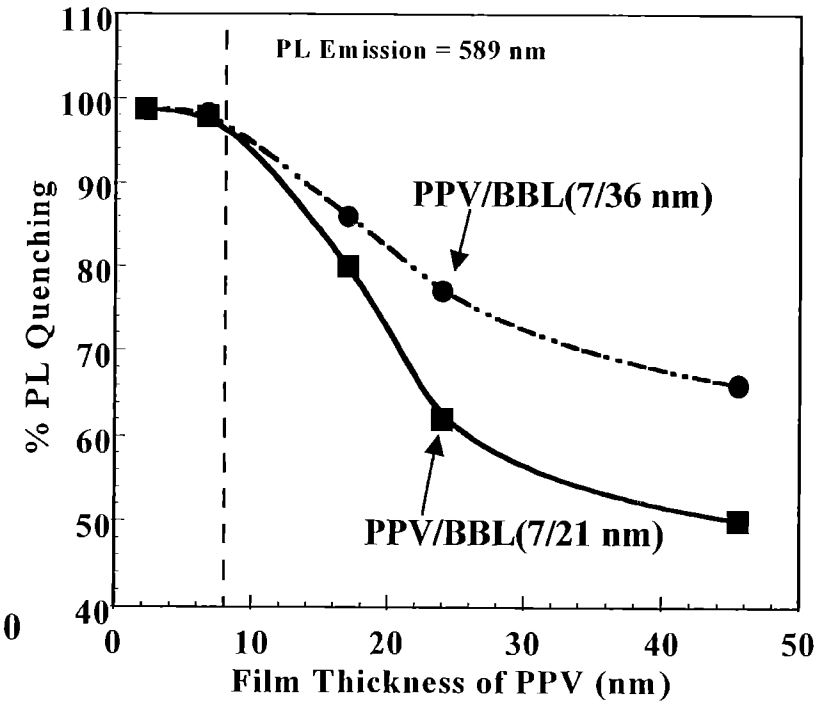

ARO TOPS MURI

S. A. JENEKHE

PHOTOVOLTAIC PROPERTIES OF SEMICONDUCTING POLYMER HETEROJUNCTIONS

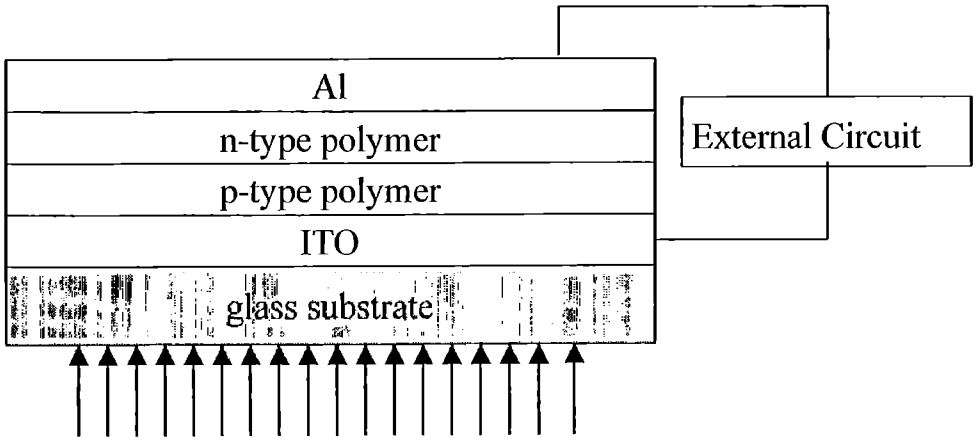

Light illumination

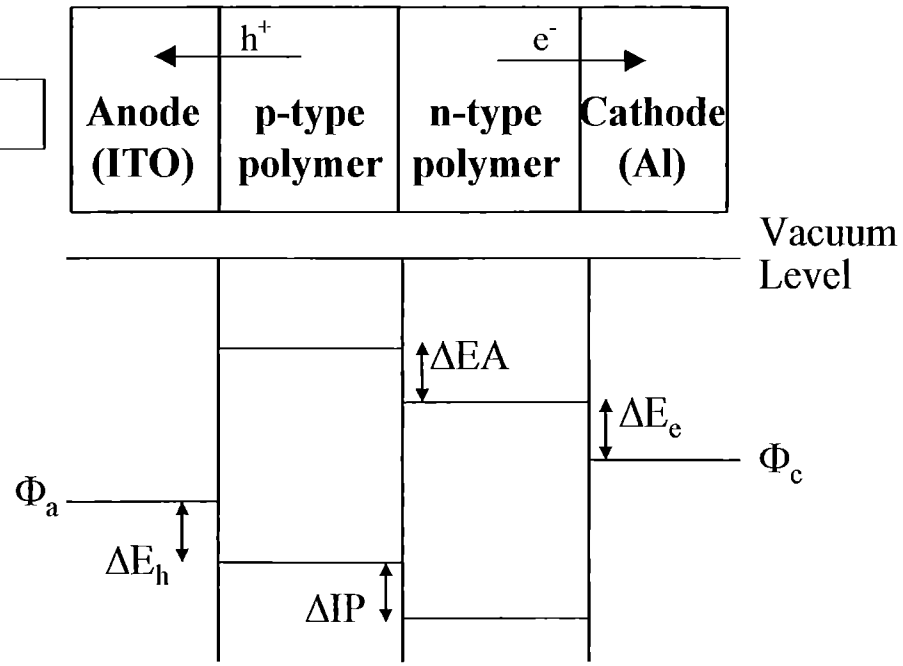

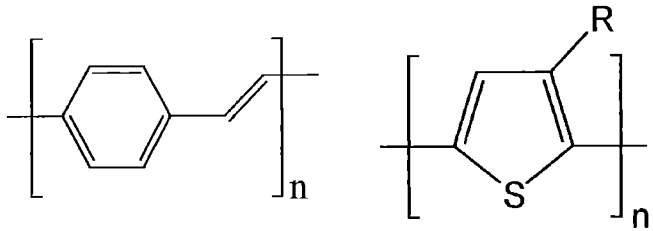

PPV P3AT

- **Role of Polymer/Polymer Interface**
  - **–(ΔIP, ΔEA)**
  - **–Charge Depletion (Space Charge) Region?**
  - **–Built-In Potential (Field)**
- **Finite Size Effects**
- **Ohmic Contacts**

PPV/BBL SOLAR CELLS

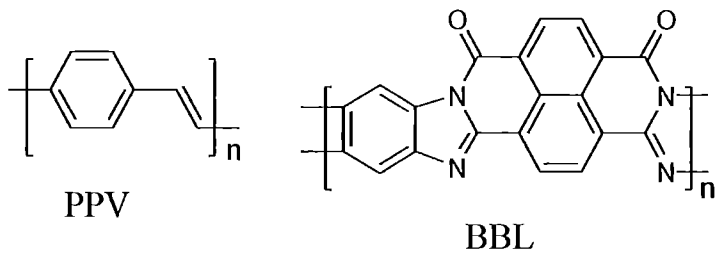

PPV BBL

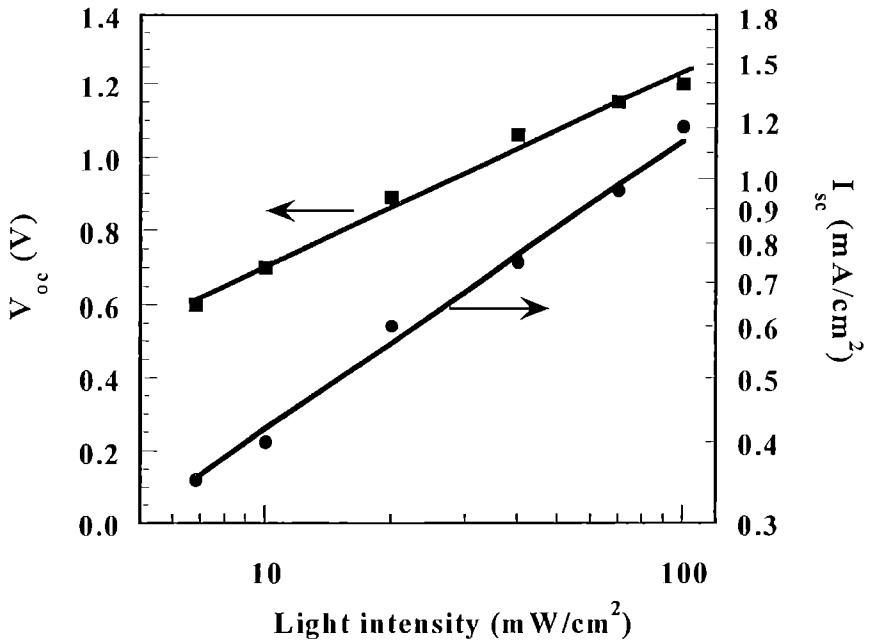

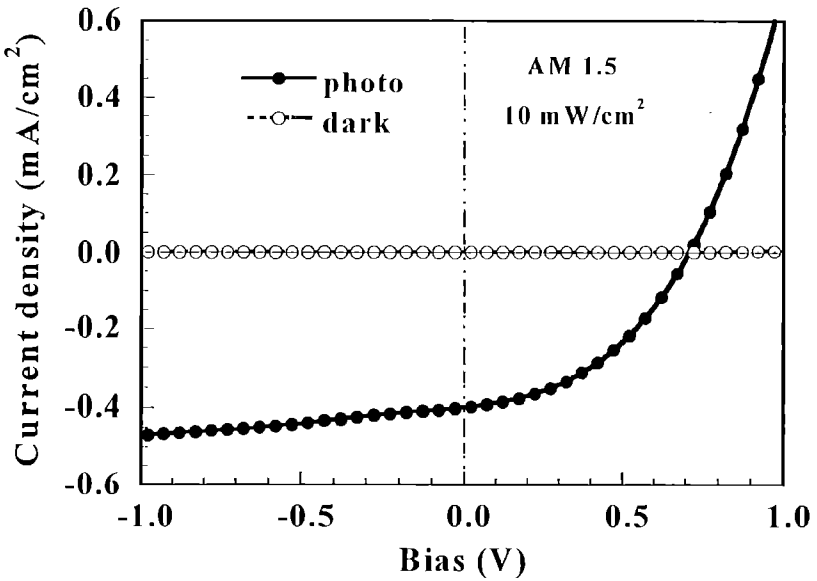

I_{sc} = 0.4 -1.2 mA/cm^2

V_{oc} = 0.7 -1.2 V

Fill Factor (FF) $= \frac{(IV)_{max}}{V_{oc} I_{sc}}$ = 0.41-0.43

Power Conversion Efficiency η_p = 1.4 - 2.0 %

CHARGE COLLECTION FROM PPV/BBL SOLAR CELLS

L = 0.4-0.5 mW/cm^2

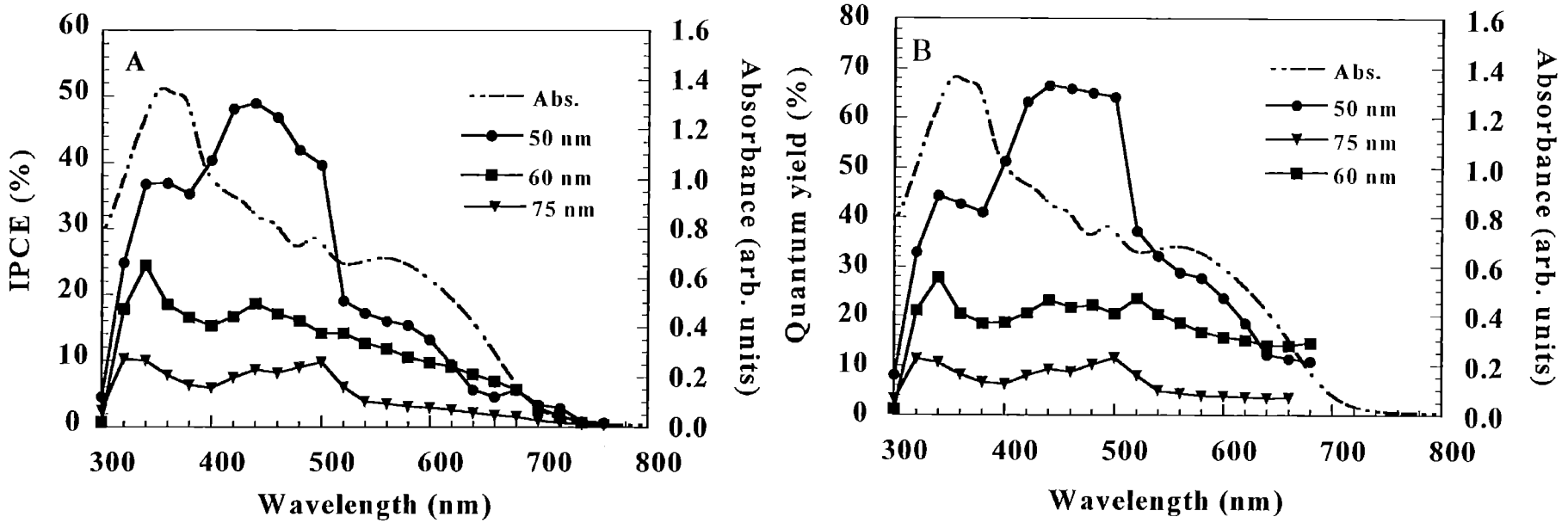

— **Maximum Photon-to-Current Conversion Efficiency = 49 %**

— **Maximum External Quantum Efficiency = 66 %**

— **Maximum Power Conversion Efficiency (η_p) = 2.0 %**

— **Finite Size Effects (Exciton Diffusion Limitations)**

Solar Cells From Polymer/Polymer Heterojunctions

SUMMARY

Efficient Solar Cells from PPV/BBL Junctions

— Photoinduced Charge Separation at Interface
(PL Quenching, Complete EL Quenching)

— Role of Electron Affinity of n-Type Polymer Critical

— Ohmic Contacts at Polymer/Metal Interfaces

— Charge Depletion (Space Charge) Region Around Interface

— Finite Size Effects (Exciton Diffusion Limitations)

Further Improvement of Polymer Solar Cells

— High Electron Affinity n-Type Conjugated Polymers

— Small Band Gap Polymers

— High Purity Materials (Trap-Free?)

Tunable Electroluminescence in Conjugated Polymers: Bilayer and Blend Structures

Kathleen Meeker

August, 2000

MURI Annual Review

Outline

- Goals and Background
- Bilayer Tunable Photoluminescence
- Bilayer Tunable Electroluminescence
  - –PPV/PCZPQ
  - –PPV/$Ru(bpy)_3^{2+}$
- Coupling Bilayers and Blends
- Environmentally Responsive EL Polymers
- Conclusions

Project Goals

Explore tunable optical properties of a variety of polymer-based systems

Extend the spectral range of tunable electroluminescence and photoluminescense in polymer thin films and other structures to encompass red, green, blue and other colors throughout the CIE color space

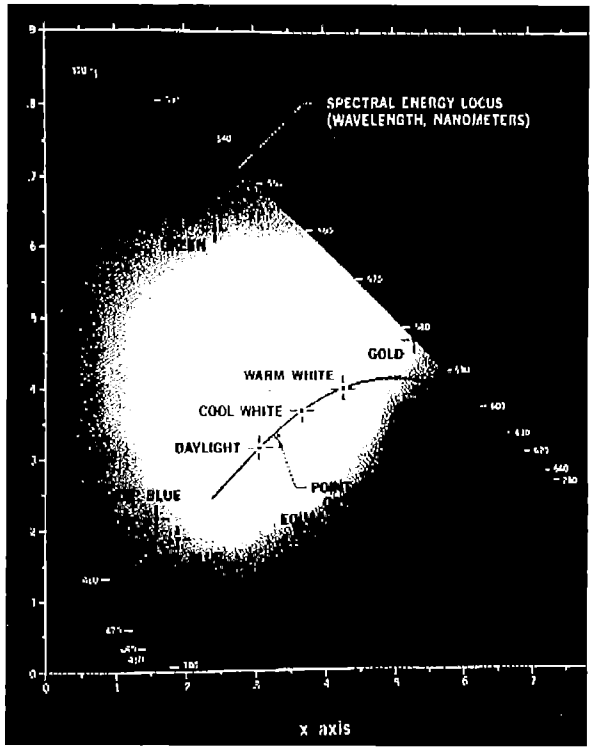

Background: Tunable EL in Polymer Heterojunctions

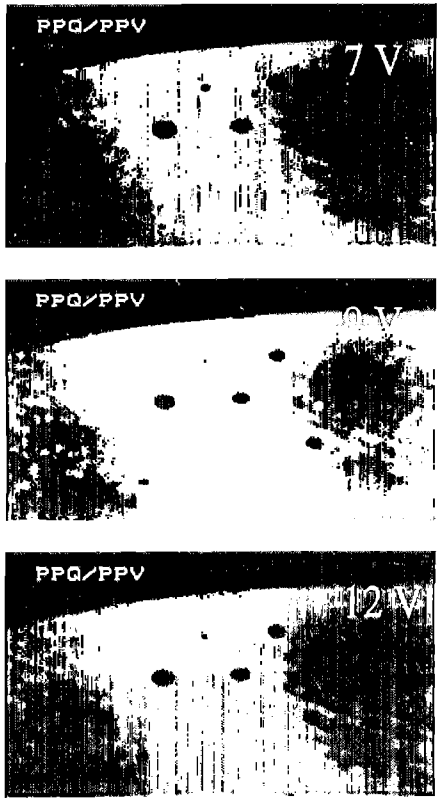

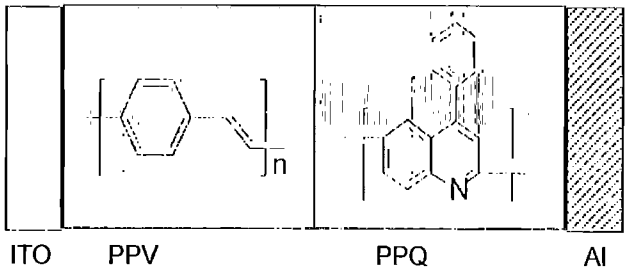

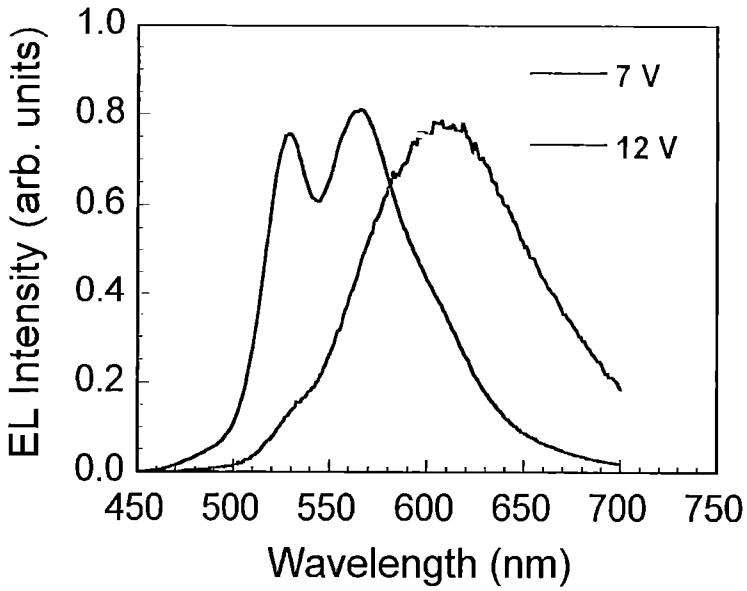

Zhang and Jenekhe, *Macromolecules* **2000**, 2069-2082.

Approaches to Tunable Electroluminescence

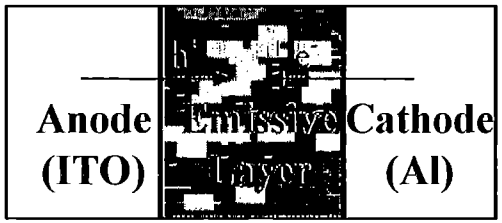

Emissive layers comprised of polymer blends can potentially provide tunable EL; each polymer contributes its emission spectrum.

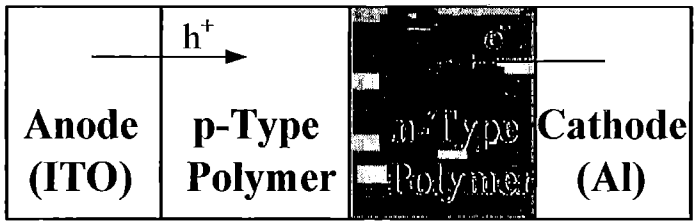

Two polymer layers can improve charge injection/transport and provide for selective excitation.

Materials Explored

Poly- and oligoquinolines

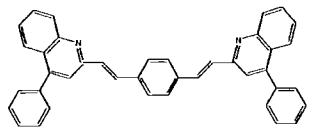

BPQ-VPV

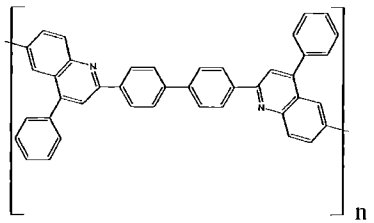

PBPQ

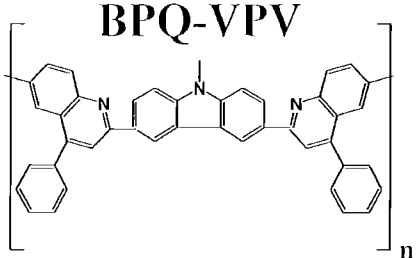

PCZPQ

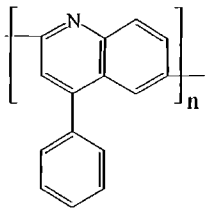

PPQ

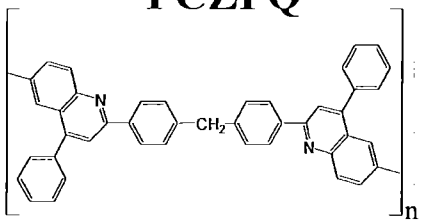

PDMPQ

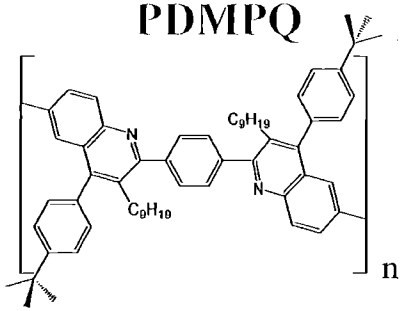

BuN-PPQ

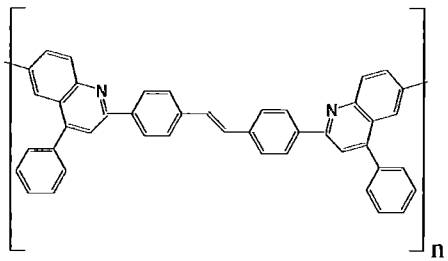

PSPQ

p-type materials

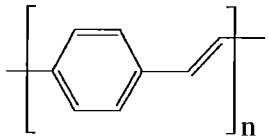

PPV

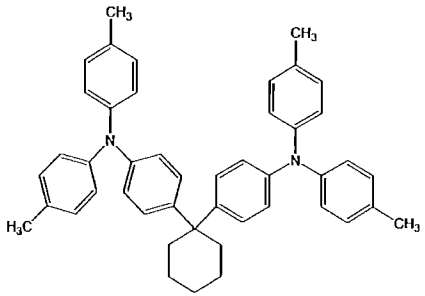

TAPC

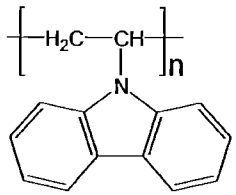

PVK

Metal Complexes

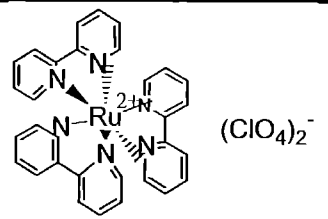

$Ru(bpy)_3(ClO_4)_2$

From the Bard group

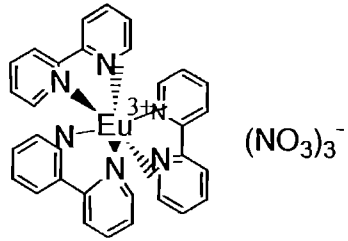

$Eu(bpy)_3(NO_3)_3$

Polyanthrazolines

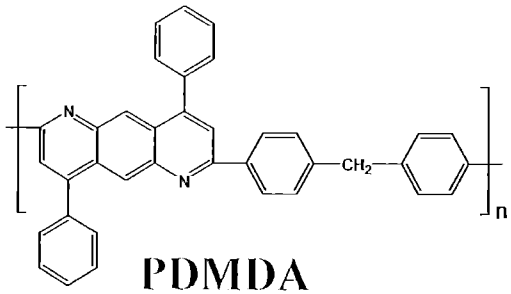

PDMDA

Tunable Bilayer Photoluminescence

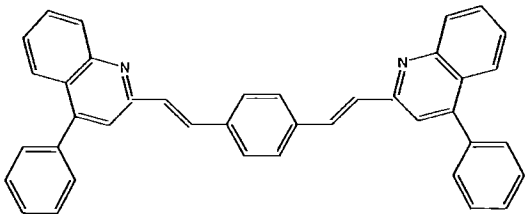

BPQ-VPV

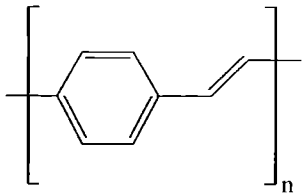

PPV

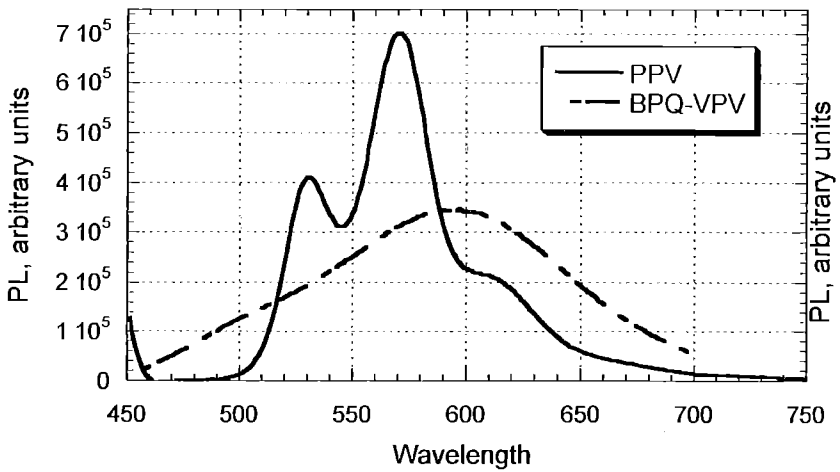

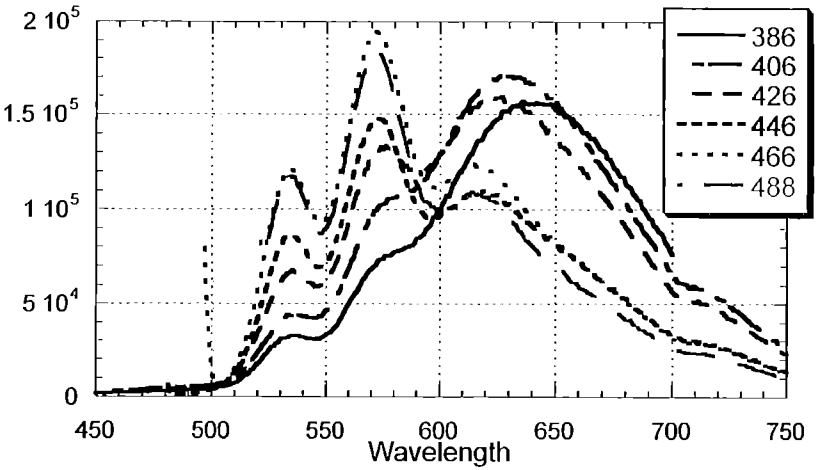

ARO TOPS MURI

KATHLEEN MEEKER

km0807s3

Voltage-Tunable EL from PPV/PCZPQ Bilayers

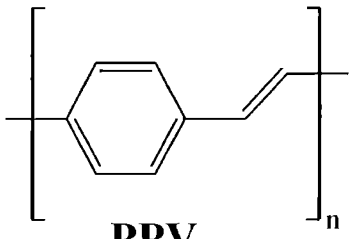

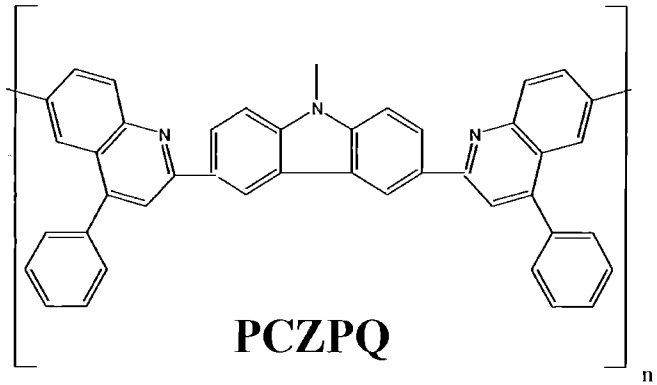

ITO/PPV/PCZPQ/Al

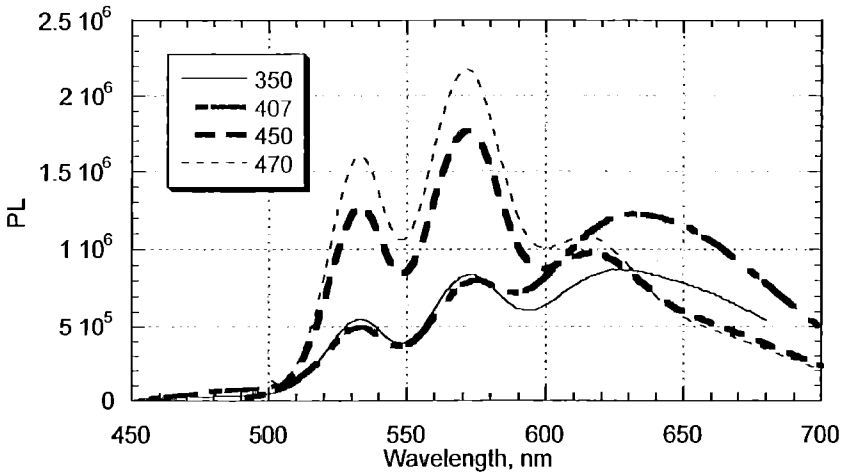

Red (6V) ⟷ Green (12V)

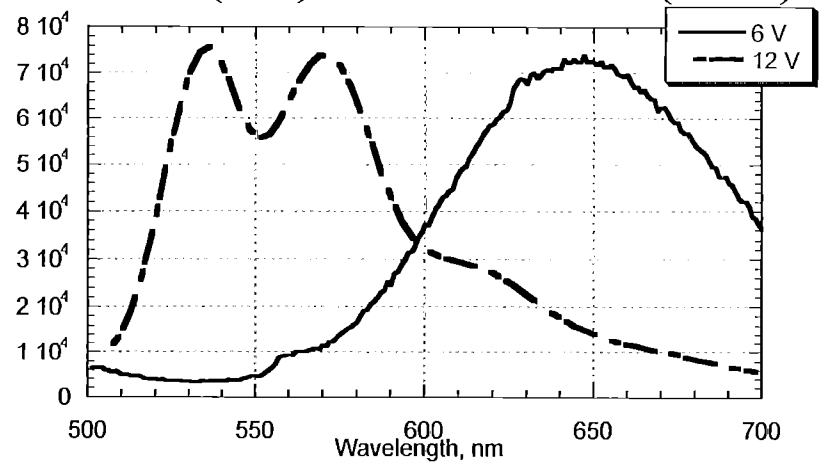

Effects of Film Thickness on Bilayer EL Color

ITO/PPV (70 nm)/ $Ru(bpy)_3(ClO_4)_2$ (30 nm) /Al

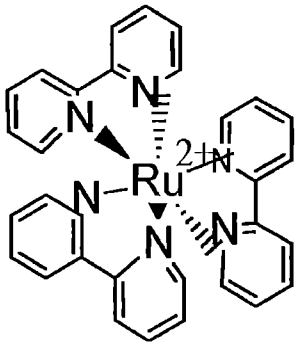

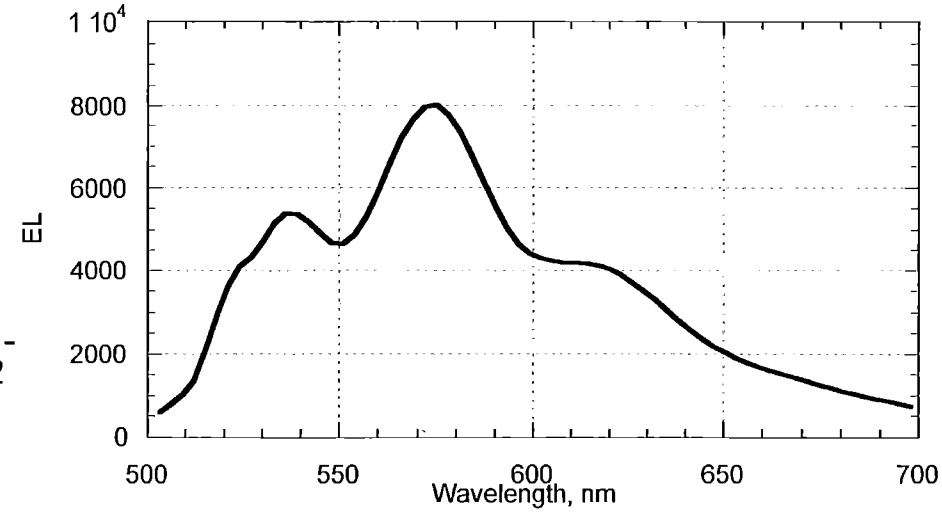

80 Cd/m²
turn on at 6 V

ITO/PPV (30 nm)/ $Ru(bpy)_3(ClO_4)_2$ (50 nm)/Al

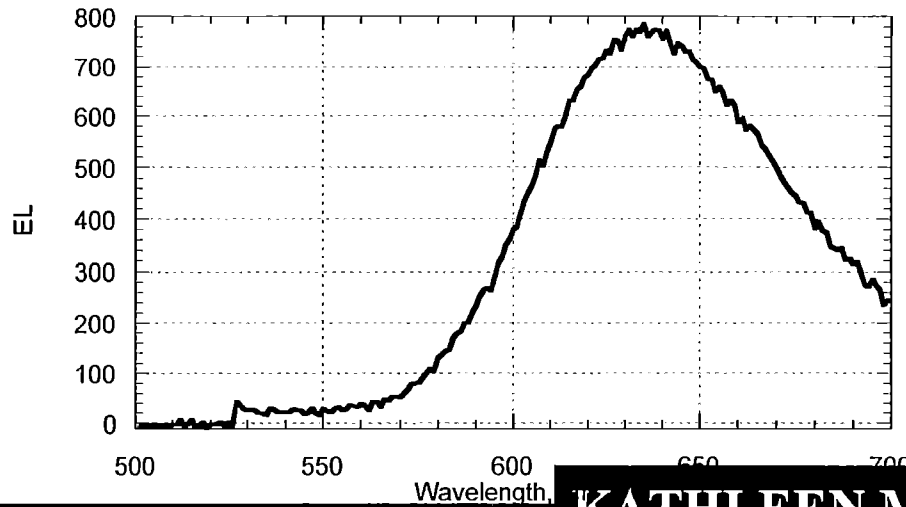

200 Cd/m²
turn on at 6 V

Tunable EL: ITO/PPV/$Ru(bpy)_3(ClO_4)_2$/Al

ITO/ PPV (40 nm) / $Ru(bpy)_3(ClO_4)_2$ (50 nm)/Al

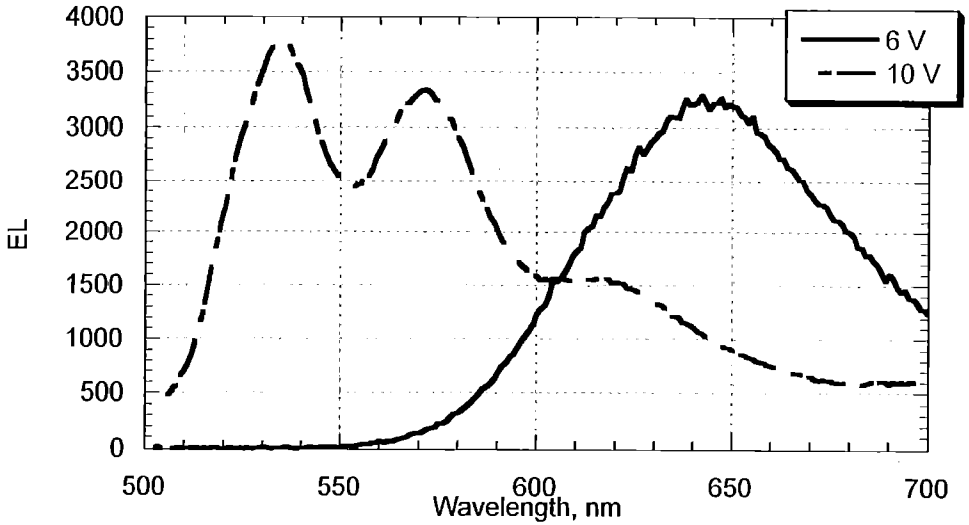

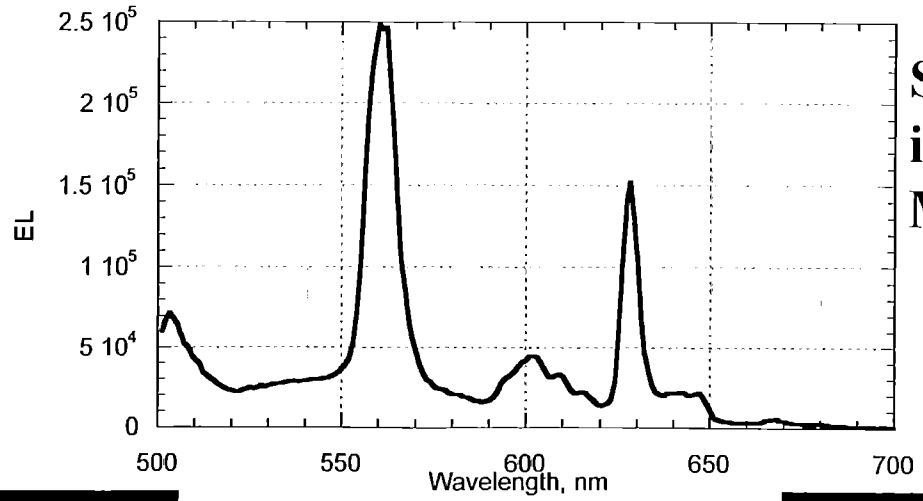

Spectrum acquired at intermediate voltage. Microcavity effects?

Bilayer LED Performance

ITO/PPV (40 nm)/$Ru(bpy)_3(ClO_4)_2$ (50 nm)/Al

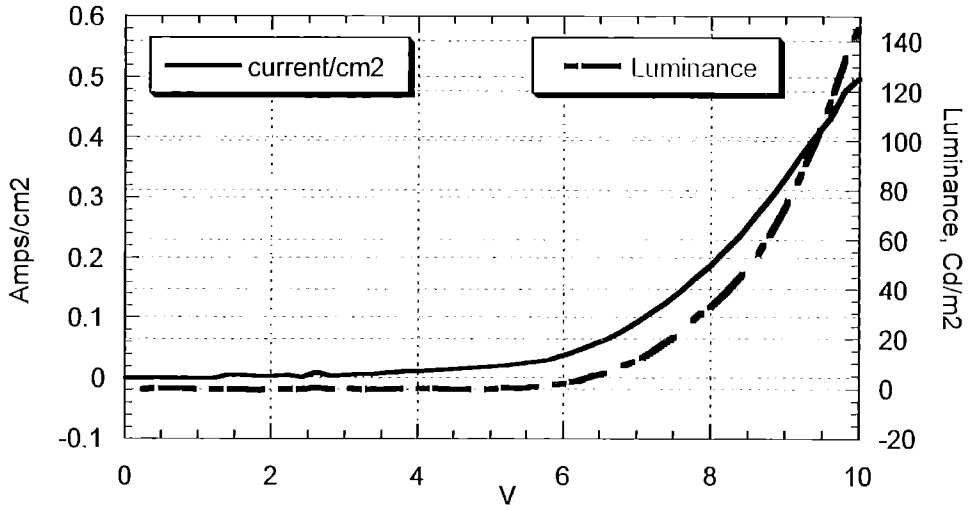

EL of Polymer Blends

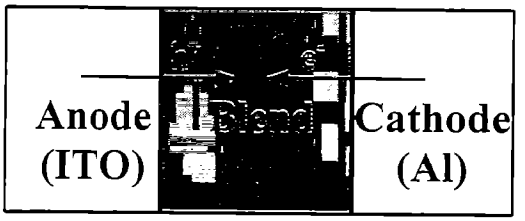

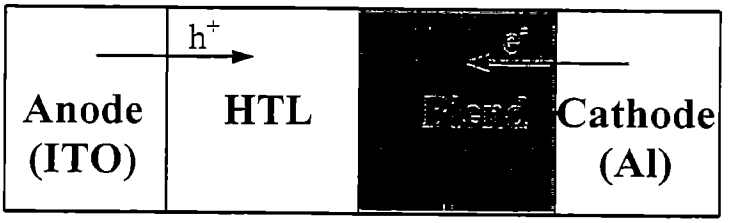

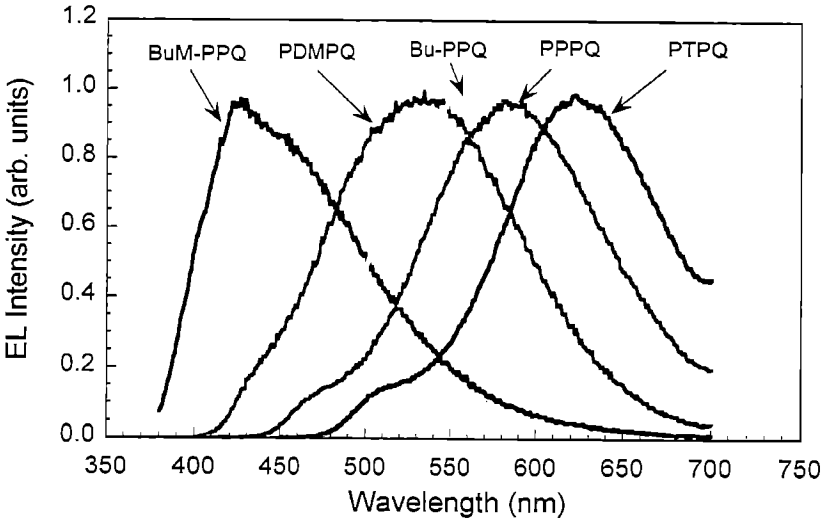

Possible Problems

A. Photophysical Processes

- **Energy Transfer**
- **Exciplex Formation**
- **Photoinduced Electron Transfer**

B. Control of Phase Separation

Polymer Blends

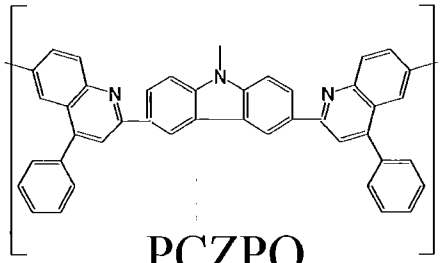

PCZPQ

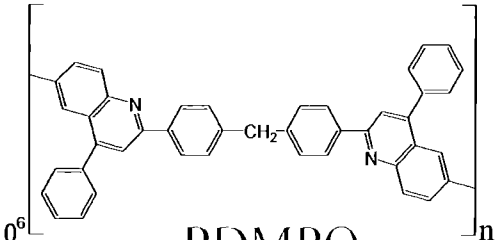

PDMPQ

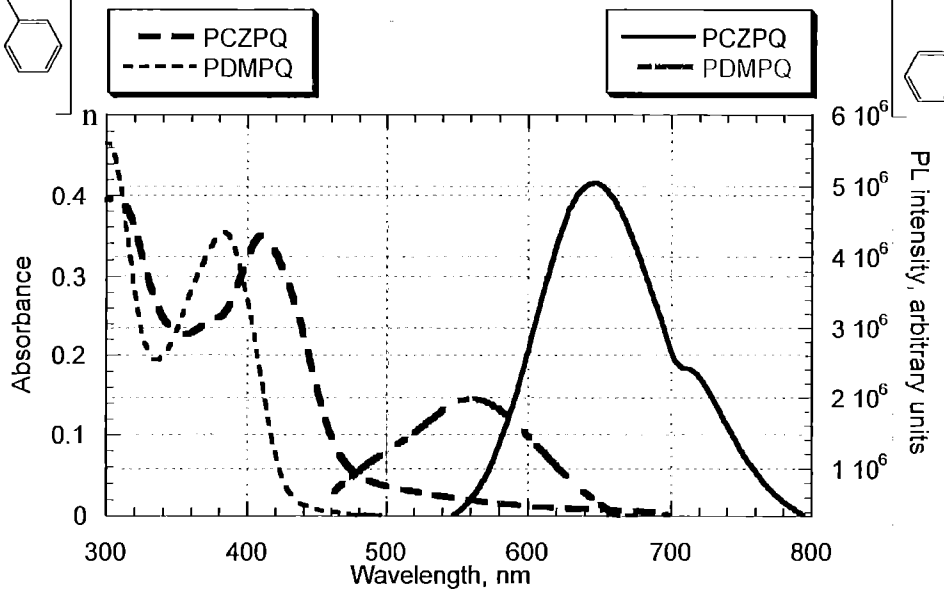

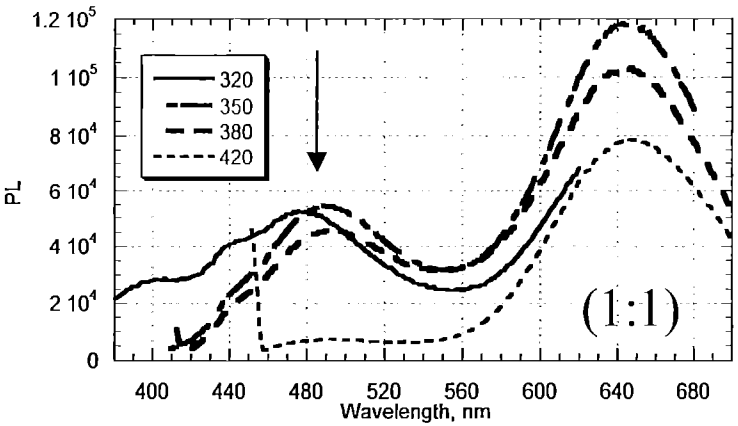

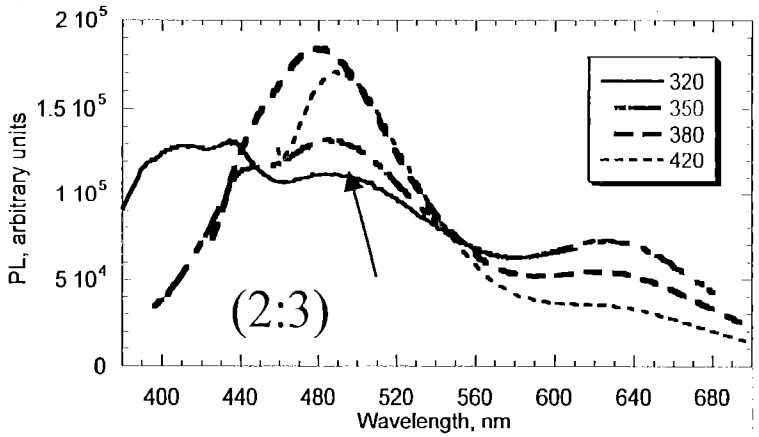

ARO TOPS MURI

KATHLEEN MEEKER

km0807s15

Origin of New Blue Peak in Blends

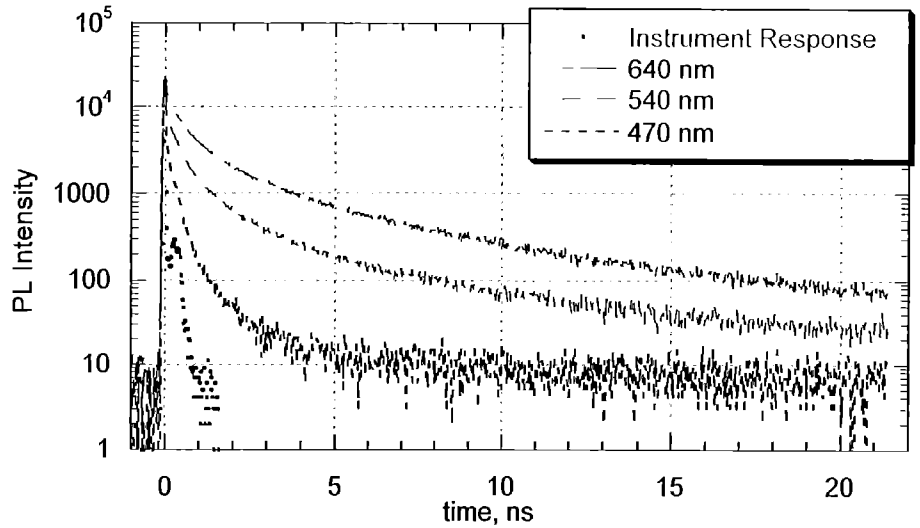

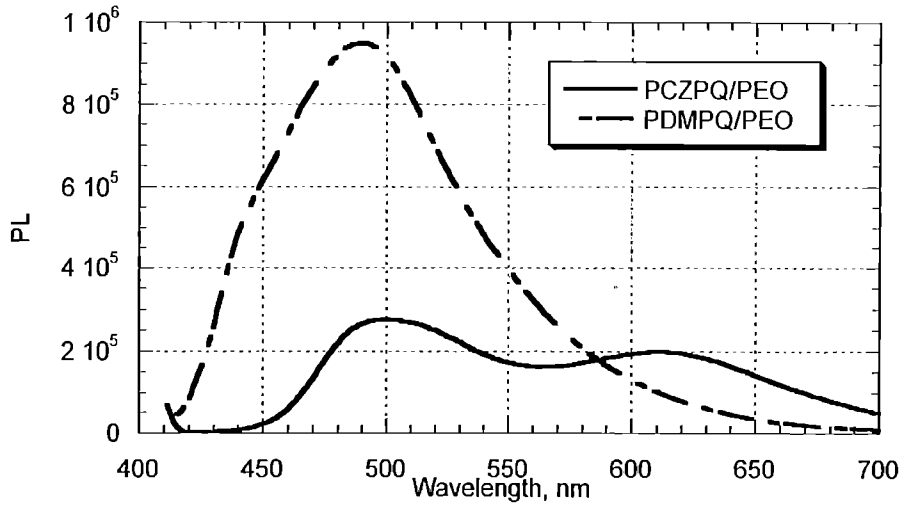

640 nm peak
4.4 ns 46%
0.91 ns 36%
0.14 ns 18%

540 nm peak
3.9 ns 32%
0.78 ns 38%
0.15 ns 30%

470 nm peak
48.5 ps 85%
0.57 ns 12%
7.9 ns 3%

- Intrachain Excitons
- Excimers in Pure Films

EL of Binary Blends

ITO/Blend/Al

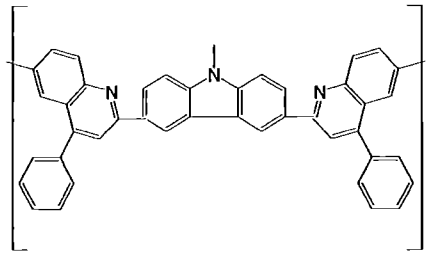

PCZPQ

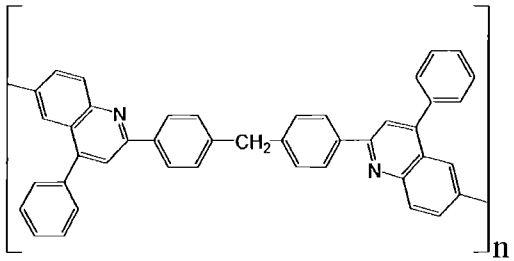

PDMPQ

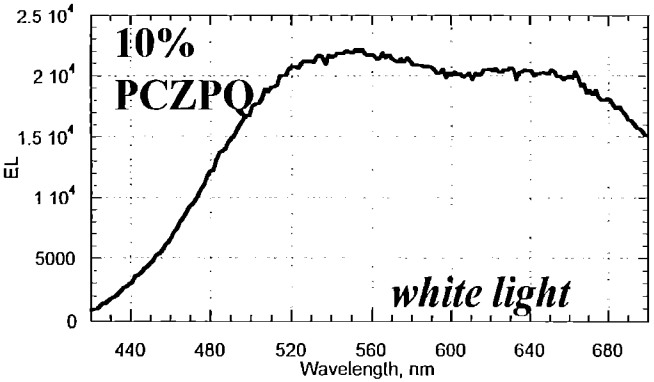

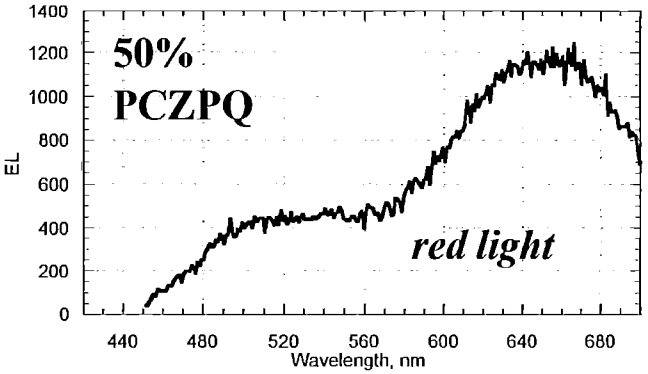

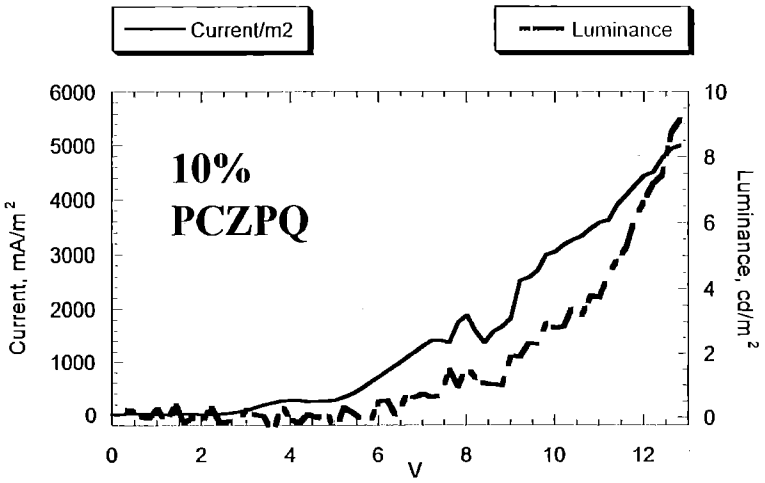

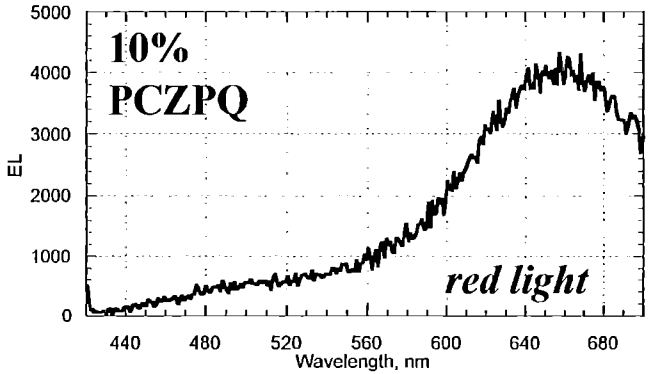

ARO TOPS MURI

KATHLEEN MEEKER

Electroluminescence of Ternary Blends: BuN-PPQ, PDMPQ, PCZPQ (2:2:1)

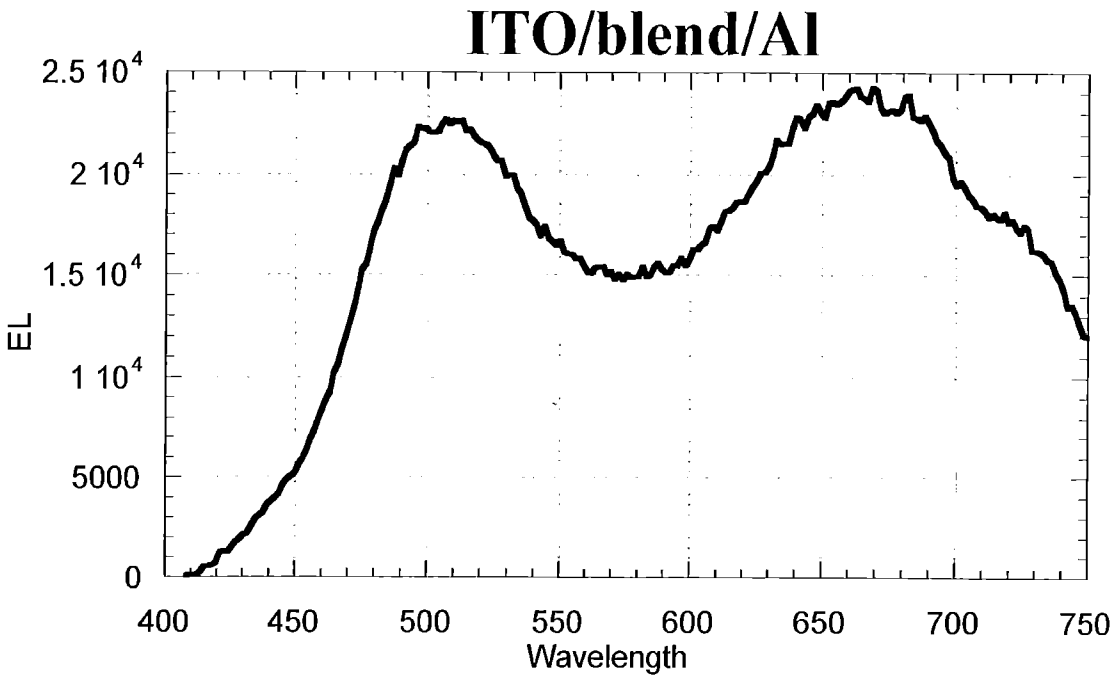

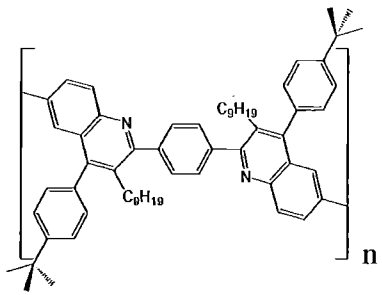

BuN-PPQ

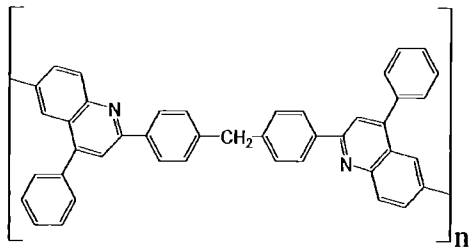

PDMPQ

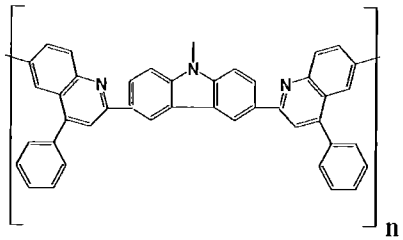

PCZPQ

Tunable EL: Ternary Blends

BuN-PPQ:PDMPQ:PCZPQ

2:2:1

ITO/PPV/Blend/Al

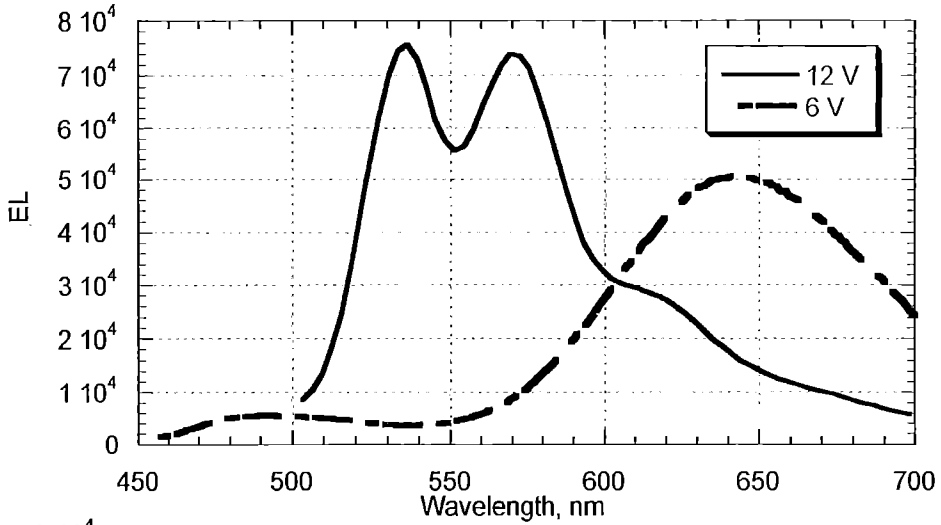

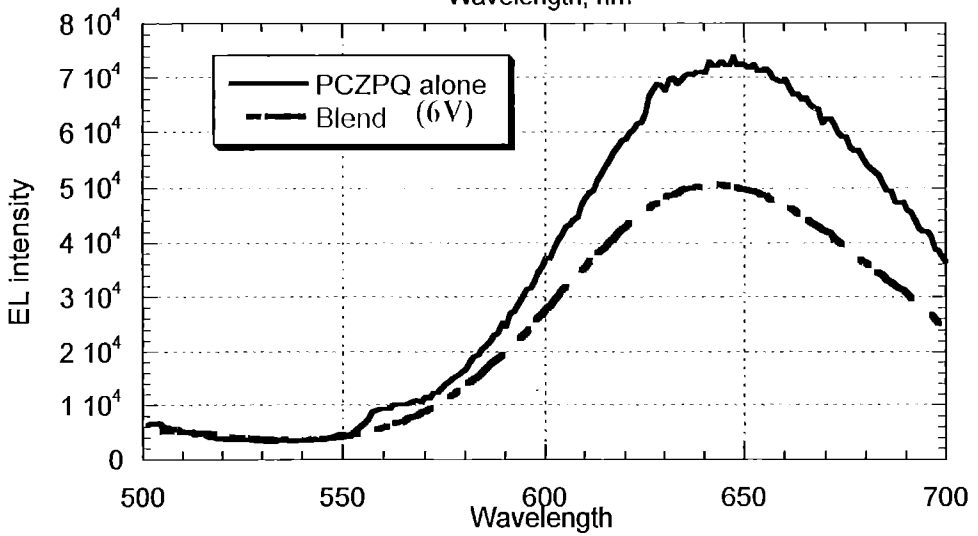

Tunability of ITO/PPV/Blend/Al identical to that of ITO/PPV/PCZPQ/Al

Selective Emission from Ternary Blends

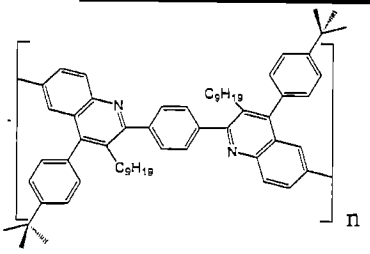

BuN-PPQ

λ_{EL} = 424 nm
IP = 5.71 eV

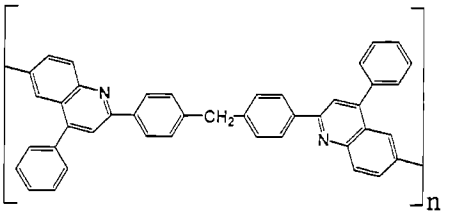

PDMPQ

λ_{EL} = 540 nm
IP = 5.44 eV

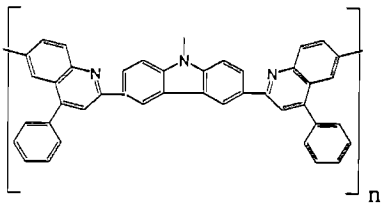

PCZPQ

λ_{EL} = 640 nm
IP = 5.27 eV

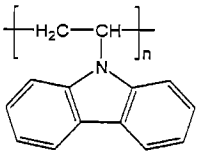

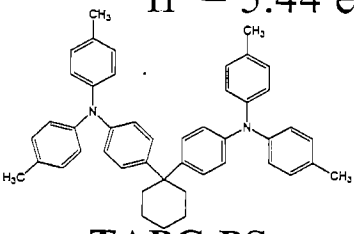

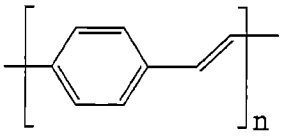

	PVK	TAPC:PS	PPV
Ionization potential?	*5.8 eV*	*5.3 eV*	*5.11 eV*
Emission from blend?	***blue***	***red***	***red***
Selective emission?	***yes***	***yes***	***yes***
Tunability?	***no***	***no***	***yes***

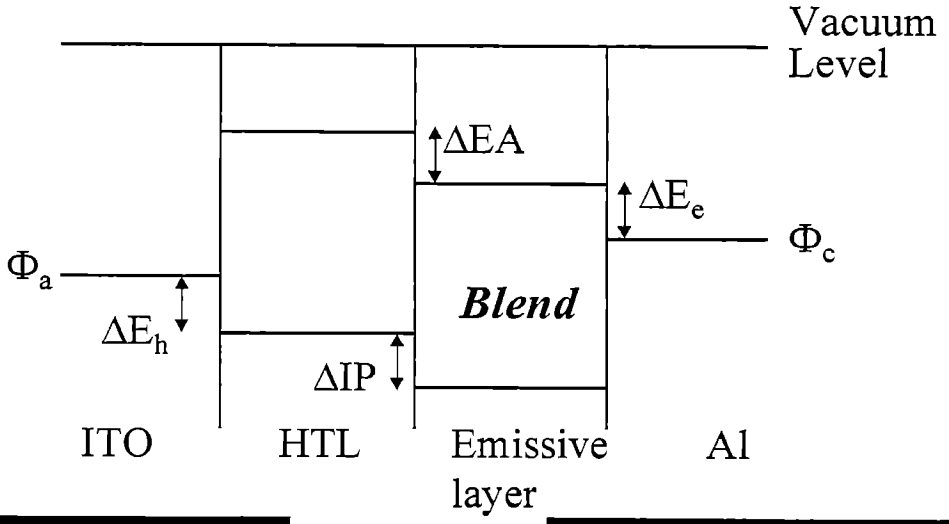

Environmentally Responsive Light Emitting Polymers

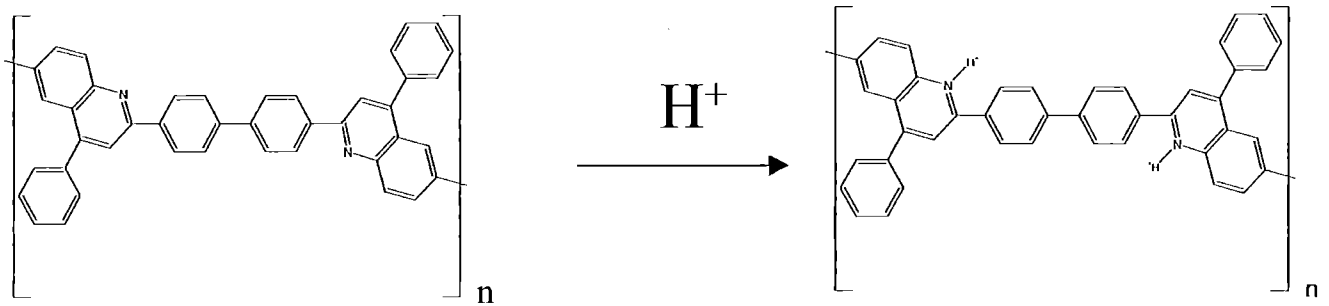

PBPQ

yellow-orange EL

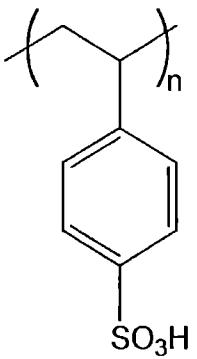

PSSA

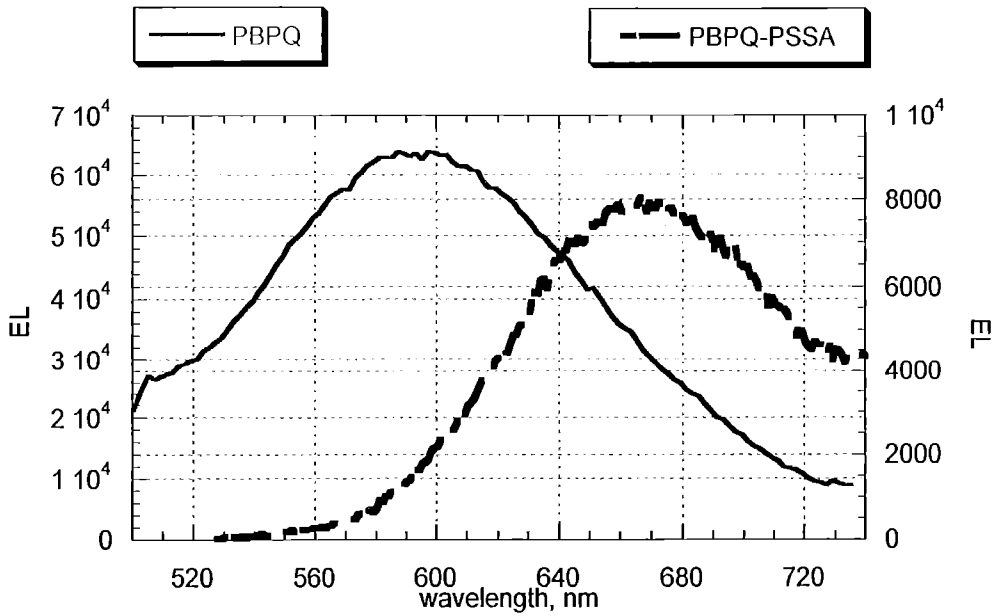

70-80 nm red shift

red EL

Conclusions

•Tunable multicolor electroluminescence obtained from bilayers of PPV/tris(bipyridine) ruthenium (II) complex

•Blending polyquinolines altered emission mechanisms; blend composition dramatically affected EL and PL spectra

•White light LEDs obtained from single-layer polyquinoline blends

•Selective emission from blend components upon incorporation of a hole-transport layer, suggests selective charge injection from hole-transport layer to individual polymers in blends

•Tunable electroluminescence from environmentally responsive light emitting polymers demonstrated; sulfonic acid molecular structure has a significant effect on PL and EL.

Acknowledgments

Army Research Office MURI
DAAD19-99-1-0206

Jenekhe Research Group

Bard Research Group

Bernard Panzarella (undergraduate student)

Dr. Chris Collison

Solvent-induced Morphological Effects on the Picosecond Photophysics of a Conjugated Polymer

Pei Wang, Chris Collison, Lewis Rothberg

Department of Chemistry, University of Rochester, New York 14627

Support: TOPS ARO MURI

Motivation: Aggregation quenching limits luminescence efficiency in solid state polymer samples. Understand the origin of aggregation quenching in order to control it and make better device.

Method: Study the photophysics while controlling aggregation by addition of poor solvents. Use femtosecond transient absorption and stimulated emission to identify excited states and investigate their dynamics.

Electroluminescent polymer: MEH-PPV
(Poly(2-methoxy, 5-(2-ethylhexoxy)-paraphenylenevinylene))

Energy Diagram illustrating the principle of pump-probe experiments

PL = Photoluminescence, PA = Photo-induced Absorption, SE = Stimulated Emission, PB = Photo Bleaching, only singlet excited states are shown.

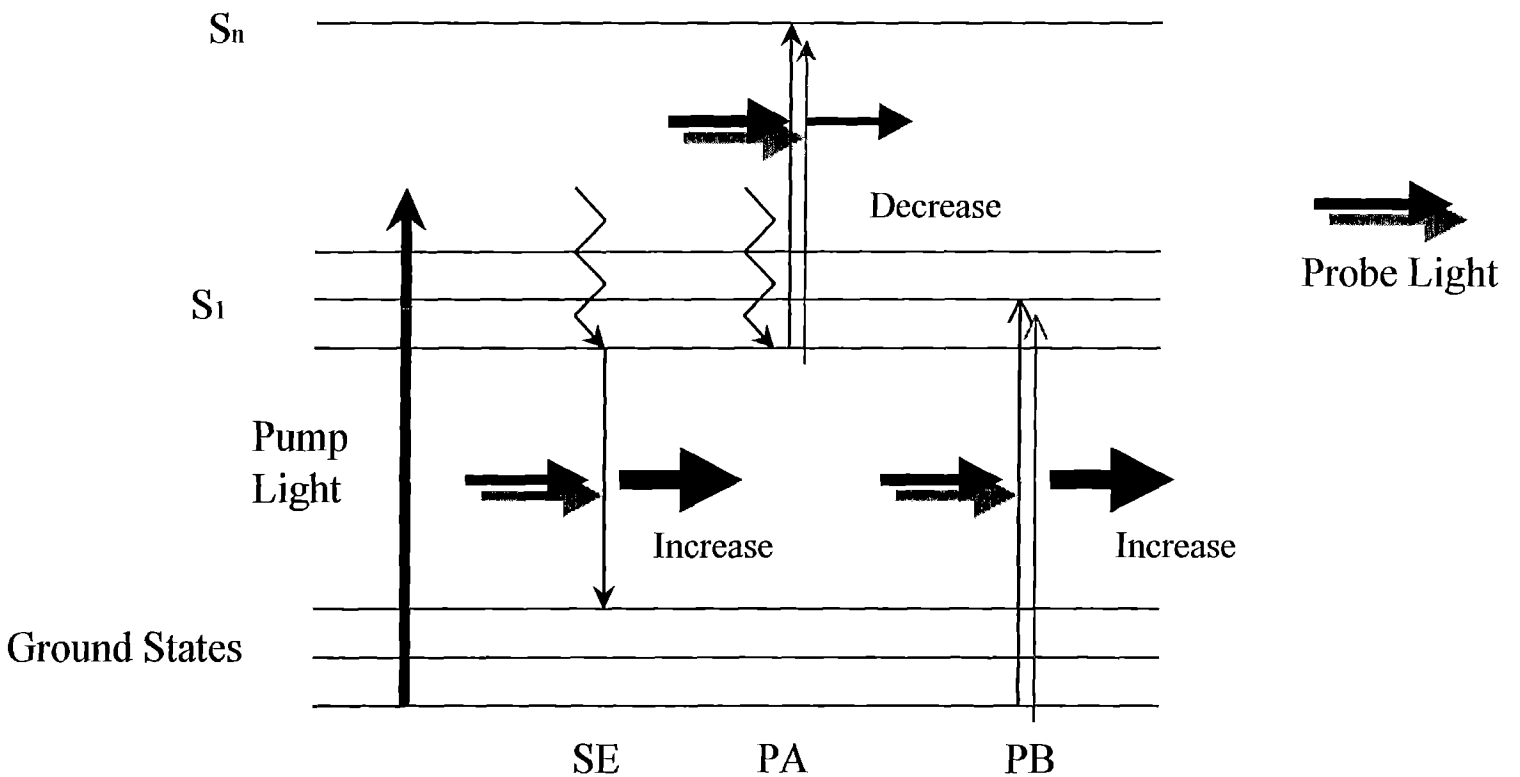

Experimental Set-up

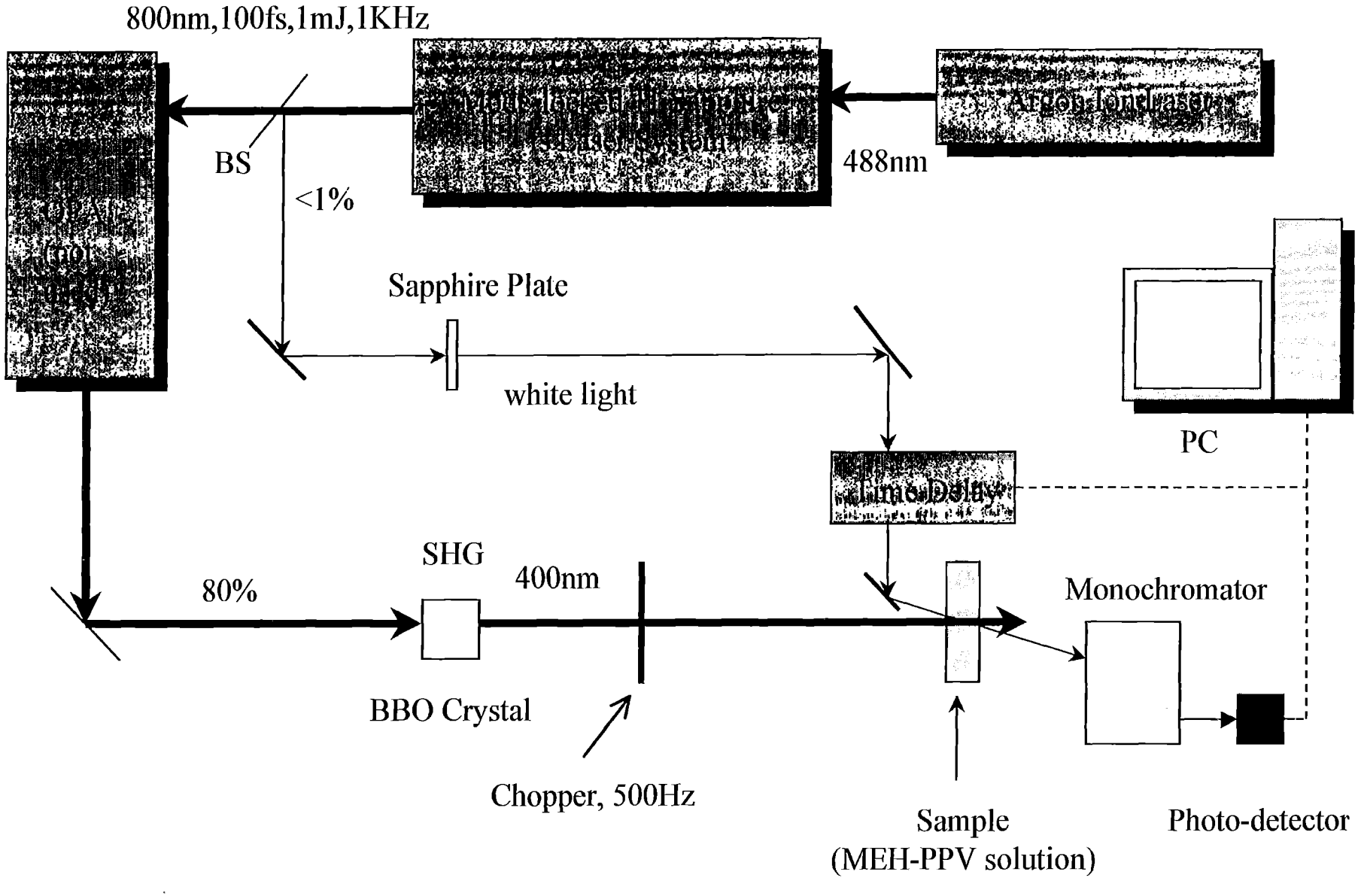

L.Rothberg, Rochester

ARO MURI

Solvatochromism in MEH-PPV

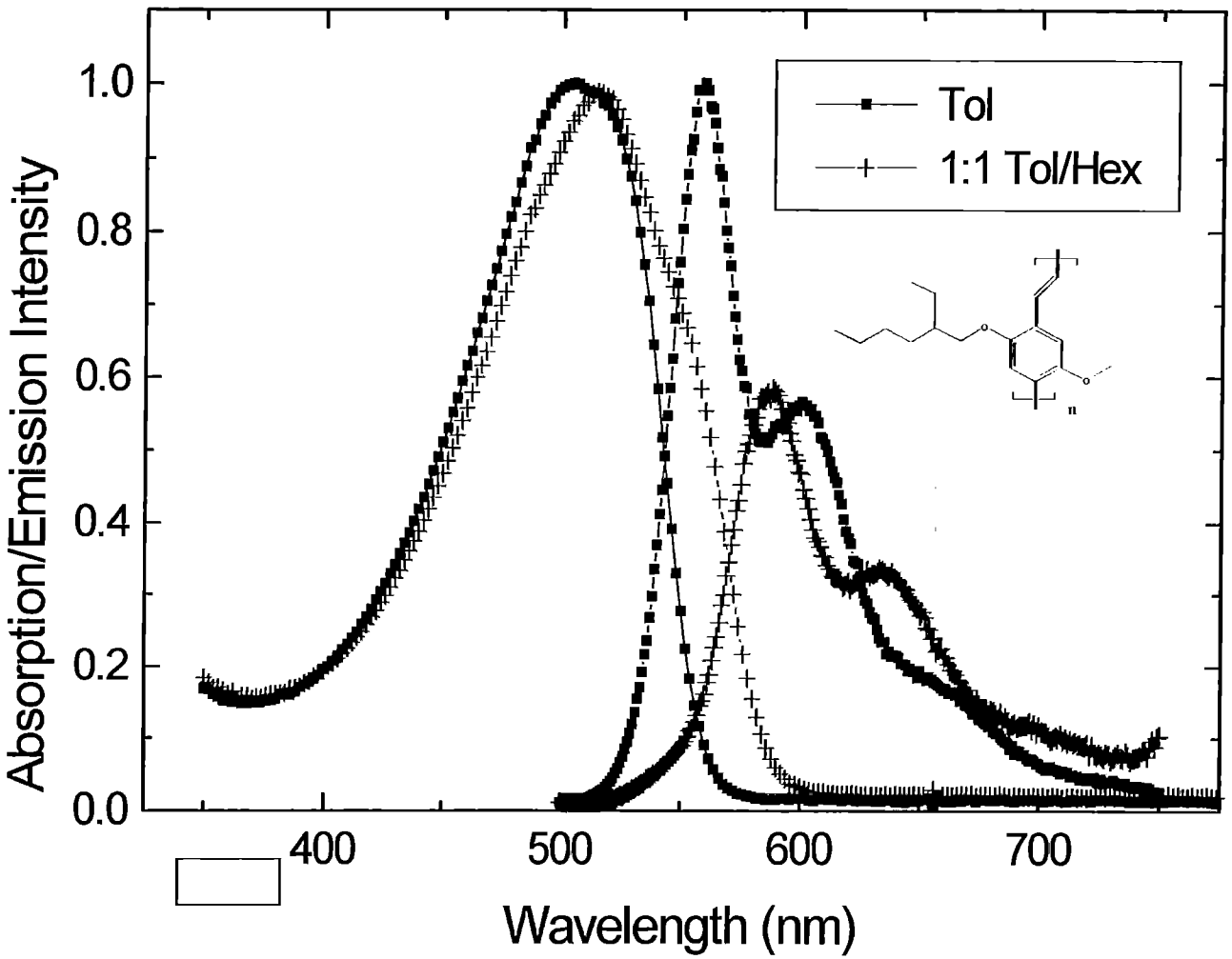

L.Rothberg, Rochester

ARO MURI

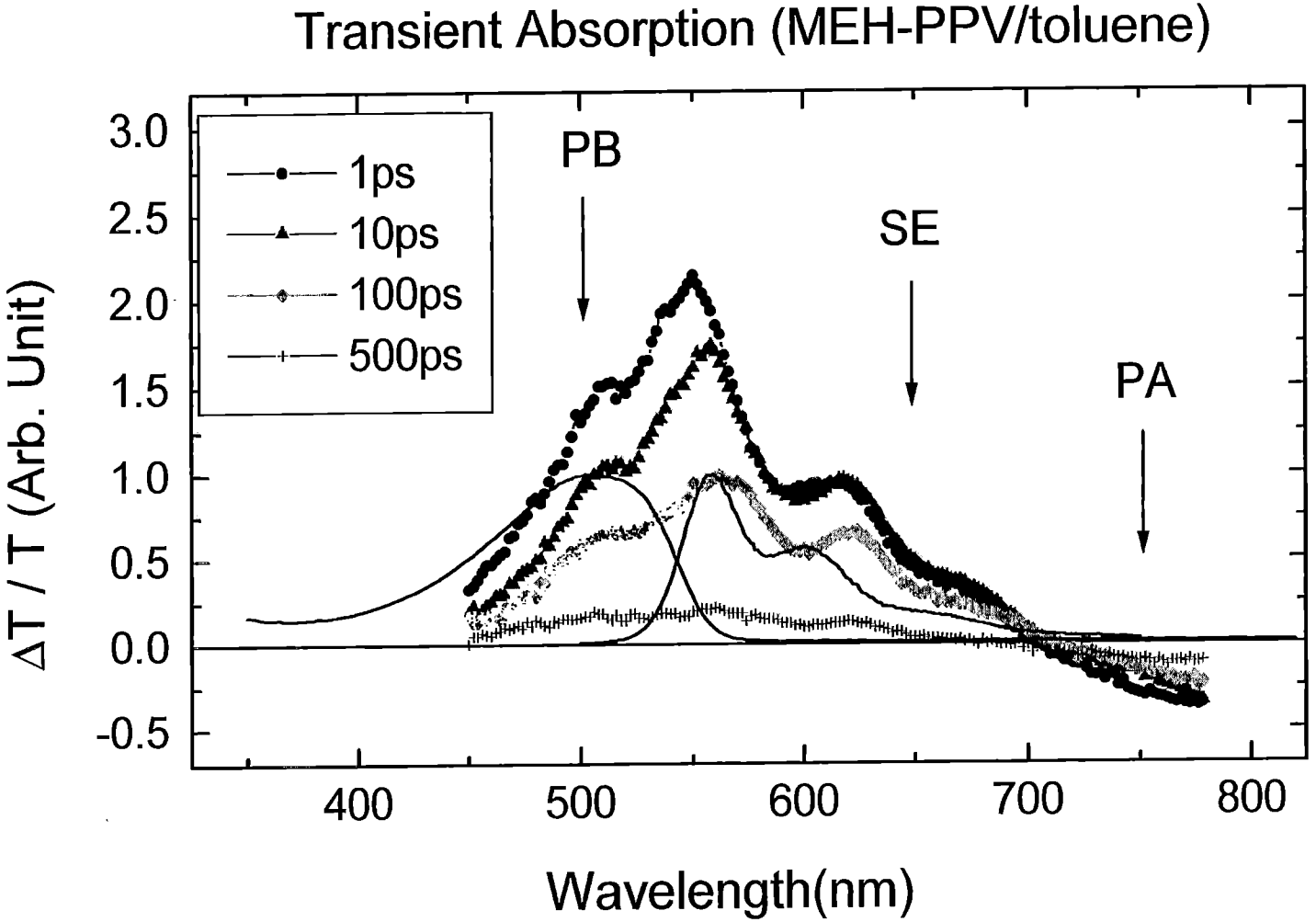

L.Rothberg, Rochester

ARO MURI

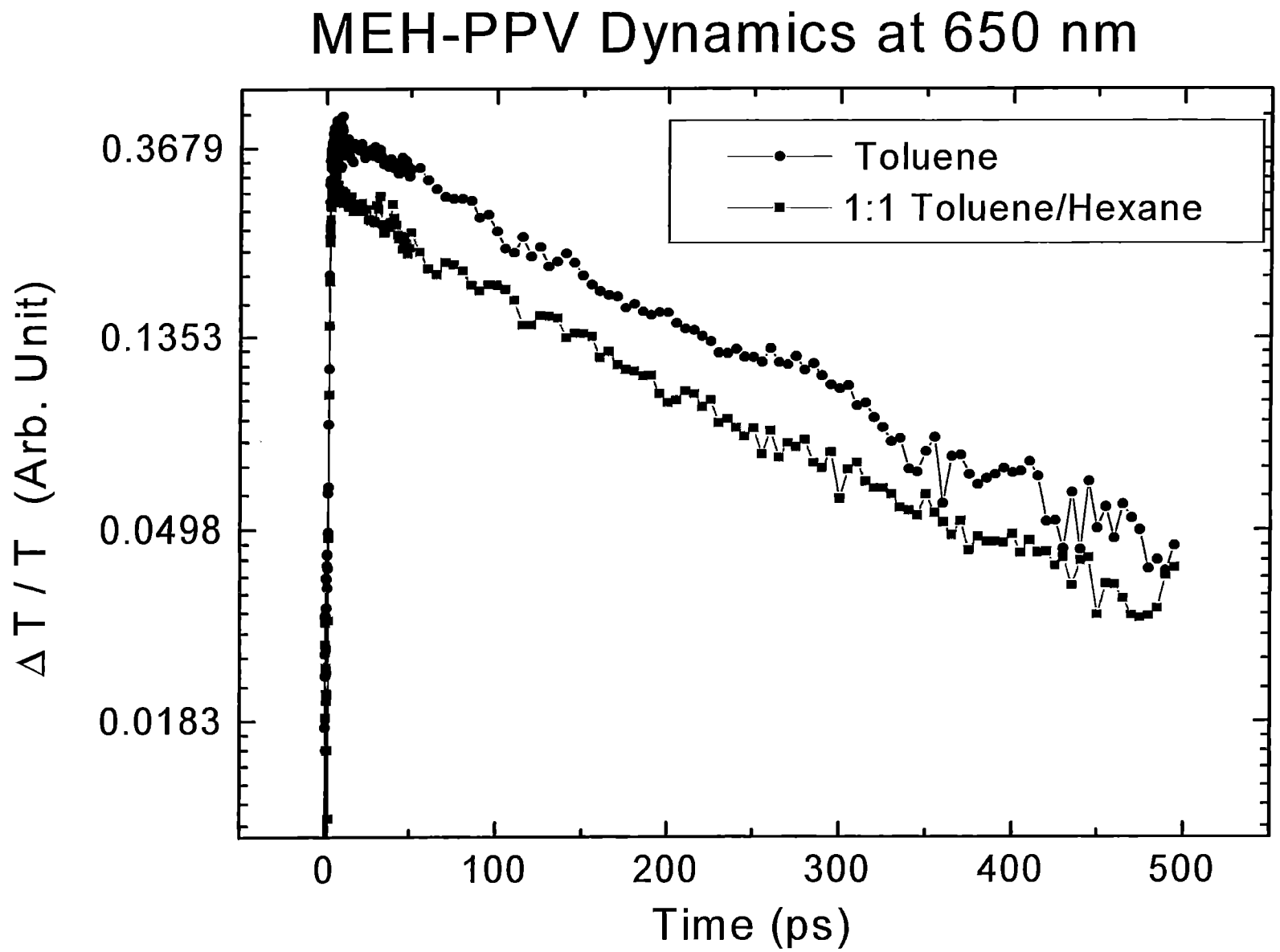

L.Rothberg, Rochester

ARO MURI

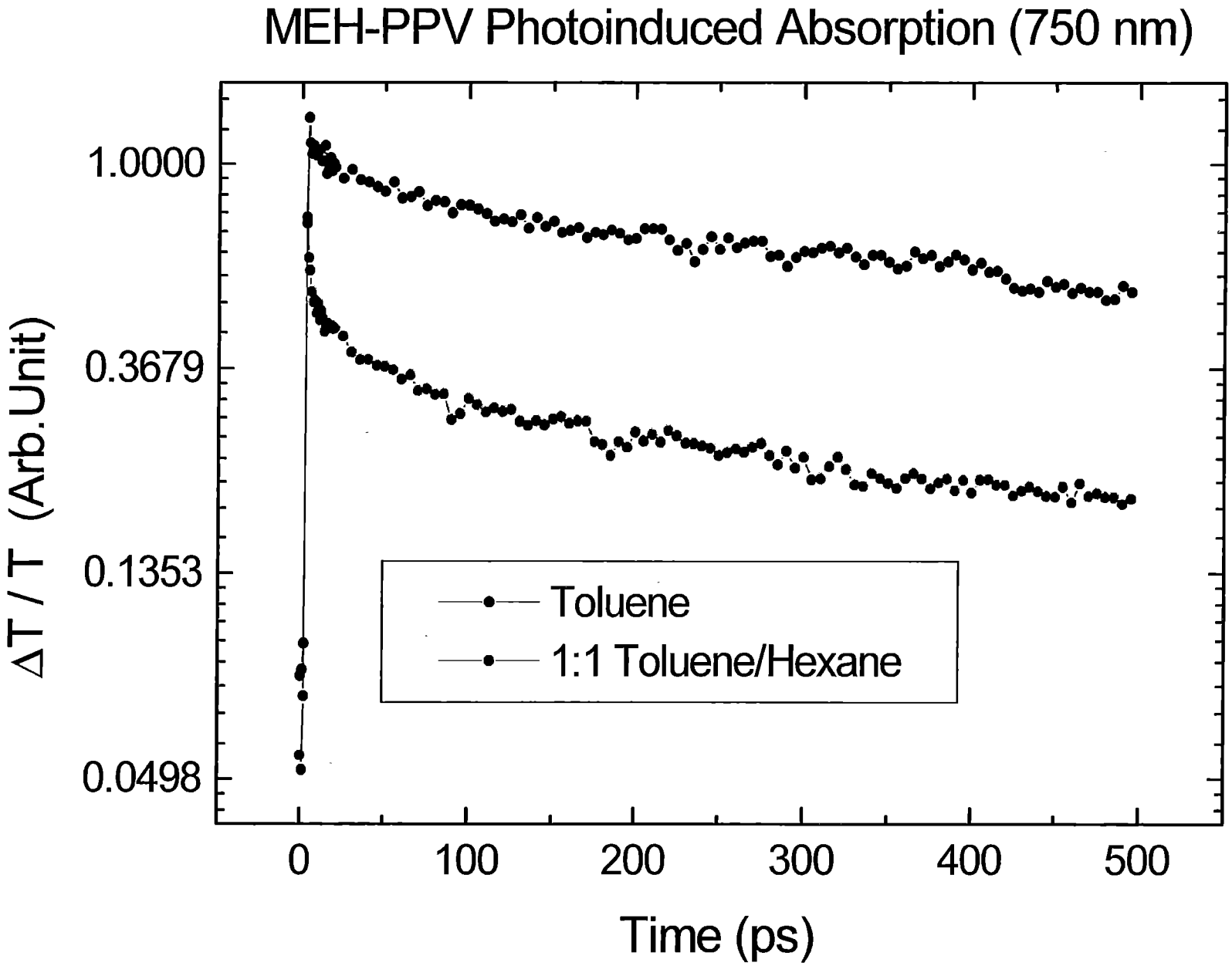

L.Rothberg, Rochester

ARO MURI

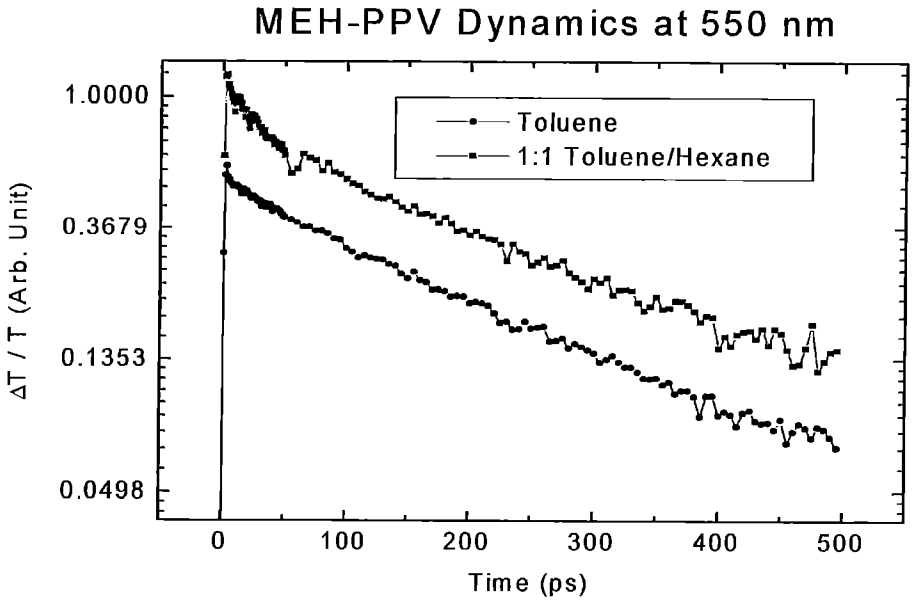
MEH-PPV Dynamics at 550 nm
1.0000
0.3679
0.1353
0.0498
ΔT / T (Arb. Unit)
Toluene
1:1 Toluene/Hexane
0
100
200
300
400
500
Time (ps)

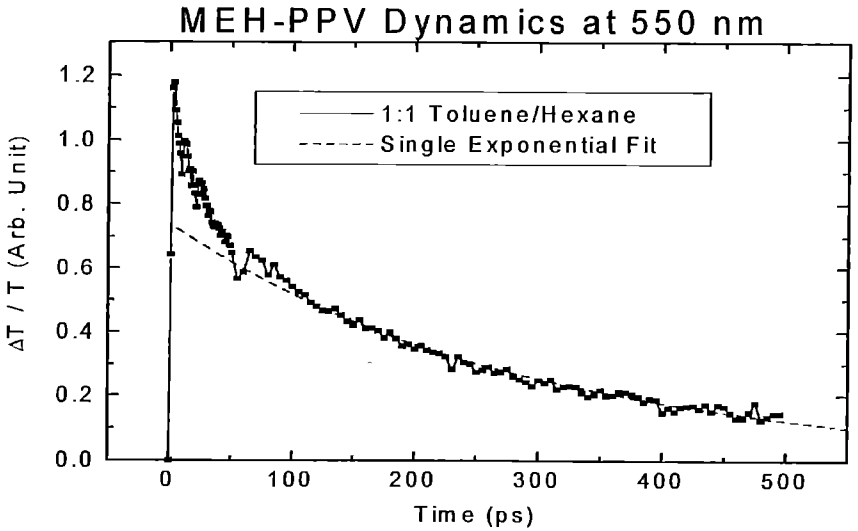
MEH-PPV Dynamics at 550 nm
1.2
1.0
0.8
0.6
0.4
0.2
0.0
ΔT / T (Arb. Unit)
1:1 Toluene/Hexane
Single Exponential Fit
0
100
200
300
400
500
Time (ps)

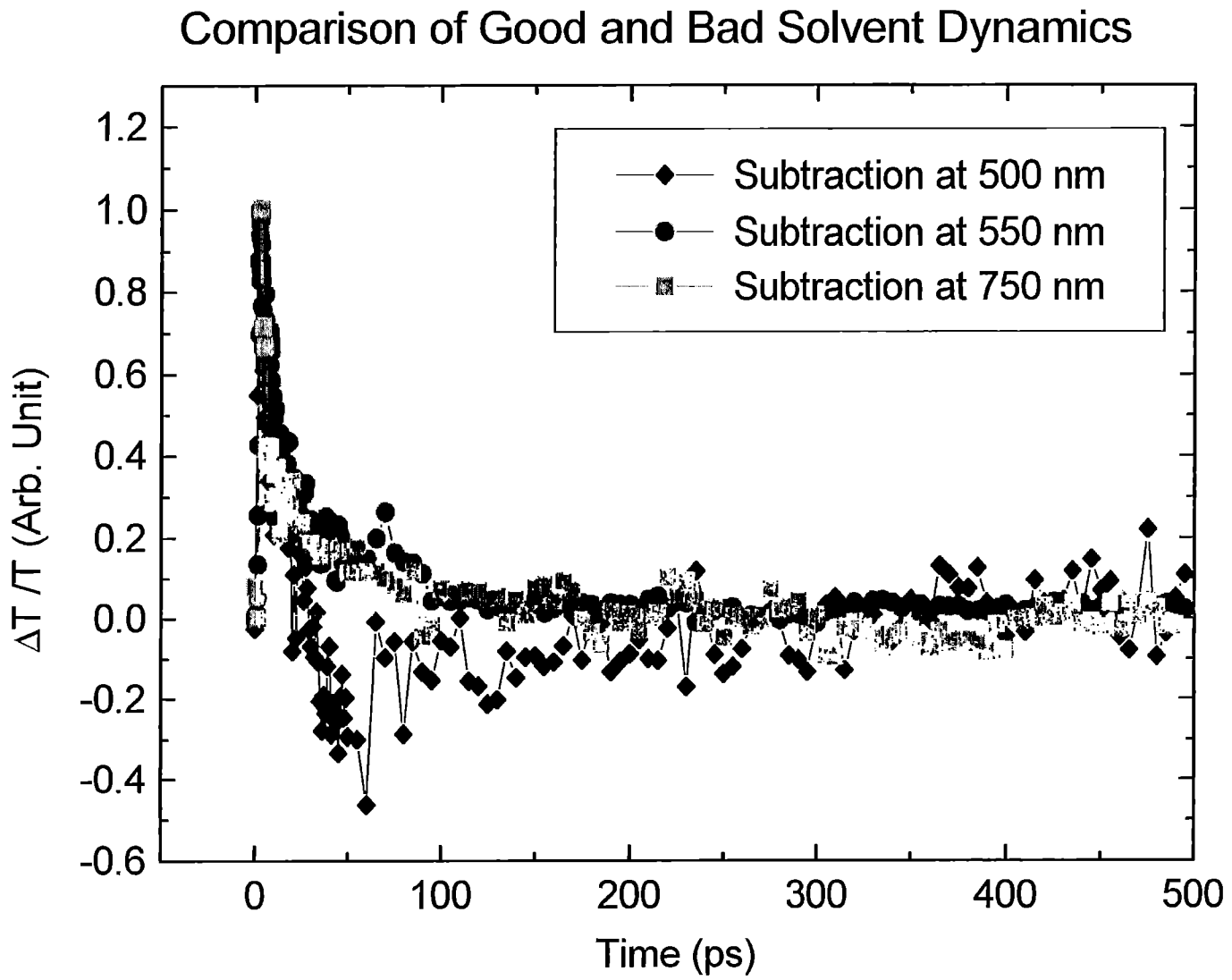

L.Rothberg, Rochester

ARO MURI

Conclusions

1. About 50% of the excitations in the more aggregated polymer solution become some species which decays non-radiatively within 50 ps at room temperature

2. The long-lived photo-induced absorption at 750 nm is due to triplet states

Future Work

Carry out measurements on film, compare the spectra of unknown species in solution and film

Electrochemiluminescent Systems

Allen Bard, Sam Jenekhe

Guoqiang Gao, Mihai Buda

Rebbeca Lai, Eve Fabrizio

Types of Electroluminescent (EL) Devices

- Inorganic EL
- Electrogenerated Chemiluminescence (ECL)
- Organic EL (Polymer, Alq)
- Hybrid Systems

- Applications
  - —Displays
  - —Lasers
  - —Analytical Devices

Key Issues - Devices

- Efficiency
- Stability (Life)
- Cost
- Manufacturability

Key Issues - Science

- Degradation mechanisms
  - ❽Materials, substrates, contacts
- Mechanism of light generation
  - —Radiative vs. nonradiative processes
  - —Singlet:triplet ratios
- Electroluminescent vs. Electrochemical Mechanisms
  - —Injection contacts
- Carrier Mobility

Solid State Organic Light-Emitting Diode (OLED)

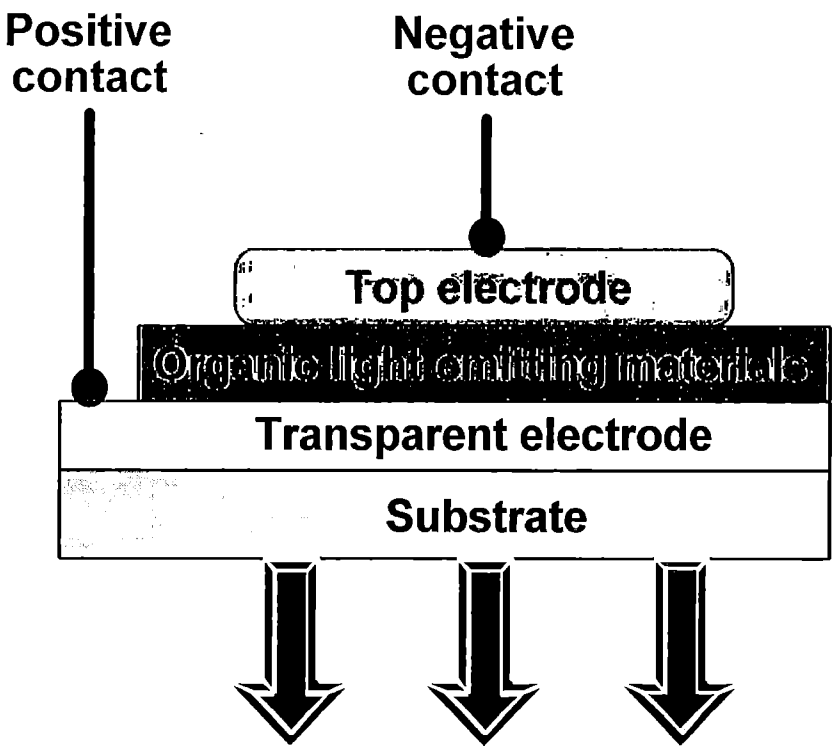

Calcium, aluminum, In/Ga

Organic molecules, polymers

ITO (Indium/Tin Oxide)

Glass or plastic

Solid State $Ru(bpy)_3(ClO_4)_2$ Cell

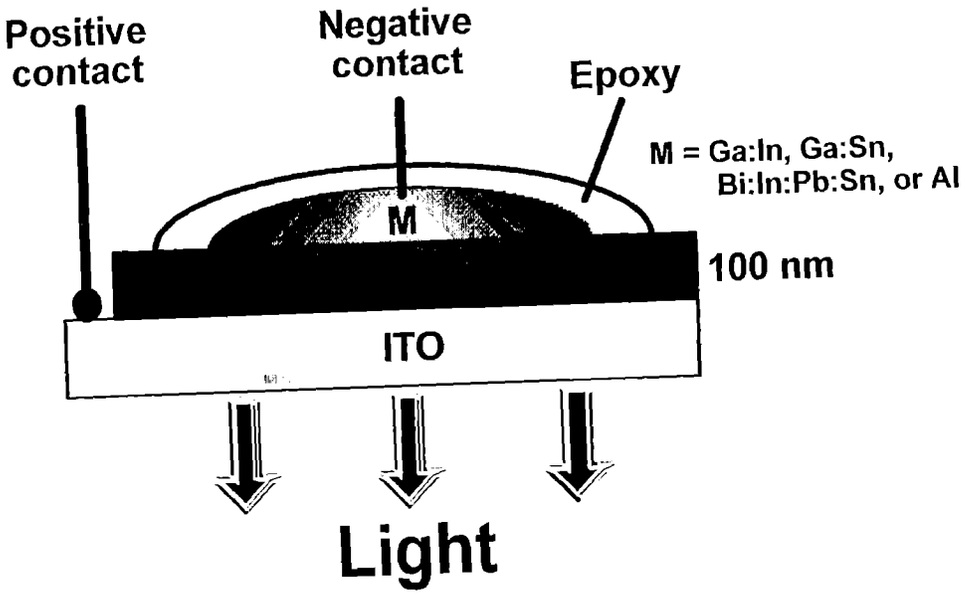

Thin Film of 3 Layers Spin-Coated On ITO

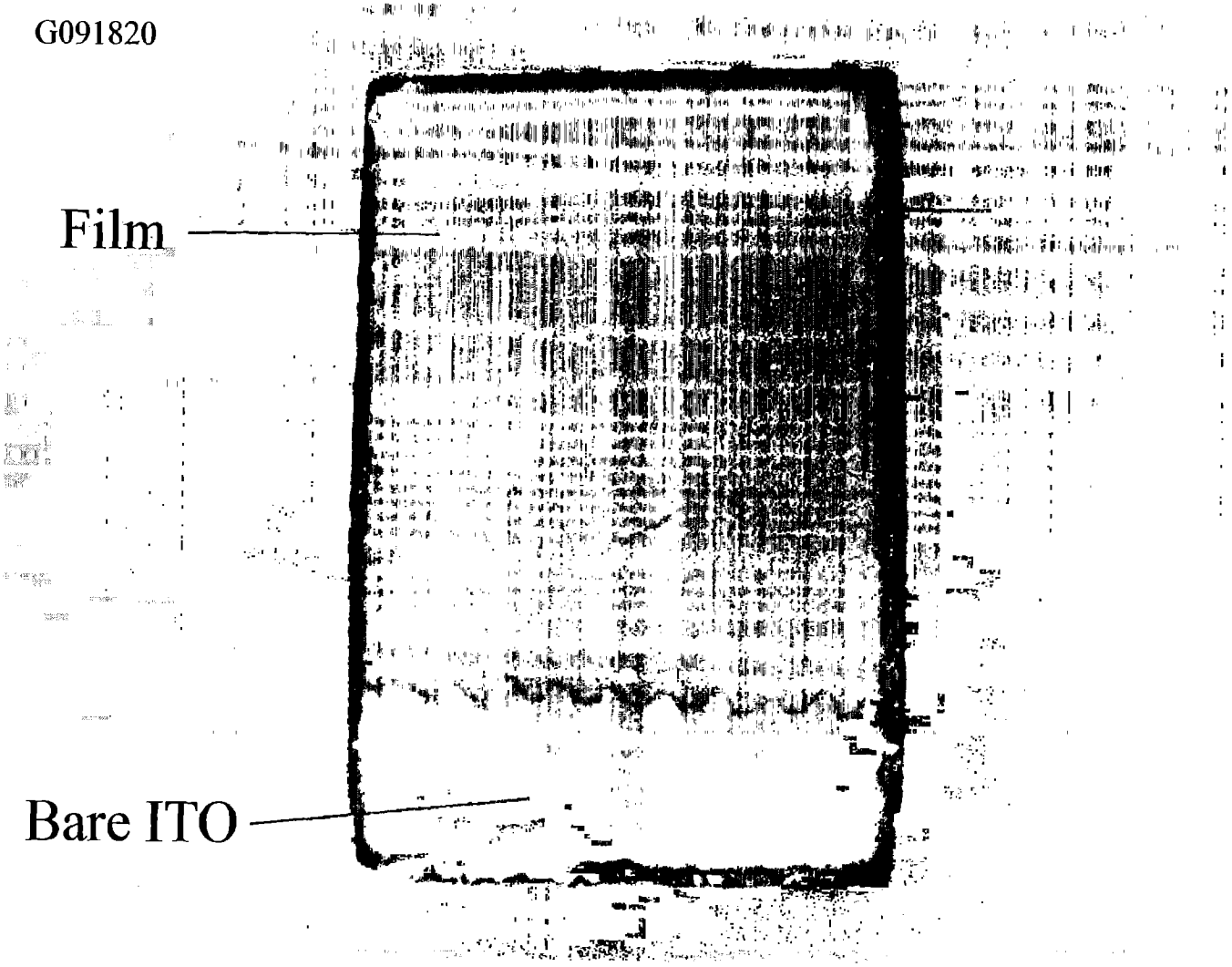

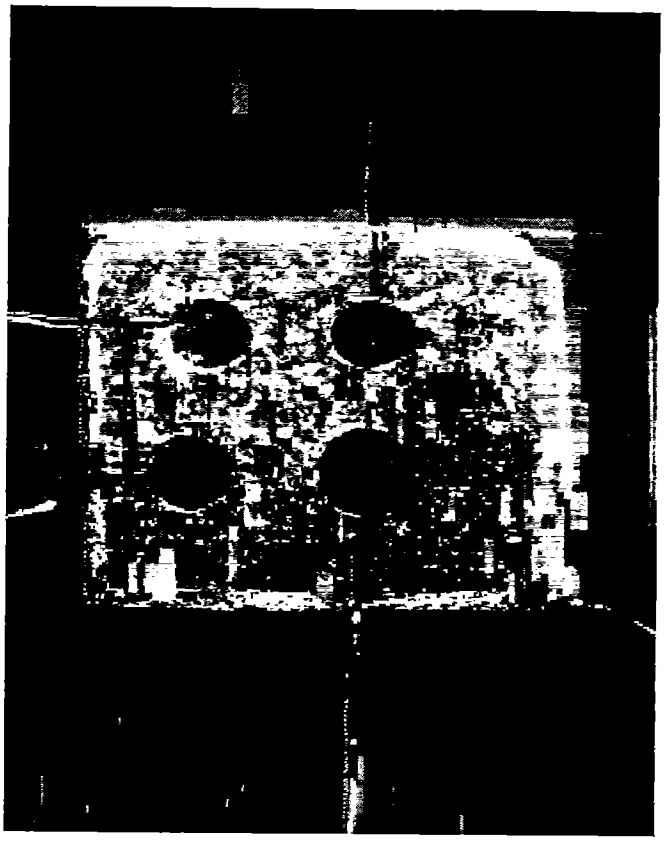

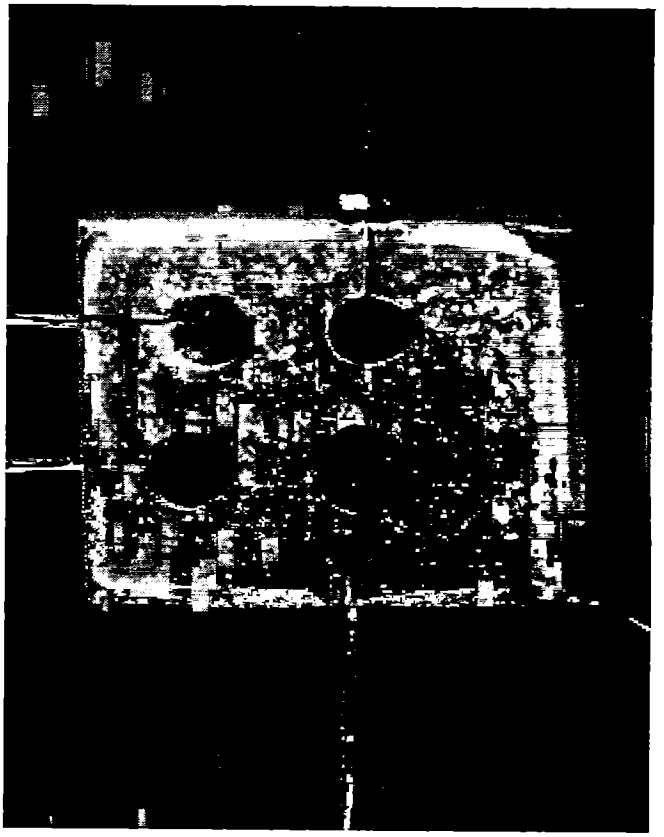

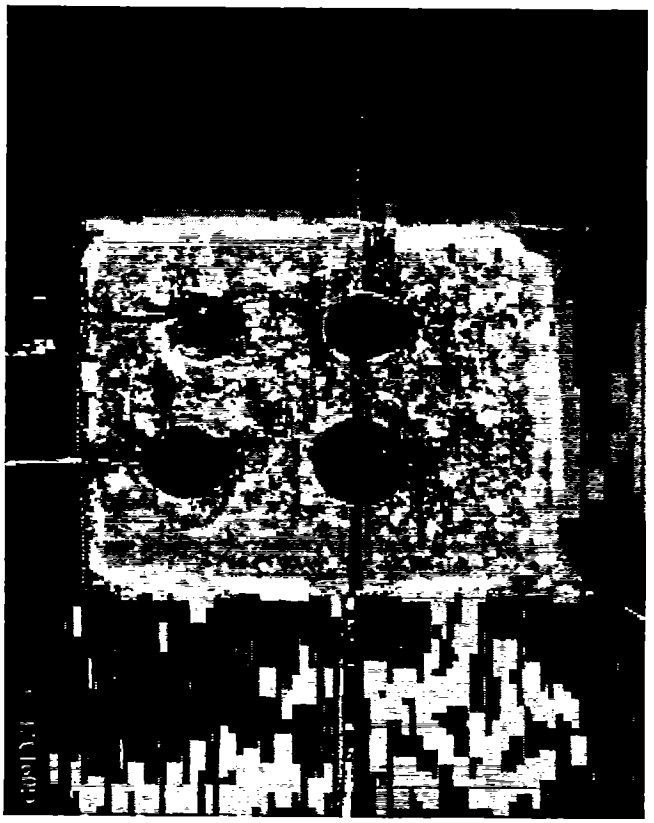

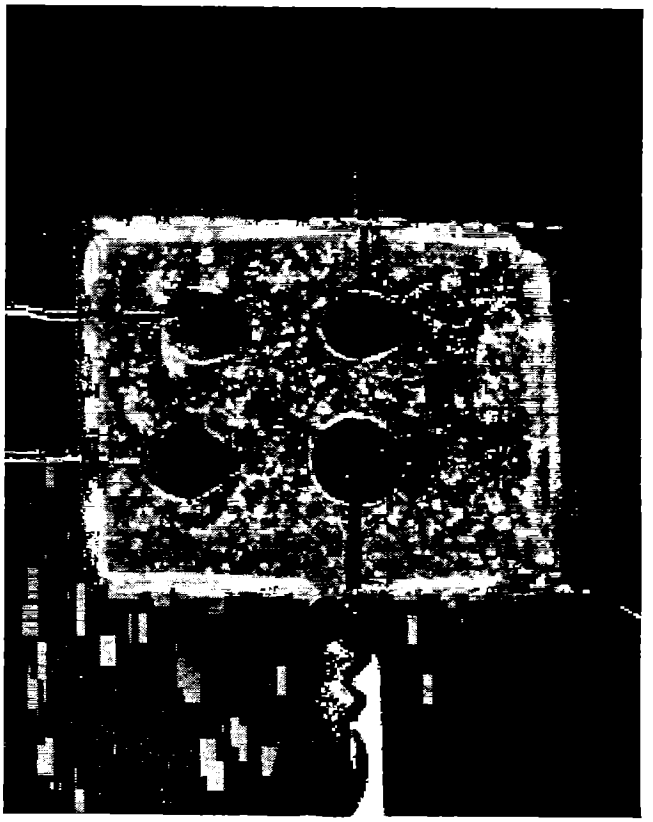

Luminescence Spectrum of An OLED

Inset: UV-vis Absorption Spectrum Of The Film

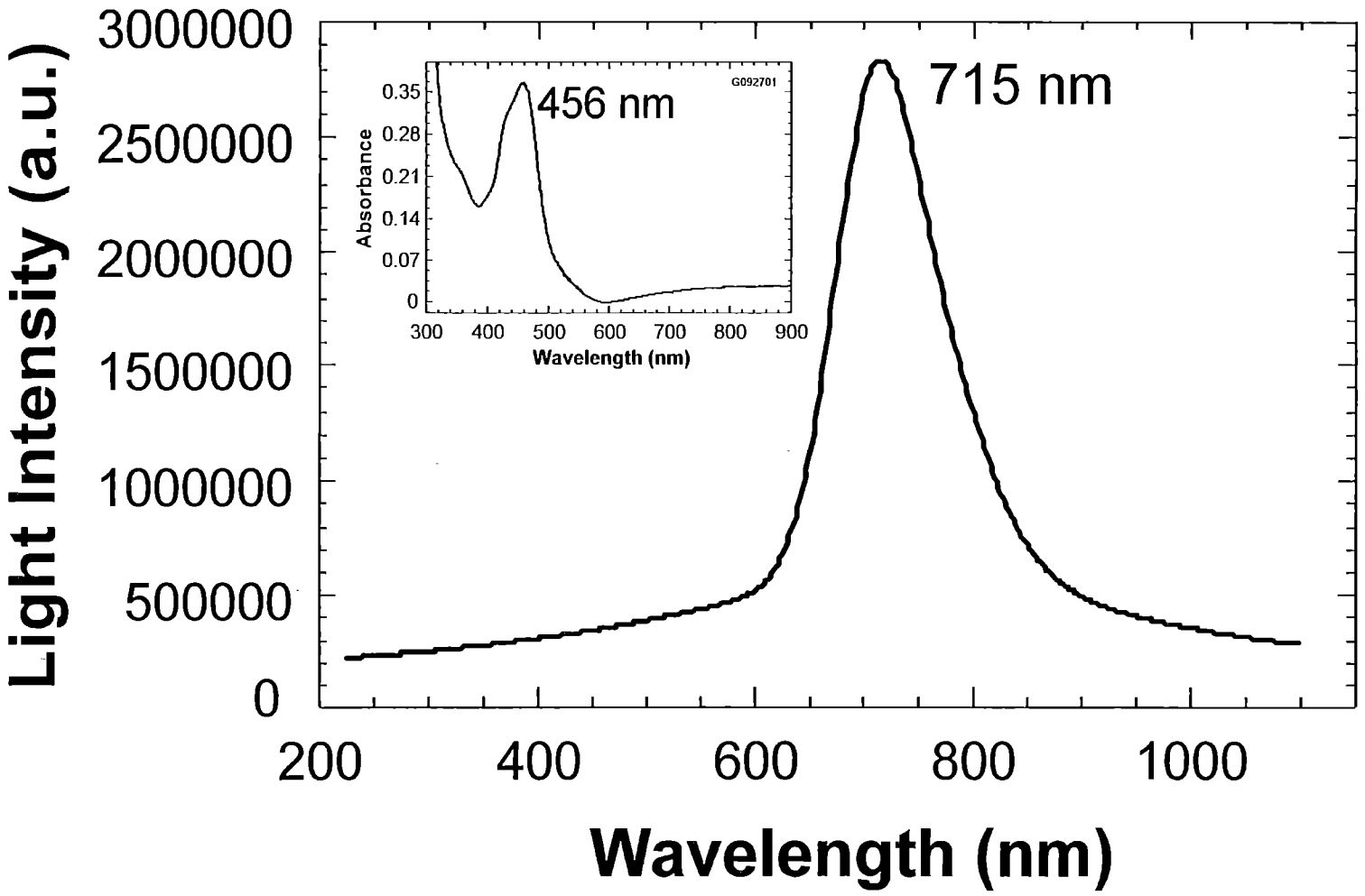

Light-Voltage (red) And Current-Voltage (blue) Plots For An OLED

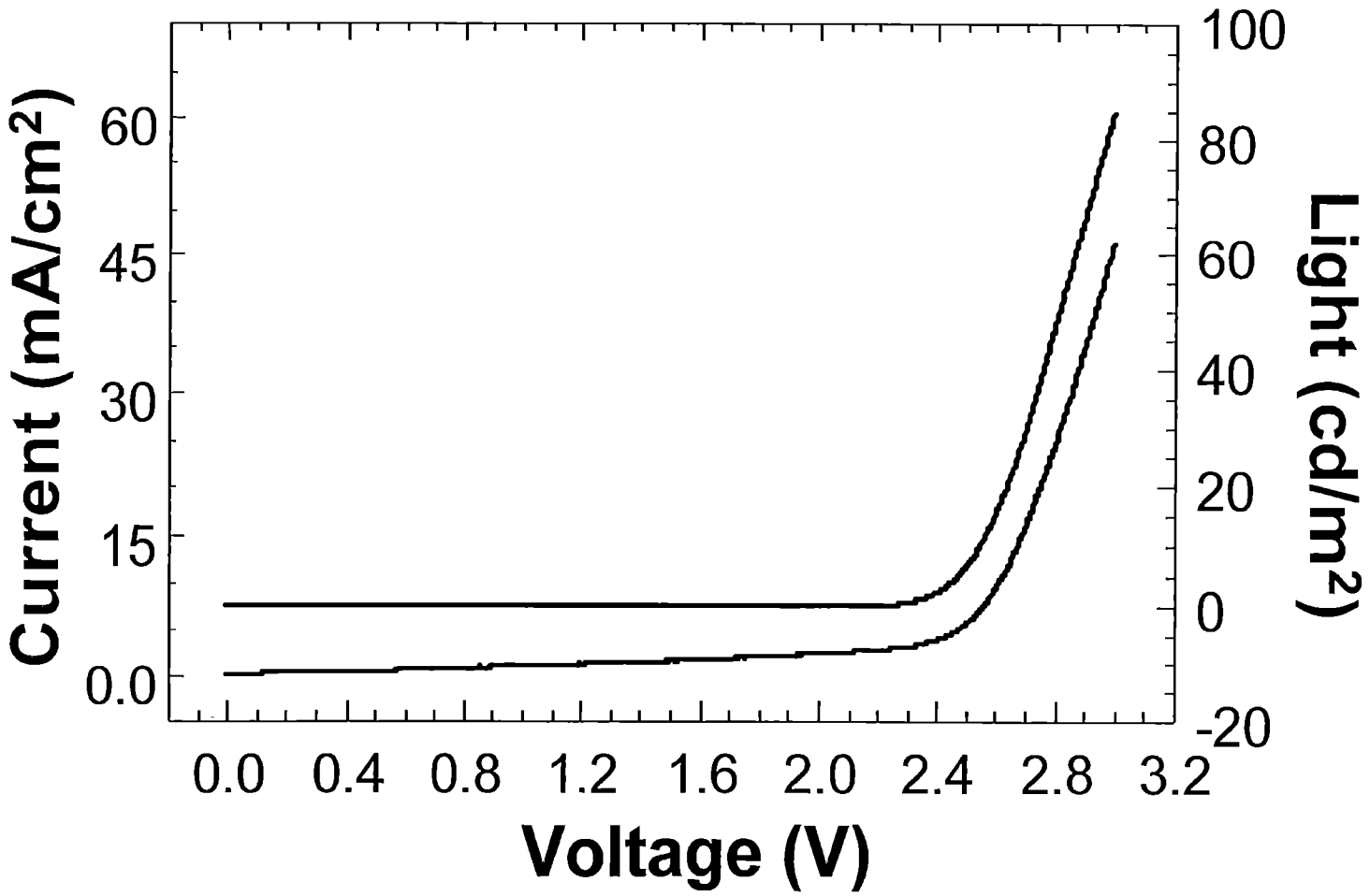

Light Emission Intensity Of 200 cd/m^2 At 5 V Was Realized For An OLED

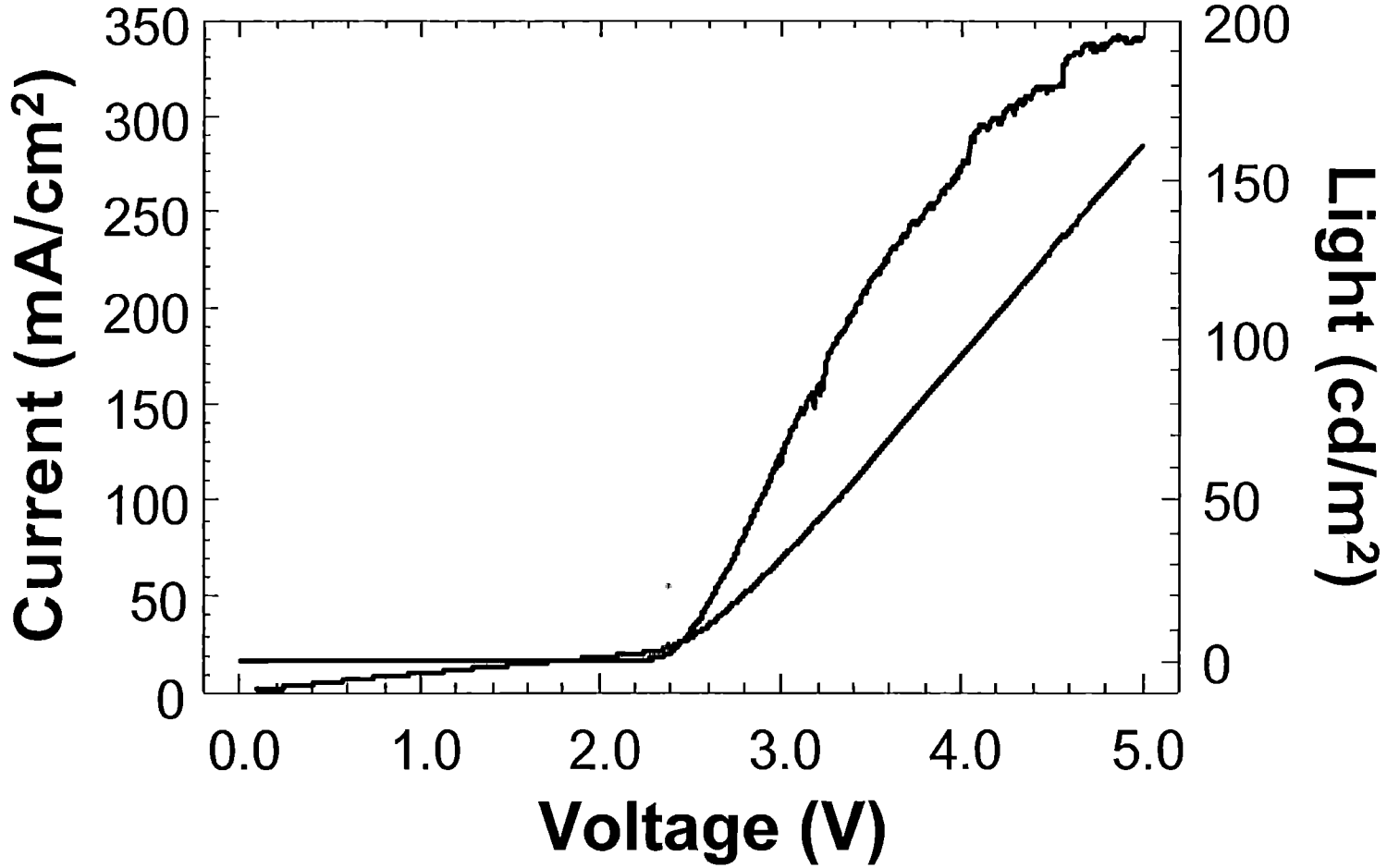

Light And Current As A Function Of Time Upon 0 - 3 V Voltage Steps

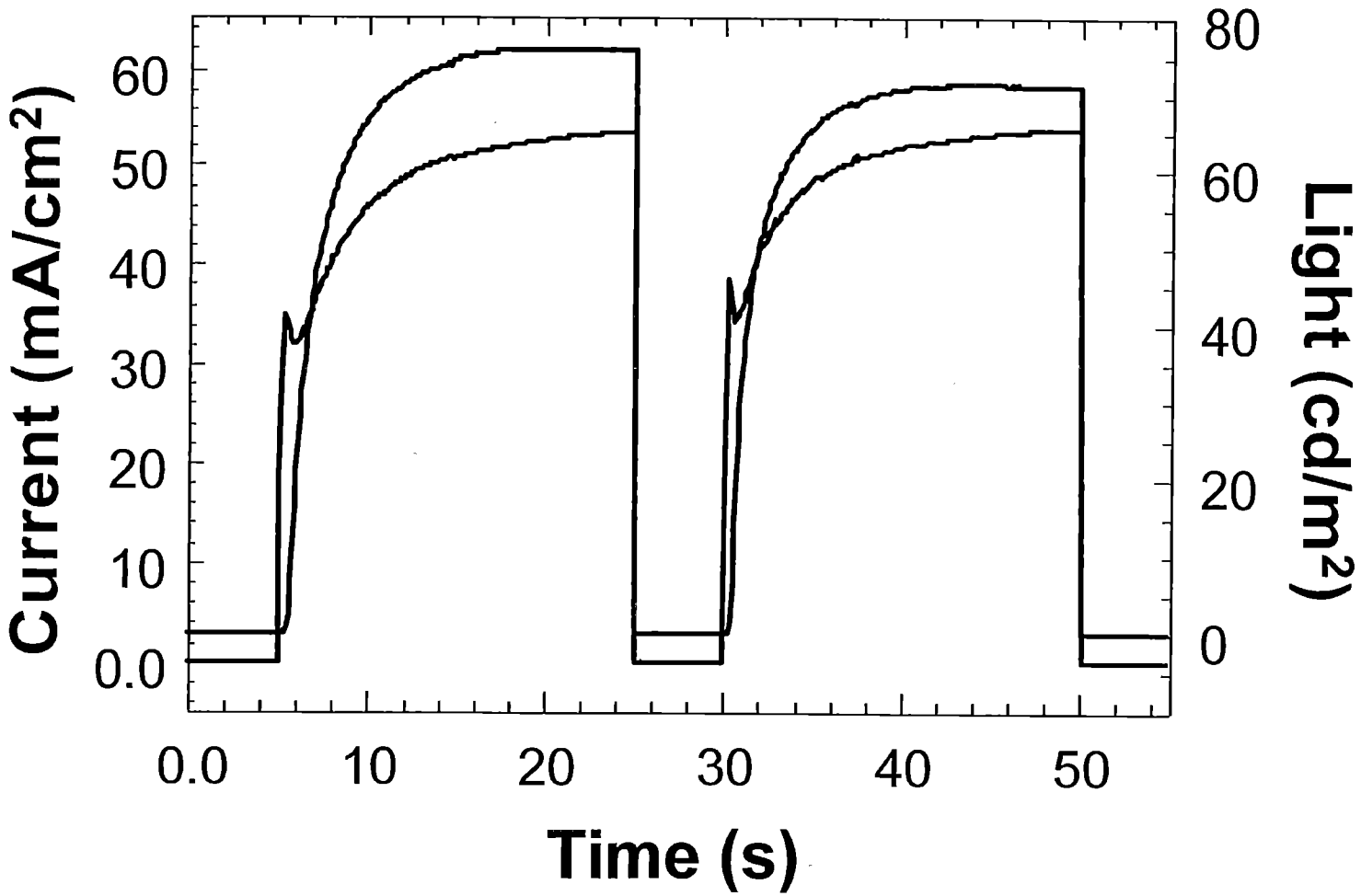

Light Output As A Function Of Time (2.8 V hold)

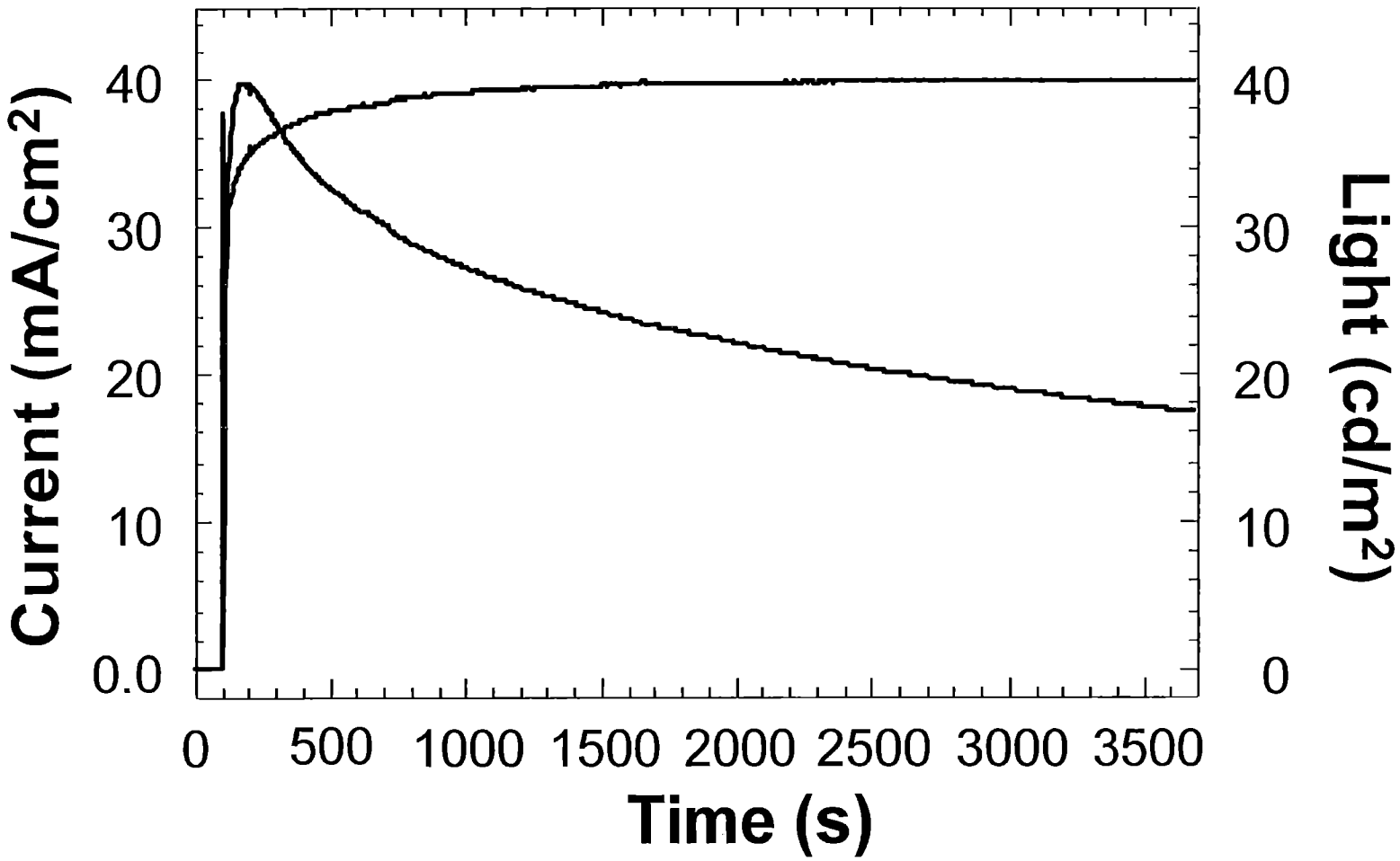

Cartoon Of The Bimolecular Hopping Transport Of Electrons Between Ru(II) And Ru(III) Sites And Ru(I) And Ru(II) Sites

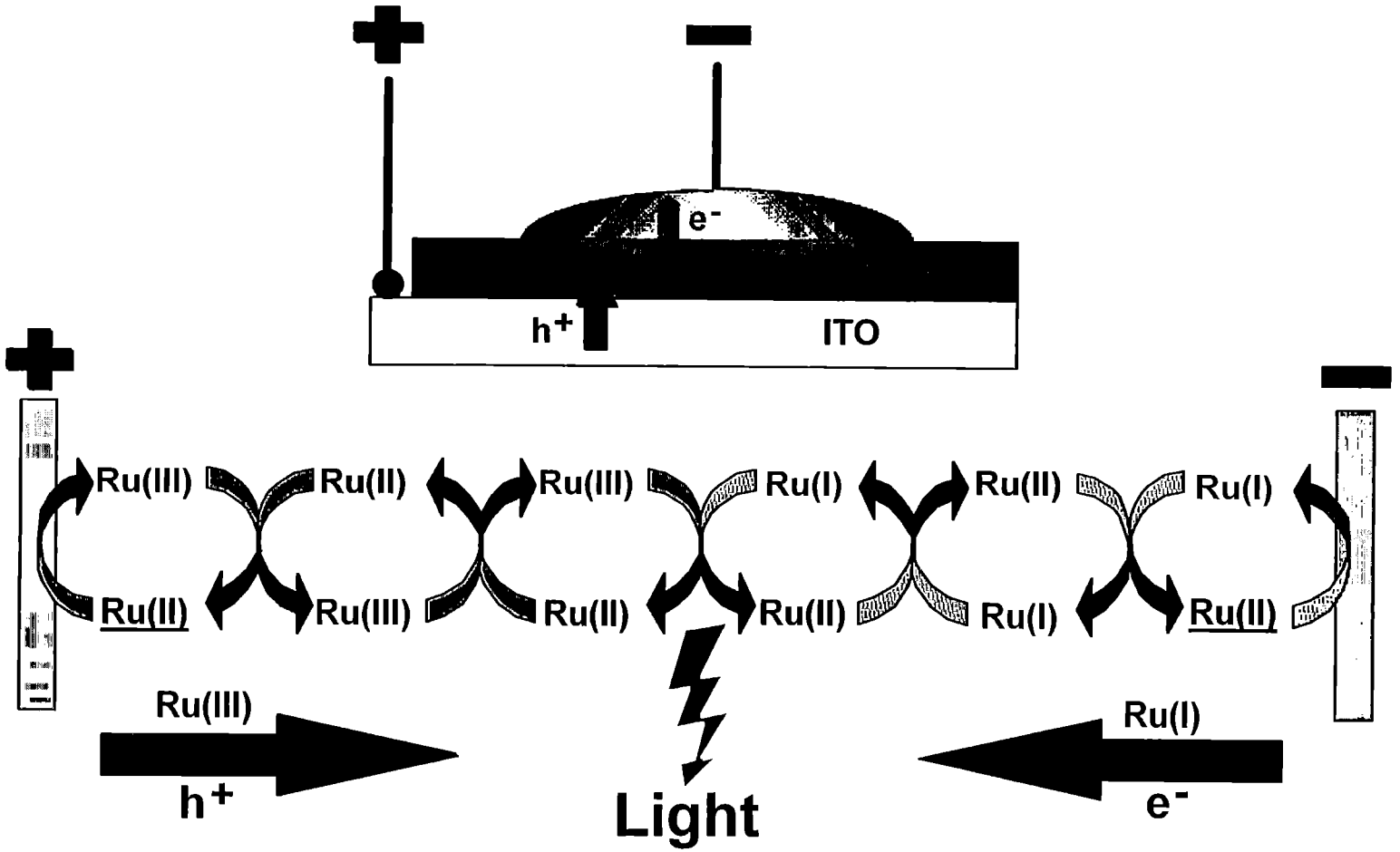

Current-voltage and luminance-voltage characteristics (50 mV/s)
ITO/$Ru(bpy)_3(ClO_4)_2$ (~150 nm)/Ga:Sn;

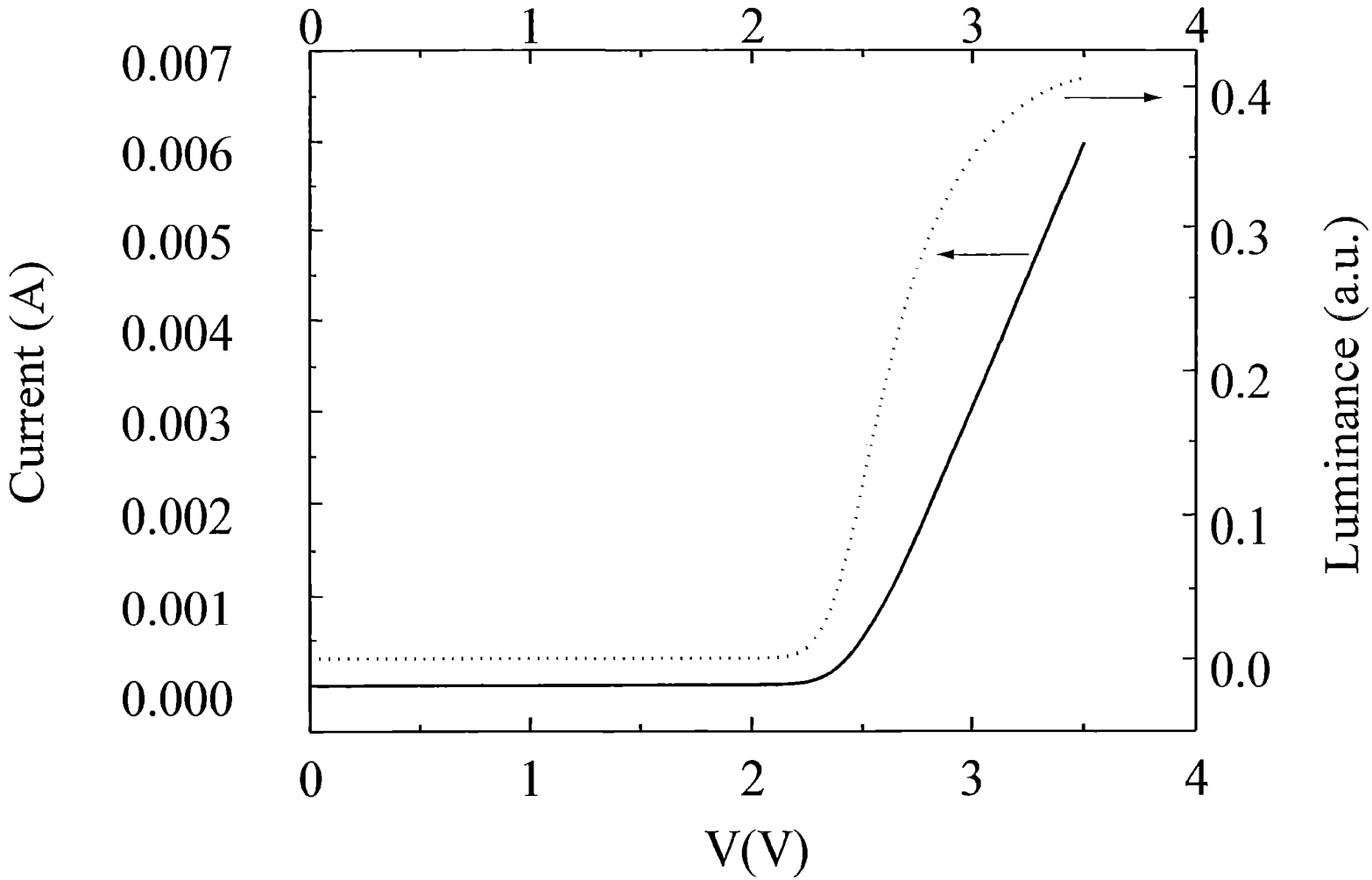

Current-voltage and luminance-voltage characteristics (50 mV/s)

ITO/$Ru(bpy)_3(ClO_4)_2$(~100 nm)/Au;

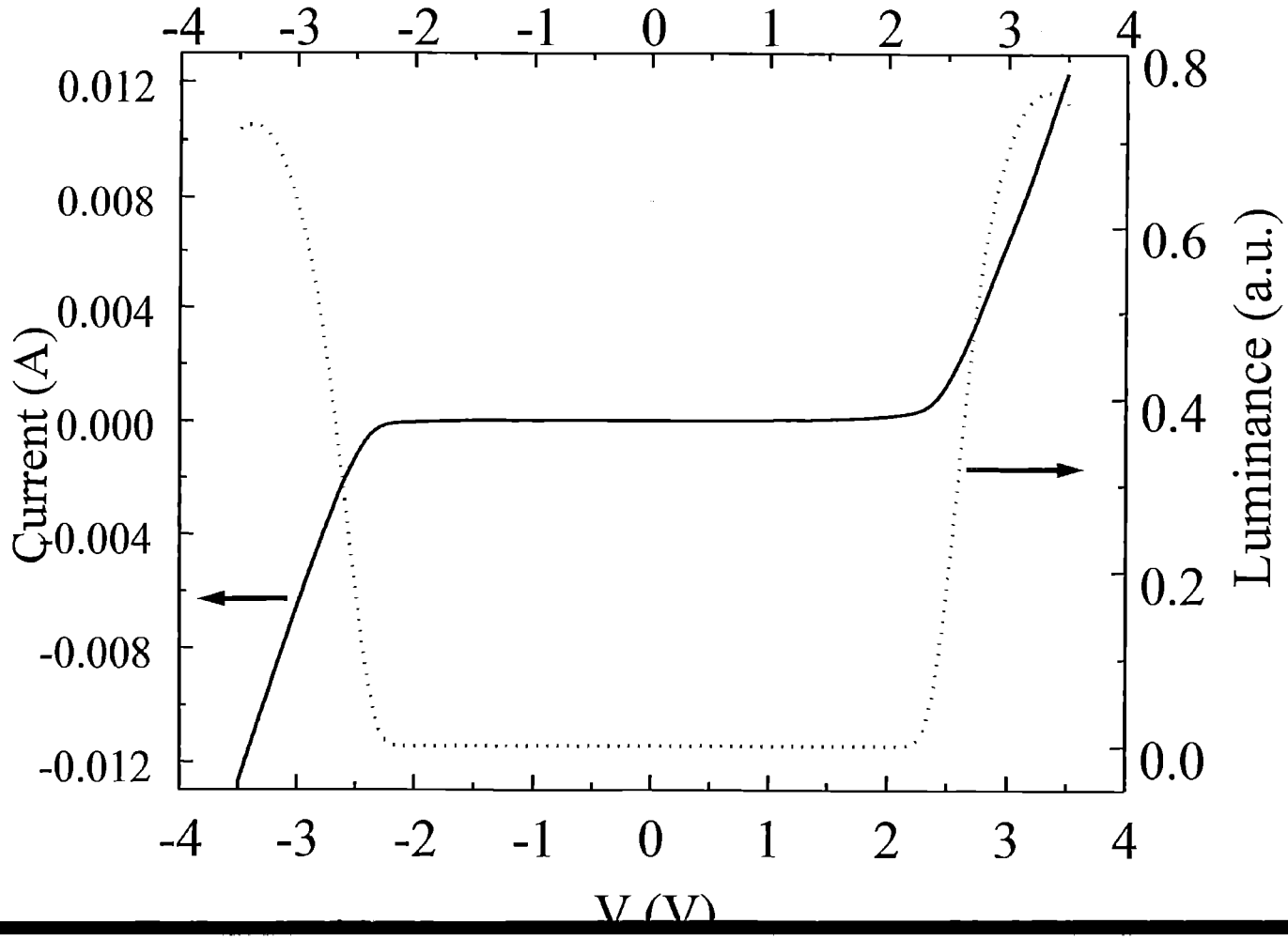

Quantum efficiencies (50 mV/s)
ITO/$Ru(bpy)_3(ClO_4)_2$/Ga:Sn

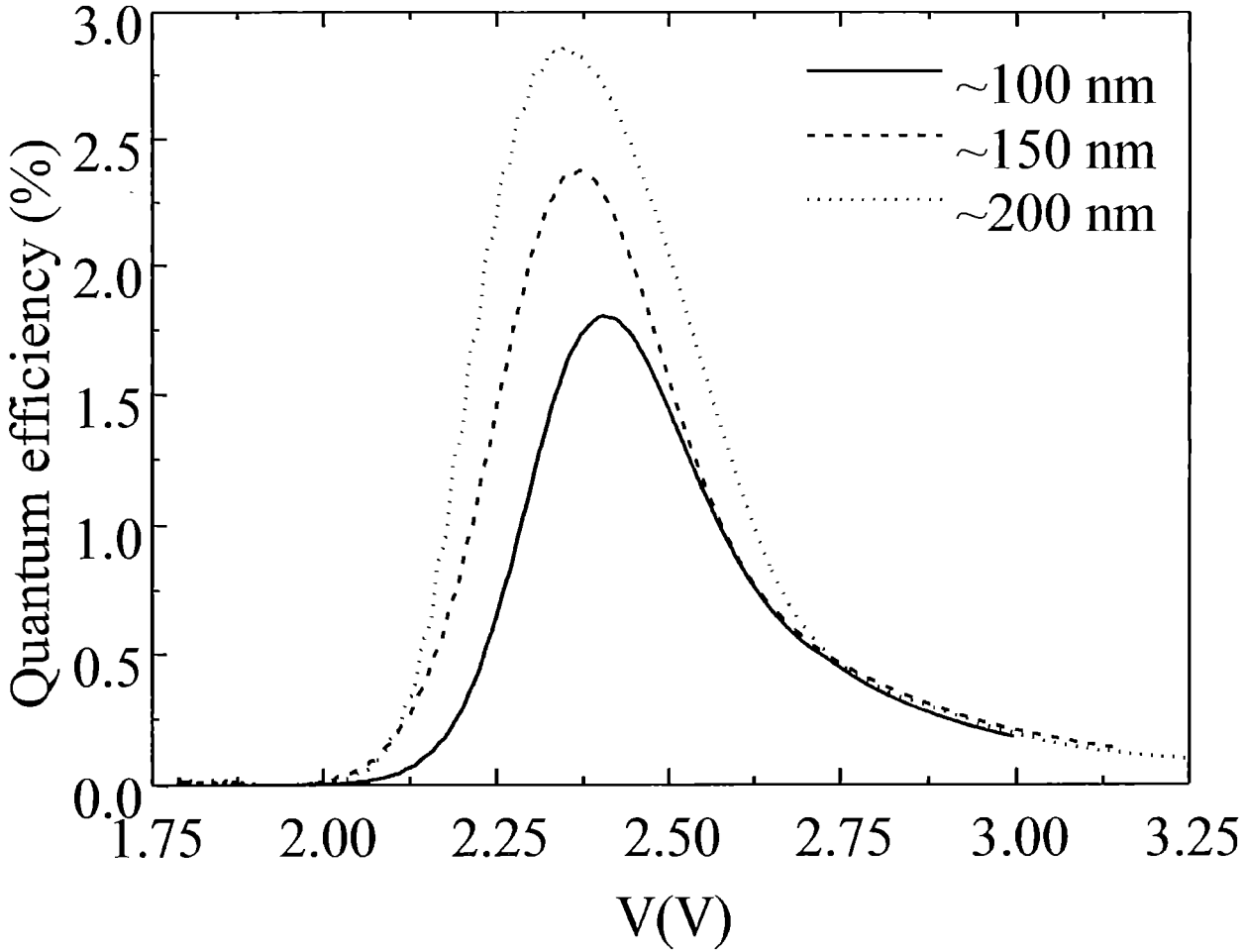

Current-time and luminance transients
2.75 V hold
ITO/$Ru(bpy)_3(ClO_4)_2$ (~150 nm)/Ga:Sn

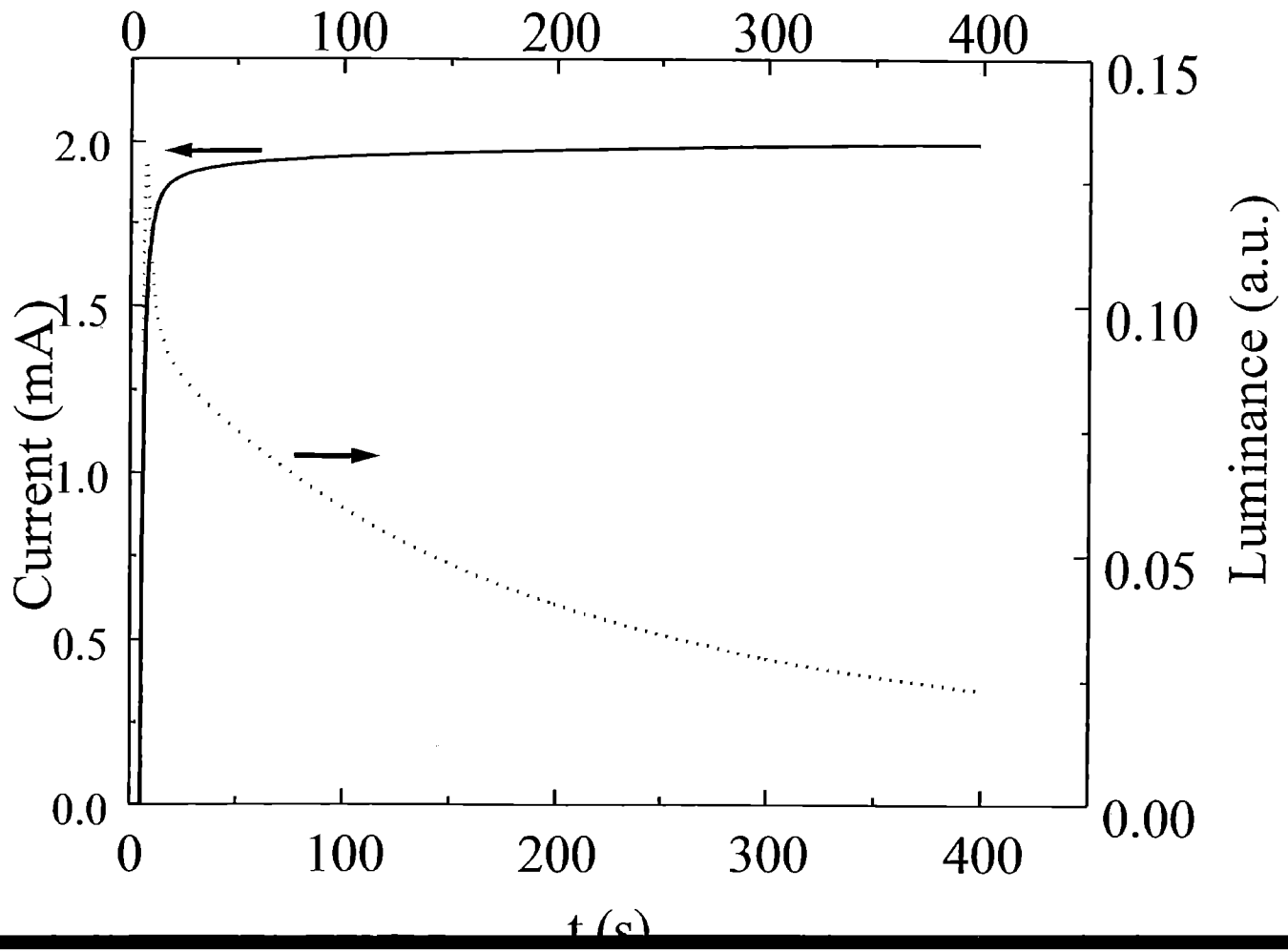

Current-time and luminance transients
2.25 V hold
ITO/$Ru(bpy)_3(BF_4)_2$ (~150 nm)/Ga:Sn

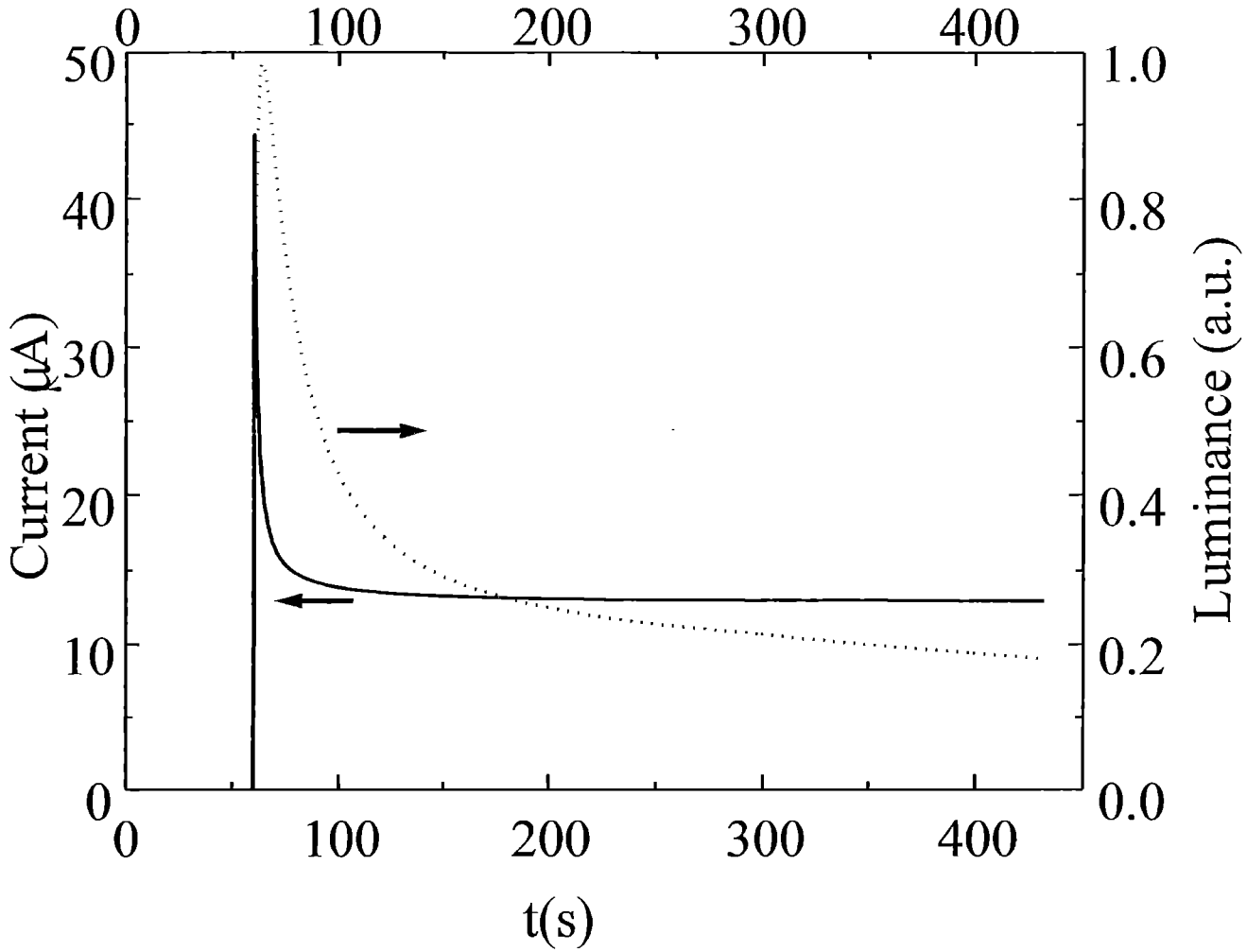

Current-time and luminance transients

2.5 V hold

ITO/$Ru(bpy)_3(PF_6)_2$ (~200 nm)/Ga:Sn

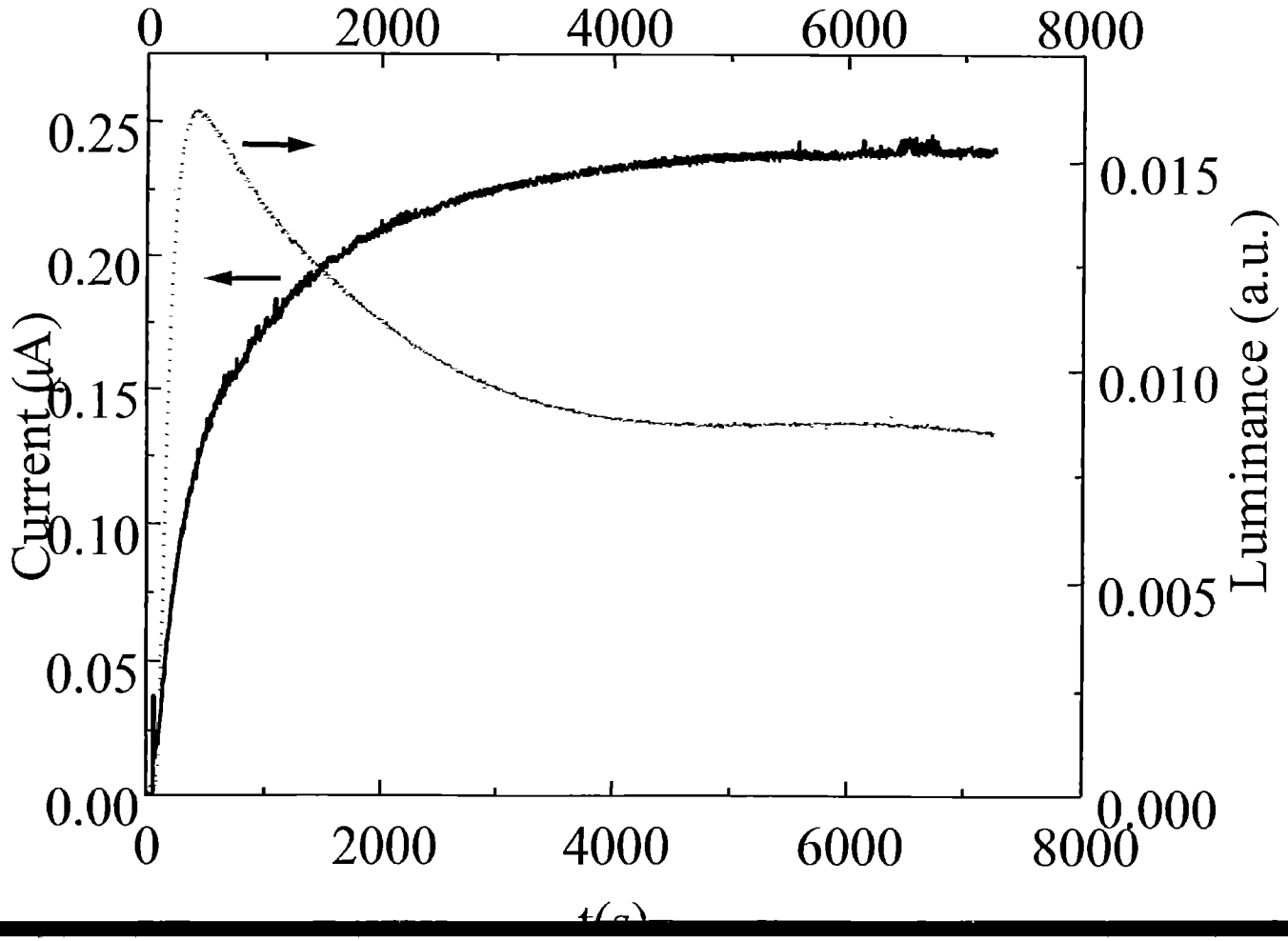

Transient luminance at short times:
ITO/$Ru(bpy)_3(ClO_4)_2$(~100 nm)/Ga;Sn

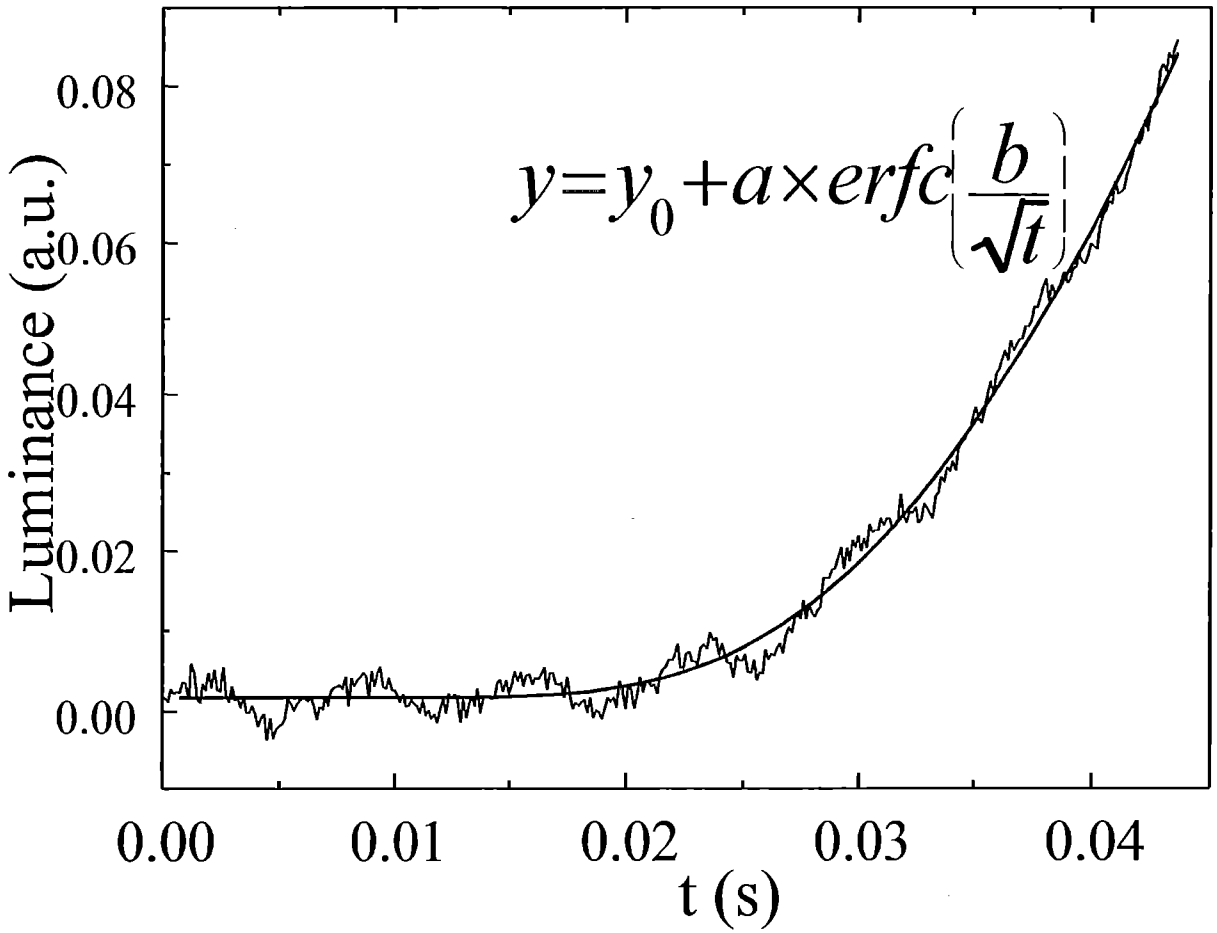

Anion	D_{app} (cm^2/s)
BF_4^-	$\sim 10^{-9}$
ClO_4^-	$\sim 10^{-10}$
PF_6^-	$\sim 10^{-13}$
AsF_6^-	$\sim 10^{-14}$

Electrochemistry and ECL of Bis(4-phenylquinoline)-10-Methylphenothiazine (BPQ-PTZ)

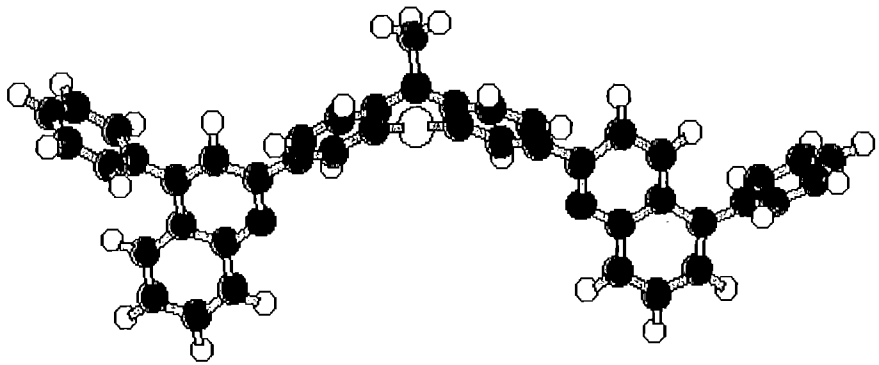

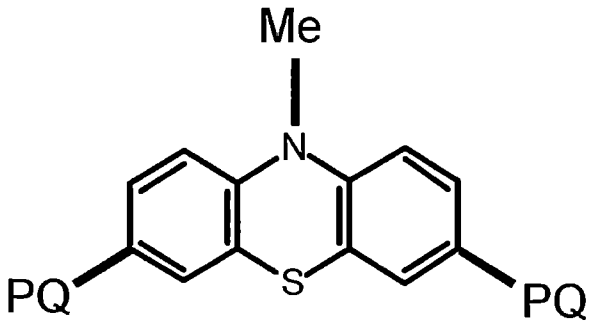

PQ =

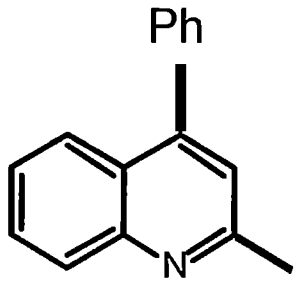

Absorption and Photoemission of BPQ-PTZ in Benzene/MeCN

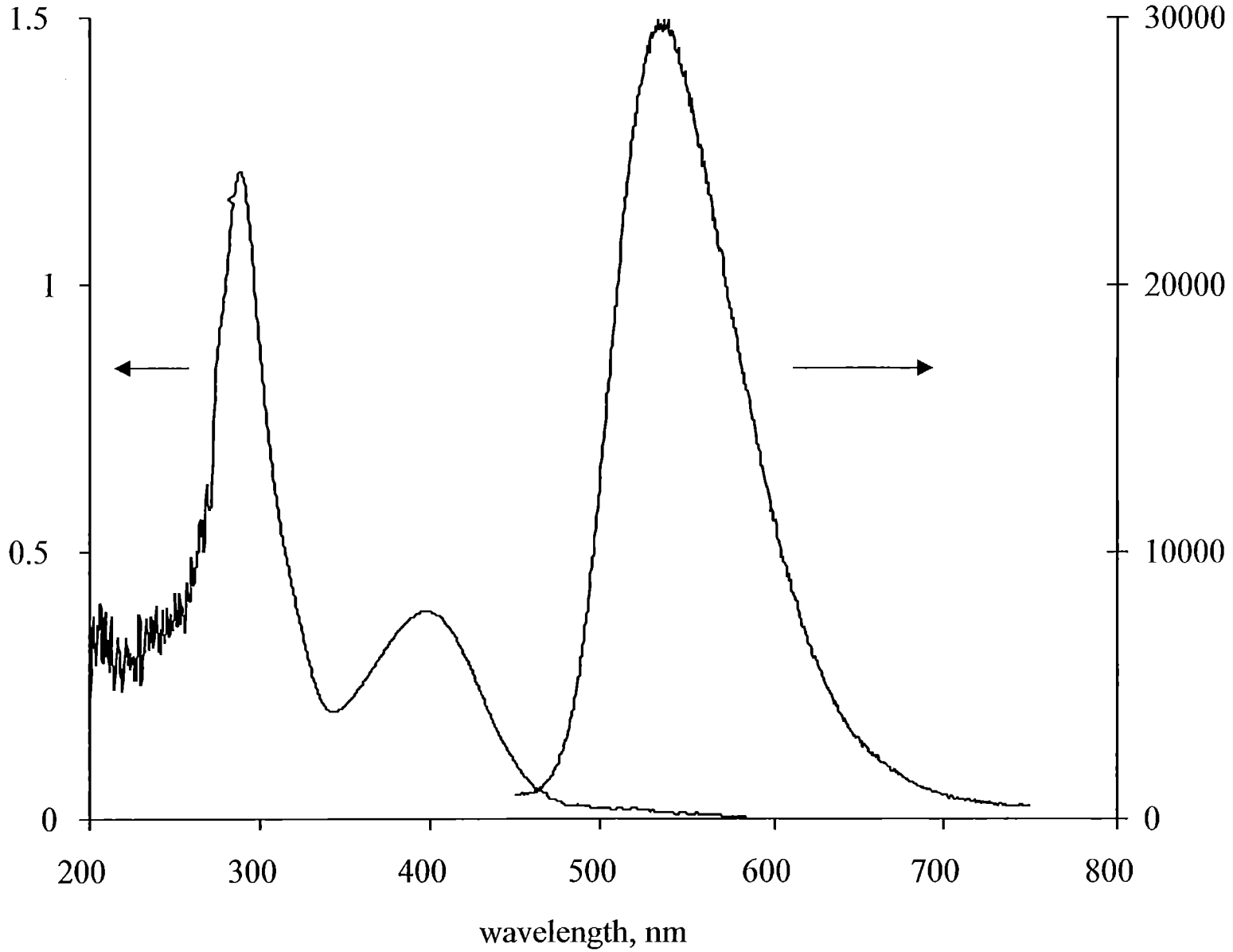

Cyclic Voltammogram of BPQ-PTZ (0.67 mM) in 0.1 M TBAP in Benzene/MeCN at Pt Electrode at 250 mV/s

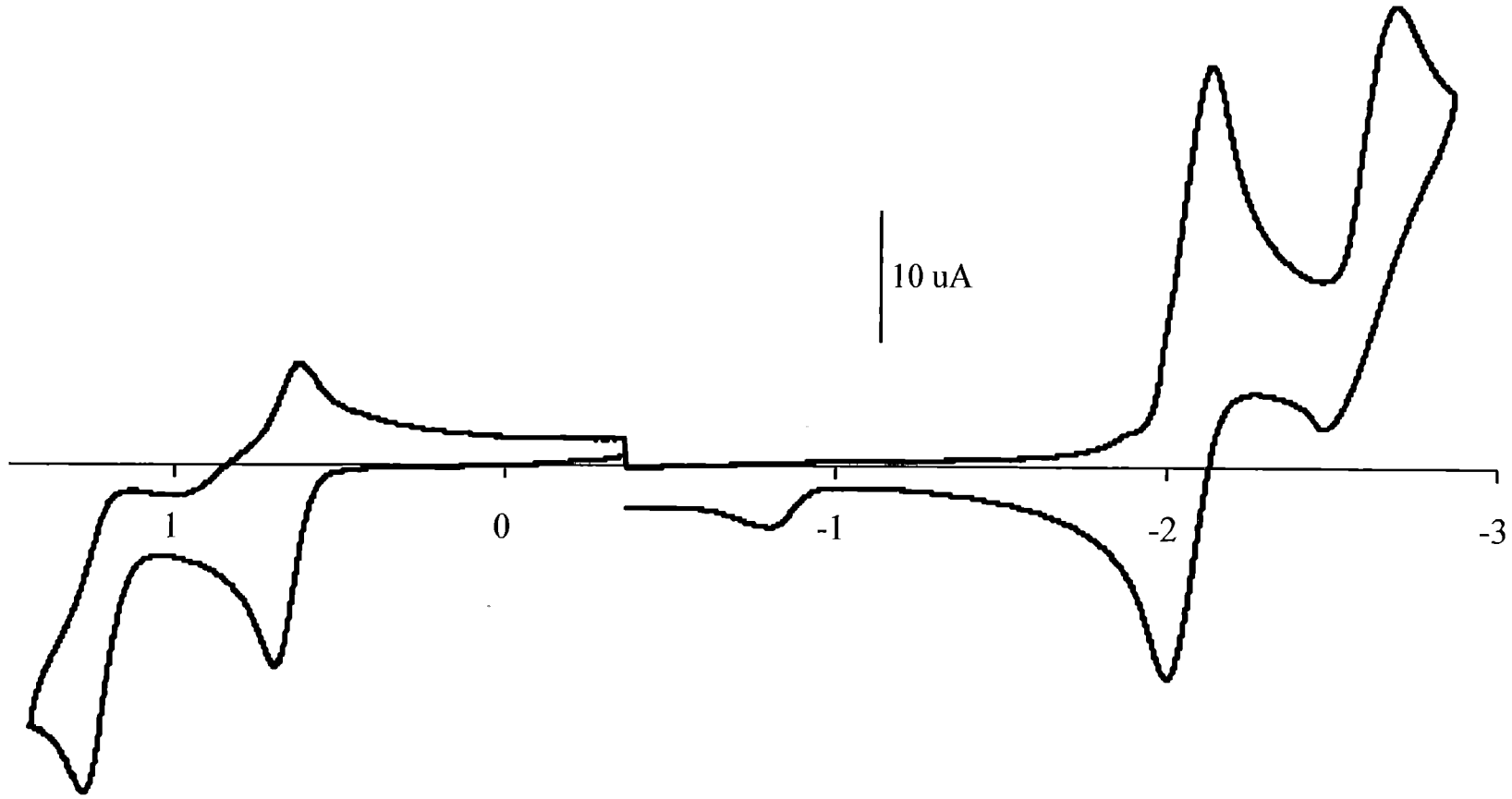

ECL of BPQ-PTZ in Benzene/MeCN

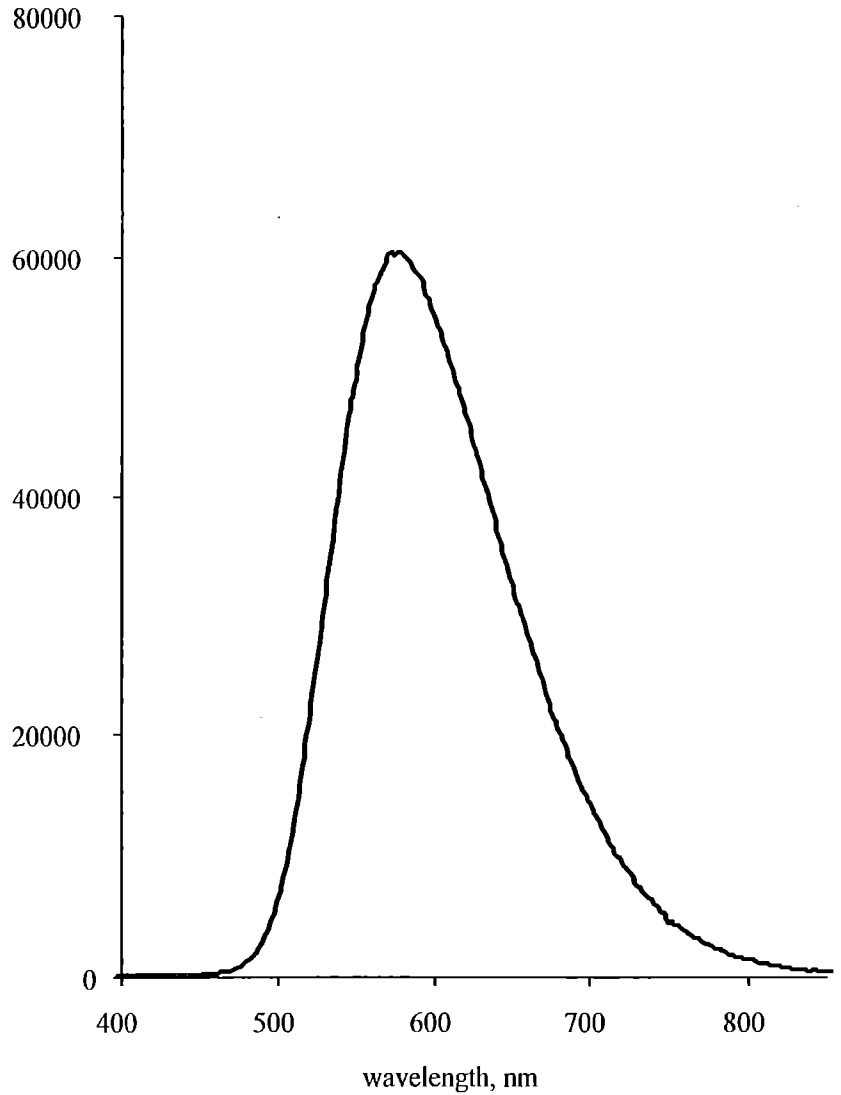

Thin Film Electrochromic Devices

ARO TOPS MURI

Dean M. DeLongchamp
Professor Paula T. Hammond

Electrochromism

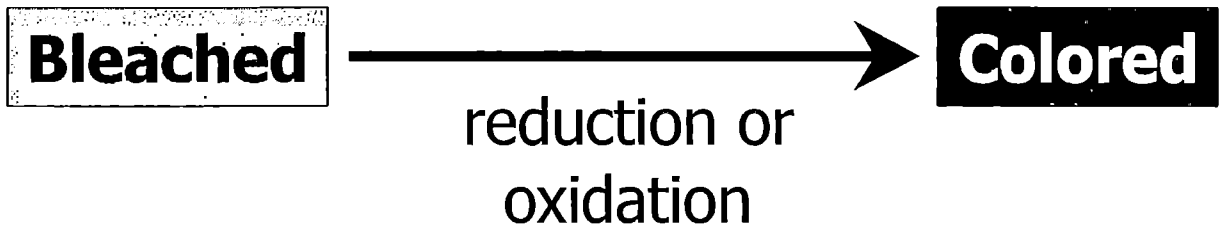

- Color by Reduction - *Cathodic electrochrome*

  + → o or **o → −**

- Color by Oxidation - *Anodic electrochrome*

  − → o or **o → +**

Transition: IR → Vis or UV → Vis

Current Shortcomings of ECDs

- Switching speed of electrochromic devices (ECDs) is too slow for advanced applications.
  - Smart Windows : seconds to minutes ☑
  - Displays: milliseconds ☒
  - Optical Switches: even faster ☒

- Cycle lifetime is too short for many products.
  - Smart Windows : 10^4-10^5 deep cycles ☑
  - Displays: 10^9-10^{10} deep cycles ☒
  - Optical Switches: 10^{17}-10^{18} deep cycles ☒

- Contrast and spectral range is often poor.

Objective

Create electrochromic devices with enhanced performance using multilayering techniques.

Optimize response time, cycle life, and spectral range by choice of materials and appropriate architecture.

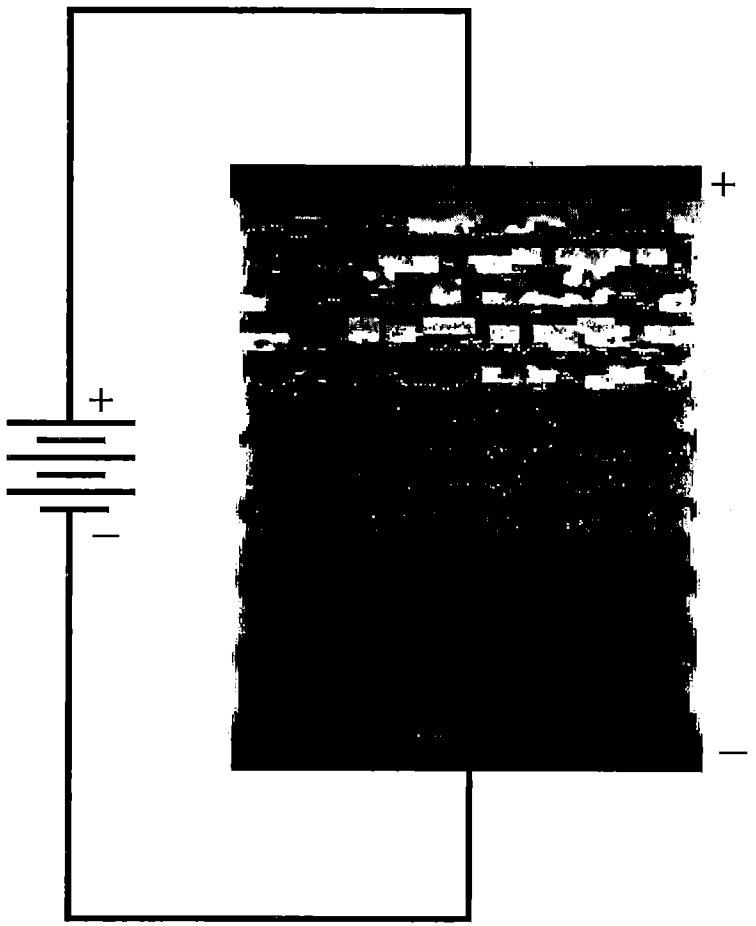

Multilayering Advantages

- Switching speed
  - Sequester polymer electrochrome at electrode
  - Combine electrochrome and transport material
  - Finely control element thicknesses
- Cycle lifetime
  - Attain high material homogeneity
  - Achieve freedom from structural defects
  - Protect from elements with cladding layers
- Contrast and spectral range
  - Influence color/contrast with counterpolyion
  - Pattern multiple electrochromes

Dual Focus

- Electrolyte
  - Evaluate the performance of ion-conducting multilayered systems
  - Determine the optimum system for ECDs
- Electrochromism
  - Characterize the electrochemistry of electrochromic multilayered systems
  - Study effects of material system and deposition conditions

Focus: Electrolyte

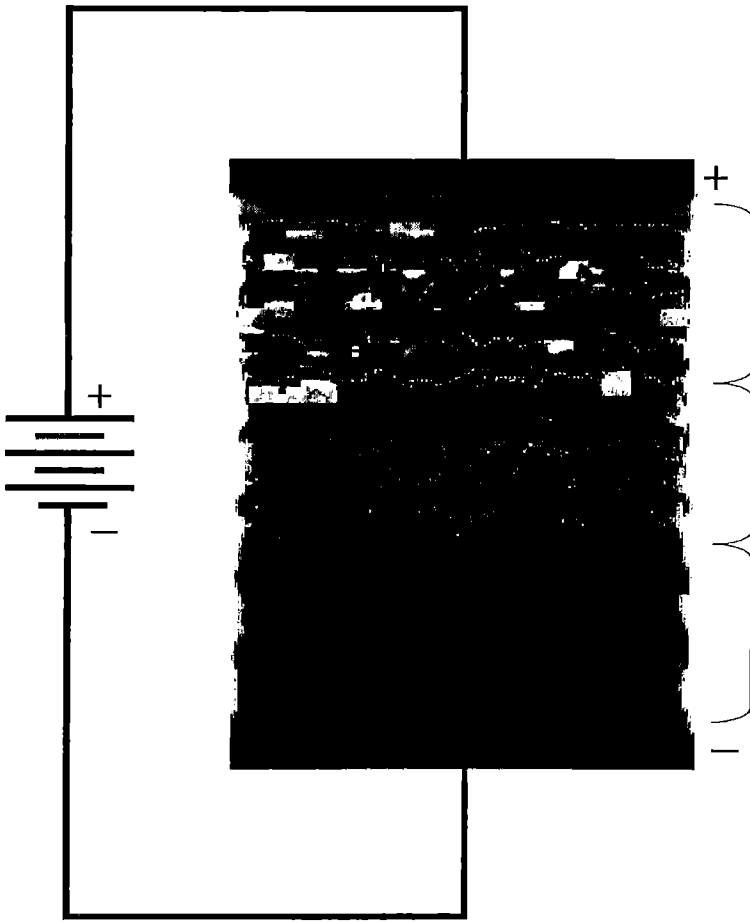

anode

electrolyte

cathode

- High ionic conductivity
- Low electronic conductivity
- Chemically robust
- Mechanically robust

Ion-Conducting Polyelectrolytes

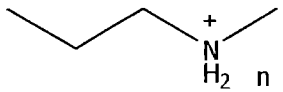

PEI

Poly(ethylene imine)

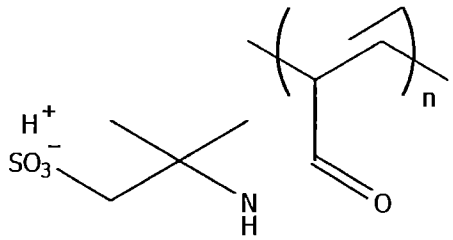

PAMPS

Poly(2-acrylamido-2-methyl-1-propanesulfonic acid)

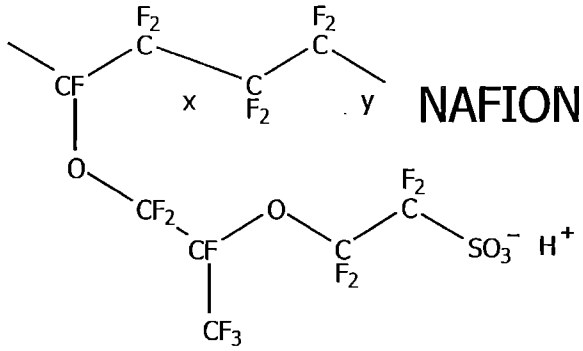

NAFION

Impedance Analysis

Impedance Analysis
Experimental Setup

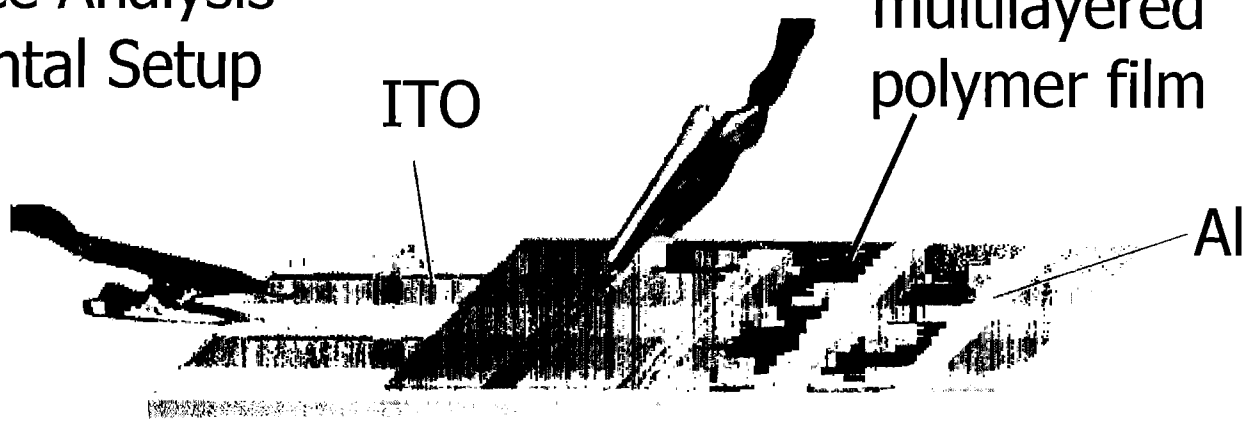

Equivalent
Circuit

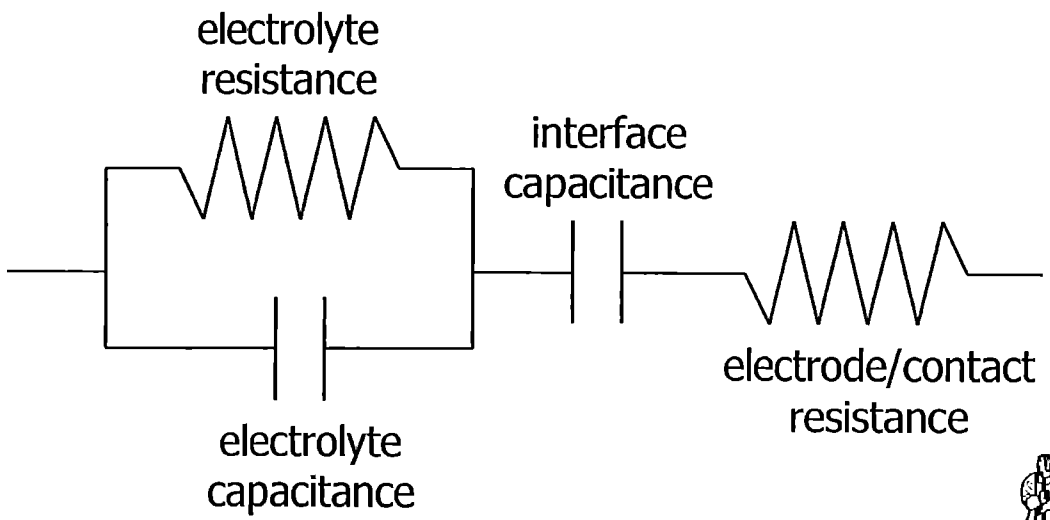

Typical Impedance Response

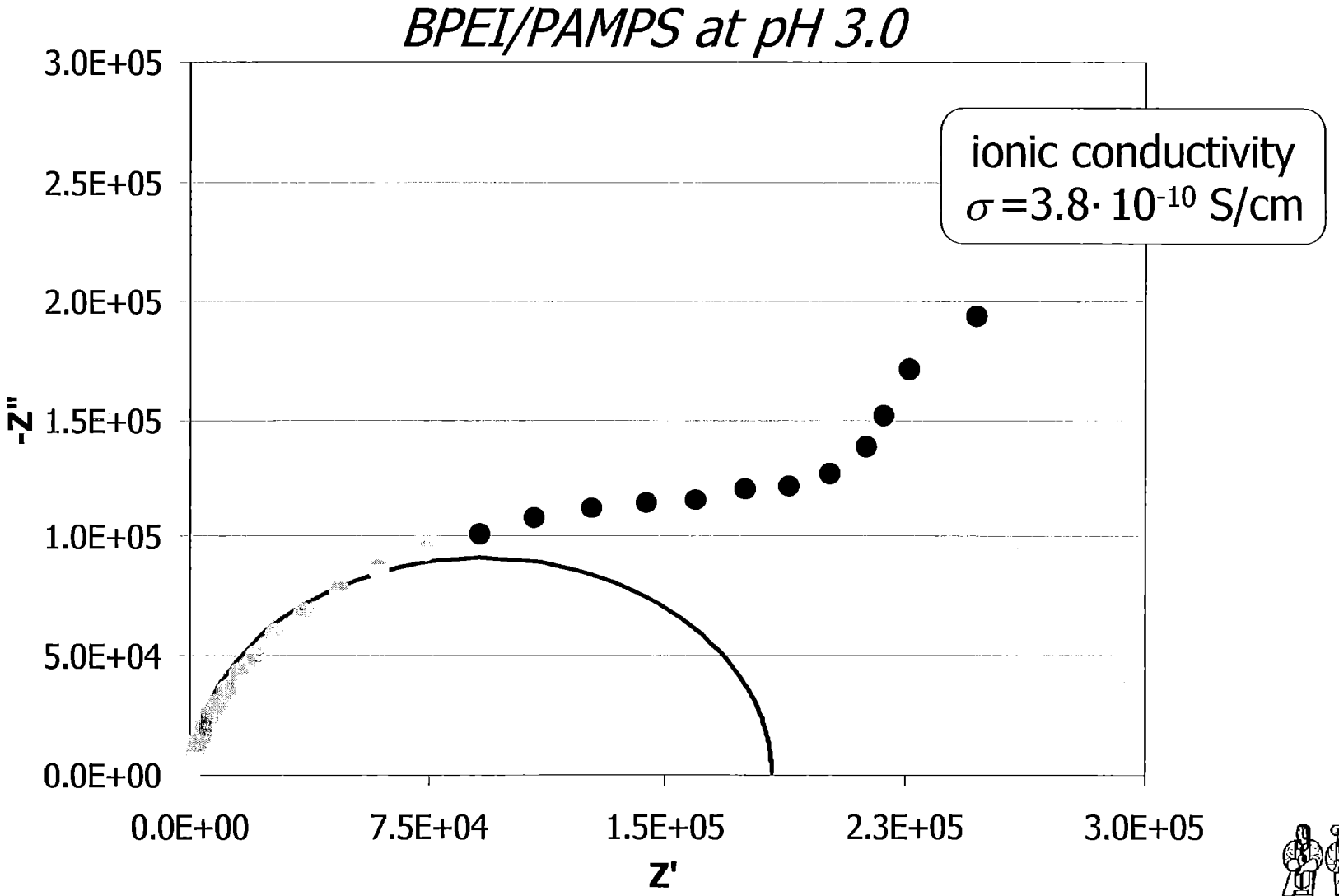

BPEI/NAFION Conductivity Trend

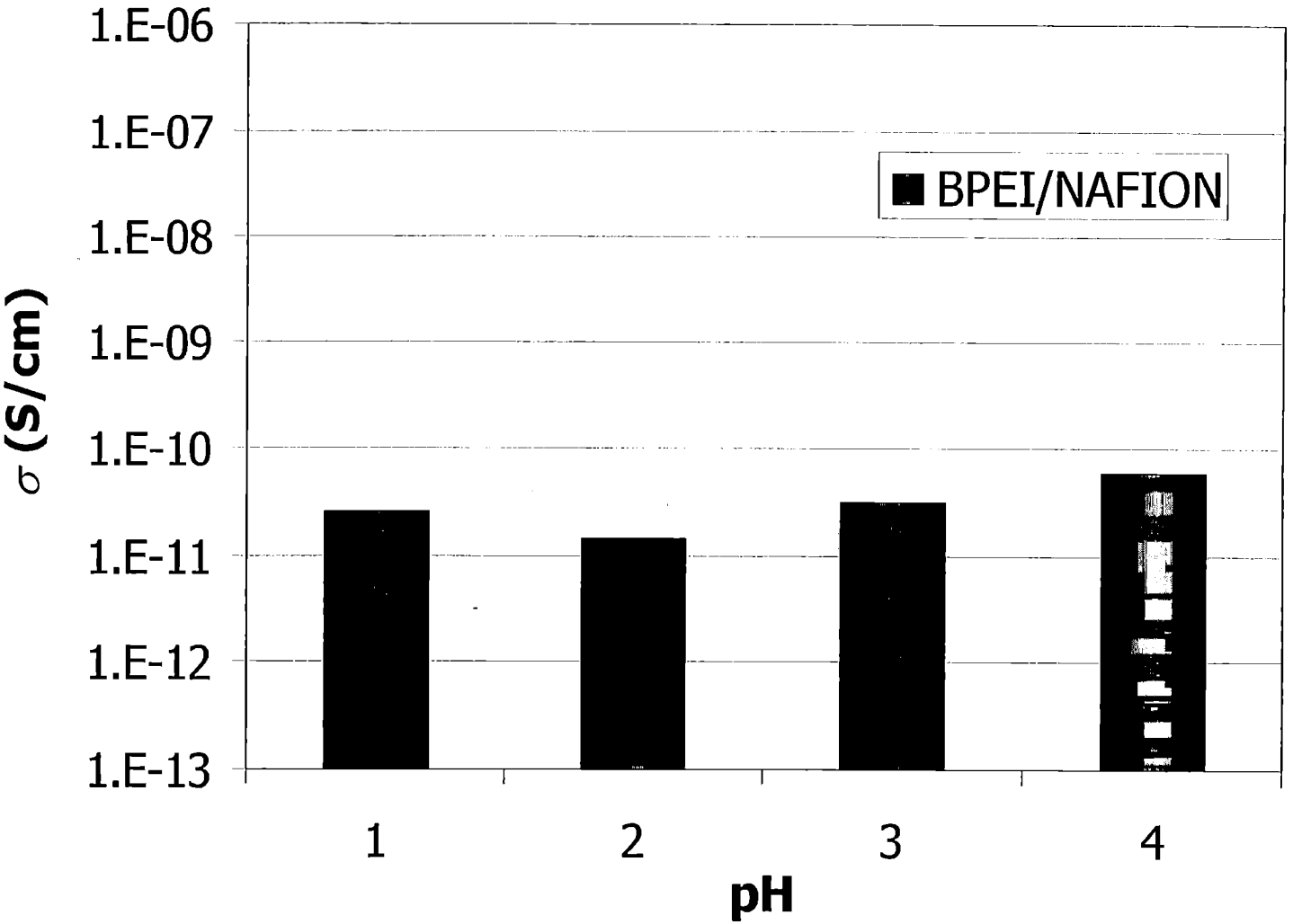

BPEI/PAMPS Conductivity Trend

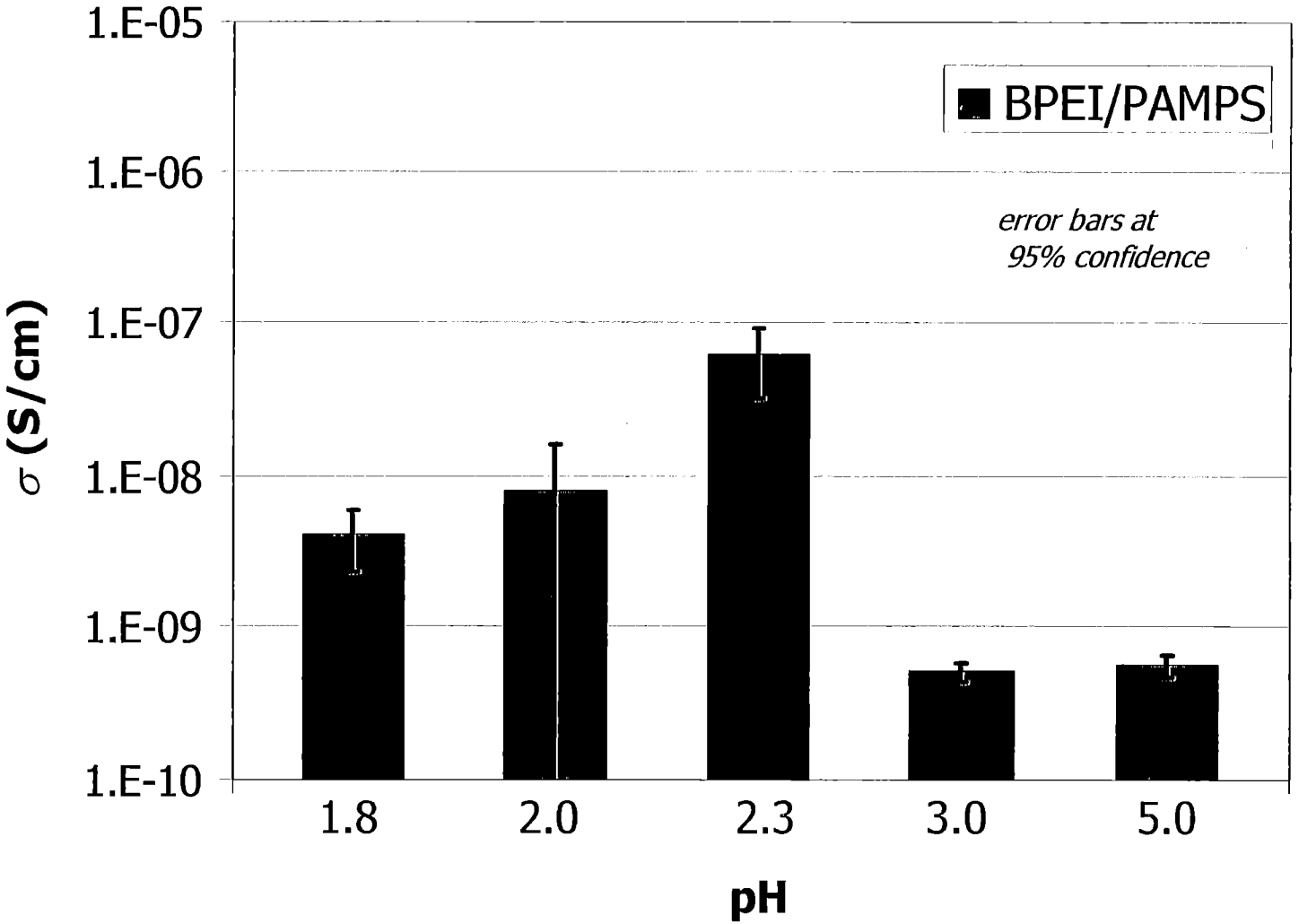

Electrolyte Summary

NAFION/BPEI System:

Thickness is greatest near acid pKa

Less charge density → more polymer per charge

No trend in conductivity observed

PAMPS/BPEI System:

Thickness is greatest near acid pKa

Conductivity is also greatest near acid pKa

Less charge density → More preserved charge carriers (protons)

Conductivity 3-4 orders of magnitude higher than NAFION/BPEI system

Focus: Electrochemistry

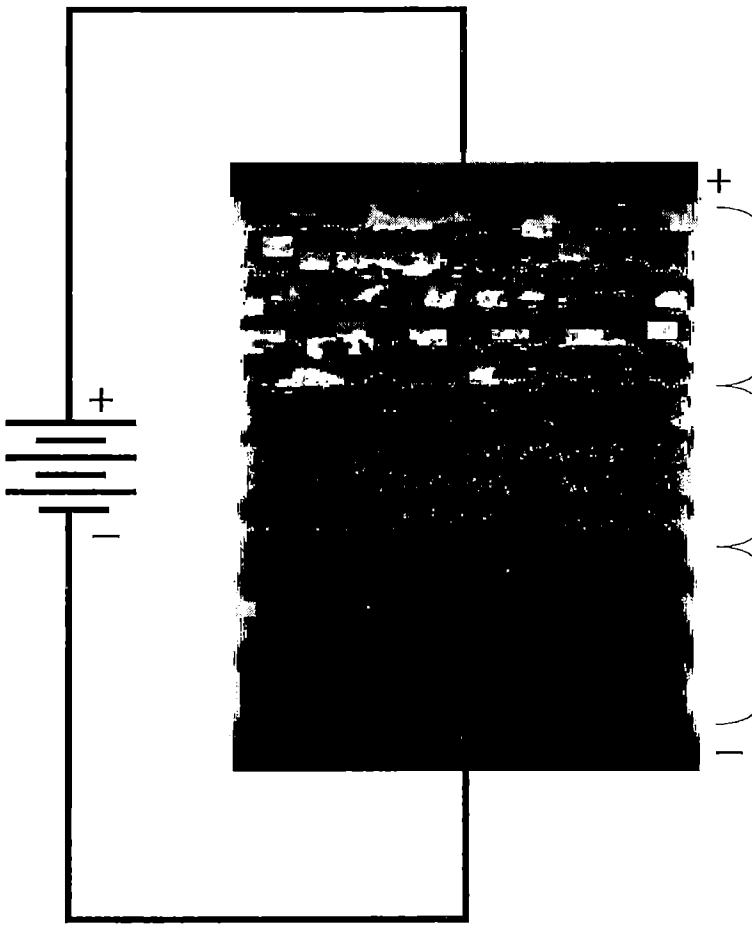

anode

electrolyte

cathode

- Ionic and electronic conductivity
- Profound chromic shift
- Well-characterized electrochemistry

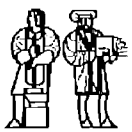

Polyelectrochromes

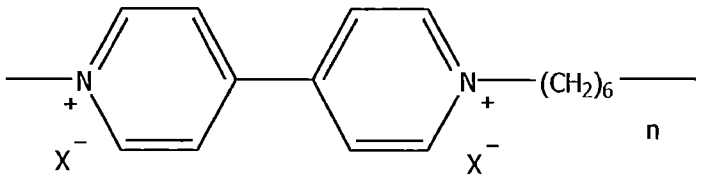

PXV
Polyhexylviologen

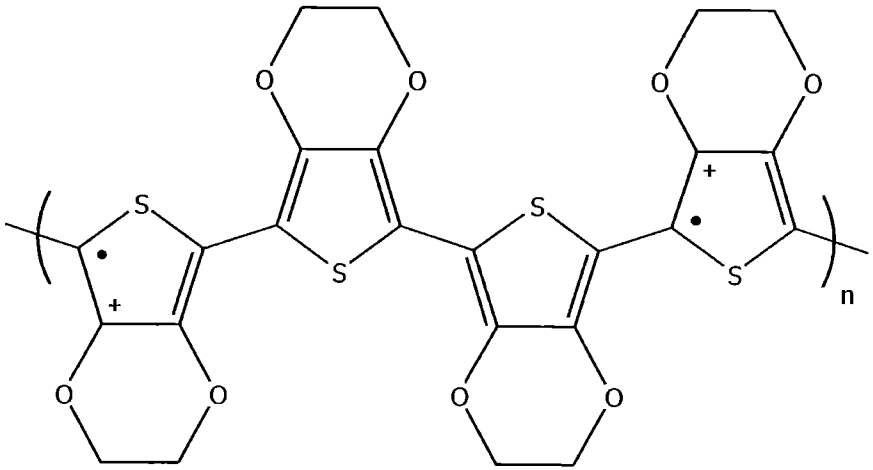

PEDOT
Poly(3,4-ethylenedioxythiophene)

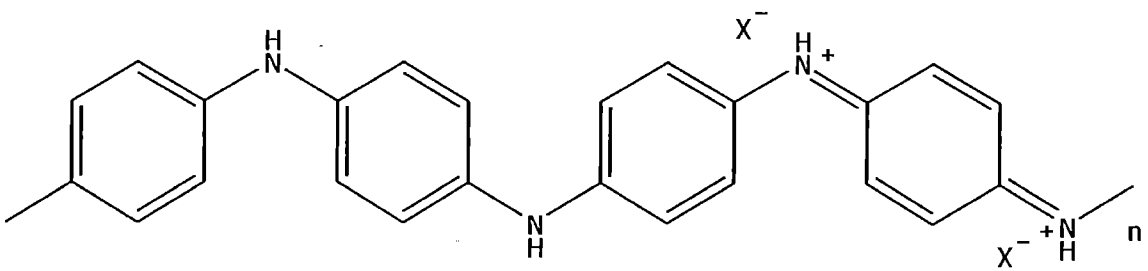

PANi
Polyaniline)

Thickness Dependence on Salt

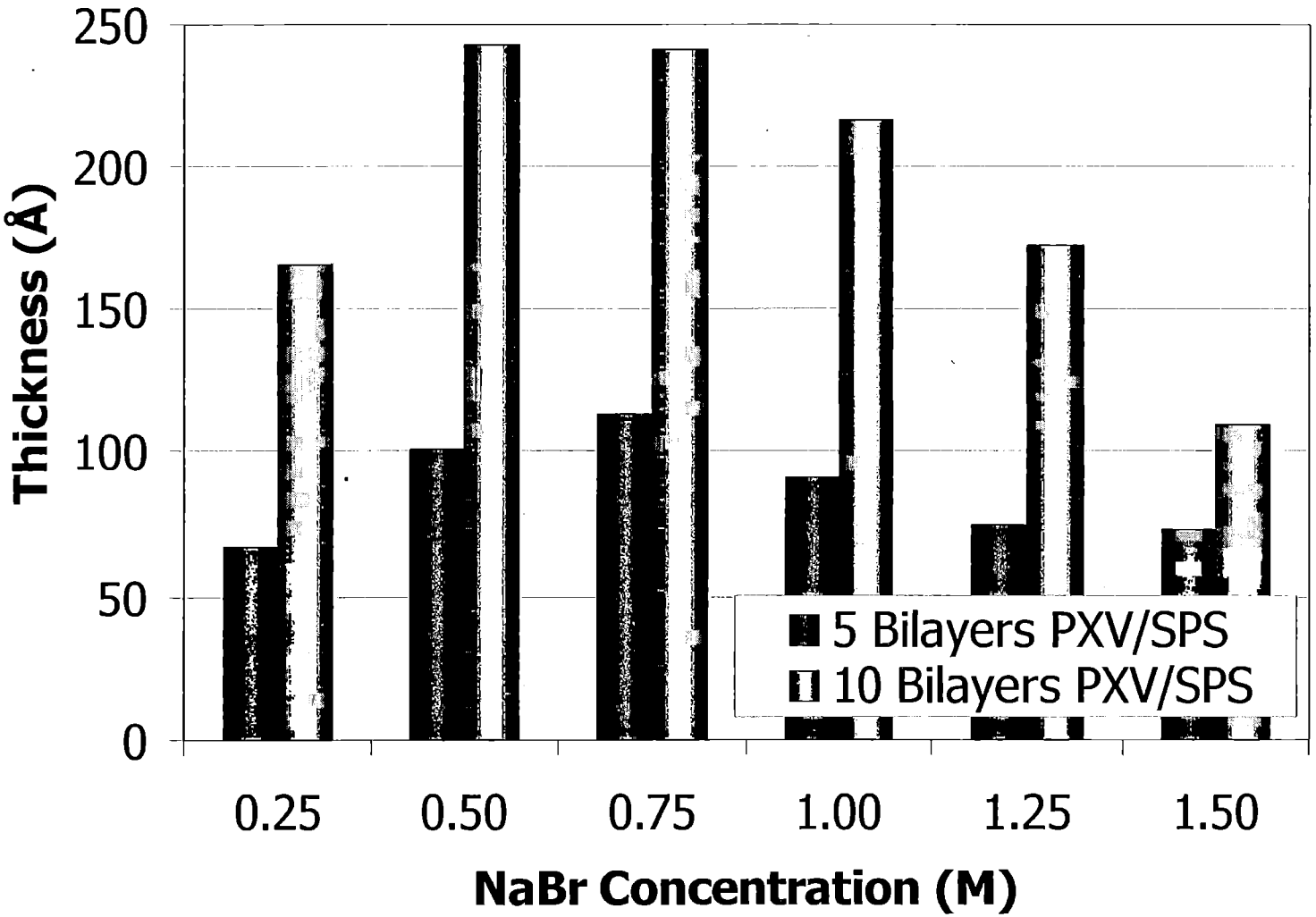

Cyclic Voltammetry Results

PXV/SPS System

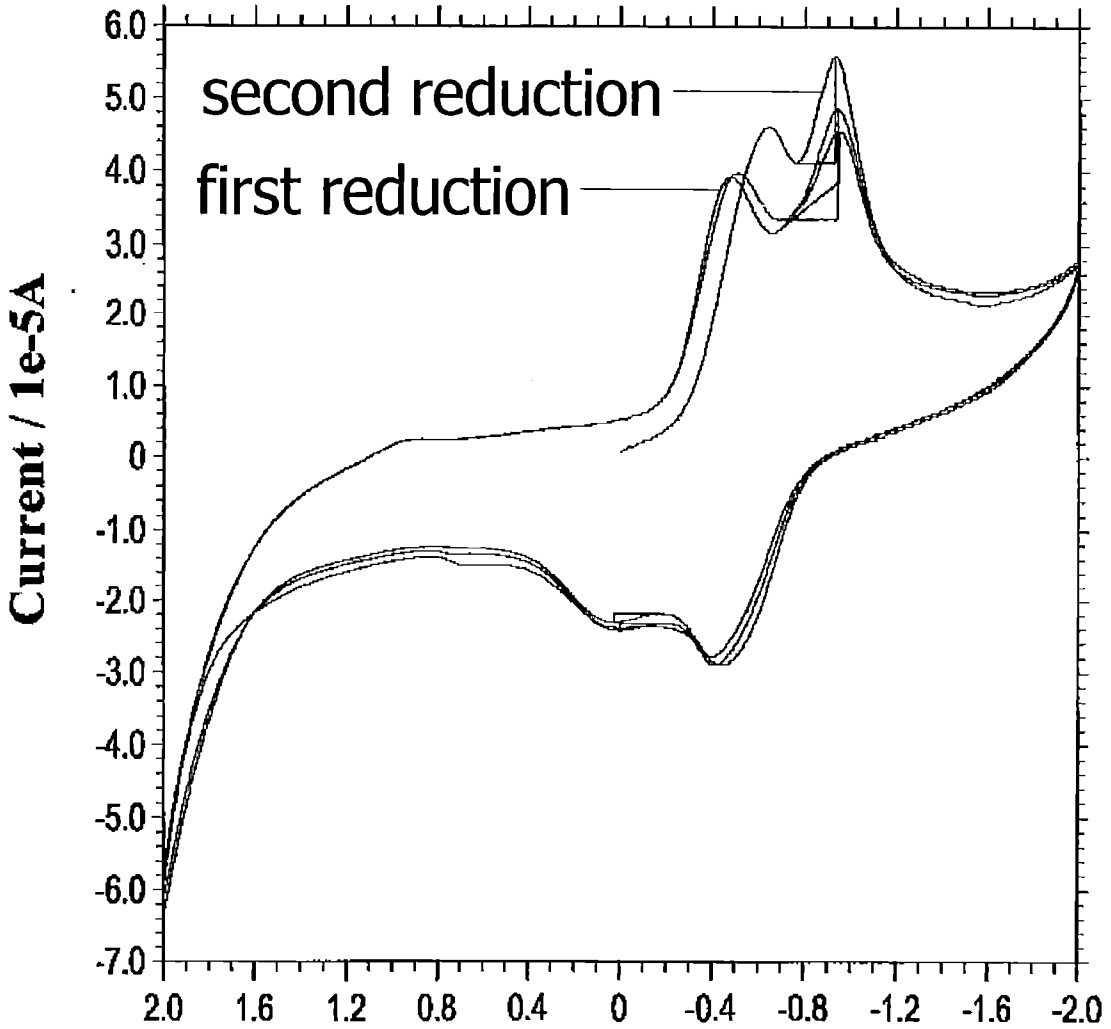

* Thanks to Bard Lab

Electrochromism Summary

PXV/BPEI System:

Thickness control achievable with salt or pH

Characterizable, reversible electrochromism

PEDOT/BPEI and PANi/BPEI Systems:

Typical film growth via multilayering

CV results pending

Single Film Device

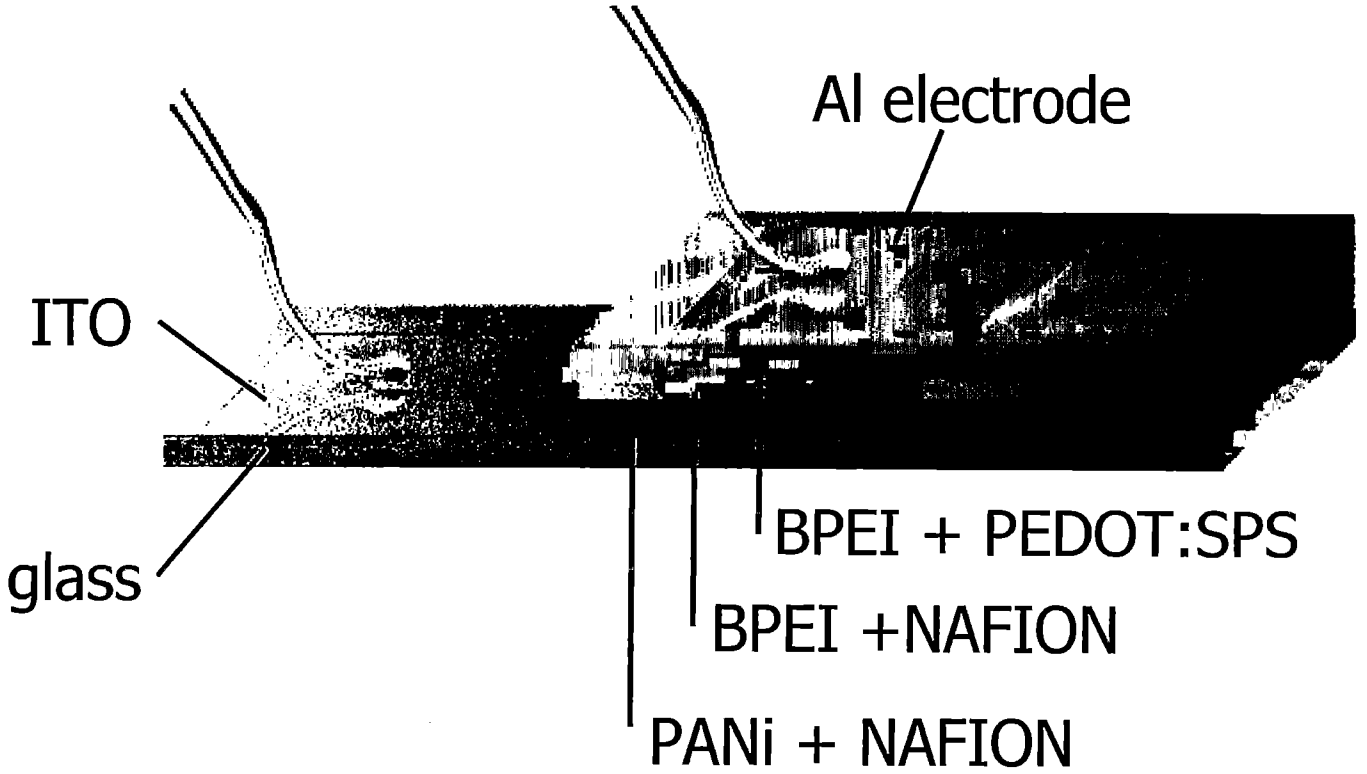

One working prototype constructed as above. Displayed blue/green color, ~5s turn-on time and required ~10V to drive the device. Failure after ~10 cycles at atmospheric conditions.

Proposed Patterned Device

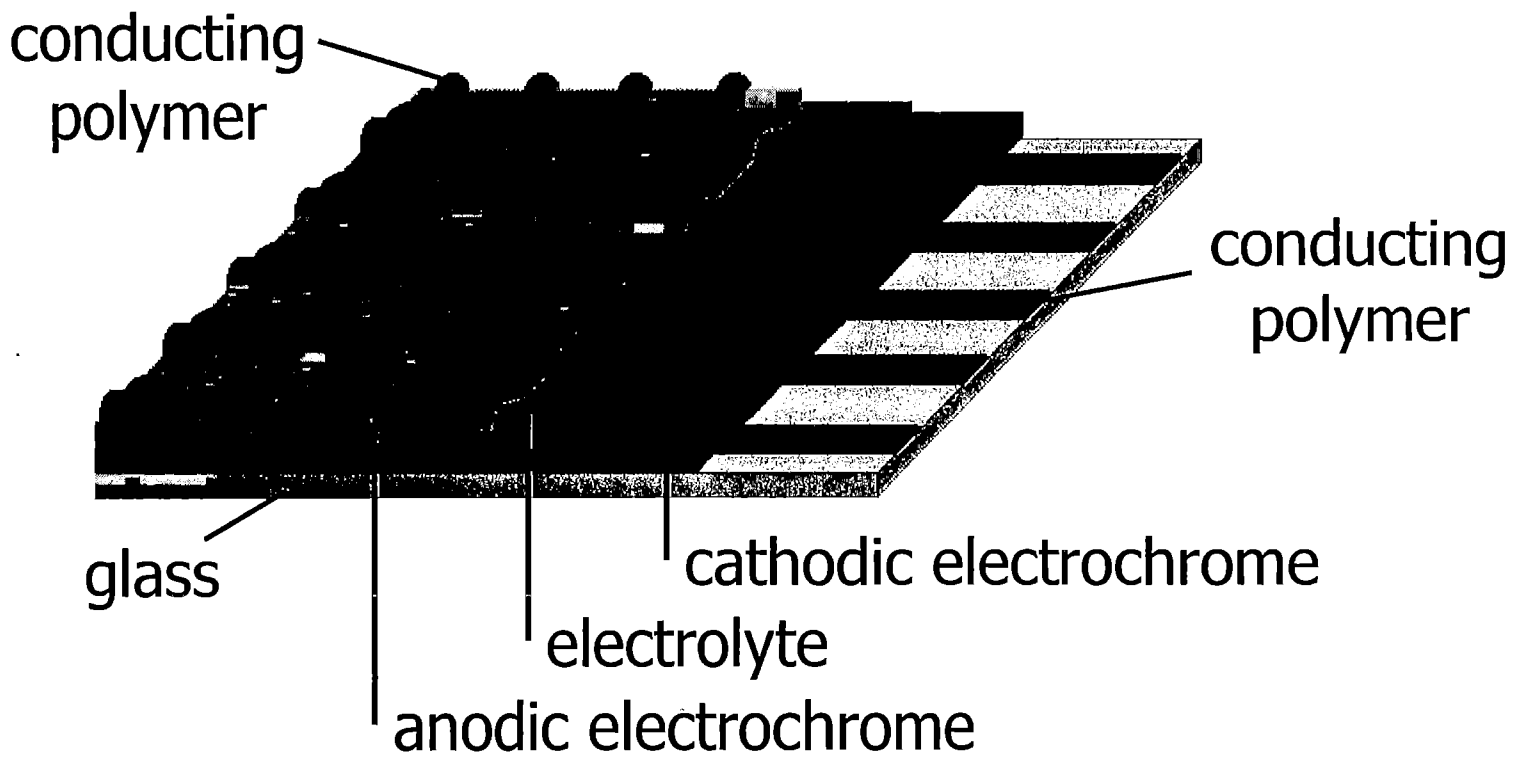

Requires deposition selectivity of electrically conducting polymer. Speed, lifetime, color contrast.

Acknowledgments

- Army Research Office (ARO TOPS MURI)
- Bard Lab
- Rubner Lab
- Hammond Lab
- Department of Defense NDSEG Fellowship

Naphthodithiophenes:
A new class of electroactive materials

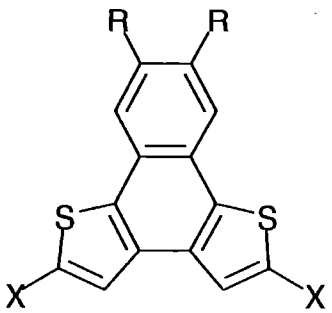

John D. Tovar and Timothy M. Swager*

Department of Chemistry
Massachusetts Institute of Technology
77 Massachusetts Avenue
Cambridge, MA (USA) 02139

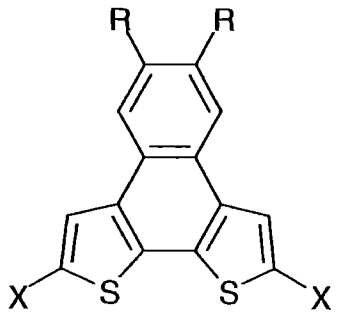

Current interest in planar fused thiophenes

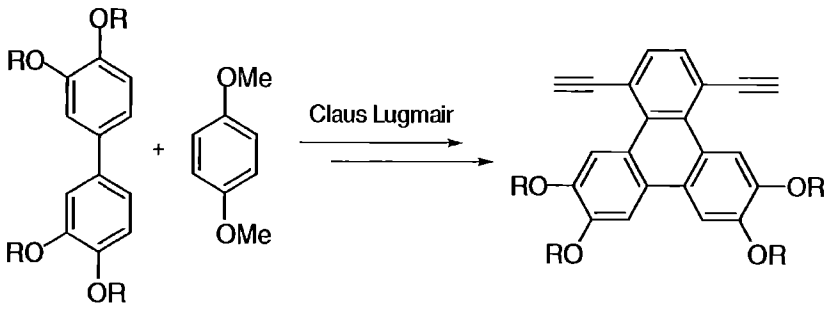

Challenging synthetic approach ... could thiophenes allow for easier functionalization?

- Halogenation to provide monomers
- Fine-tuning of molecular properties
- Incorporation into LC or sensory polymers

High mobility organic FET materials

- polycyclic aromatics
- well-defined oligomers

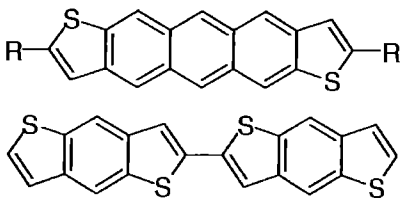

H. E. Katz *et. al. Adv. Mater.* **1997**, *9*, 36; *J. Am. Chem. Soc.* **1998**, *120*, 664-672.

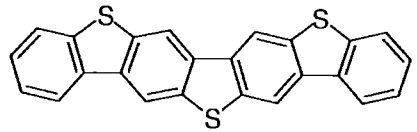

Sirringhaus, Friend, Müllen *et. al.* *J. Mater. Chem.* **1999**, *9*, 2095-2101.

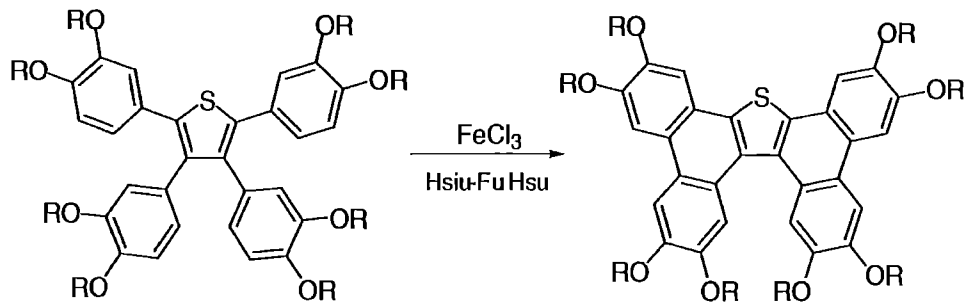

Structural similarity to triphenylene: New discotic core mesogens?

Synthesis of α-thienyl systems

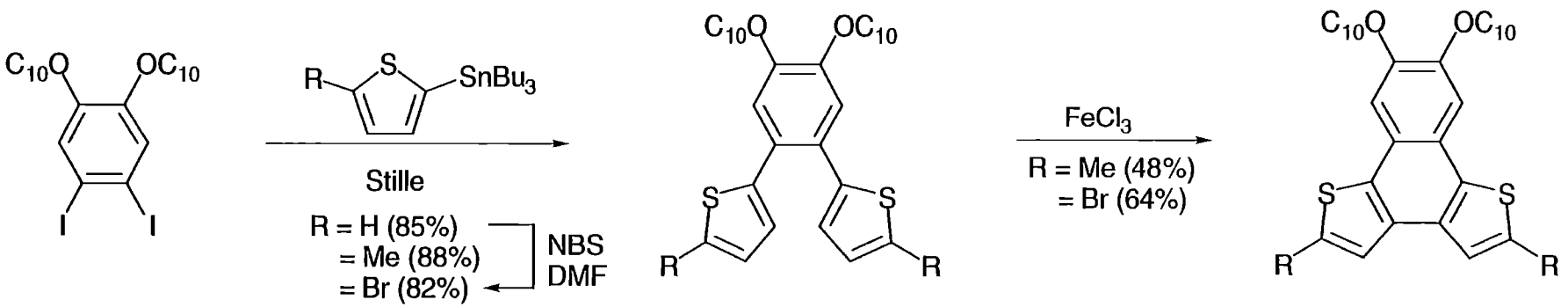

This strategy also applies to extended aromatic systems:

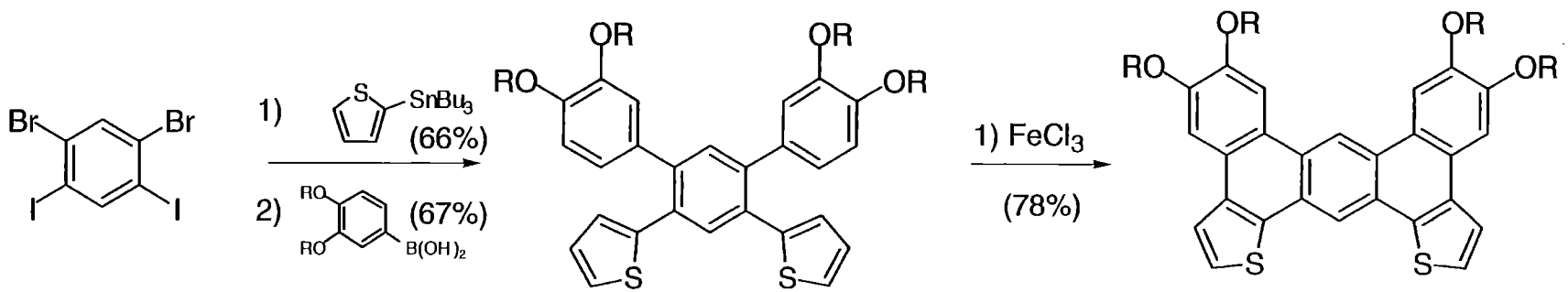

Cyclization-redox activity: α-blocked models

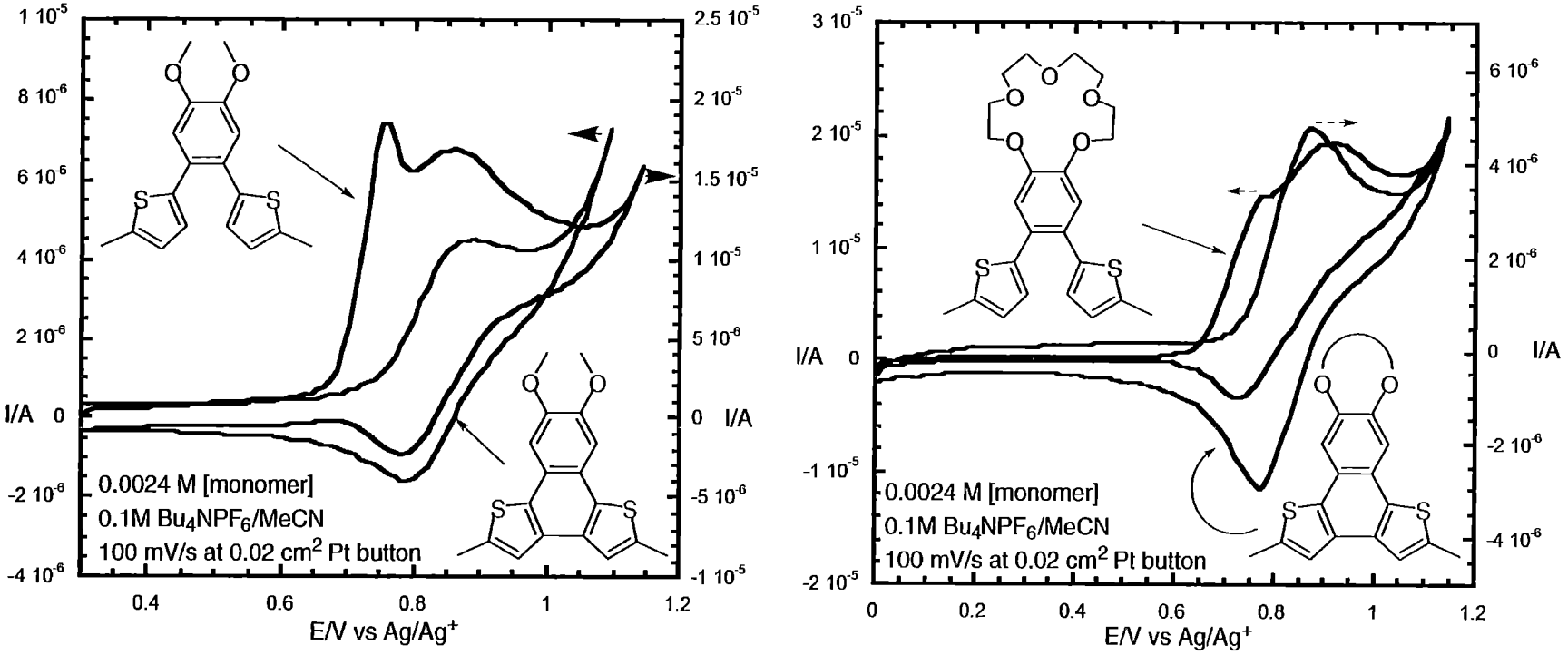

Both display a loss of irreversible oxidation after chemical cyclization

Sodium binding with a 15-crown-5 monomer

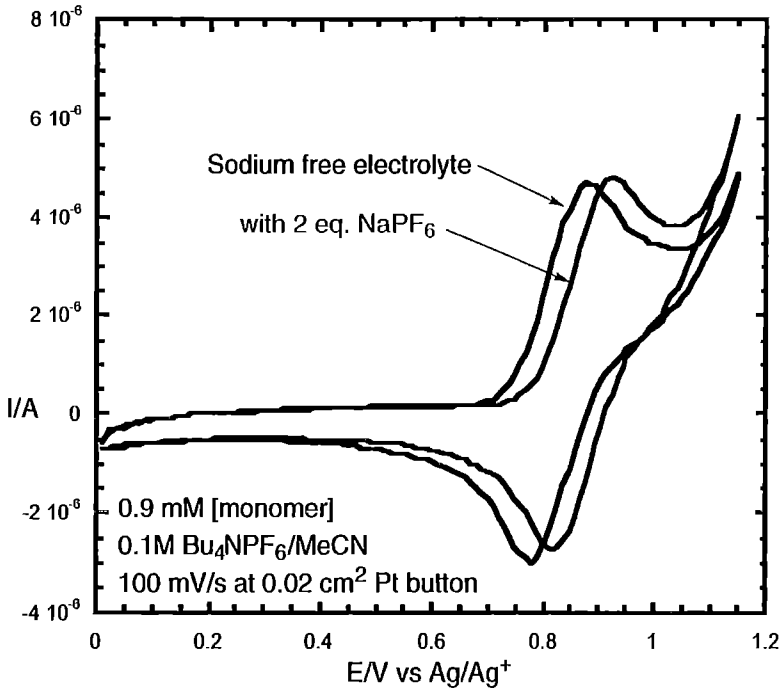

The shift to higher potential suggests communication between the **benzeno** bridge and the fused **bithiophene** moiety

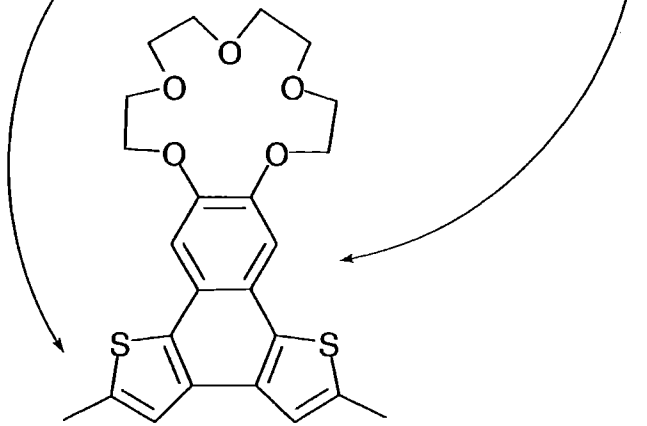

Could this be exploited in a polymer?

Moving on to β-thiophenes

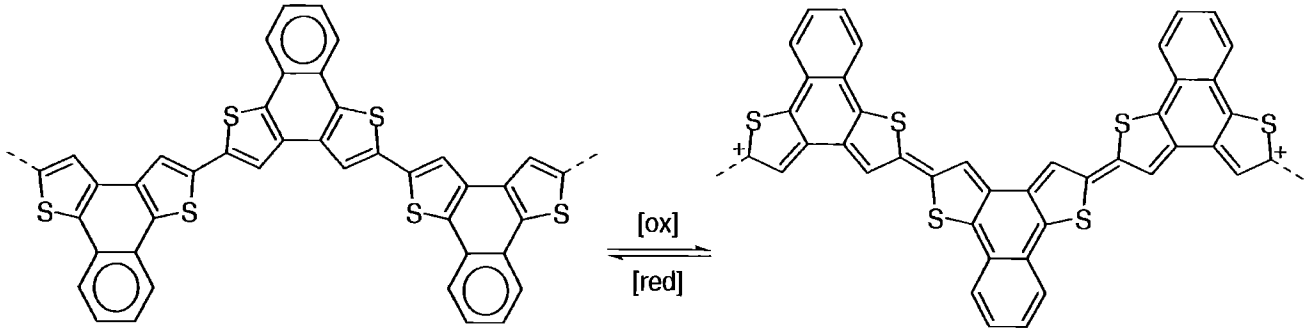

Here, quinoid resonances must disrupt pendant ring aromaticity ...

... while here, conjugation mainly through the planar poly(bithiophene) backbone

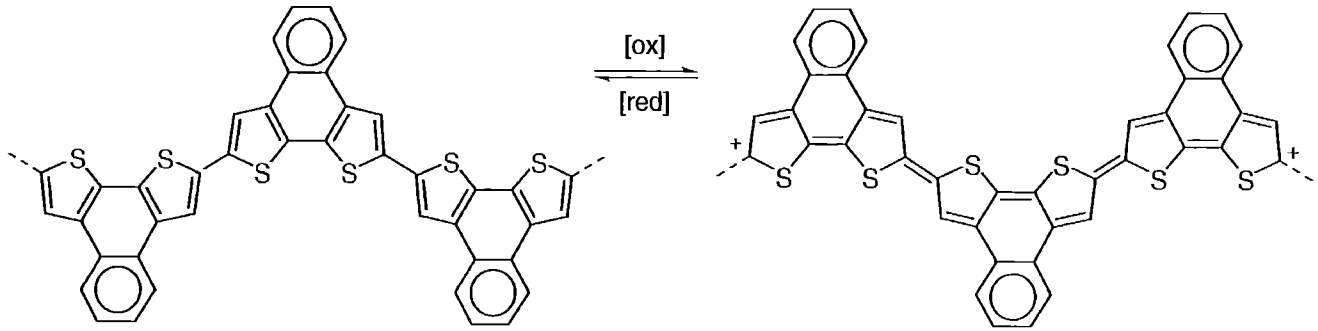

Planar thiophene polymerizations:

Chemical and electrochemical methods

Thiophene polymerizations:

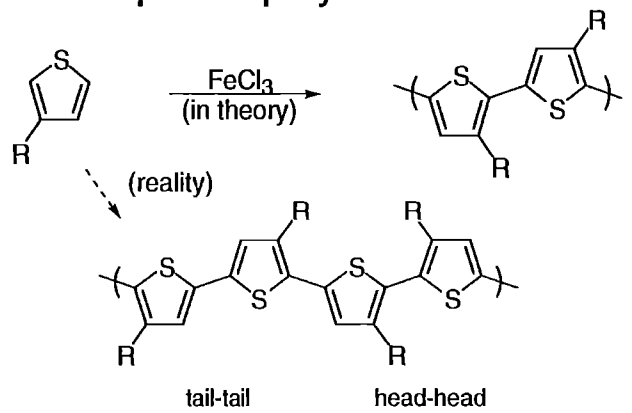

Lack of regioregularity leads to lower conductivities

Planarized monomers

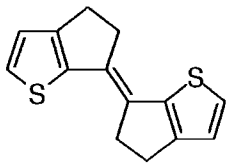

Roncali, *J. Chem. Soc. Chem. Commun.* **1994**, 2249-2250

Ferraris, *ibid.* **1991**, 1268-1270

Quinoidal monomers

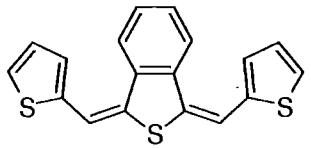

Hanack, *Synth. Met.* **1993**, *55-57*, 827-832

Disruption of planarity

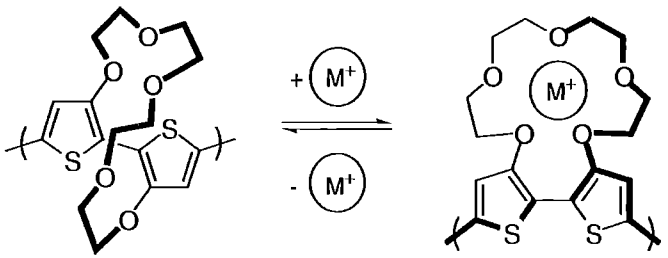

Swager, *J. Am. Chem. Soc.* **1993**, *115*, 12214-12215

Synthesis of β-thienyl monomers

Preliminary CV studies

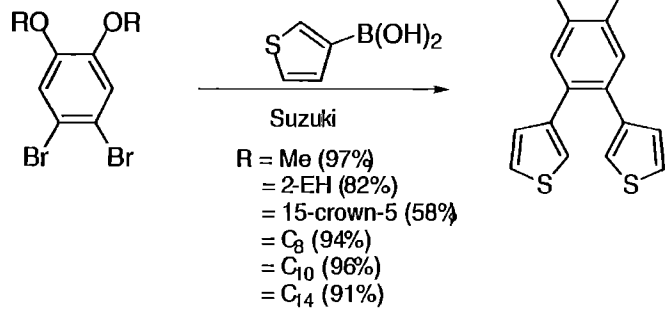

Polymer redox after growth

Leads to cyclization?

Oxidation of aromatic monomer?

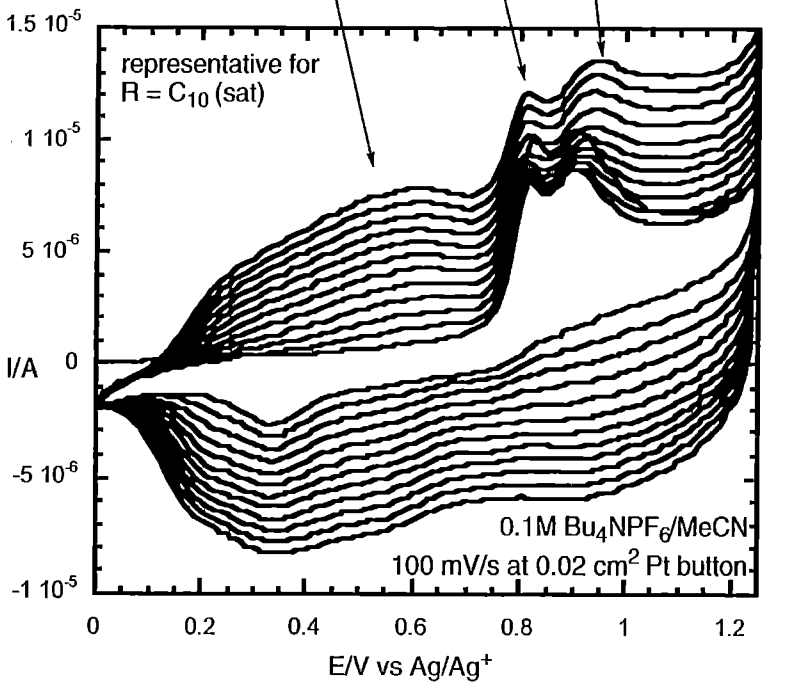

Lack of reduction activity implies discrete chemical reactions ...

No polymer growth is observed until scanning to the second oxidation potential.

Deconvoluting the electrochemistry:

Synthesis of model compounds ...

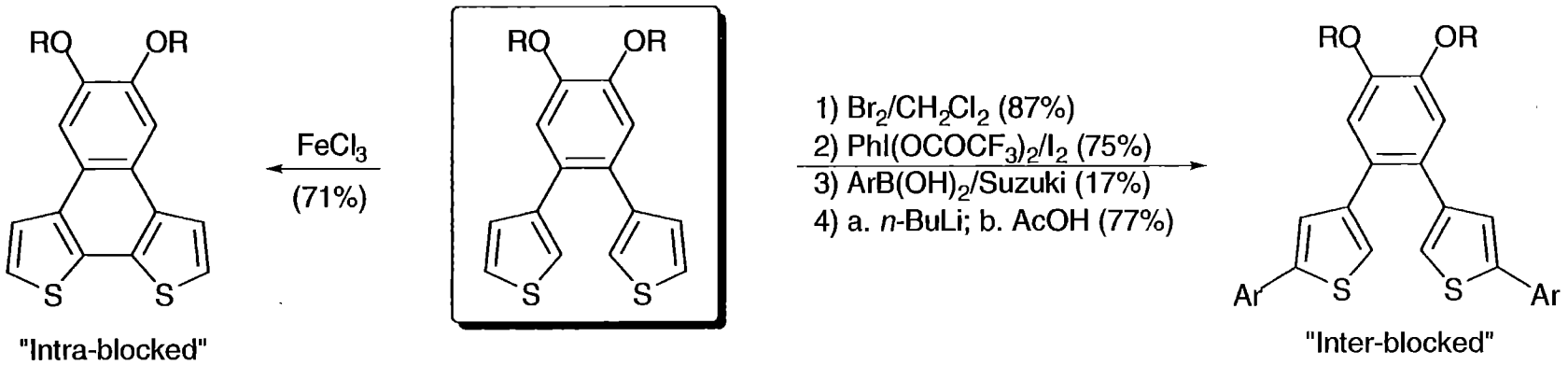

... and verification of the connectivity through independent syntheses

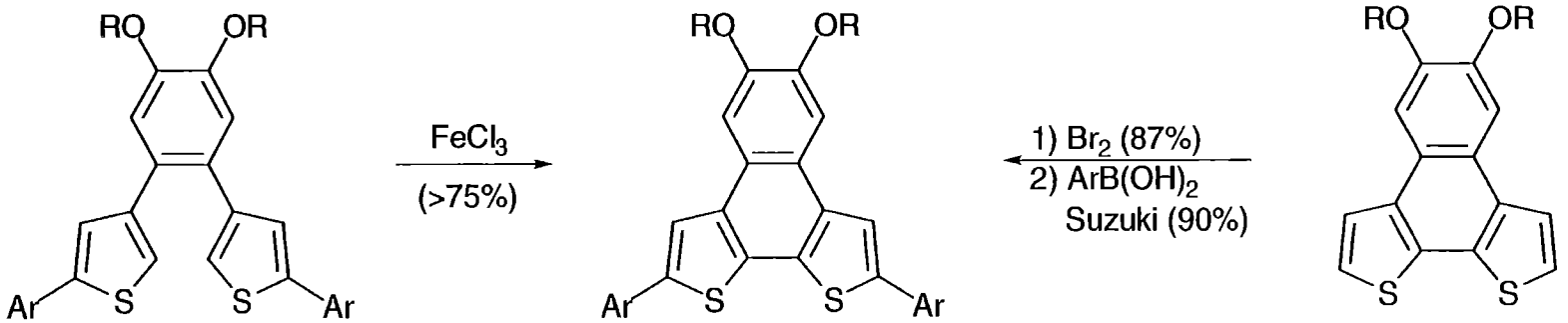

No evidence for β-coupling

Selective α-bromination

CV studies: Tandem cyclization-polymerization

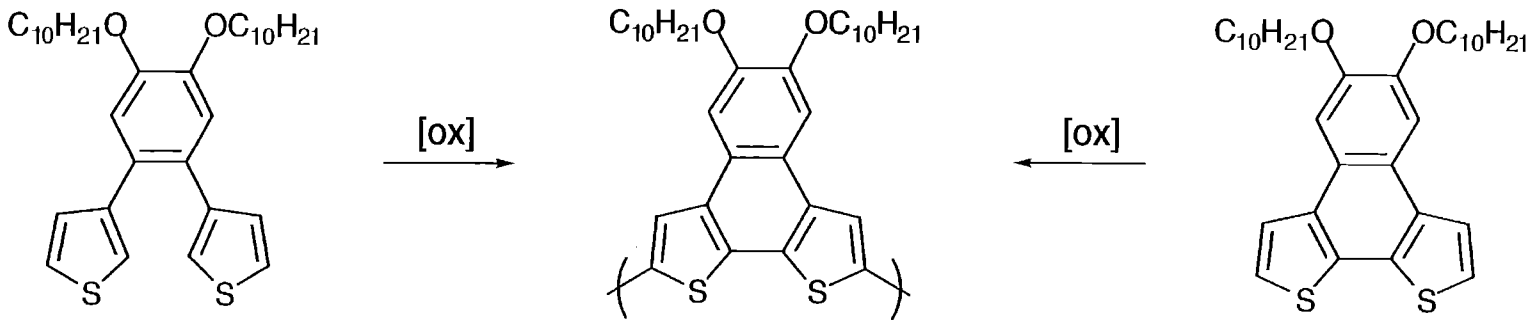

Two distinct monomer oxidations

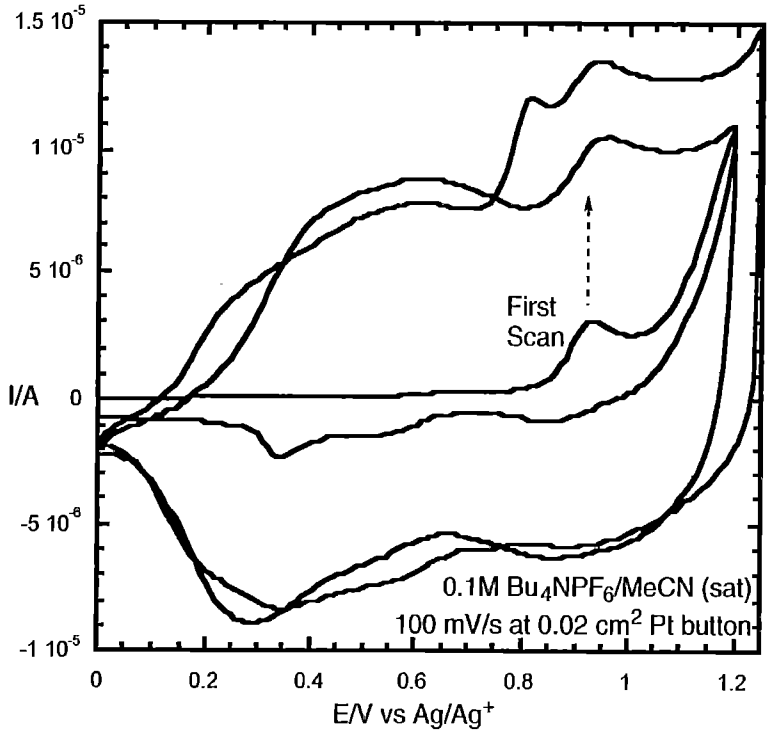

Only one monomer oxidation!

Assessing the regioregularity:

bulk electrolysis

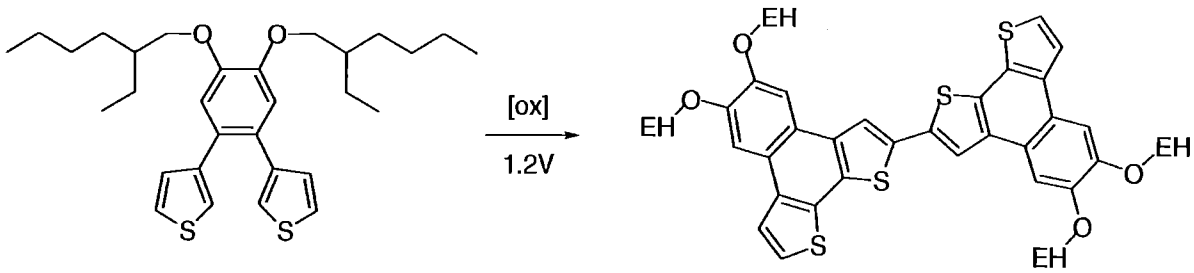

(Isolate the cyclized dimer alongside oligomers)

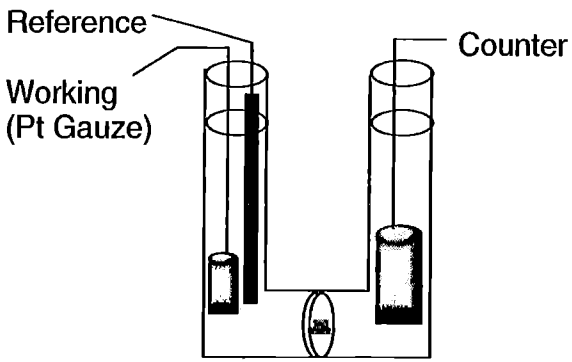

Ethylhexyl for solubility:

- GPC shows oligomers

Constant potential electrolyses:

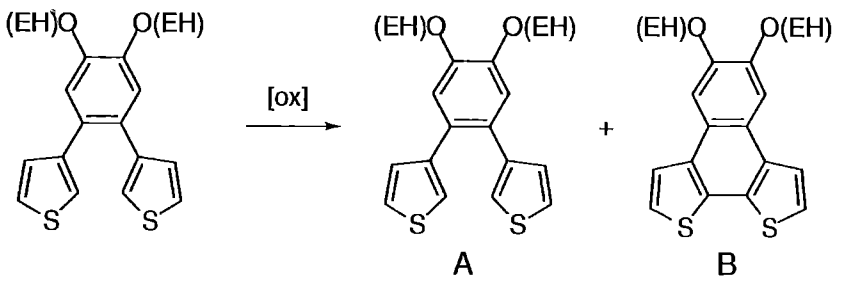

Potential/V	e-/mol	A	B	
0.75		0.96	0.04	
0.85	1.09	0.49	0.51	
0.85	2.02	0.03	0.97	(74% isolated)

Attempts toward more diverse systems

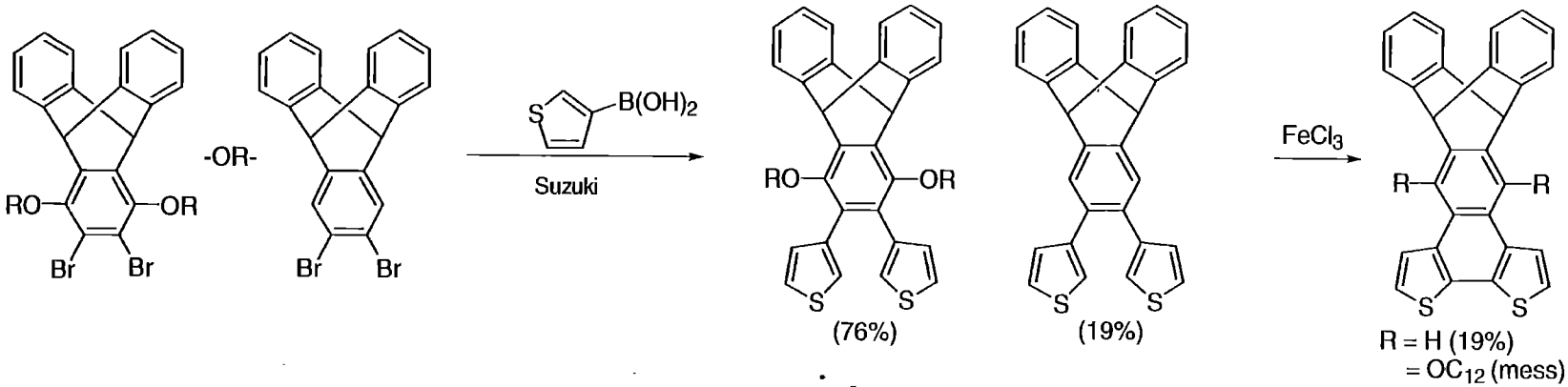

For redox-active NO sensors?

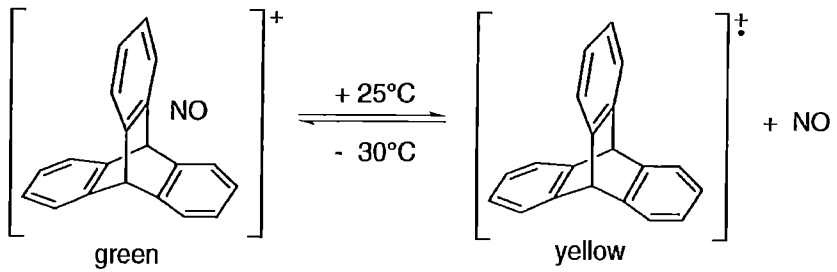

Kochi, *J. Org. Chem.* **1998**, *63*, 8630-8631

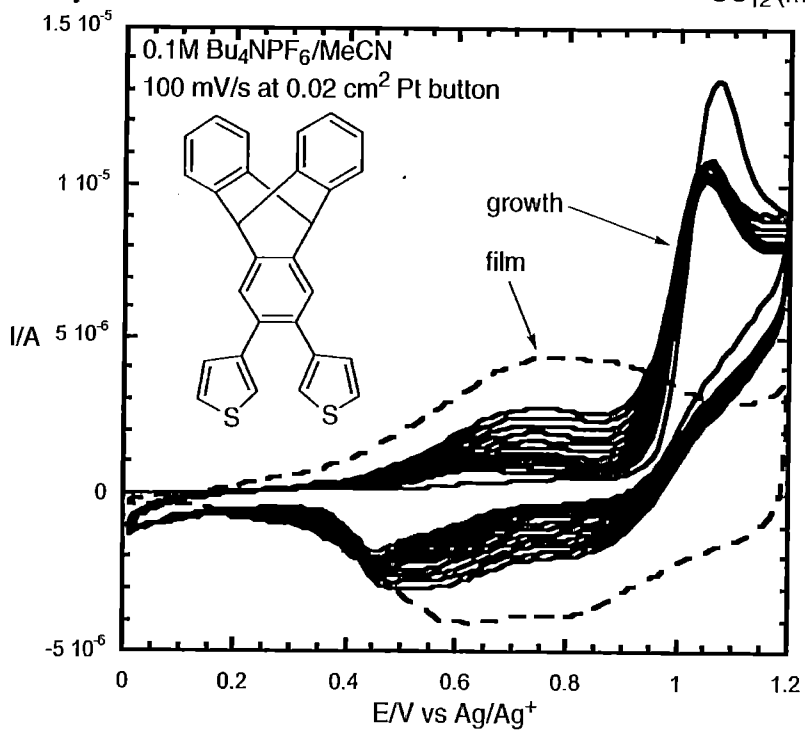

Spectroelectrochemical studies:

assessing the electrochromicity

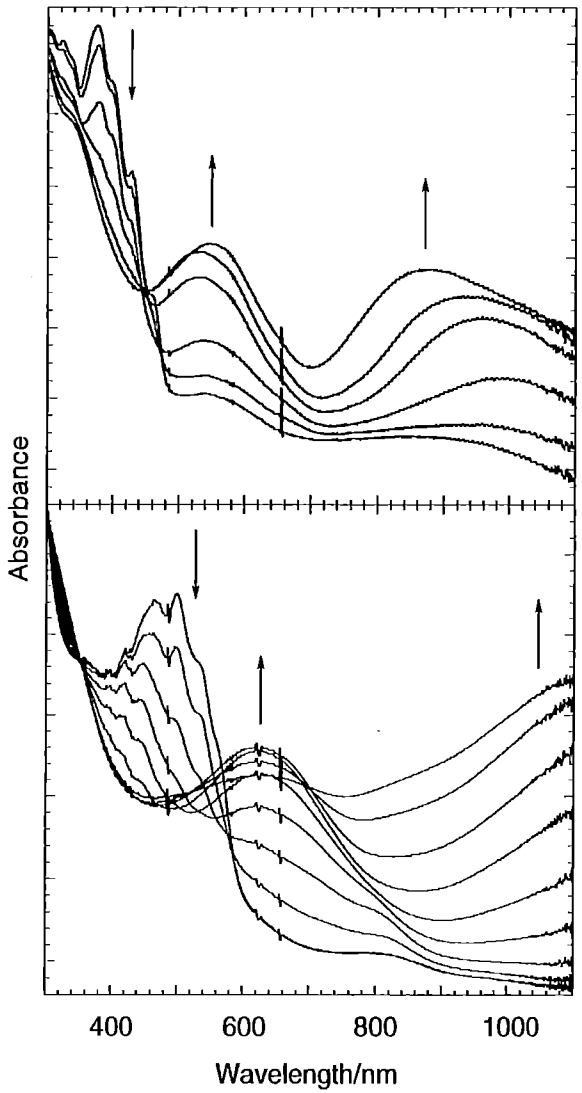

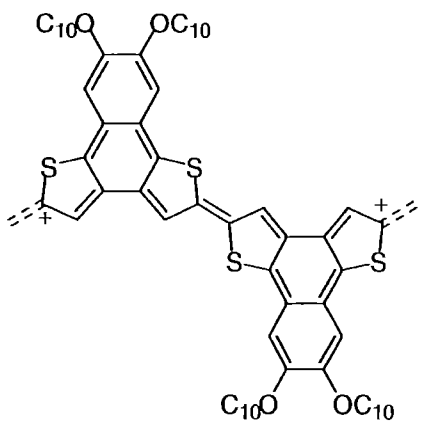

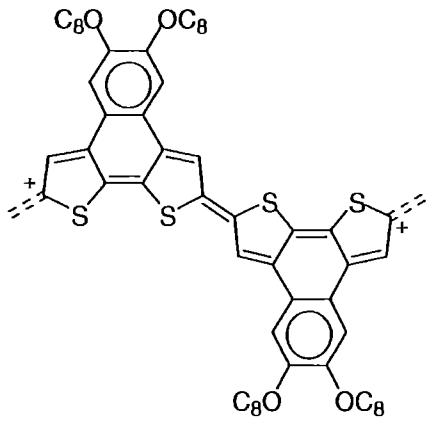

Substitution on the pendant phenyl moities should allow for tuning of optical absorption/ conductivity

Demonstrations of facile functionalization

future directions

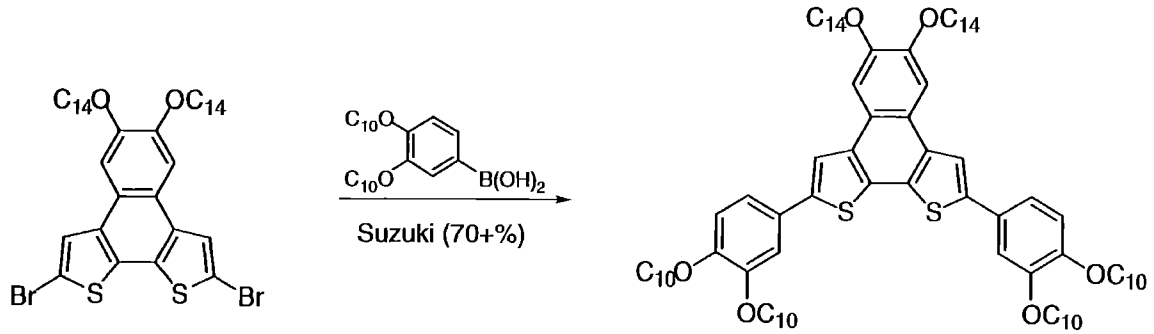

Liquid crystals?

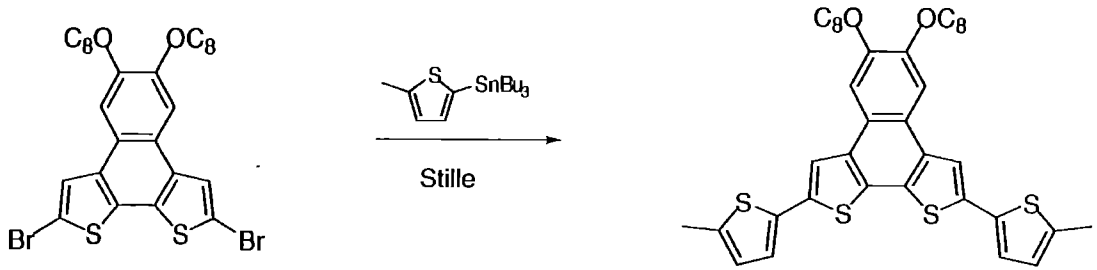

Tuneable electroactivity?

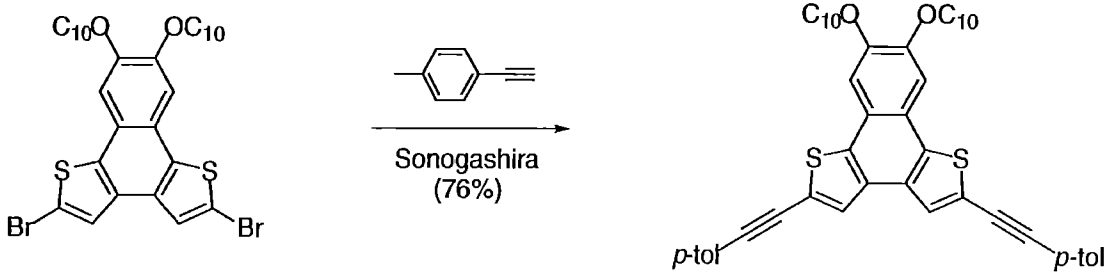

Incorporation into conducting polymers?

Acknowledgements

Prof. Timothy M. Swager

The Swager Group
Dr. Anthony E. Pullen
Mr. Hsiao-hua Yu

Prof. Hsiu-Fu Hsu
Dr. Hindy E. Bronstein
Dr. Zhengguo Zhu

ARO (MURI)
DARPA

MODEL SYSTEMS

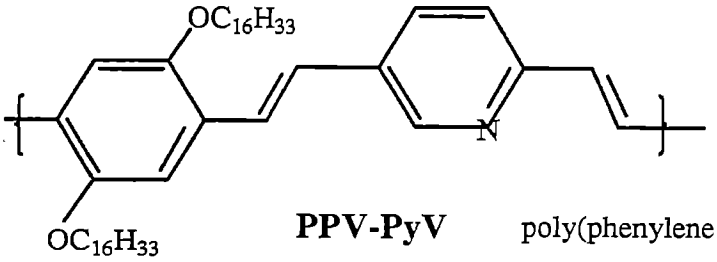

absorption shifted to red by protonation

PPV-PyV poly(phenylene vinylene pyridyl vinylene)

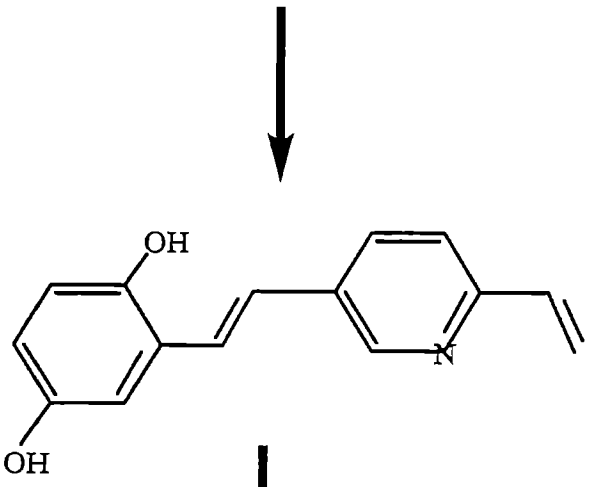

replace hydrocarbon chain by H

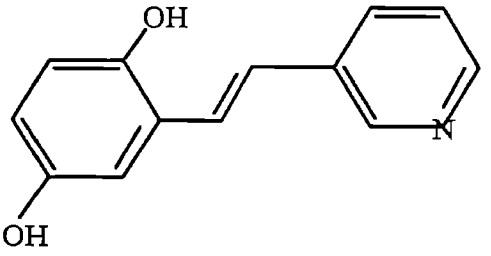

may not need terminal vinyl group

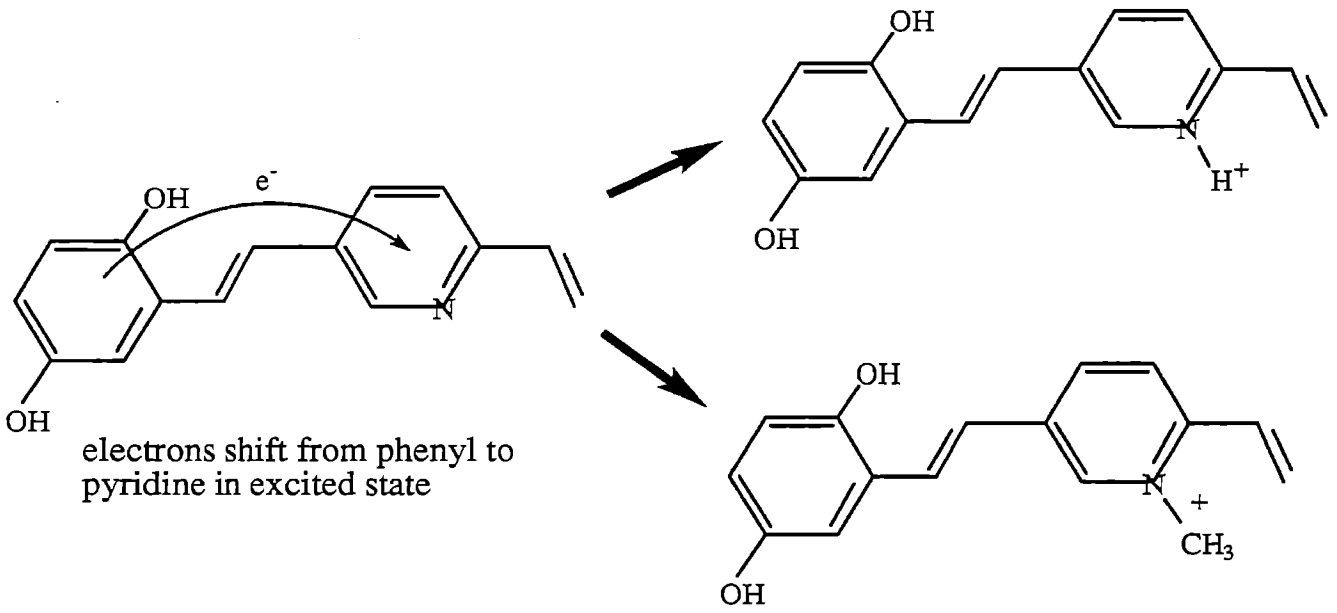

electrons shift from phenyl to pyridine in excited state

substituent enhances pyridine's ability to hold electrons.
ought to lower band gap

L

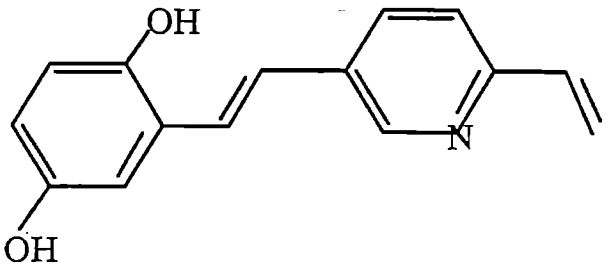

PROCEDURE

- Optimize geometry

INDIVIDUAL MOs

- Calculate MOs
- Display HOMO and LUMO

  a) Does LUMO in fact have more density on right than HOMO?
- LUMO - HOMO energy difference as measure of absorption wavelength

TOTAL ELECTRON DENSITY ρ

- Display ρ for ground state
- Display ρ for first excited state ($^1\pi\pi^*$)
- Display $\rho_{excited} - \rho_{ground}$

  Does excited state in fact have more density on right than ground state?

- $E_{excited} - E_{ground}$ as measure of absorption wavelength

- Repeat entire process for protonated and methylated molecule
- Use the analysis to identify important parts of molecule for modification

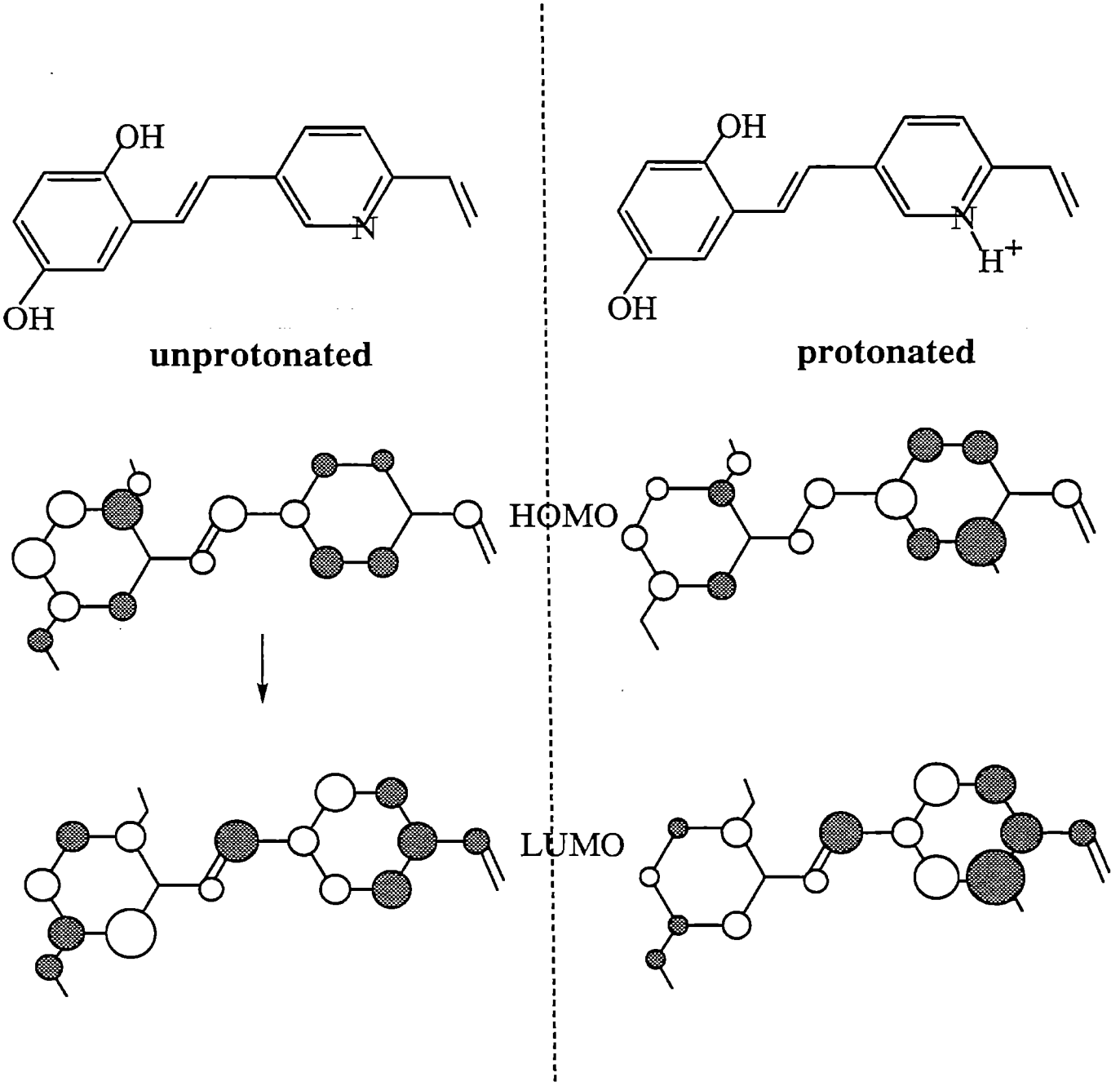
OH
N
OH
unprotonated
OH
N
H+
OH
protonated
HOMO
LUMO

Energy Levels

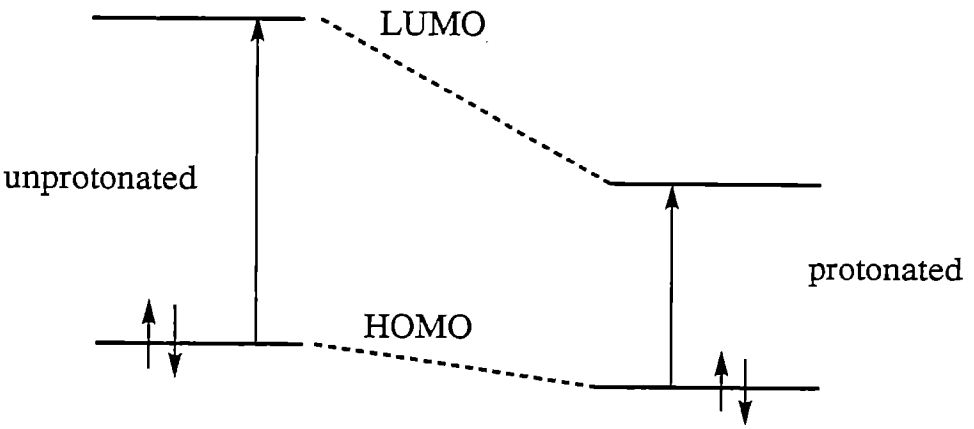

identification of "hot spots"

unprotonated **protonated**

HOMO

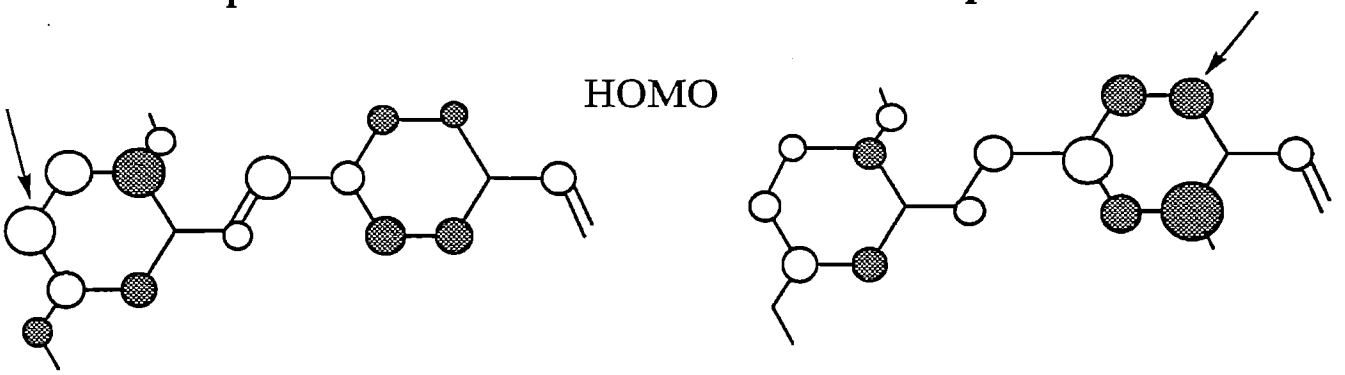

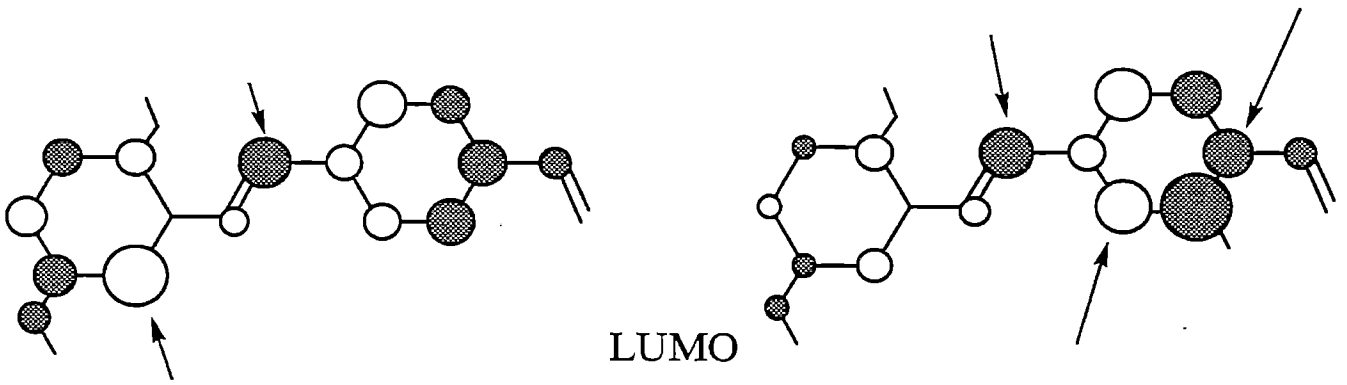

LUMO

areas of potential substitution

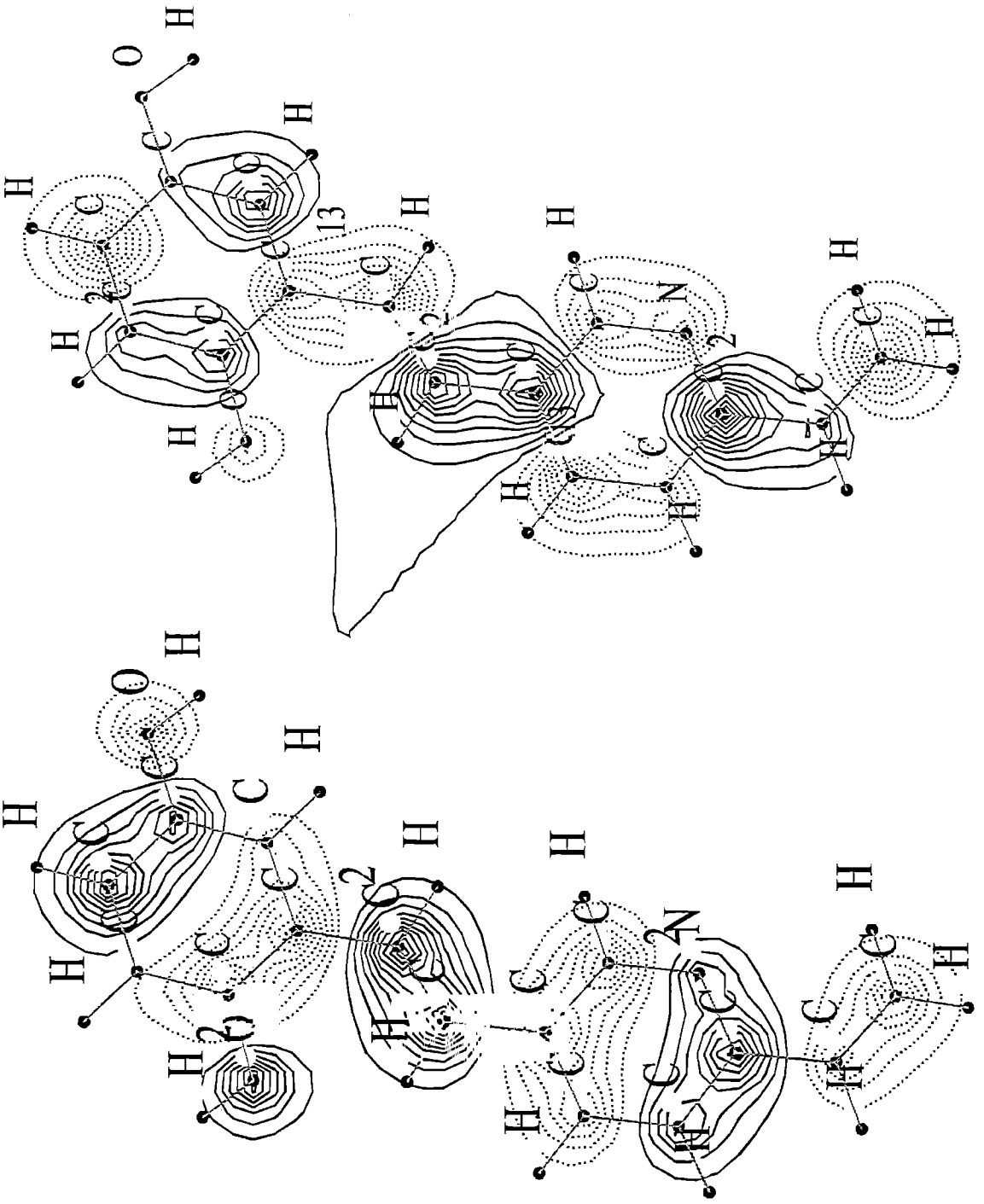

UNPROTONATED HOMO/LUMO

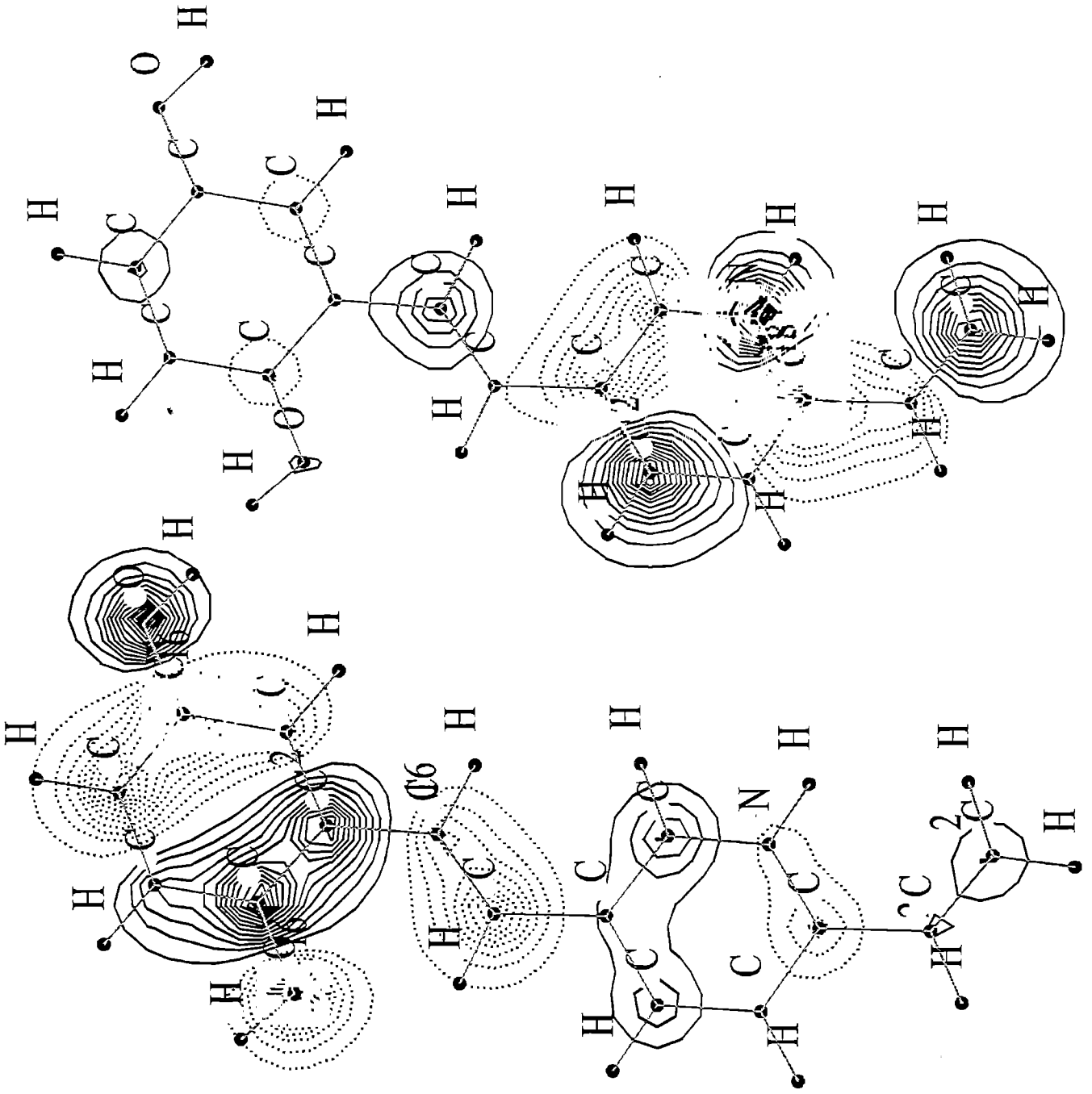

PROTONATED HOMO/LUMO

total electron density shifts caused by excitation

unprotonated (blue=gain; red=loss)

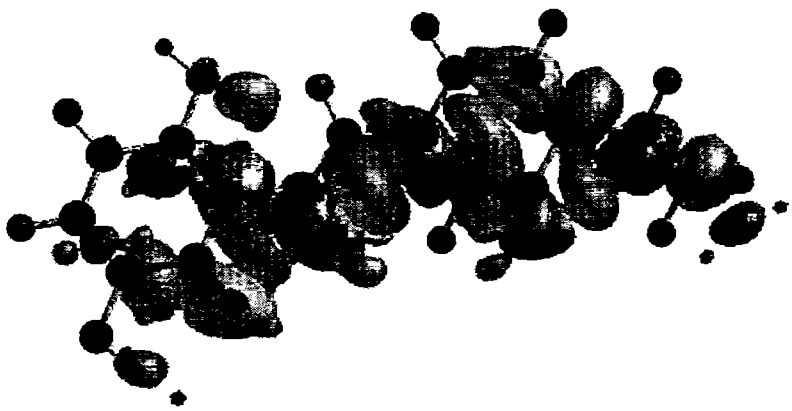

protonated

difference in density shifts:

shift in protonated – shift in unprotonated

(blue=gain; red=loss)

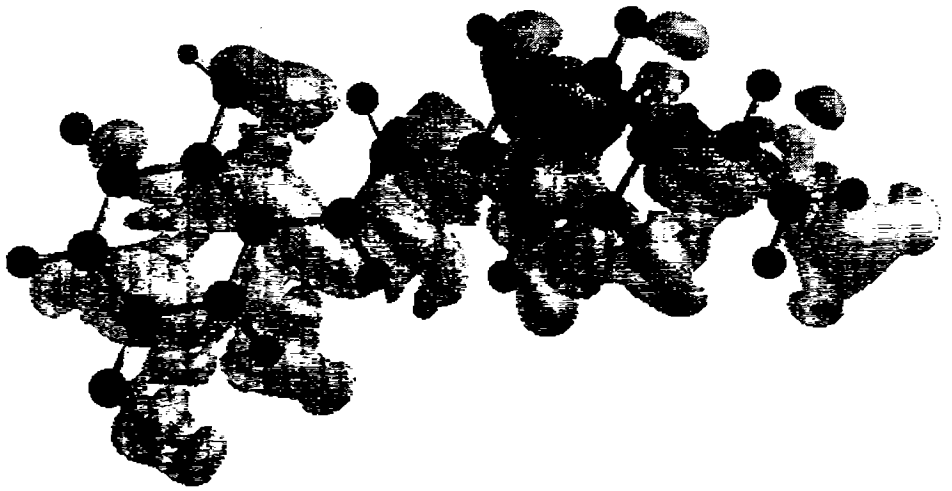

Using frontier MOs and total density as a guide, there would appear to be a great deal of excitation-induced density shift from first to second aromatic ring in protonated case, little if any when unprotonated.

check to see if this is correct:

Natural population atomic charges

	unprotonated	
	ring 1	ring 2
S_o charge	-0.028	-0.063
$\pi\pi^*$ charge	-0.014	-0.073
change	+0.014	-0.010
	protonated	
S_o charge	0.053	0.751
$\pi\pi^*$ charge	0.297	0.483
change	+0.245	-0.268

protonation does in fact cause electron density to shift from ring 1 to ring 2 upon excitation

very similar results are obtained when N is methylated
or when Mulliken charges are used

atomic charges in ground and excited states confirm and quantify ideas arising from HOMO/LUMO shapes

EXCITATION ENERGIES

Differences in energy between ground and excited states (eV)

	unprotonated	protonated	difference
6-31G*	4.72	4.33	-0.39
3-21G	4.90	4.48	-0.42

protonation lowers excitation energy by 0.39 – 0.42 eV
good consistency from one basis set to the next

PROBLEM: What modifications of the molecule might produce a large effect upon the magnitude of this protonation-induced change in excitation energy?

Attack problem by replacing various H atoms by F
big change in electronegativity

Where to make these replacements?
use MOs as a preliminary guide.

changes in individual atomic charges caused by excitation:

	unprotonated		protonated	
atom	Mulliken	natural	Mulliken	natural
C1	0.011	0.021	0.021	0.041
C2	-0.006	-0.002	0.022	0.047
C3	-0.005	-0.021	-0.008	-0.029
C4	0.016	0.037	0.036	0.068
C5	-0.005	-0.005	0.027	0.064
C6	-0.015	-0.037	-0.013	-0.043
C7	0.002	0.010	-0.021	-0.055
C8	-0.007	-0.009	0.058	0.127
C9	0.003	0.016	-0.038	-0.068
C10	-0.017	-0.034	-0.080	-0.136
C11	0.020	0.027	0.041	0.062
C12	-0.024	-0.028	-0.088	-0.125
N13	0.008	0.004	-0.013	-0.027
C14	-0.003	0.007	0.039	0.069
C15	0.008	0.004	0.031	0.041
C16	-0.007	-0.005	-0.042	-0.070
O17	0.003	0.002	0.015	0.014
O18	0.012	0.011	0.030	0.028

in unprotonated case, atomic charges are largely unaffected by excitation, generally less than 0.03.

for protonated molecule, charge changes are much larger.
note especially C8, C10, and C12, also C16.

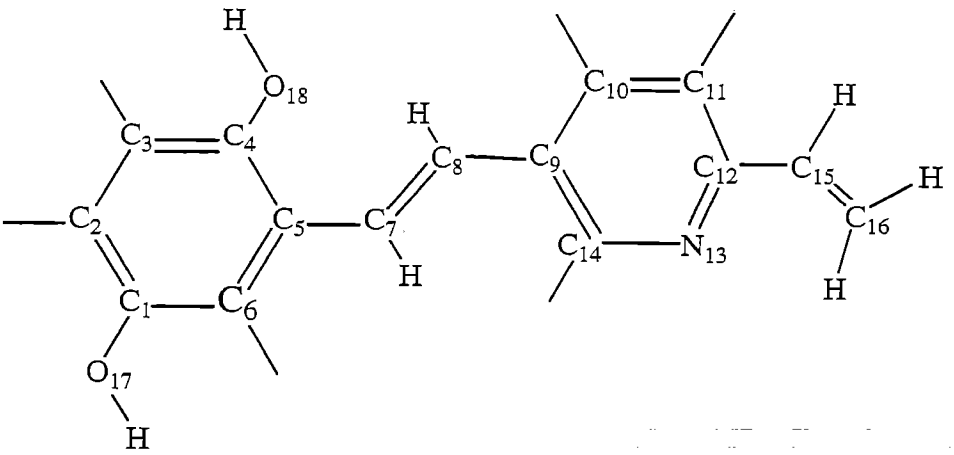

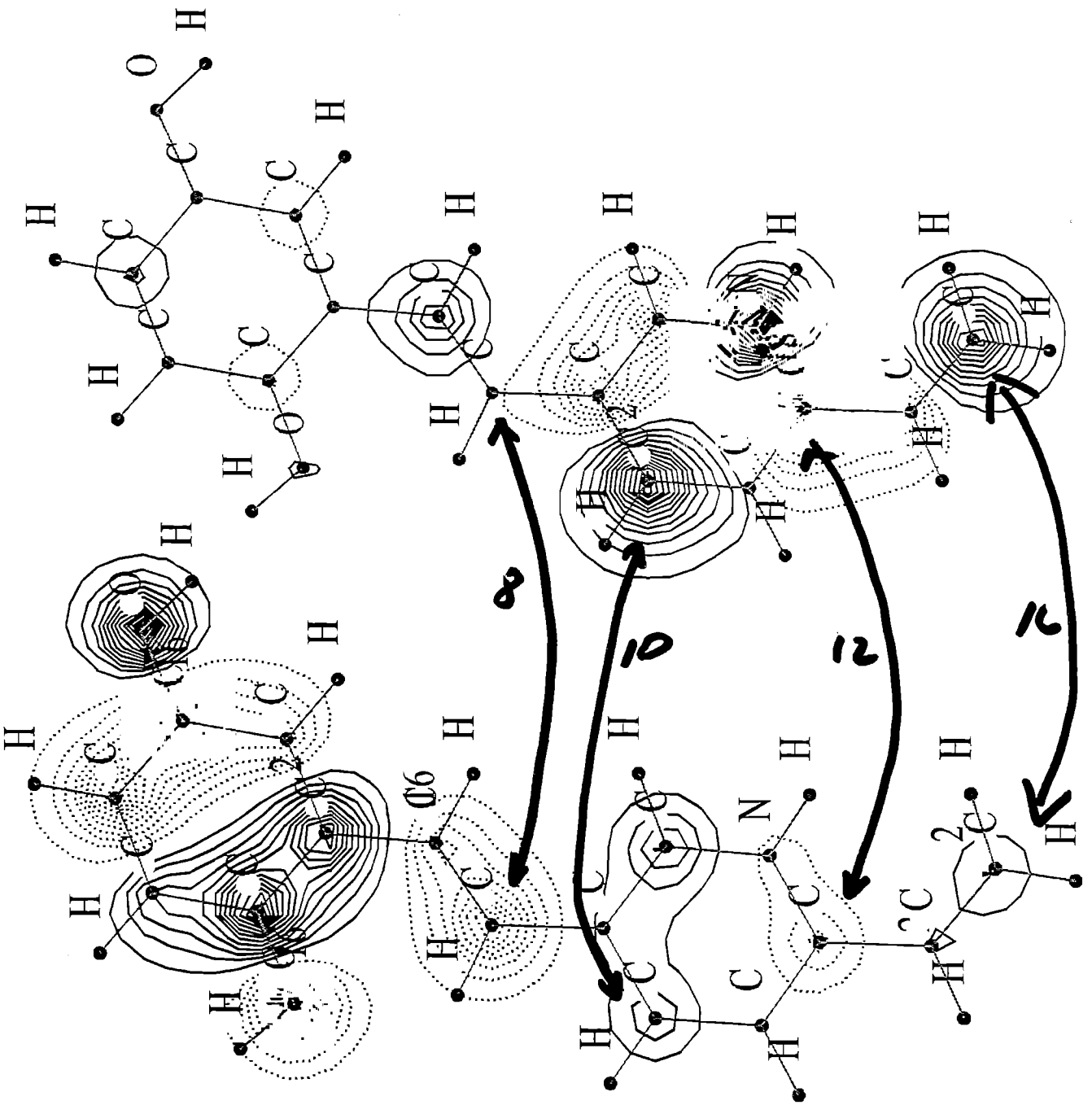

PROTONATED HOMO/LUMO

EXCITATION ENERGIES

Differences in energy between ground and excited states (eV)
all calculated with 6-31G* basis set

F-substitution	unprotonated	protonated	difference
none	4.72	4.33	-0.39
C2	4.76	4.35	-0.40
C6	4.75	4.45	-0.31
C8*	4.78	4.30	-0.48
C10*	4.75	4.36	-0.38
C14	4.73	4.19	-0.54

*predicted to change excitation energy drop based on atomic charge changes

C8 is predicted correctly to change and C2 to be static
however, C10 shows little change in excitation energy drop
despite charge sensitivity
C6 shows a substantial decrease in excitation energy drop
even though not much change in charge
C14 opposite of C6, large increase in excitation energy
drop (perhaps due to proximity to N?)

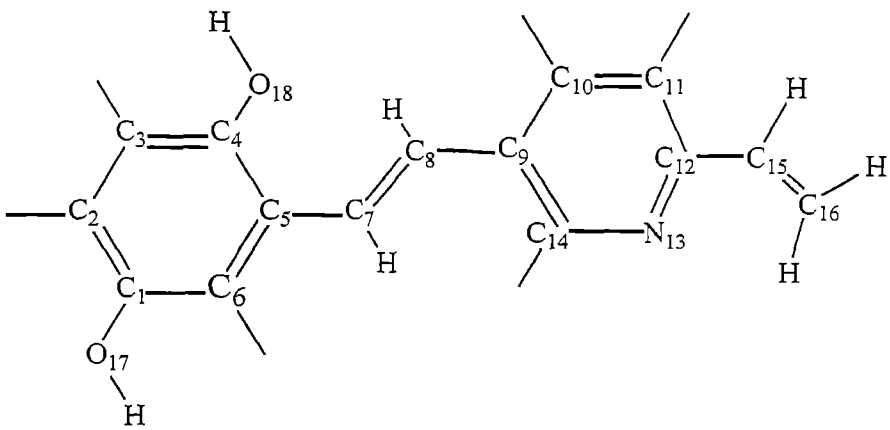

calculations with smaller 3-21G basis set

F-substitution	unprotonated	protonated	difference
none	4.90	4.48	-0.42
C2	4.92	4.51	-0.41
C6	4.93	4.61	-0.32
C14	4.89	4.28	-0.61
C8*	4.95	4.44	-0.51
C10*	4.91	4.46	-0.45
C16*	4.91	4.44	-0.47

*predicted to change excitation energy based on atomic charge changes

consistent with larger basis set:
- increase in excitation energy drop at C8, decrease at C6
- large increase at C14
- some small increases at C10 and C16

other substitution – nitro group

	unprotonated	protonated	difference
none	4.90	4.48	-0.42
C8-F	4.95	4.44	-0.51
C8-NO_2	4.50	4.51	0.01*
C10-F	4.91	4.46	-0.45
C10-NO_2	*4.49*	*4.14*	*-0.35*

*strong repulsions make this planar structure not a minimum

nitro group has effect opposite to F, reducing excitation energy drop in C10

removal of planarity constraint

3-21G basis set

F-substitution	unprotonated	protonated	difference
none pl	4.72	4.33	-0.39
none npl	5.00	4.68	-0.32
			+0.07
C10-F pl	4.75	4.36	-0.38
C10-F npl	4.91	4.65	-0.26
			+0.12
C8-F pl	4.78	4.30	-0.48
C8-F npl	5.27	4.72	-0.54
C8-F npl (HB)	5.13	4.70	-0.43

relaxing planarity constraint
lowers the amount of the excitation energy drop for unsubstituted molecule and for C10-F
raises it for C8 (if no H-bond), lowers in case of H-bond

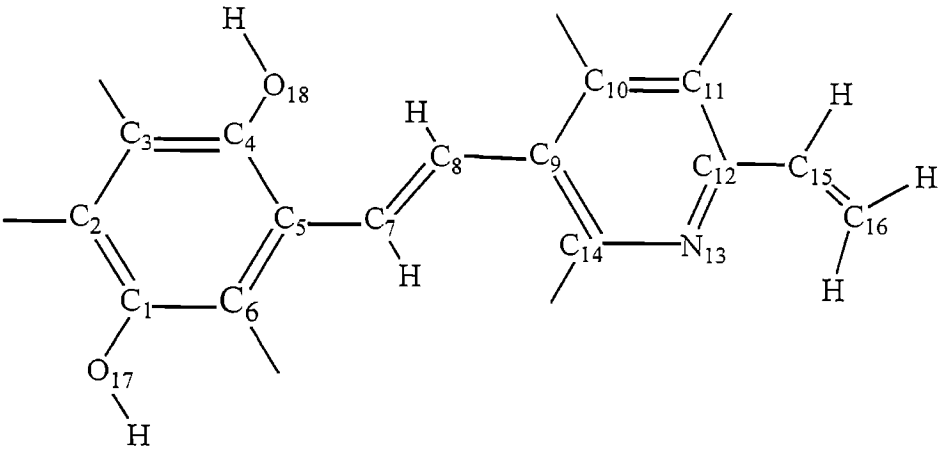

other substitutions - (all nonplanar)

none	5.00	4.68	-0.32
C10-F	4.91	4.65	-0.26
C10-CH_3	5.15	4.78	-0.37
C10-NO_2	4.33	3.75	-0.58
C10-NH_2	5.96	5.65	-0.30
none	5.00	4.68	-0.32
C8-F	5.13	4.70	-0.43
C8-NO_2	4.42	4.26	-0.16

for C10, NH_2 has little effect, F lowers drop, CH_3 and NO_2 increase drop
for C8, F raises drop, NO_2 decreases drop

in both cases, F and NO_2 are opposite to one another

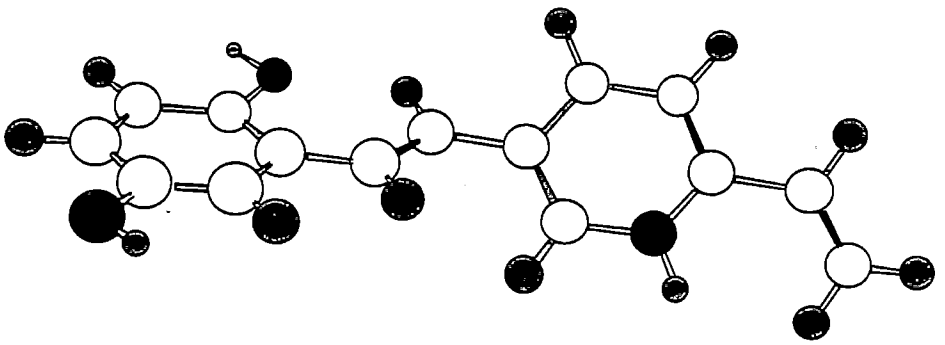

CONCLUSIONS

- **calculations support notion that protonation acts to promote a red shift via a mechanism involving charge transfer from one ring to another as a result of electronic excitation**

- **atomic charges are of some help in identifying "hot spots", but this help is limited**

- **for F substitution, C14 and C8 enhance the magnitude of the red shift, C6 does the reverse.**

- **C2 does very little, C10 and C16 mild increases.**

- **so this is not just a matter of substitution on one ring or another**

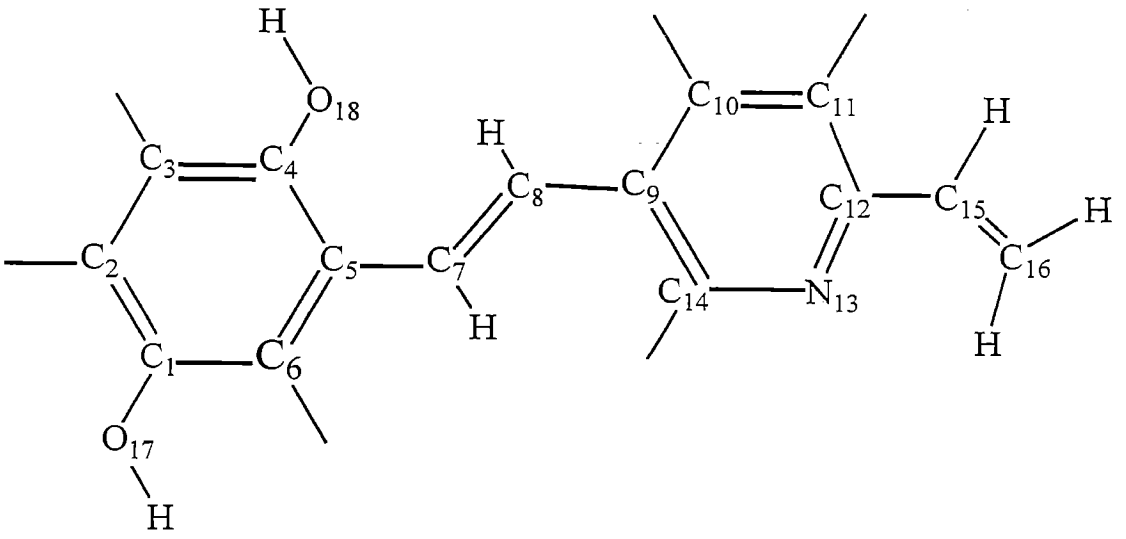

- changing from F to other substituents produces results that are not easily understood yet
- nitro group produces large perturbations, but not the same as F
- removing planarity constraint tends to lower the magnitude of red shift
- other substituents (methyl, nitro, amino) produce results which are not yet easily interpreted

A 1996 paper (Toshima & Tominaga, Bull. Chem. Soc. Jpn. 1996, 69, 2111) had found interesting redox properties of complexes between several transition metals and phthalocyanine (pc) in thin films.

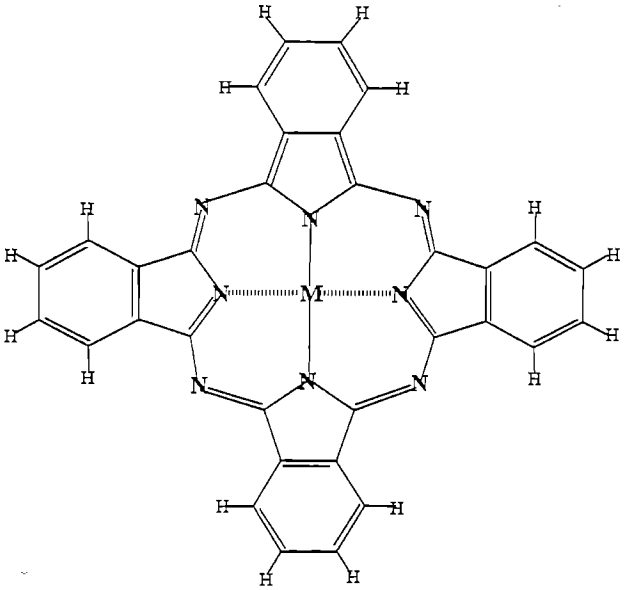

When M=Cu, Ni, reversible electrochromism
Zn, Co, Fe irreversible.

The authors had little understanding of this difference.
Their hypothesis: M changes electron state of the pc ring.

If M highly electronegative
•sucks density out of pc ring, making latter more difficult to oxidize, i.e. higher oxidation potential.
•after ionization to cation, positive charge will tend to localize on pc ring.

when M less electronegative, get the reverse.
also hypothesize that positive charge of cation is localized at certain positions of the pc ring. these can be thought of as electrically isolated domains, subject to attack by anions present in the solution.

M	Electronegativity	reversible?
Fe	1.7	no
Co	1.7	no
Ni	1.8	yes
Cu	1.8	yes
Zn	1.6	no

can such small changes in electronegativity (~0.1) account for these differences?

Address problem by ab initio calculations.
Large size of system, coupled with close-lying electronic states, makes routine application of high-level ab initio theory problematic.

HF	Hartree-Fock	standard workhorse, questionable for transition metals
MP2	perturbation theory	means of including electron correlation. but also questionable for transition metals
B3LYP	density functional	"standard" variant of DFT; includes electron correlation
LANL2DZ	basis set	effective core potential on M
6-31G*		no effective cores used
ADF		less standard DFT, does not use "basis sets" as such

Binding Energies of Metals to Pc[a], eV

	FePc	CoPc	NiPc	CuPc	ZnPc	MgPc
B3LYP (A)[b]	-4.39	-9.38	-7.81	-6.03	-5.12	
HF (A)	1.67		-6.11	-3.16		
MP2 (A)			-8.35			
B3LYP (B)[c]	-7.87	-8.44	-10.21	-10.06	-7.56	-8.07
HF (B)	-6.74	-4.79	-9.04	-5.51	-5.66	
MP2 (B)	-11.25	-10.95	-13.43	-8.87	-9.57	
ADF	-9.81	-10.49	-9.90	-6.96	-5.66	-8.14

[a]negative quantity indicates favorable binding
[b]LanL2DZ [c]6-31G*

HF probably useless; correlation very important
MP2: Ni > Fe > Co > Zn > Cu
B3LYP: Ni ~ Cu > Co > Fe ~ Zn
B3LYP makes Cu a better binder
ADF: Co > Ni ~ Fe > Cu > Zn
Co,Ni,Fe > Cu,Zn
binding energies are in the 5 – 10 eV range

MO DIAGRAM

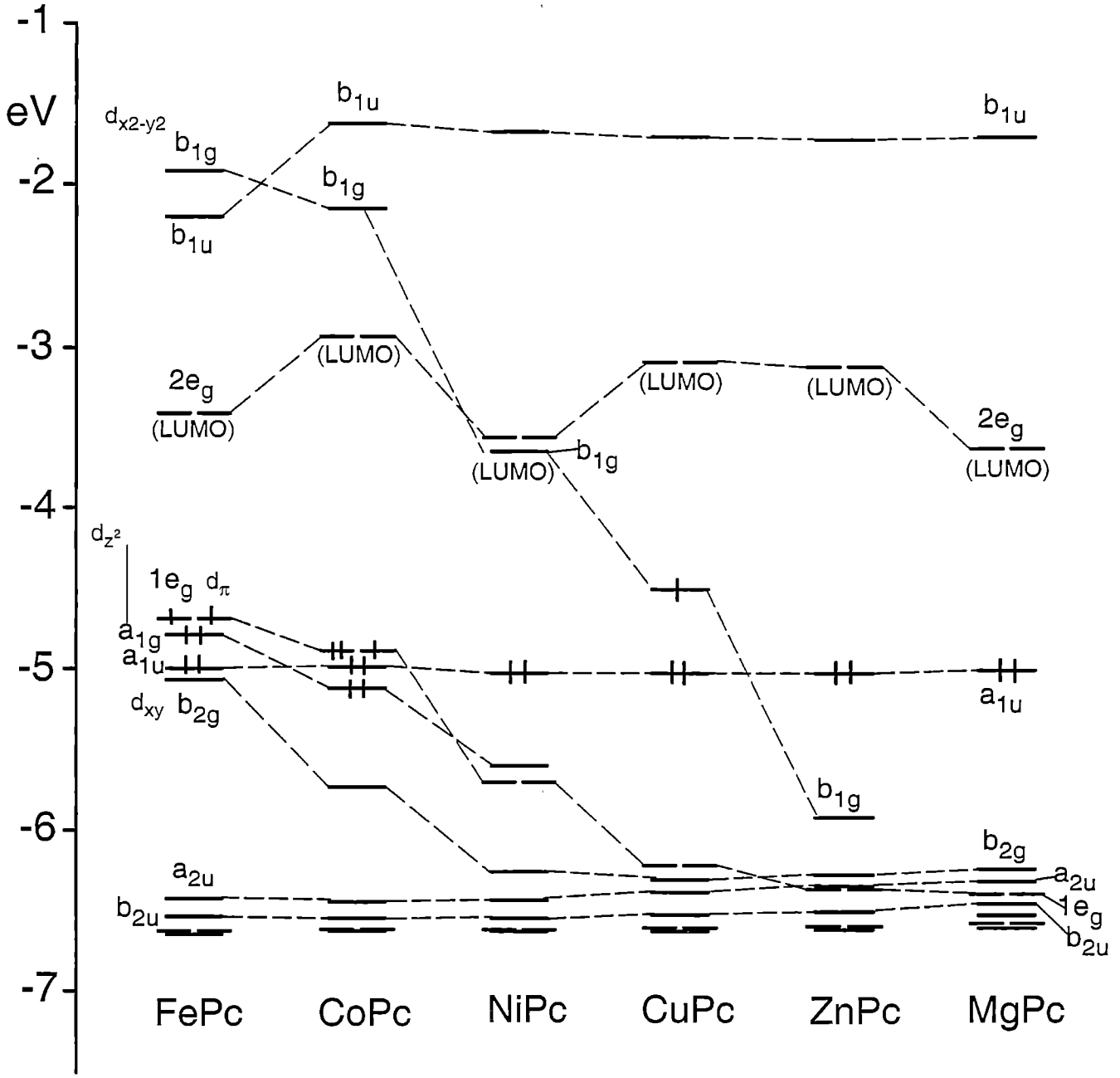
-1
eV
-2
-3
-4
-5
-6
-7
d_{x2-y2}
b_{1g}
b_{1u}
b_{1u}
b_{1g}
b_{1u}
$2e_g$
(LUMO)
(LUMO)
(LUMO)
(LUMO)
(LUMO)
b_{1g}
$2e_g$
(LUMO)
d_{z^2}
$1e_g$ d_π
a_{1g}
a_{1u}
d_{xy} b_{2g}
a_{1u}
b_{1g}
b_{2g}
a_{2u}
a_{2u}
b_{2u}
$1e_g$
b_{2u}
FePc
CoPc
NiPc
CuPc
ZnPc
MgPc

IONIZATION POTENTIALS, eV

	Pc	FePc	CoPc	NiPc	CuPc	ZnPc	MgPc
B3LYP (A)		3.83	7.58	6.08	7.65	6.00	
HF (A)				4.54			
MP2 (A)				7.31			
B3LYP (B)	6.93	6.02	6.24	6.08	7.30	6.06	5.97
HF (B)		4.50	4.72	4.54	4.66	4.54	
MP2 (B)							
ADF	7.02	6.46	6.47	6.56	6.51	6.56	6.52
ADF (T)	6.98	6.49	6.47	6.51	6.51	6.52	6.48

B3LYP (B): Cu hardest to ionize, harder than uncomplexed pc
all other metals have lower IP, roughly the same.

ADF: all metals lower IP, little to distinguish one metal from another

(ADF) HOMO - LUMO SEPARATIONS, eV

Fe	Co	Ni	Cu	Zn	Mg
1.38	1.96	1.47	1.42	1.91	1.38
$1e_g \rightarrow 2e_g$	$1e_g \rightarrow 2e_g$	$a_{1u} \rightarrow b_{1g}$	$b_{1g} \rightarrow 2e_g$	$a_{1u} \rightarrow 2e_g$	$a_{1u} \rightarrow 2e_g$

Fe, Ni, Cu have lowest separation, followed by Zn and Co.
except for Fe, this conforms to expt.

note also: HOMO-LUMO separation pattern different than IPs.

Charge assigned to metal atom

	FePc	CoPc	NiPc	CuPc	ZnPc	MgPc
B3LYP (A)	0.27	0.60	0.55	0.73	1.15	
HF (A)	0.45	0.57	1.02			
MP2 (A)			0.63			
B3LYP (B)	1.20	0.71	0.80	0.88	0.94	1.07
HF (B)	1.46	0.75	1.28	0.83	1.34	
MP2 (B)	1.23	0.66	0.90	0.74	1.04	
ADF	0.71	0.59	0.50	0.65	0.64	0.77

B3LYP: Zn > Cu > Co ~ Ni
but Fe very sensitive to basis set

MP2: Zn high, but now followed by Ni > Cu > Co

ADF: Zn ~ Cu > Co > Ni

no obvious patterns here, except high charge of Zn

whereas low electronegativity of Zn is manifest by high + charge, high electronegativities of Ni and Cu don't seem to be apparent in charges

ELECTRON AFFINITIES, EV

	Fe	Co	Ni	Cu	Zn	Mg
MPc	-2.92	-3.19	-2.14	-1.74	-2.23	-2.16

electrons are drawn to each species (negative values)
Cu and Ni the weakest, with Cu < Ni
among others, Zn < Fe < Co

this pattern generally consistent with electronegativities:
Zn < Fe ~ Co < Cu ~ Ni
in that Ni and Cu have weakest pull for an electron,
but Zn out of place here.

MORE DETAIL OF METAL CHARGE

orbital	Fe	Co	Ni	Cu	Zn	Mg
3d	6.59	7.63	8.61	9.50	10.0	0.42 (3d)
4s	0.42	0.41	0.42	0.39	0.55	0.36 (3s)
4p	0.29	0.37	0.48	0.46	0.81	0.45 (3p)
Q_M	0.71	0.59	0.50	0.65	0.64	0.77

total (positive) charge: Ni < Co < Zn ~ Cu < Fe
orbital populations (invert charge)
3d shell: Zn < Cu < Ni < Co < Fe
4s shell: Zn < Fe ~ Co ~ Ni < Cu
4p shell: Zn < Ni ~ Cu < Co < Fe
none of these show expt behavior

ATOMIC CHARGES AROUND THE PC SYSTEM

	M = Fe	M = Co	M = Ni	M = Cu	M = Zn	M = Mg
Q_M	0.71	0.59	0.50	0.65	0.64	0.87
Q_{N1}	-0.53	-0.50	-0.48	-0.51	-0.49	-0.57
Q_{N2}	-0.33	-0.33	-0.33	-0.33	-0.33	-0.33
Q_{C1}	0.32	0.32	0.32	0.32	0.32	0.33
Q_{C2}	0.09	0.09	0.09	0.09	0.08	0.08
Q_{C3}	0.14	0.14	0.14	0.14	0.14	0.13
Q_{C4}	0.17	0.17	0.17	0.17	0.17	0.17
Q_{H1}	-0.18	-0.18	-0.19	-0.18	-0.18	-0.18
Q_{H2}	-0.18	-0.18	-0.18	-0.18	-0.18	-0.18

Nature of metal has very little effect upon the charges of the atoms around the pc ring. This belies the idea that the different behavior is moderated by the electron density on the periphery of the pc system, induced by change in metal electronegativity.

same properties of cation:

orbital	Fe	Co	Ni	Cu	Zn	Mg
3d	6.59	7.64	8.61	9.50	10.0	0.40
4s	0.40	0.36	0.40	0.37	0.54	0.31
4p	0.27	0.39	0.47	0.45	0.80	0.40
Q_M	0.74	0.62	0.52	0.68	0.65	0.90

total (positive) charge: Ni < Co < Zn < Cu < Fe
orbital populations (invert charge)
3d shell: Zn < Cu < Ni < Co < Fe
4s shell: Zn < Fe ~ Ni < Co ~ Cu
4p shell: Zn < Ni ~ Cu < Co < Fe

patterns in cation very much the same as in neutral

CONCLUSIONS

- problem is a difficult one
- metal electronegativity oversimplified and not indicative enough
- electron correlation needed for accuracy
  different methods can be at odds with one another
- ionization potentials of MPc are all quite similar
- HOMO-LUMO separation pattern different than IPs
  (HOMO not the same symmetry for all)
- b_{1g} orbital most sensitive to nature of metal (d_{x2-y2})
- atomic charges (metal or PC atoms) not helpful indicators
  same true for individual atomic orbitals (4s, 4p, 3d)
- electron affinities are smallest for CuPc and NiPc

Timothy M. Swager

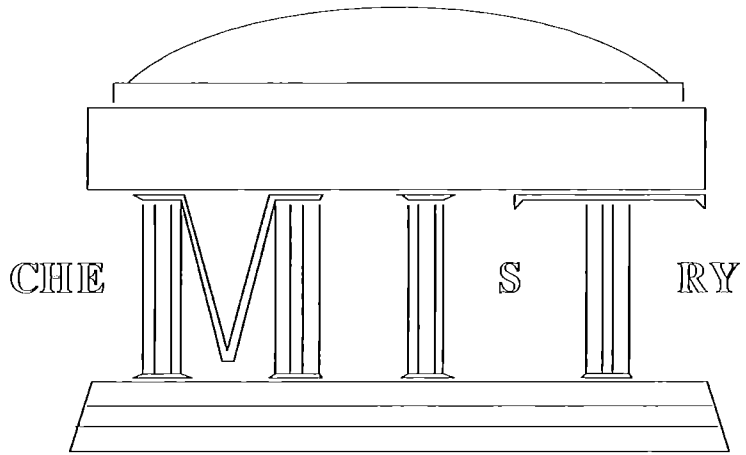

Synthesis of Electroactive and Emissive Conjugated Polymers

MIT Team: J.D. Tovar (100 % MURI effort)
Dr. Anthony Pullen (now at E-ink)
Ashleigh H. Hegedus (UG-Yale)
Irina Gorodetskaya (UG)
Bruce Yu (50% MURI effort)
D. Tyler McQuade (NIH PD fellow)
Dr. Zhengguo Zhu (Funded by DARPA)

Cationic PPEs

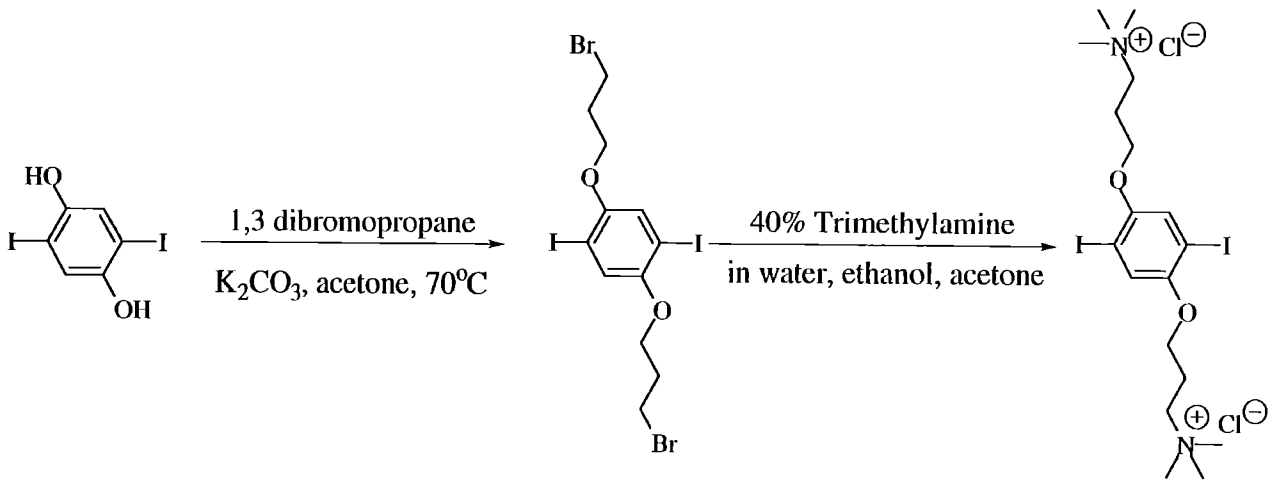

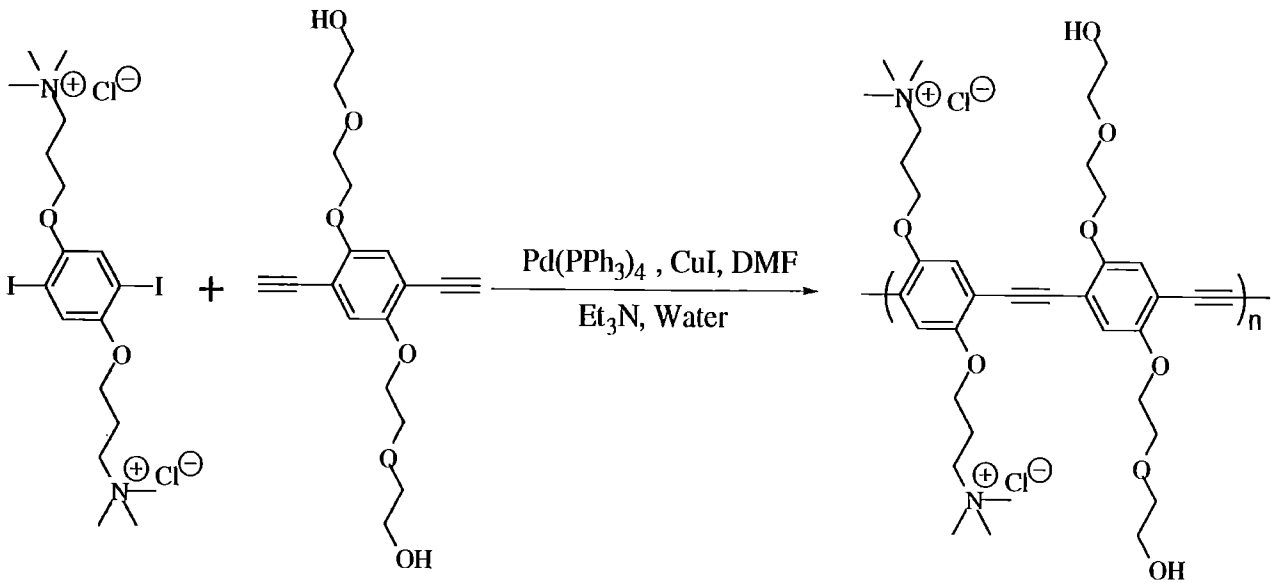

Water Soluble Ionic PPEs

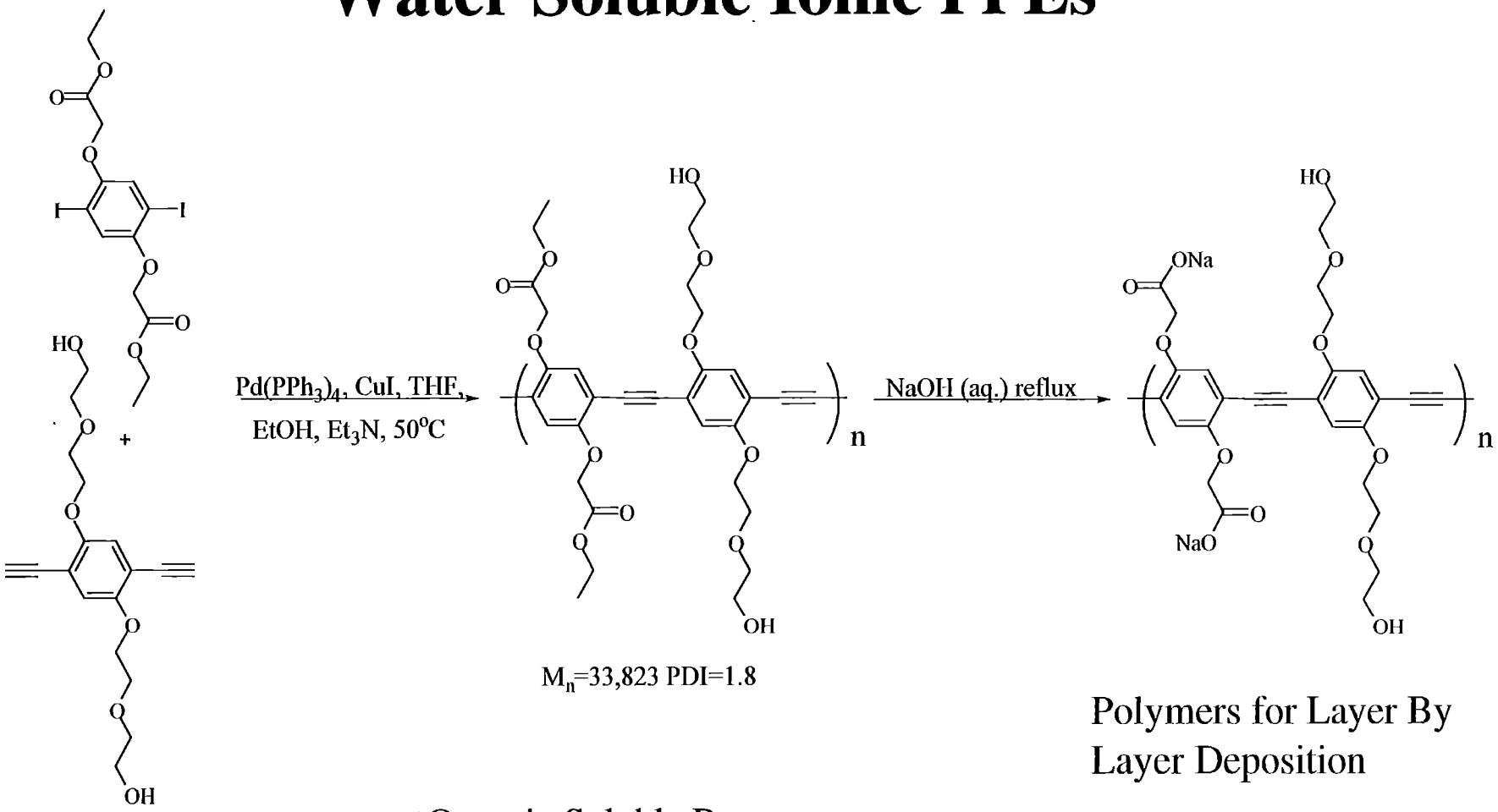

Organic Soluble Precursor

Polymers for Layer By Layer Deposition

Formation of a pH Sensitive Polymeric Dye

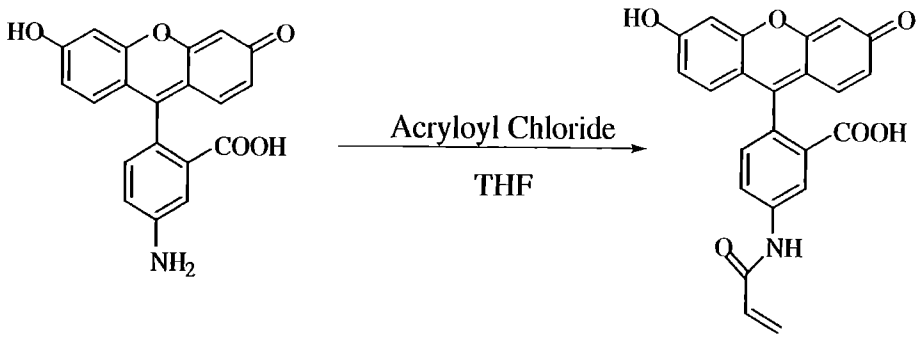

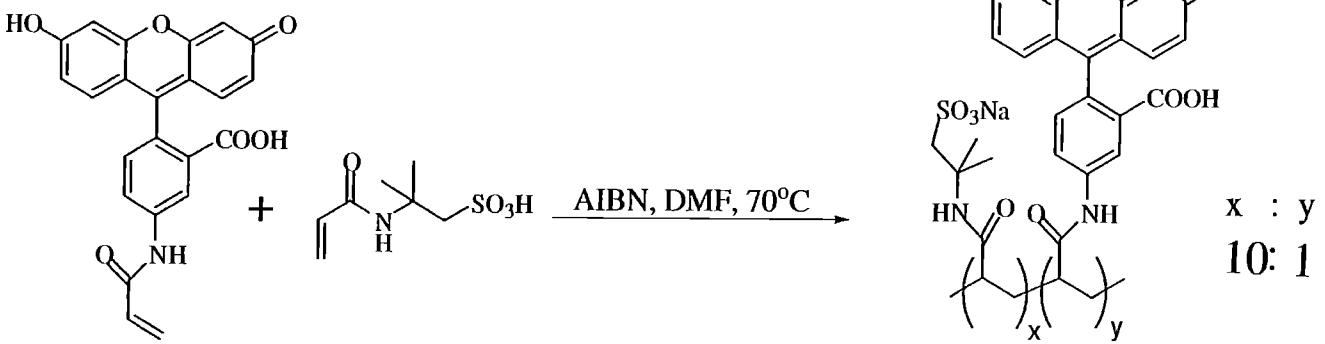

Fluoresceinamine
Emissive at High pH

Emission/Absorption of Donor and Acceptors

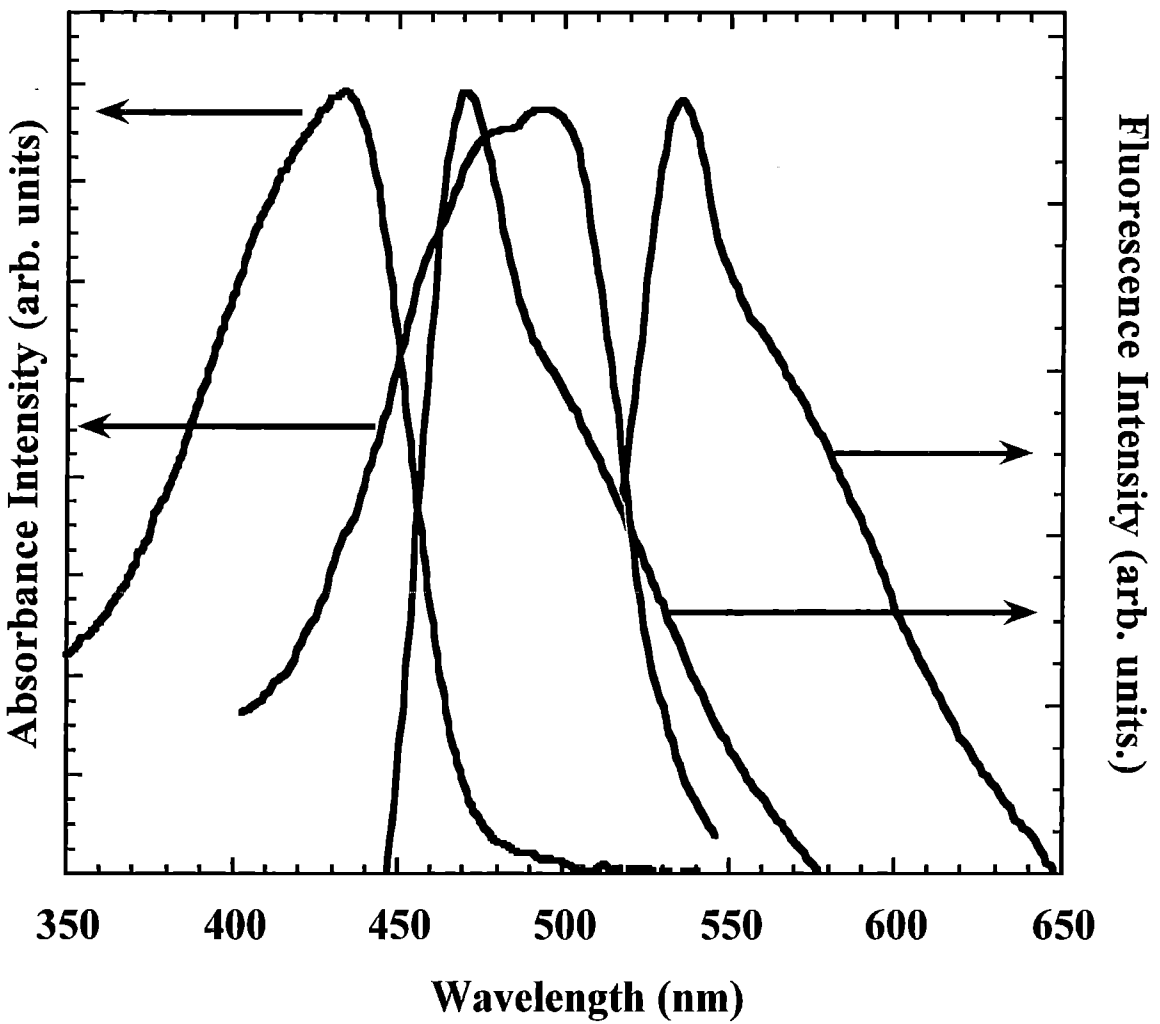

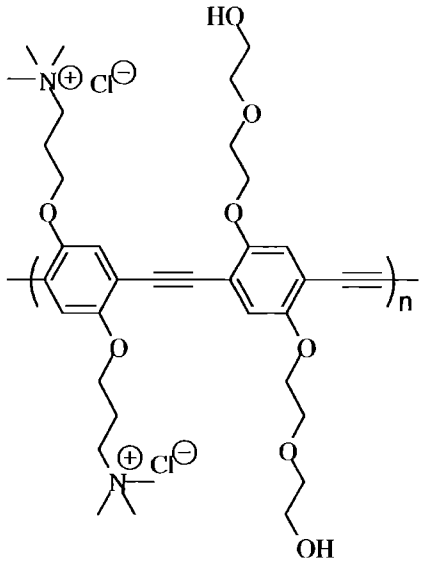

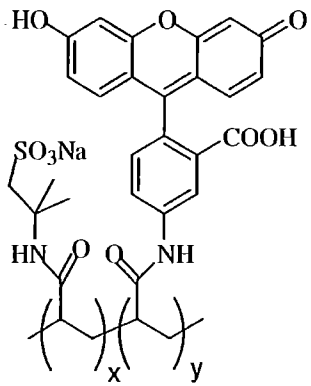

TOPS-MURI, T.M. Swager, MIT

Two Layer Film
Produced in A Layer By Layer Method

The Difference Between the Ex. 420 and 500
Indicates Efficient Energy Transfer

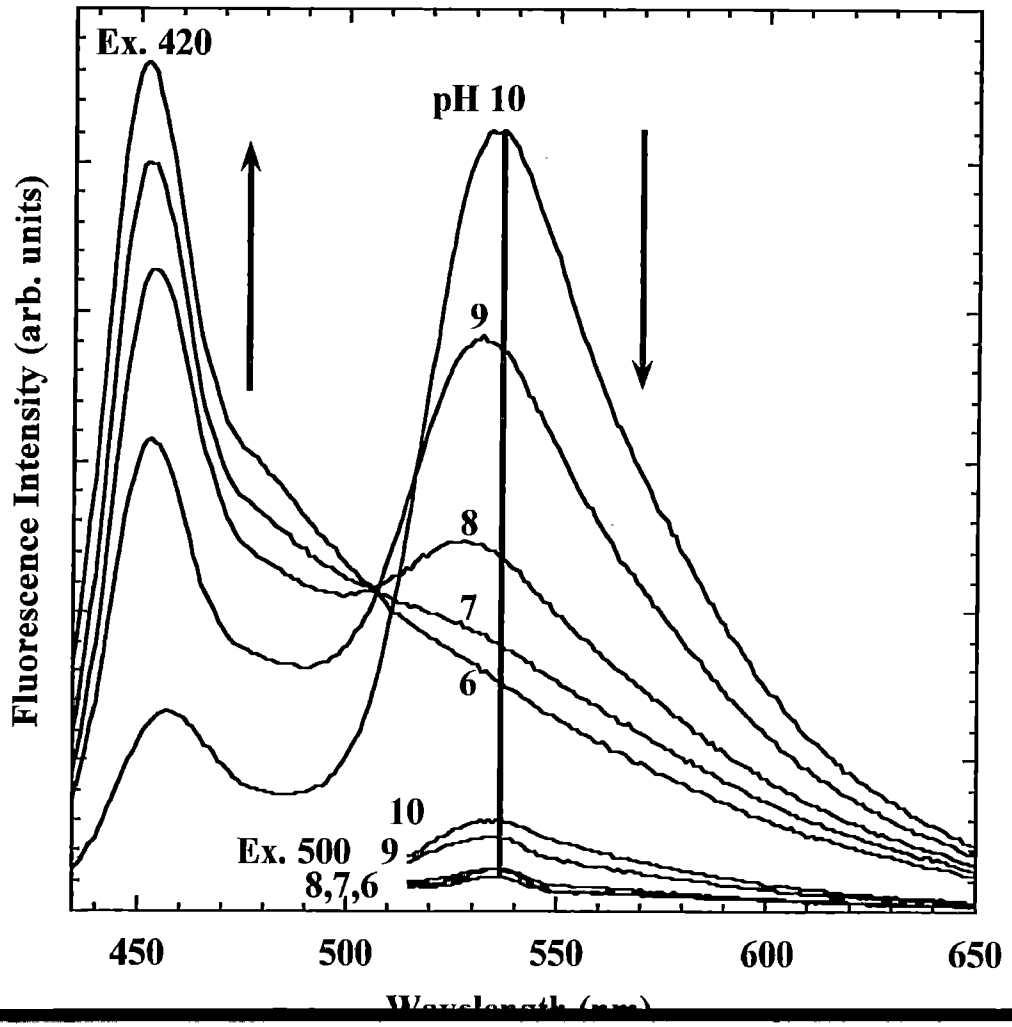

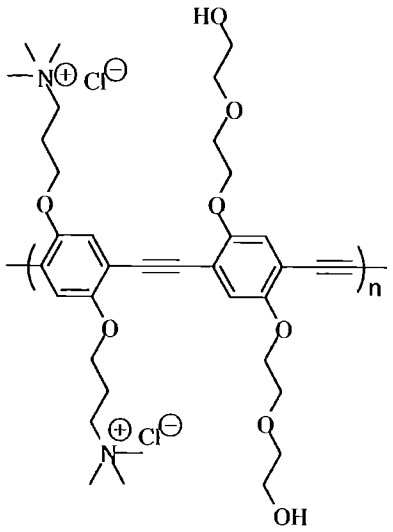

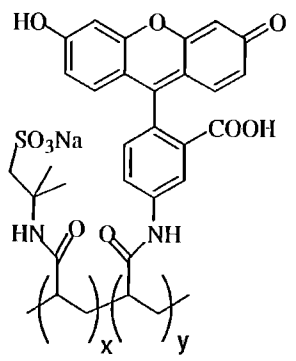

pH Response of Three-Layer Films

Get a Lower QY of the Polymer

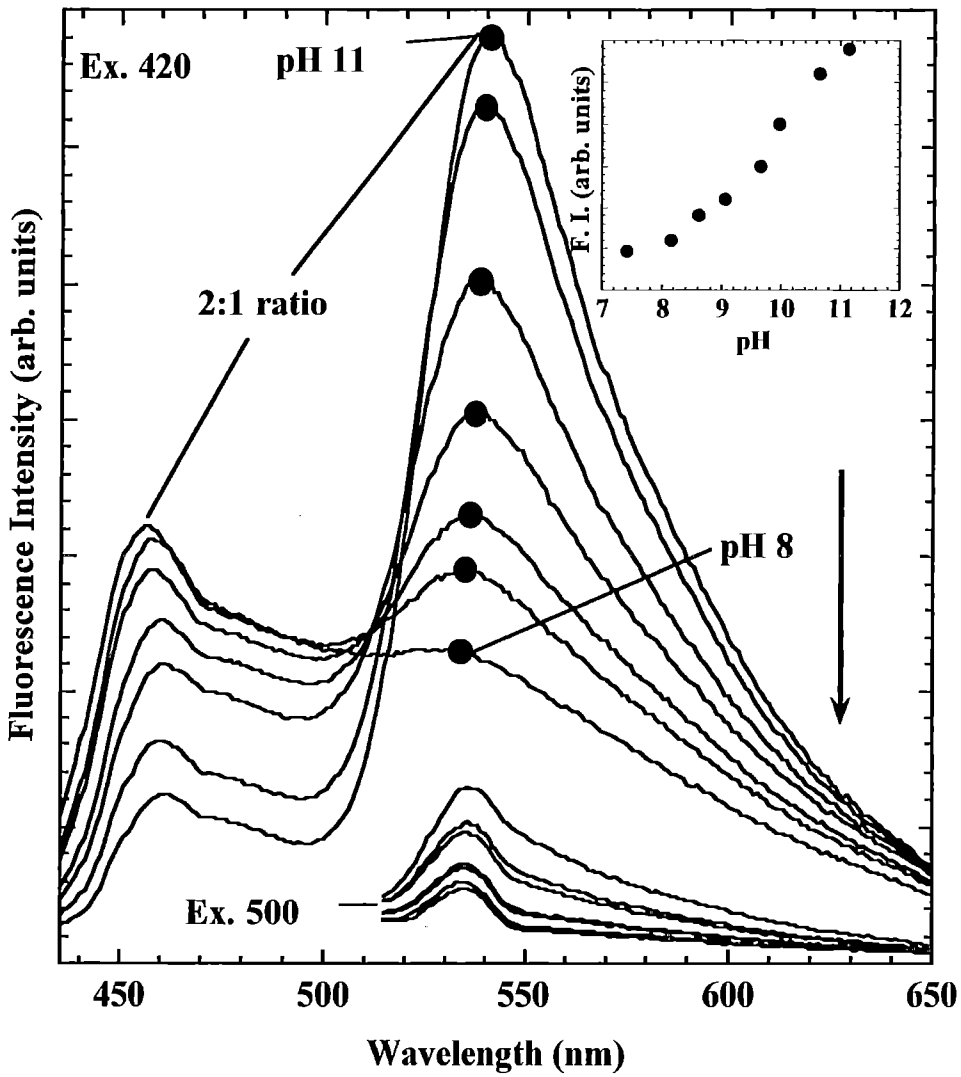

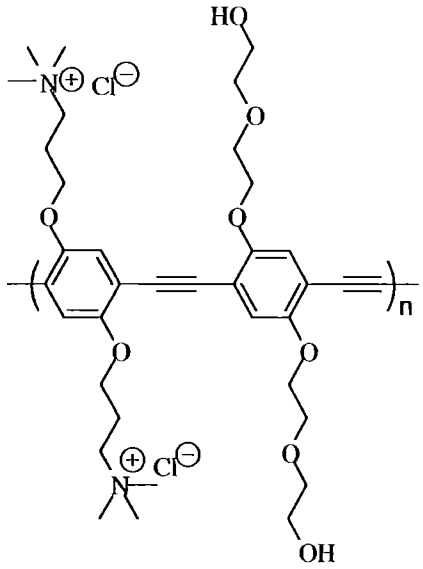

2 Layers

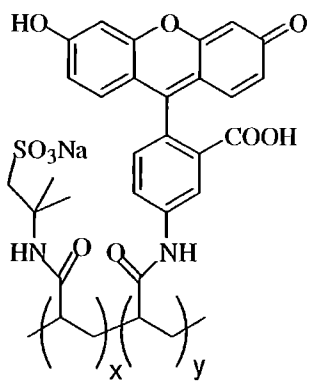

1 Layer

Regiospecific Synthesis of Aniline Copolymers

By Using Step-Wise Coupling
Precise More Structures can be Created

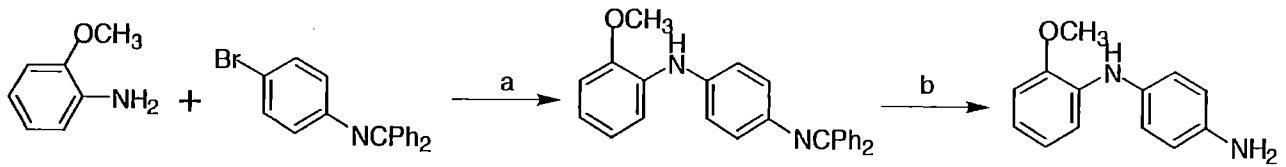

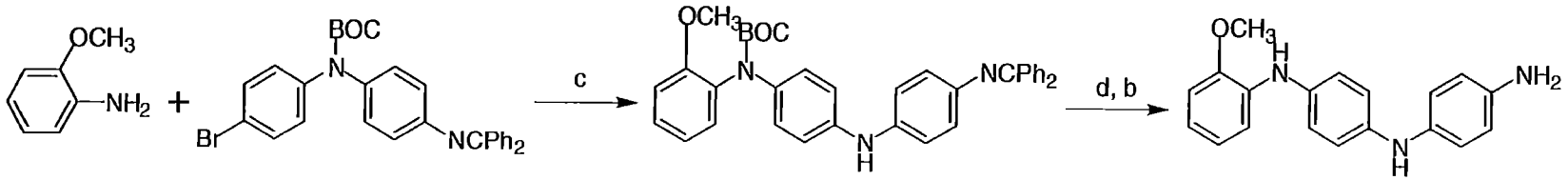

[a](a) Pd_2dba_3, *rac*-BINAP, NaOtBu, THF, reflux; (b) 10% Pd/C, NH_4HCO_2, THF, EtOH, 60° C; (c) Pd_2dba_3, *rac*-BINAP, NaOtBu, THF, reflux; (d) 160° C

Electro-deposition of Dimer and Trimers

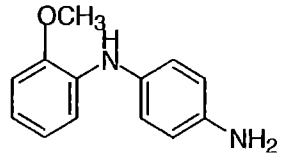

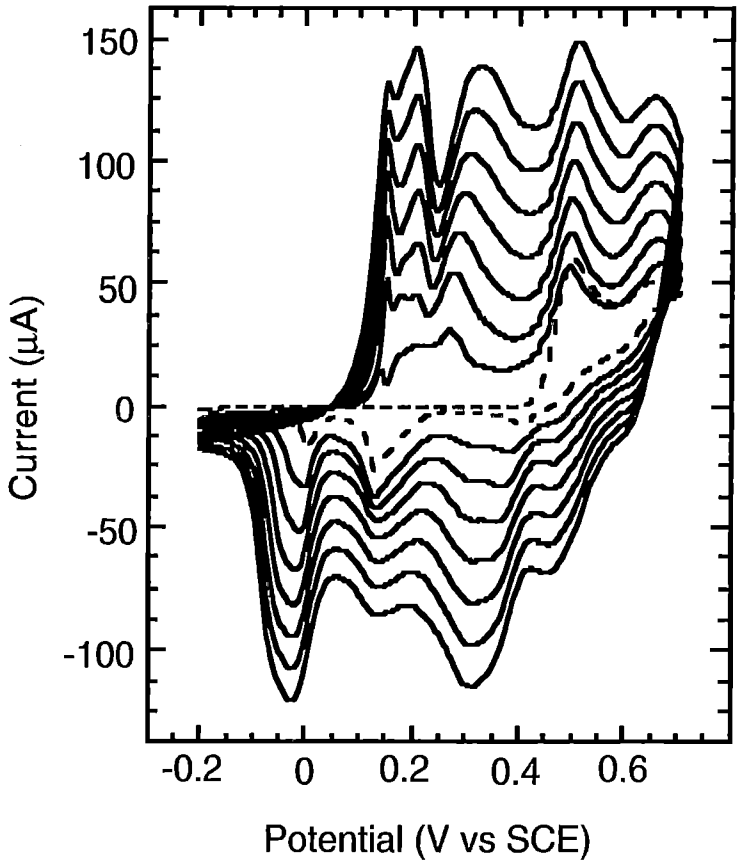

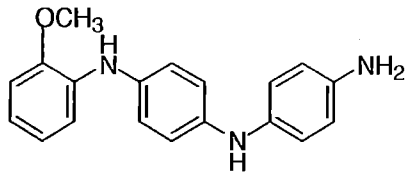

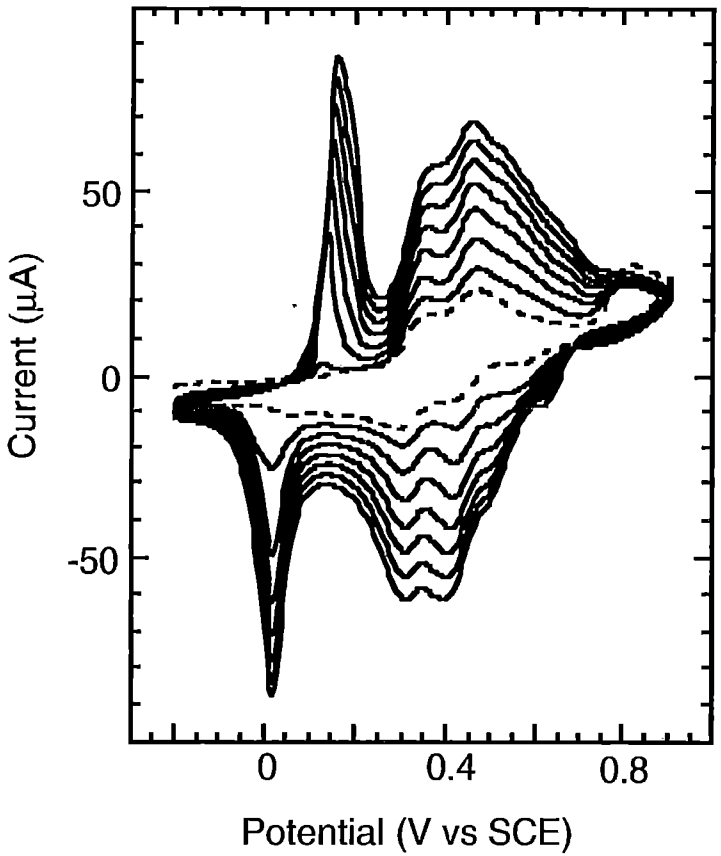

Dotted Line Indicates Initial Scan

CV and Conductivity Profiles of Dimer and Trimer

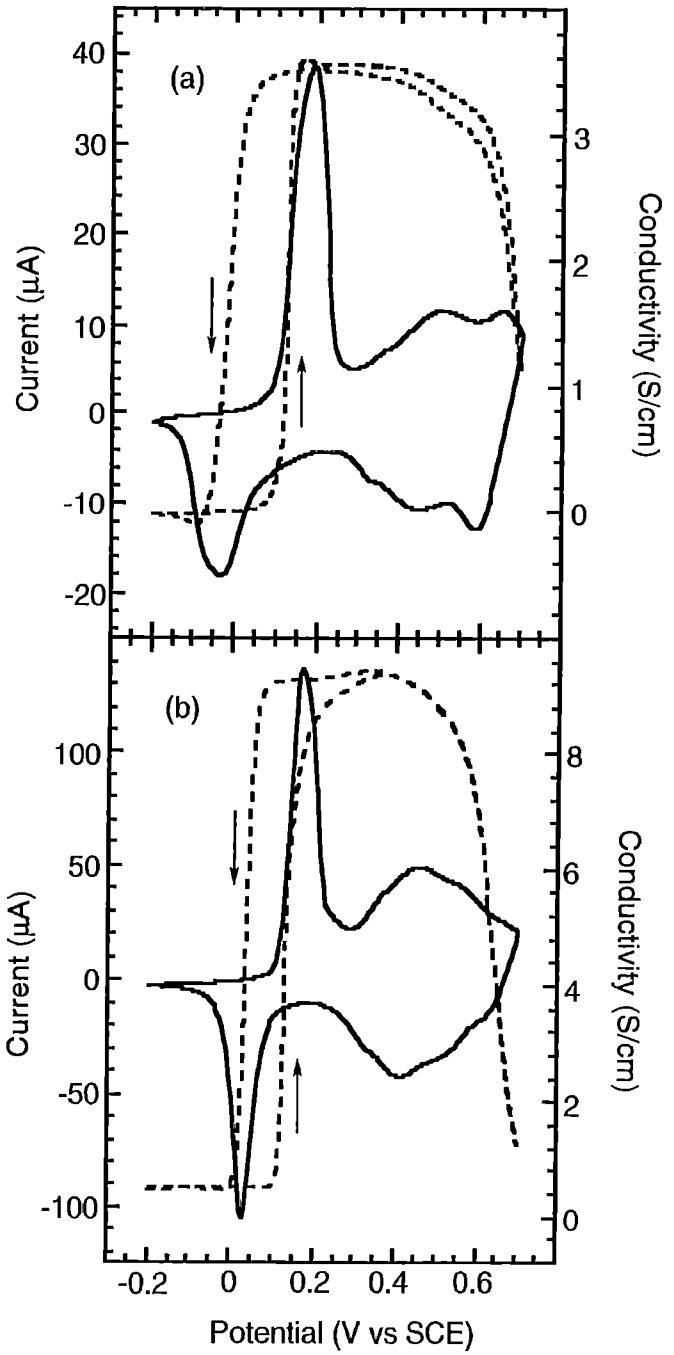

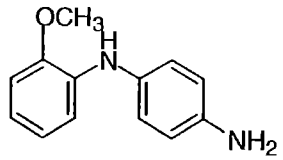

Sharp CVs

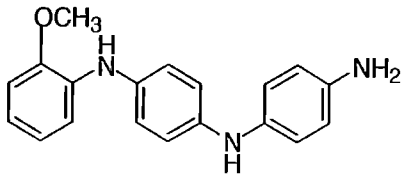

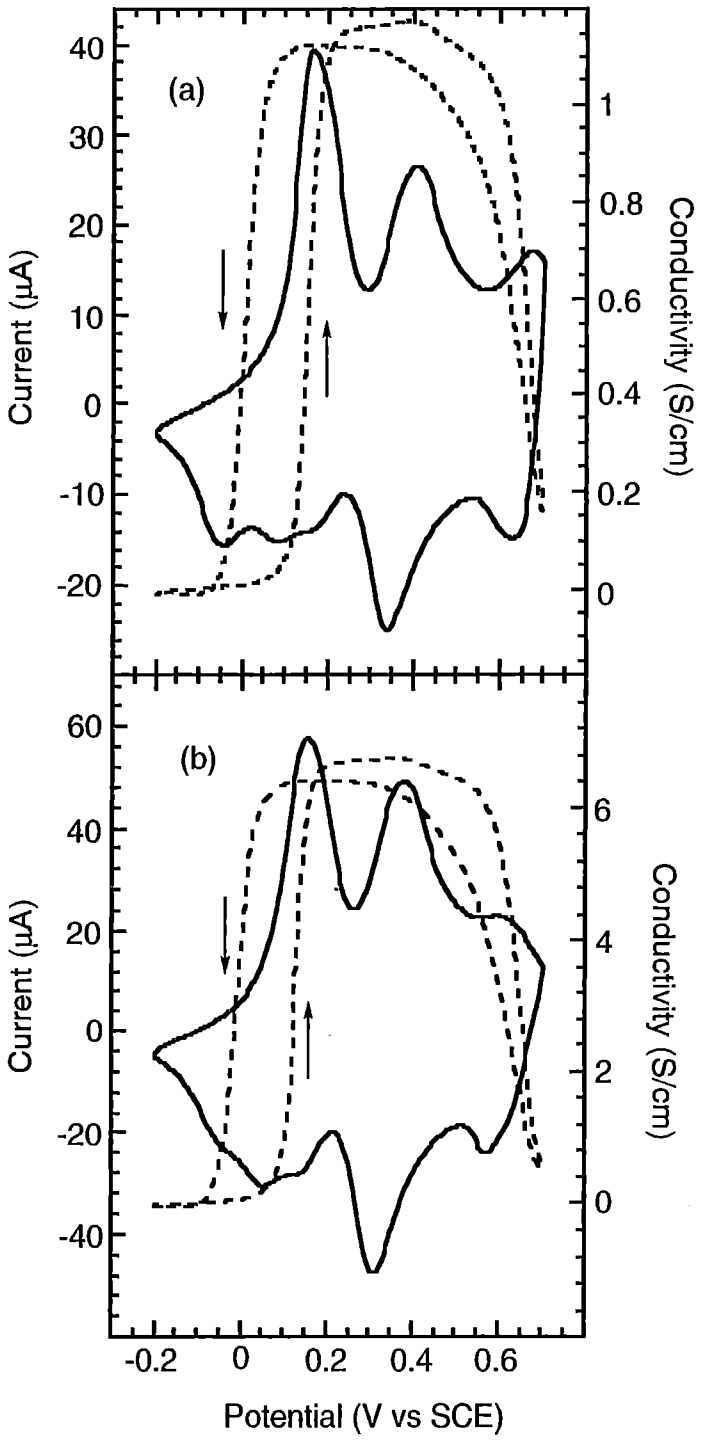

Random Copolymers of Methoxy Aniline and Aniline

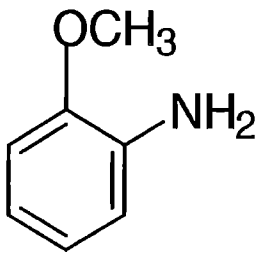

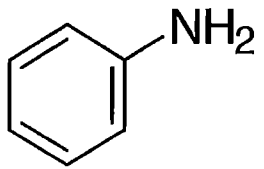

(a) Equal Amounts
(b) 2:1 (Aniline Excess)

Broader Electrochemistry
Slightly Lower Conductivity

Resonance Structures and The Charged States of Co-Polyanilines

An Organic Chemist's View

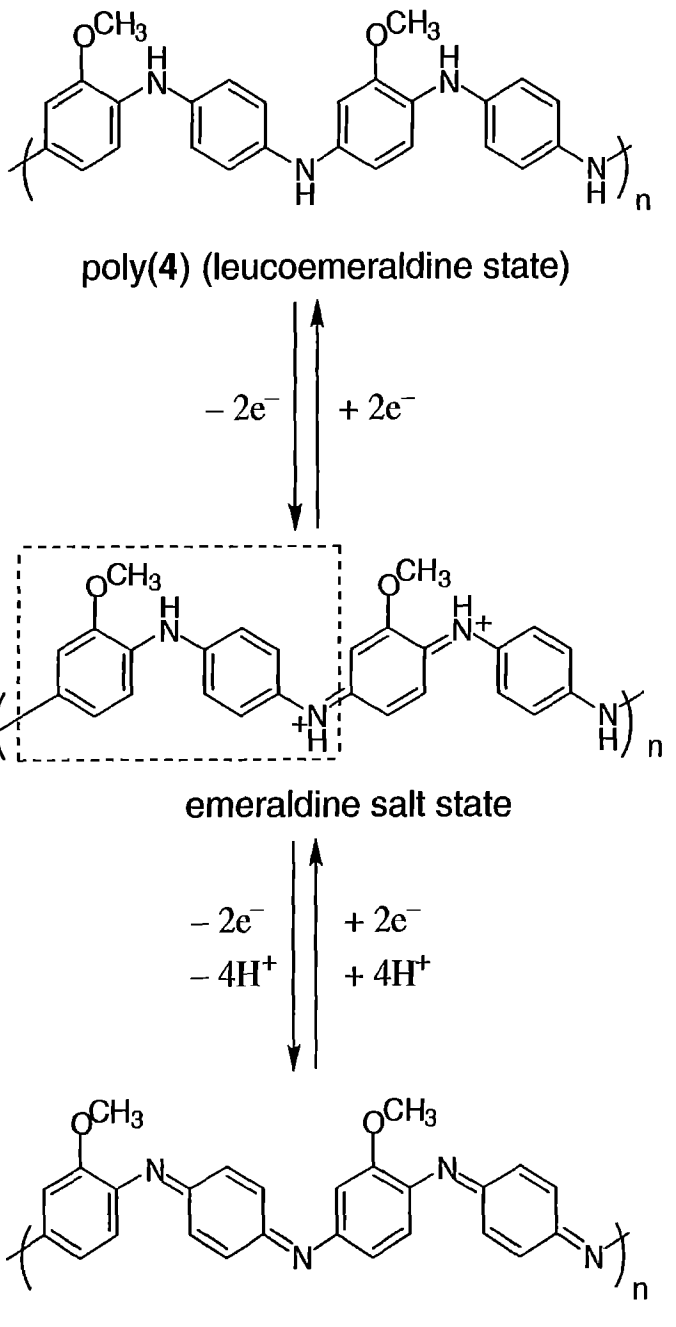

Examples of Highly Luminescent PPVs

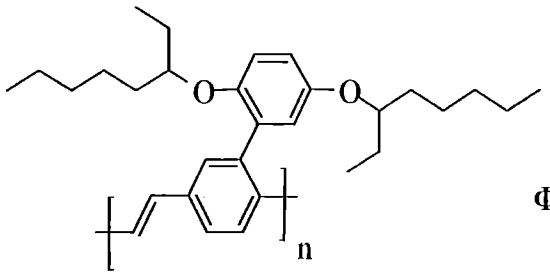

Φ=28%

Johansson,D. M.; Srdanov,G.; Yu, G.; Theander, M.; Inganäs, O.; Andersson, M. R. *Macromolecules* **2000**, *33*, 2525 -2529 .

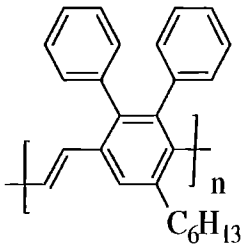

Φ=65%

Hsieh, B. R.; Yu, Y.; Forsythe, E. W.; Schaaf, G. M.; Feld, W. A. *J. Am. Chem. Soc.* **1998**, *120*, 231-232.

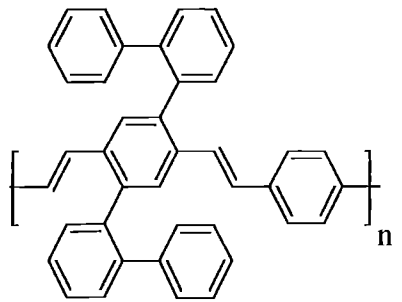

Φ=82%

Peng, Z.; Zhang, J.; Xu, B. *Macromolecules* **1999**, *32*, 5162-5164.

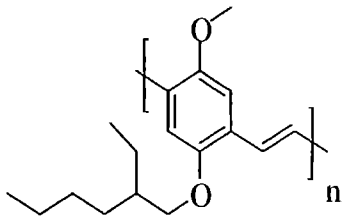

Braun, D.; Heeger, A. J.; *Appl. Phys. Lett.* **1991**, *58*, 1982

PPVs with Alternate Triptycene Units

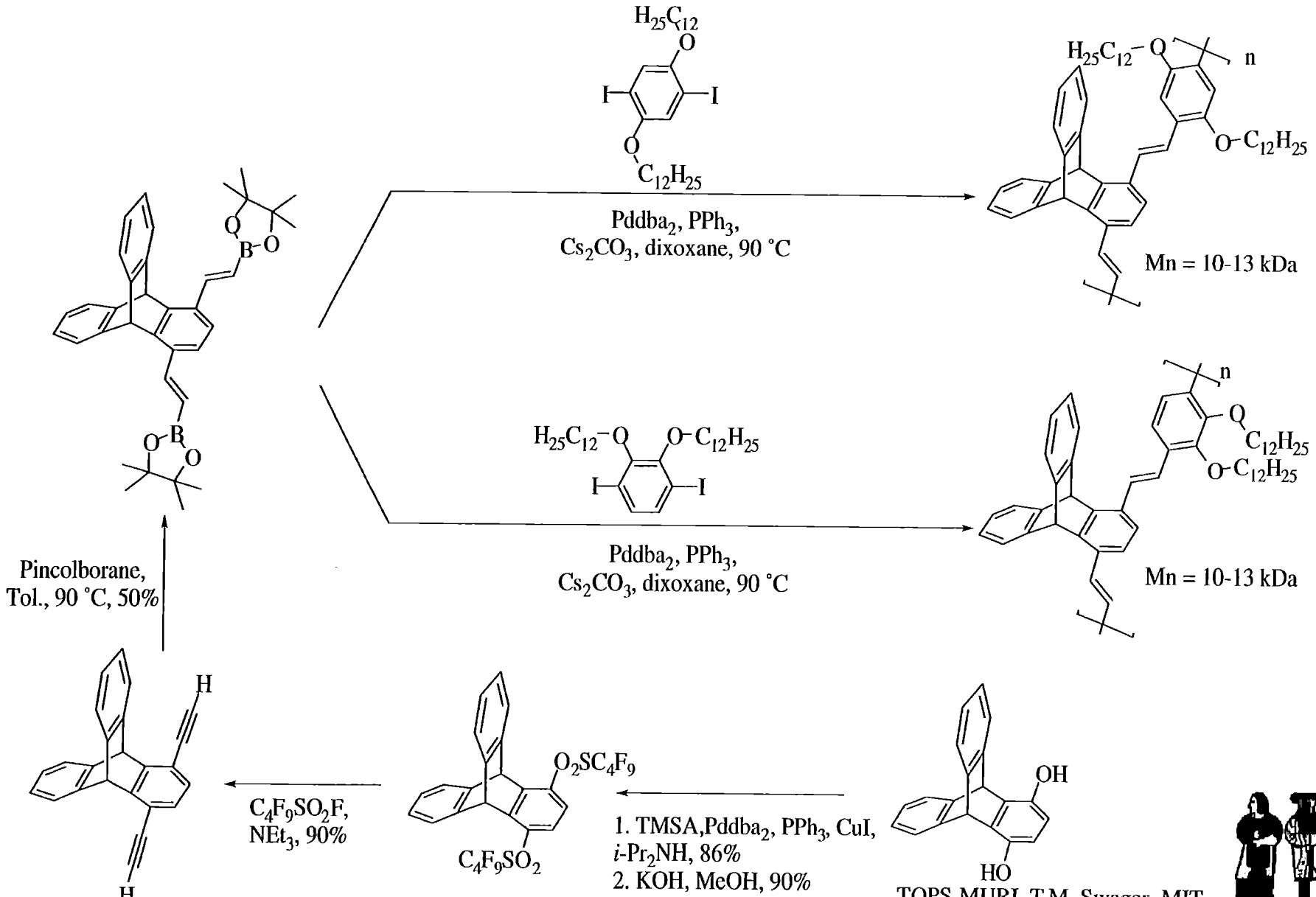

Emission Spectra

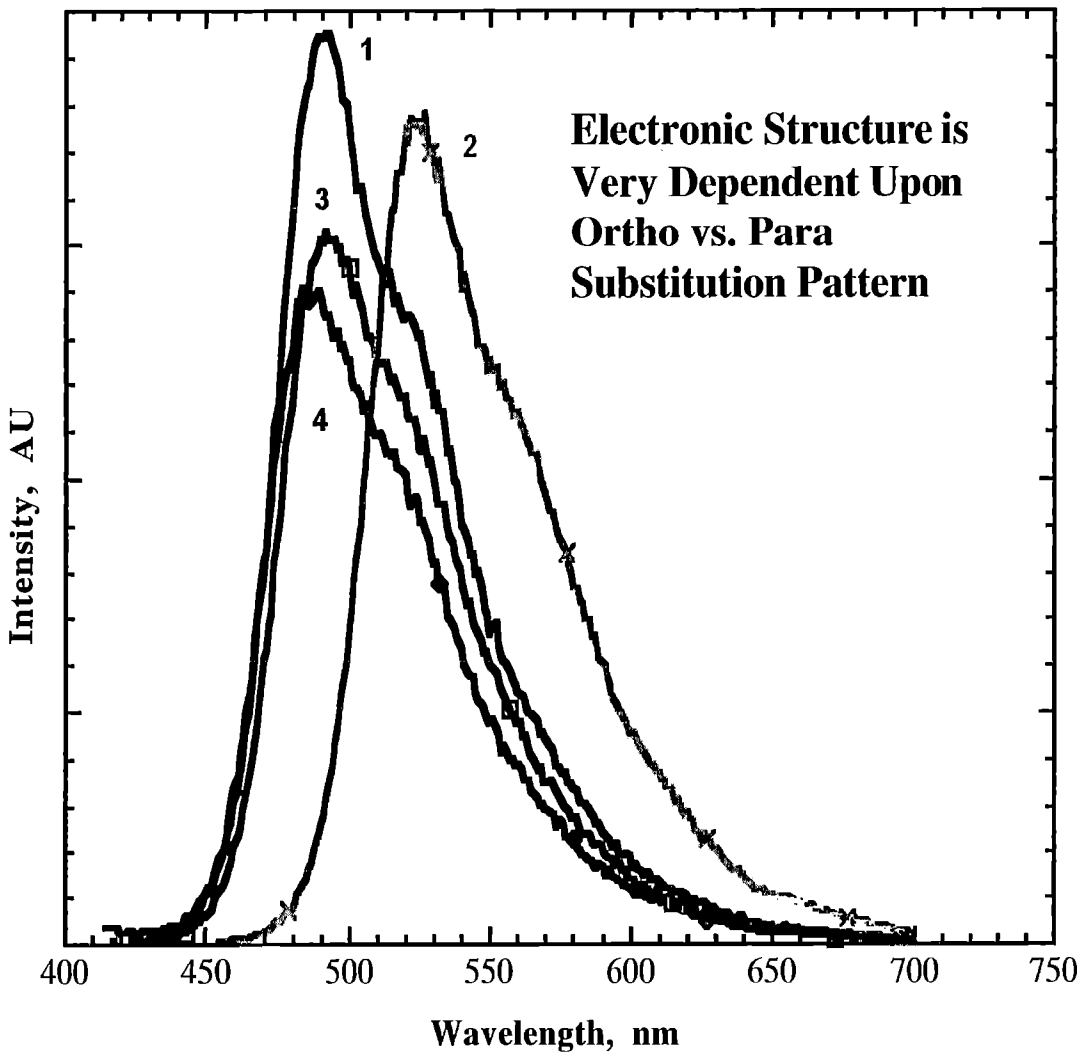

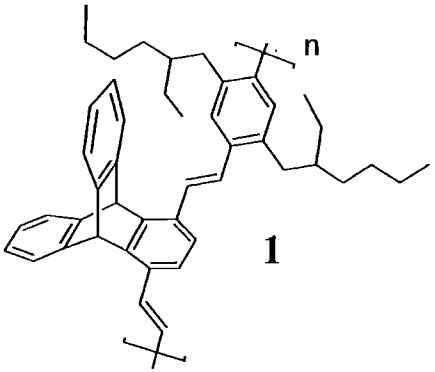

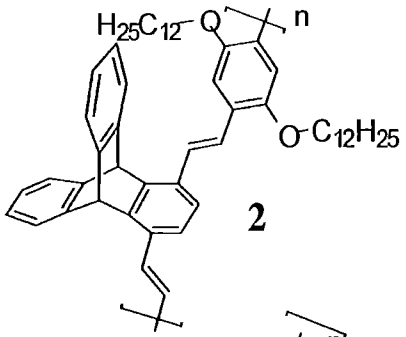

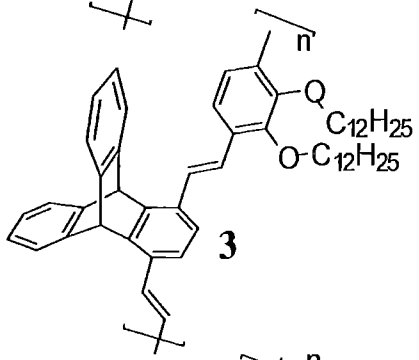

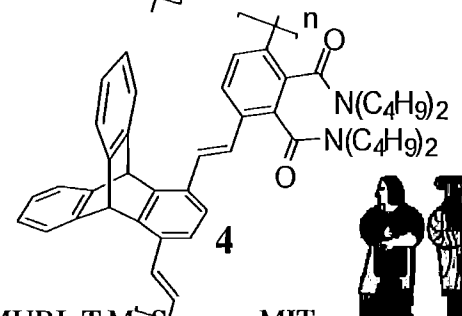

PPVs with Greater Larger Interchain Distances

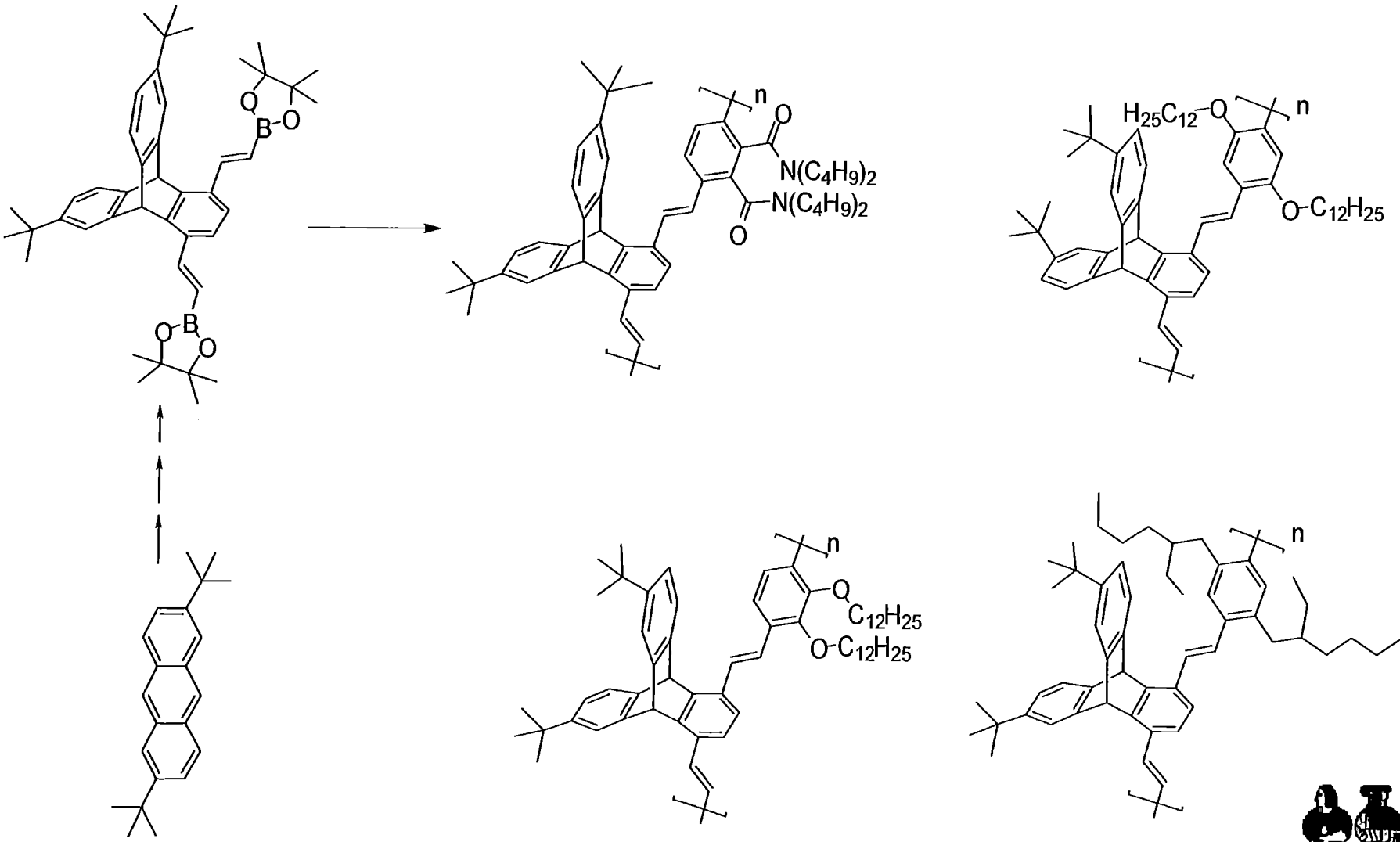

Synthesis of Triptycene PPV

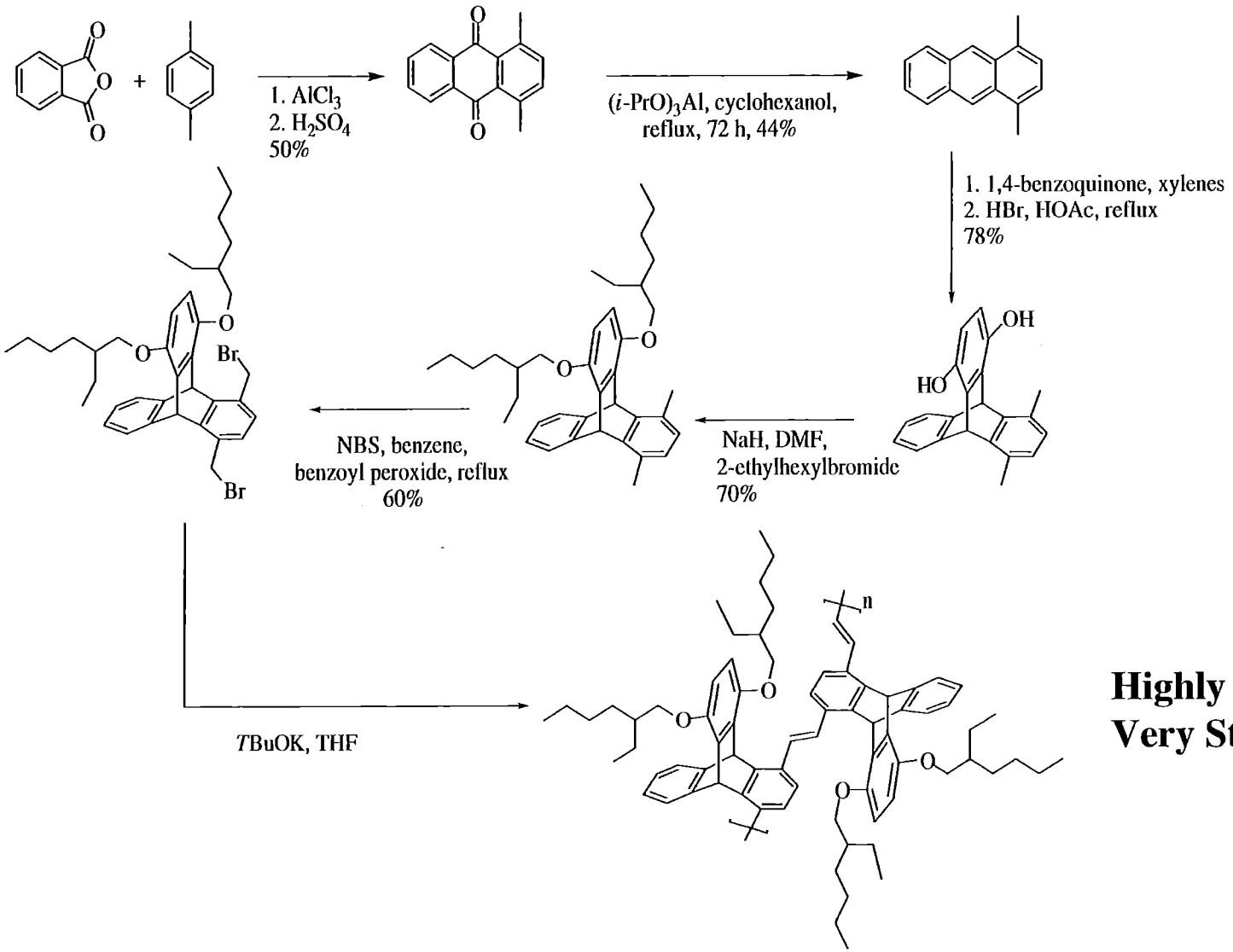

Highly Emissive
Very Stable

TOPS-MURI, T.M. Swager, MIT

Random Triptycene/MEH PPV Copolymers

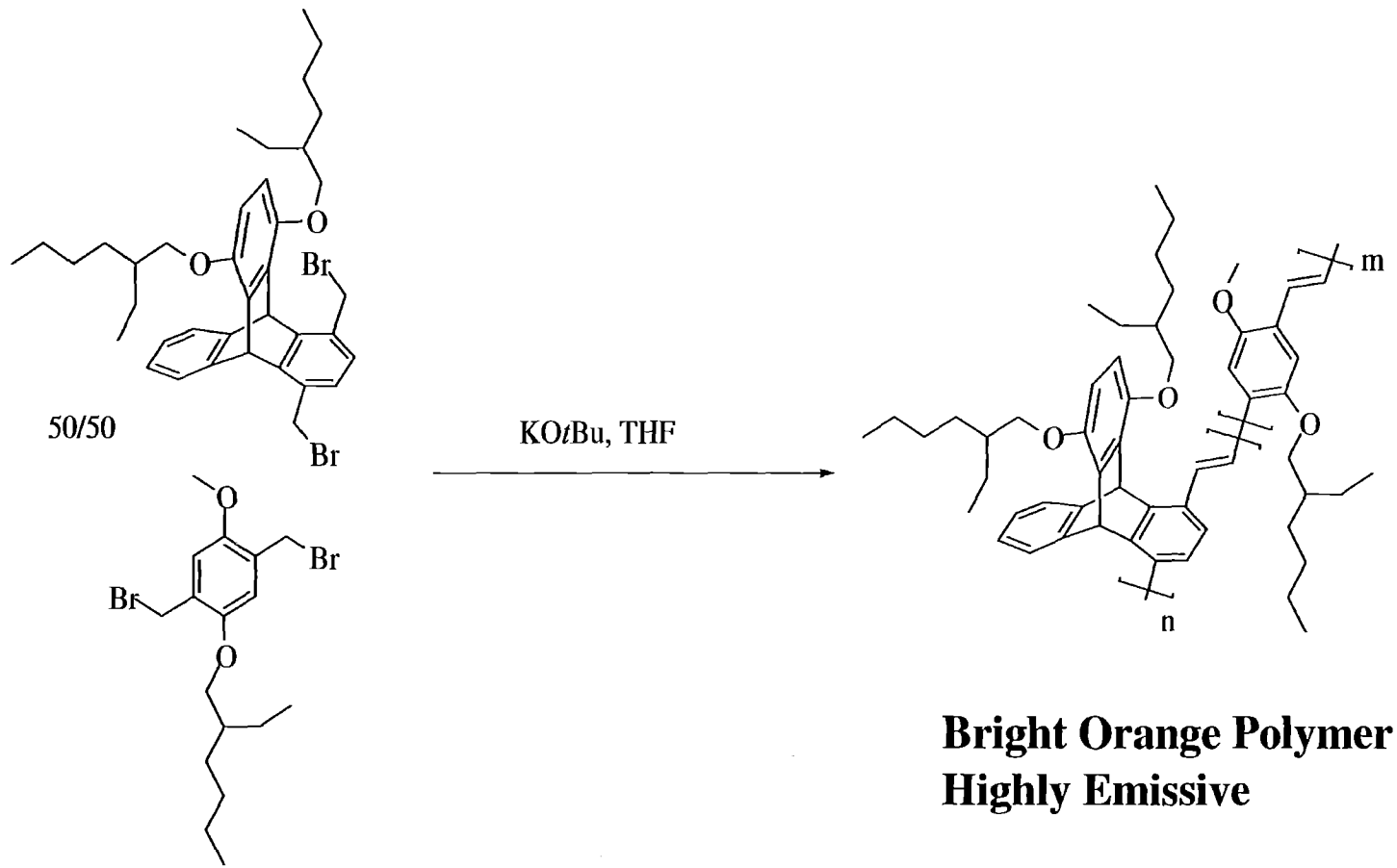

Bright Orange Polymer
Highly Emissive

Emission of Triptycene PPV and Copolymer

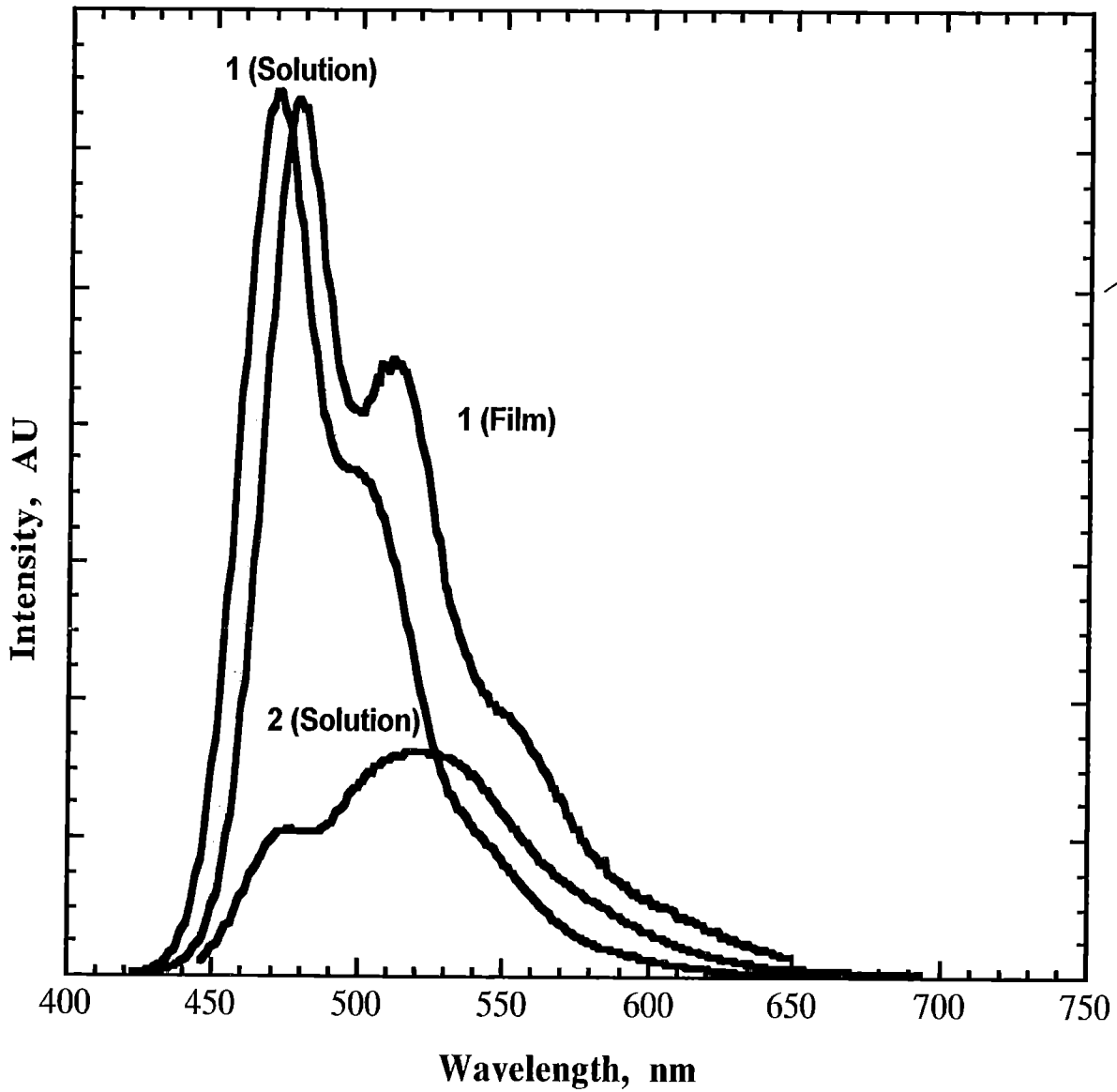

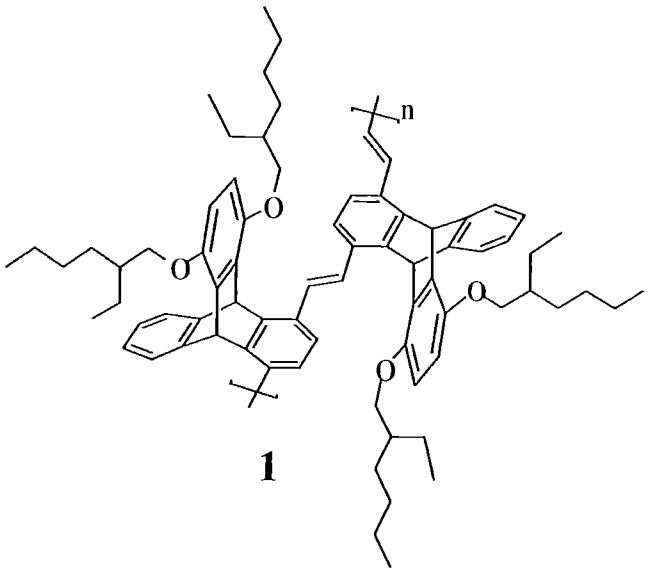

1

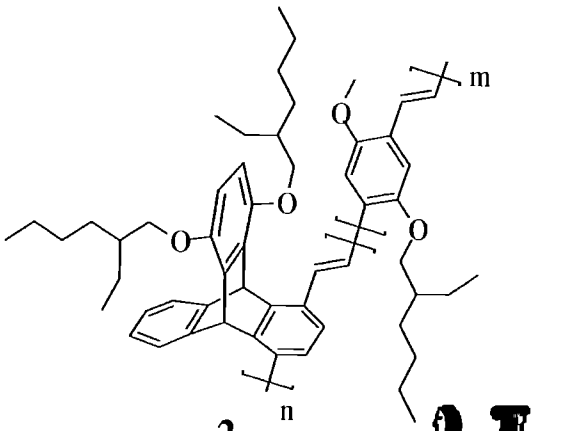

2

New Water Soluble PPVs

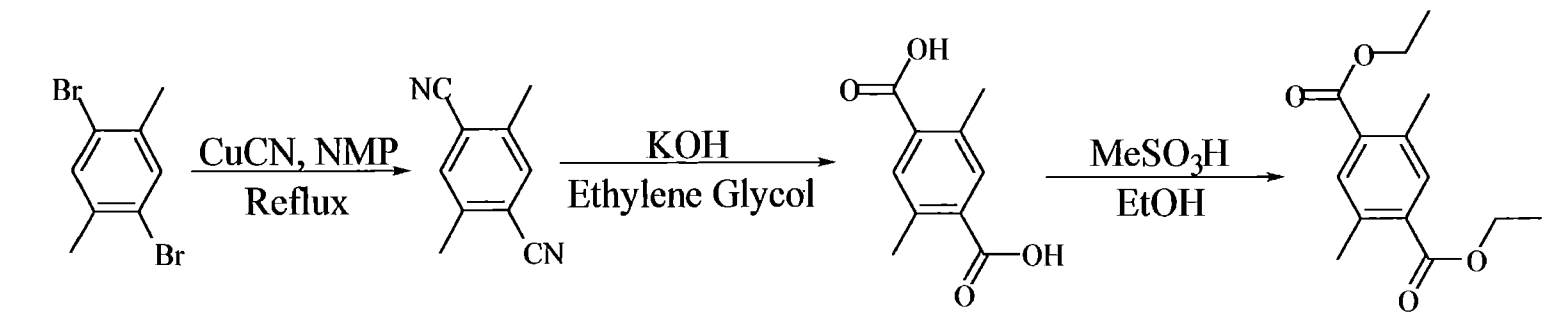

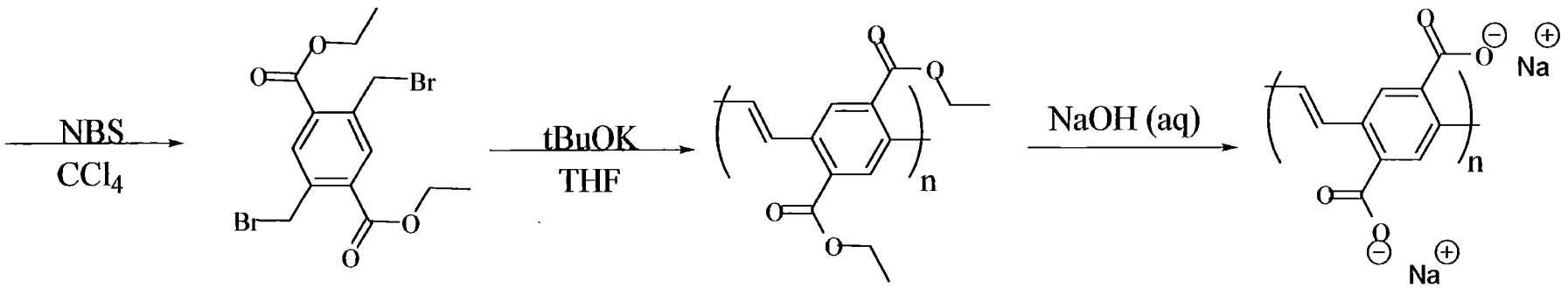

Carboxylates: Electron Withdrawing
Excellent for Functionalization

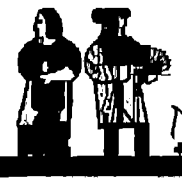

ROUTING AND ACTION MEMORANDUM

ROUTING

TO: (1) Chemistry Division Division
(Kiserow, Douglas)
Report is ATTACHED for review.

(2) Proposal Files

Report Number 39836.3-CH-MUR

Date Received in Library: 15 Oct 2001

Date Processed: 15 Oct 2001

Number of Copies: 3

DESCRIPTION OF MATERIAL

CONTRACT OR GRANT NUMBER: DAAD19-99-1-0206

INSTITUTION: University of Rochester
Office of Research & Project Administration
518 Hylan Bldg.
Rochester, NY 14627
USA

PRINCIPAL INVESTIGATOR: Professor Samson A. Jenekhe

SCIENTIFIC LIAISON: Dave Meeker
SCIENTIFIC LIAISON: Dr. Jack E. Rowe
SCIENTIFIC LIAISON: Dr. Henry Everitt
SCIENTIFIC LIAISON: Ken Wynne
SCIENTIFIC LIAISON: Dr. Gary Hagnauer
SCIENTIFIC LIAISON: CHARLES LEE
SCIENTIFIC LIAISON: Mr. David J. Thomas
SCIENTIFIC LIAISON: Lisa Hepfinger
SCIENTIFIC LIAISON: Dr. Donald Woodbury

TYPE REPORT: Old Reprint
Period Covered (if applicable):

TITLE: Thermotropic Chiral-Nematic Poly(P-Phenylene)s as a Paradigm of Helically Stacked pi-Conjugated Systems

ACTION TAKEN BY DIVISION

(X) Report has been reviewed for technical sufficiency and [X] *IS* [ ] *IS NOT* satisfactory.

(X) Material has been given an OPSEC review and it has been determined to be nonsensitive and, except for manuscripts and progress reports, suitable for public release.

( ) Further action requested:

(Signature)

11-1-01
(Date)

ARO FORM 36-E
15 Mar 89

REPORT DOCUMENTATION PAGE

Form Approved
OMB NO. 0704-0188

1. AGENCY USE ONLY *(Leave blank)*	2. REPORT DATE	3. REPORT TYPE AND DATES COVERED
		Reprint

4. TITLE AND SUBTITLE

TITLE ON REPRINT

5. FUNDING NUMBERS

DAAD19-99-1-0206

6. AUTHOR(S)

AUTHOR(S) ON REPRINT

7. PERFORMING ORGANIZATION NAMES(S) AND ADDRESS(ES)

University of Rochester

8. PERFORMING ORGANIZATION REPORT NUMBER

9. SPONSORING / MONITORING AGENCY NAME(S) AND ADDRESS(ES)

U.S. Army Research Office
P.O. Box 12211
Research Triangle Park, NC 27709-2211

10. SPONSORING / MONITORING AGENCY REPORT NUMBER

ARO 39836.3-CH-MUR

11. SUPPLEMENTARY NOTES

The views, opinions and/or findings contained in this report are those of the author(s) and should not be construed as an official Department of the Army position, policy or decision, unless so designated by other documentation.

12a. DISTRIBUTION / AVAILABILITY STATEMENT

Approved for public release; distribution unlimited.

12 b. DISTRIBUTION CODE

13. ABSTRACT *(Maximum 200 words)*

ABSTRACT ON REPRINT

14. SUBJECT TERMS

15. NUMBER IF PAGES

16. PRICE CODE

17. SECURITY CLASSIFICATION OR REPORT	18. SECURITY CLASSIFICATION OF THIS PAGE	19. SECURITY CLASSIFICATION OF ABSTRACT	20. LIMITATION OF ABSTRACT
UNCLASSIFIED	UNCLASSIFIED	UNCLASSIFIED	UL

MEMORANDUM OF TRANSMITTAL

U.S. Army Research Office
ATTN: AMSRL-RO-RI. Mrs. Sylvia Hall
P.O. Box 12211
Research Triangle Park, NC 27709-2211

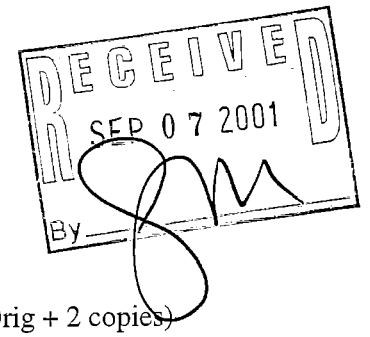

☒ Reprint (Orig + 2 copies)

☐ Technical Report (Orig + 2 copies)

☐ Manuscript (1 copy)

☐ Final Progress Report (Orig + 2 copies)

☐ Related Materials, Abstracts, Theses (1 copy)

CONTRACT/GRANT NUMBER: DAAD19-99-1-0206

REPORT TITLE: *Thermotropic chiral-nematic poly(p-phenylene)s as a paradigm of helically stacked π-conjugated systems*

is forwarded for your information.

SUBMITTED FOR PUBLICATION TO (applicable only if report is manuscript):

Sincerely,

Shaw H. Chen

Professor Shaw H. Chen
Department of Chemical Engineering
Room 1210 COI, University of Rochester
240 East River Road
Rochester, New York 14623-1212

Thermotropic Chiral−Nematic Poly(*p*-phenylene)s as a Paradigm of Helically Stacked π-Conjugated Systems

H. P. Chen,[†,‡] D. Katsis,[†,‡] J. C. Mastrangelo,[†,§] K. L. Marshall,[∥] and S. H. Chen*[,†,‡,§,∥]

Department of Chemical Engineering, Materials Science Program, NSF Center for Photoinduced Charge Transfer, and Laboratory for Laser Energetics, Center for Optoelectronics and Imaging, University of Rochester, 240 East River Road, Rochester, New York 14623-1212

T. H. Mourey

Analytical Technology Division, Kodak Research Laboratories, B82 Eastman Kodak Company, Rochester, New York 14650-2136

Received March 17, 2000. Revised Manuscript Received May 24, 2000

As an emerging class of multifunctional optical materials, chiral−nematic poly(*p*-phenylene)s with cyanobiphenyl and (*S*)-1-phenylethyl pendants were synthesized and characterized. Nematic homopolymer was also synthesized for preparation into a uniaxially aligned film. Linearly polarized photoluminescence (LPPL) and FTIR dichroism revealed that both the conjugated backbone and the nematic pendant are oriented along the director with an orientational order parameter, $S = 0.62$ and 0.73, respectively. Films prepared with chiral−nematic copolymers were found to selectively reflect left-handed circularly polarized light in the ultraviolet, visible, and infrared region at a decreasing chiral content. The helically stacked poly(*p*-phenylene)s were further characterized in terms of circularly polarized photoluminescence (CPPL). On the basis of a recent theory, $S = 0.67$ was found for the orientational order of conjugated backbones within quasinematic layers comprising the chiral−nematic film. Within experimental uncertainty, the S values determined with the LPPL and CPPL techniques are in good agreement, thereby validating the proposed supramolecular structure on the basis of which theories governing light absorption, emission, and propagation in structured media were constructed.

I. Introduction

Conjugated polymers represent one of the most extensively investigated classes of advanced materials in the past two decades. Reasons for the extraordinary intensity of interest include the diverse structures and properties afforded by molecular design and synthesis, the ease of processing and low costs compared to inorganic materials, and the technological potential for advanced technologies, such as electronics, optics, photonics, and optoelectronics.[1] In particular, feasibility has been demonstrated with amorphous or crystalline conjugated polymers for light-emitting diodes,[2] organic lasers,[3] thin film transistors,[4] photoconductors,[5] and nonlinear optical devices.[6] Liquid crystalline conjugated polymers characterized by various modes of macroscopic order have added a new dimension in recent years. Mediated by nematic or smectic mesomorphism, axial alignment of π-conjugated segments has been shown to enhance electrical conductivity by orders of magnitude[7] and to induce linearly polarized light emission.[8] Conjugated polymers of the chiral−nematic (i.e., cholesteric) type, in which conjugated segments self-assemble into helically stacked, quasinematic layers, have remained literally unexplored. As a matter of fact, there exists only one paper at present[9] reporting loosely pitched conjugated systems. This is an emerging class of multifunctional optical materials potentially capable of selective reflection accompanied by circular polarization of incident unpolarized light,[10] circularly polarized luminescence,[11] and electrochromism inherent to π-con-

* To whom all correspondence should be addressed.
† Department of Chemical Engineering.
‡ Materials Science Program.
§ NSF Center for Photoinduced Charge Transfer.
∥ Laboratory for Laser Energetics.

(1) Salaneck, W. R., Lundström, I., Rånby, B., Eds. *Conjugated Polymers and Related Materials*; Oxford University Press: Oxford, 1993.
(2) Burroughes, J. H.; Bradley, D. D. C.; Brown, A. R.; Marks, R. N.; Mackay, K.; Friend, R. H.; Burn, P. L.; Kraft, A.; Holmes, A. B. *Nature* **1990,** *347,* 539.
(3) Tessler, N.; Denton, G. J.; Friend, R. H. *Nature* **1996,** *382,* 695.
(4) Horowitz, G. *Adv. Mater.* **1998,** *10,* 365.
(5) Bleïr, H. In *Organic Materials for Photonics*; Zerbi, G., Ed.; Elsevier: Amsterdam, 1993; p 77.
(6) Marder, S. R.; Kippelen, B.; Jen, A. K.-Y.; Peyghambarian, N. *Nature* **1997,** *388,* 845.
(7) Akagi, K.; Shirakawa, H. *Macromol. Symp.* **1996,** *104,* 137.
(8) Weder, C.; Sarwa, C.; Montali, A.; Bastiaansen, C.; Smith, P. *Science* **1998,** *279,* 835.
(9) Chen, S. H.; Conger, B. M.; Mastrangelo, J. C.; Kende, A. S.; Kim, D. U. *Macromolecules* **1998,** *31,* 8051.
(10) Schadt, M.; Fünfschilling, J. *Jpn. J. Appl. Phys.* **1990,** *29,* 1974.
(11) Chen, S. H.; Katsis, D.; Schmid, A. W.; Mastrangelo, J. C.; Tsutsui, T.; Blanton, T. N. *Nature* **1999,** *397,* 506.

10.1021/cm000238m CCC: $19.00
Published on Web 07/14/2000

Scheme 1. Synthesis of Nematic and Chiral–Nematic Poly(*p*-phenylene)s

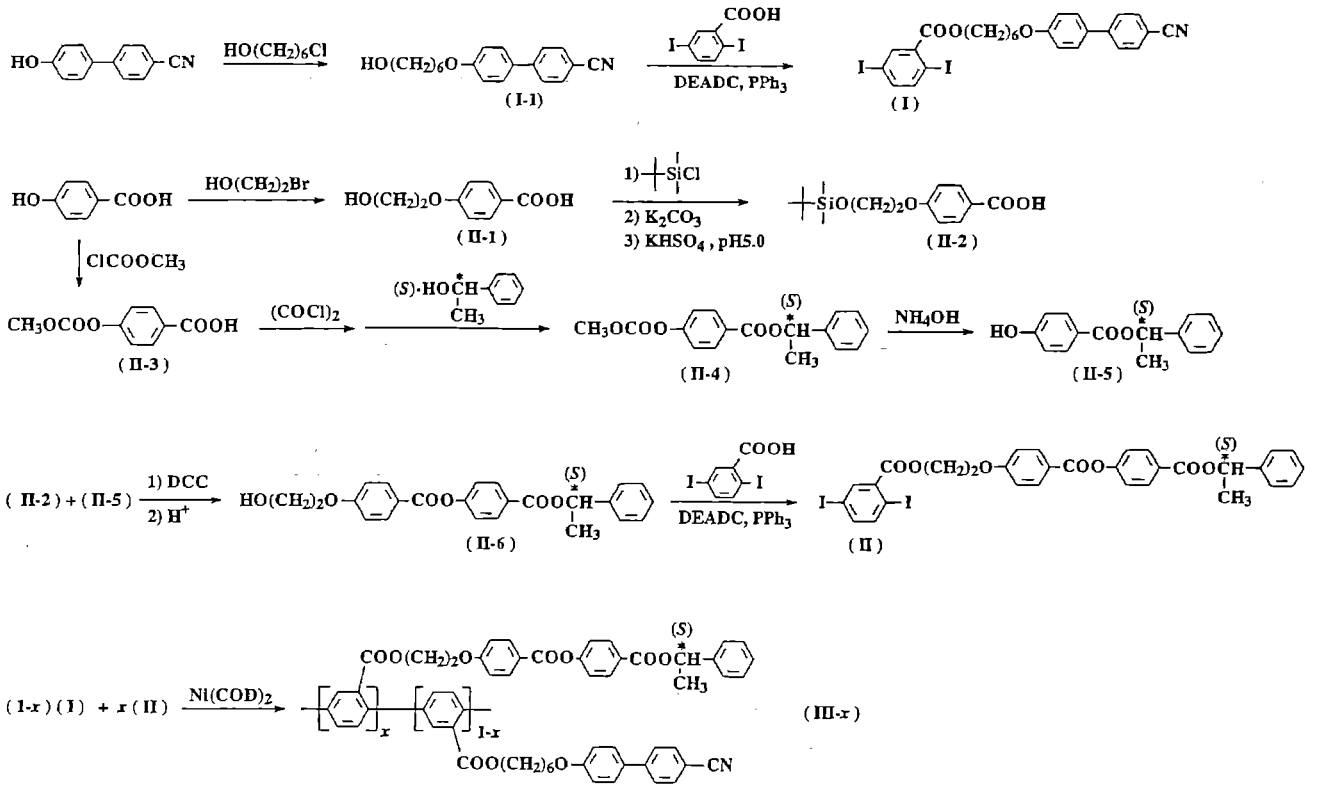

jugation.[12] Nonetheless, no existing conjugated polymers possess a tight enough pitch to show selective wavelength reflection in the visible region. In what follows we report on the synthesis and characterization of tightly pitched, chiral–nematic conjugated polymers with supramolecular structure fully characterized by polarized photoluminescence and infrared dichroism.

II. Experimental Section

Reagents and Chemicals. All chemicals, reagents, and solvents were used as received from the Aldrich Chemical Co. or VWR Scientific with the following exceptions. Bis(1,5-cyclooctadiene)nickel(0) (98+%, Strem Chemicals) was used without further purification. Tetrahydrofuran (99%) was dried by being refluxed over sodium in the presence of benzophenone until blue and then distilled. Silica gel 60 (EM Science, 230–400 mesh) was used for liquid chromatography.

Material Synthesis. Syntheses of monomers and polymers were performed following Scheme 1 with the experimental procedures as described in what follows.

4-(6-Hydroxyhexyloxy)-4′-cyanobiphenyl, (**I-1**). 4-Hydroxy-4′-cyanobiphenyl (4.92 g, 25.2 mmol), 6-chloro-1-hexanol (4.40 g, 32.2 mmol), cesium carbonate (9.18 g, 28.1 mmol), and potassium iodide (0.43 g, 2.6 mmol) were dissolved in 65 mL of DMF. The reaction mixture was stirred at 80 °C for 5 h. The resultant salt was removed by hot filtration. The filtrate was slowly added to 600 mL of water, and the crude product was collected for recrystallization from methanol to produce 5.75 g in 76% yield.

2,5-Diiodobenzoic Acid, 6-[4-(4′-Cyanobiphenyl)oxy]hexyl Ester (**I**). 2,5-Diiodobenzoic acid (6.65 g, 17.8 mmol), triphenylphosphine (5.33 g, 20.3 mmol), and **I-1** (5.00 g, 16.9 mmol) were dissolved in 85 mL of anhydrous tetrahydrofuran, to which diethyl azodicarboxylate (DEADC; 4.43 g, 25.4 mmol) was slowly added. Under argon the reaction mixture was stirred at room temperature overnight. Upon evaporation of the solvent under reduced pressure, the solid residue was dissolved in a small amount of methylene chloride for purification by flash column chromatography on silica gel, with a 98/2 mixture of methylene chloride and acetone as the eluent, followed by recrystallization from methanol to obtain 10.26 g in 93% yield. ^{1}H NMR: δ 8.08–7.00 (m, aromatic, 11H), 4.38 (t, $COOCH_2$, 2H), 4.04 (t, $ArOCH_2$, 2H), 1.86 (m, $COOCH_2CH_2$-$(CH_2)_2CH_2CH_2OAr$, 4H), 1.58 (m, $COOCH_2CH_2(CH_2)_2CH_2CH_2$-OAr, 4H). Anal. Calcd: C, 47.95; H, 3.56; N, 2.15; I, 38.97. Found: C, 47.98; H, 3.34; N, 2.21; I, 39.40.

4-(2-Hydroxyethyloxy)benzoic Acid, (**II-1**), *4-[2-[(tert-Butyldimethylsilyl)oxy]ethoxy]benzoic acid* (**II-2**), *4-Methoxycarbonyloxybenzoic Acid* (**II-3**), *4-Methoxycarbonyloxybenzoic Acid (S)-(−)-1-Phenylethyl Ester* (**II-4**), *and 4-Hydroxybenzoic Acid (S)-(−)-1-Phenylethyl Ester* (**II-5**). The synthesis of all the intermediates leading to the chiral monomer **II** except **II-6** has been reported previously.[13,14]

4-[(S)-(−)-1-Phenylethyl]-4-[(2-hydroxyethoxy)benzoyloxy]-benzoate (**II-6**). Intermediate **II-2** (9.62 g, 32.5 mmol) **II-5** (7.50 g, 30.8 mmol), *N,N′*-dicyclohexylcarbodiimide (DCC; 7.38 g, 35.8 mmol), and 4-pyrrolidinopyridine (0.46 g, 3.3 mmol) were dissolved in 60 mL of anhydrous tetrahydrofuran. The reaction mixture was stirred at room temperature overnight under nitrogen. Upon evaporation of the solvent under reduced pressure, the crude product was purified by column chromatography on silica gel with a 75/25 mixture of methylene and *n*-hexane as the eluent. The resultant silyl ether was hydrolyzed by being stirred in a 60/20/20 mixture of acetic acid, tetrahydrofuran, and water. Upon neutralization with a $NaHCO_3$ solution, column chromatography was carried out on silica gel with methylene chloride containing 0.5% acetone as

(12) Hyodo, K. *Electrochim. Acta* **1994**, *39*, 265.

(13) Krishnamurthy, S. Ph.D. Thesis, University of Rochester, Rochester, NY, 1992, pp 97–99.

(14) Katsis, D.; Chen, P. H. M.; Mastrangelo, J. C.; Chen, S. H.; Blanton, T. N. *Chem. Mater.* **1999**, *11*, 1590.

the eluent. Recrystallization from hexane containing 2% ethanol produced 7.50 g in 60%.

2,5-Diiodobenzoic Acid, 4′-{4″-[(S)-(−)-1‴-Phenylethyl)benzoyloxy]benzyloxy}-2-ethyloxy Ether (**II**). Chiral monomer **II** was prepared following the same procedure as for the nematic monomer **I**, except recrystallization from a 20/80 mixture of acetone and ethanol to obtain a 86% yield. ^{1}H NMR: δ 8.20–7.00 (m, aromatic, 16 H), 6.16 (q, $-COOCH(CH_3)$, 1H), 4.75 (t, $COOCH_2$, 2H), 4.43 (t, $ArOCH_2$, 2H), 1.70 (d, $CHCH_3$, 3H). Anal. Calcd: C, 48.84; H, 3.17; N, 0.00; I, 33.29. Found: C, 49.03; H, 2.98; N, 0.00; I, 33.69.

Nematic and Chiral–Nematic Polymers **III-x**. The procedure for Ni(0)-mediated polymerization is illustrated with copolymer **III-0.23** as follows. Bis(1,5-cyclooctadiene)nickel(0) ($Ni(COD)_2$; 0.84 g, 3.03 mmol), 2,2′-dipyridyl (0.47 g, 3.03 mmol), and 1,5-cyclooctadiene (0.33 g, 3.03 mmol) were dissolved in 8 mL of anhydrous DMF. To this solution were added **I** (0.90 g, 1.38 mmol) and **II** (0.45 g, 0.59 mmol). Precautions against oxygen and moisture were taken by preparing the reaction mixture in a glovebox. Polymerization was carried under argon at 55 °C overnight. The crude product was precipitated into 100 mL of methanol containing 2 mL of concentrated hydrochloric acid. The precipitate was filtered and washed sequentially with ethanol, basic EDTA, acidic EDTA, water, and ethanol. The resultant solid was slurried in methylene chloride, and the insolubles were filtered off. The methylene chloride solution was washed sequentially with basic EDTA, acidic EDTA, water, and brine before being dried over anhydrous $MgSO_4$. The solution was reduced to 6 mL in volume for precipitation into 80 mL of methanol. A 0.61 g (59%) of copolymer **III-0.23** was collected. (**III-0.00**) ^{1}H NMR: δ 8.50–6.80 (m, aromatic, 11H), 4.50–3.70 (m, $COOCH_2(CH_2)_4CH_2OAr$, 4H), 2.00–1.00 (m, $COOCH_2(CH_2)_4CH_2OAr$, 8H). Anal. Calcd: C, 78.56; H, 5.84; N, 3.53. Found: C, 78.42; H, 6.03; N, 3.41. (**III-0.07**) ^{1}H NMR: δ 8.50–6.50 (m, aromatic, x(26H) + (1 − x)(11H)), 6.14 (br, $-COOCH(CH_3)$, xH), 4.70–3.70 (m, $COOCH_2$-$(CH_2)_4CH_2$-OAr and $COO(CH_2)_2OAr$, x(4H) + (1 − x)(4H)), 1.90–1.10 (m, $-CH_3$ and $COOCH_2(CH_2)_4CH_2OAr$, x(3H) + (1 − x)(8H)). Anal. Calcd: C, 78.07; H, 5.74; N, 3.20. Found: C, 77.60; H, 5.83; N, 3.12. (**III-0.12**) ^{1}H NMR: δ 8.50–6.50 (m, aromatic, x(26H) + (1 − x)(11H)), 6.13 (br, $-COOCH(CH_3)$, xH), 4.70–3.70 (m, $COOCH_2(CH_2)_4CH_2OAr$ and $COO(CH_2)_2OAr$, x(4H) + (1 − x)-(4H)), 1.90–1.10 (m, $-CH_3$ and $COOCH_2(CH_2)_4CH_2OAr$, x(3H) + (1 − x)(8H)). Anal. Calcd: C, 77.77; H, 5.68; N, 3.01. Found: C, 77.46; H, 5.75; N, 3.01. (**III-0.17**) ^{1}H NMR: δ 8.50–6.50 (m, aromatic, x(26H) + (1 − x)(11H)), 6.14 (br, $-COOCH(CH_3)$, xH), 4.70–3.70 (m, $COOCH_2(CH_2)_4CH_2OAr$ and $COO(CH_2)_2$-OAr, x(4H) + (1 − x)(4H)), 1.90–1.10 (m, $-CH_3$ and $COOCH_2$-$(CH_2)_4CH_2OAr$, x(3H) + (1 − x)(8H)). Anal. Calcd: C, 77.55; H, 5.63; N, 2.86. Found: C, 76.87; H, 5.77; N, 2.67. (**III-0.23**) ^{1}H NMR: δ 8.50–6.50 (m, aromatic, x(26H) + (1 − x)(11H)), δ 6.14 (br, $-COOCH(CH_3)$, xH), 4.70–3.70 (m, $COOCH_2(CH_2)_4$-CH_2OAr and $COO(CH_2)_2OAr$, x(4H) + (1 − x)(4H)), δ 1.90–1.10 (m, $-CH_3$ and $COOCH_2(CH_2)_4CH_2OAr$, x(3H) + (1 − x)-(8H)). Anal. Calcd: C, 77.06; H, 5.54; N, 2.54. Found: C, 76.53; H, 5.58; N, 2.49.

General Characterization Techniques. Chemical structures were elucidated with elemental analysis (performed by Oneida Research Services, Whitesboro, NY) and FTIR (Nicolet 20 SXC) and ^{1}H and ^{13}C NMR (Avance-400, Brüker) spectroscopic techniques. Thermal transition temperatures were determined by differential scanning calorimetry (Perkin-Elmer DSC-7) with a continuous N_2 purge at 20 mL/min. Liquid crystal mesomorphism was characterized with a polarizing optical microscope (DMLM, Leica) equipped with a hot stage (FP82, Mettler) and a central processor (FP90, Mettler); the nematic and cholesteric mesomorphisms were identified with the threaded textures and oily streaks, respectively. Three PLgel mixed-C, 7.5 × 300 mm columns (Polymer Laboratories) were used in a size-exclusion chromatograph equipped with serially arranged UV–vis absorbance detector, 15° and 90° light scattering detector, differential viscometer, and differential refractometer, as described previously.[15] The size-exclusion chromatograph system was operated at 35 °C with uninhibited tetrahydrofuran as the eluent at a flow rate of 0.1 mL/min. A universal calibration curve was constructed using 15 polystyrene standards with a molecular weight ranging from 580 to 2 300 000. Samples in 100 μL were injected at a concentration of 2 mg/mL. The weight-average molecular weight was calculated from the 15° light scattering with correction for anisotropic scattering.

Preparation of Films and Characterization of Optical Properties. Optical elements for the order parameter measurement were fabricated using optically flat, calcium fluoride substrates (1.00 in. diameter × 0.04 in. thickness, Optovac) that are transparent from the infrared region down to 200 nm. Optical elements for the reflection, transmission, and circular polarization measurements were fabricated using optically flat, fused silica substrates (1.00 in. diameter × 1/8 in. thickness, Esco Products) transparent down to 200 nm. In both cases, the substrates were cleaned, spin-coated with Nylon 66, and then buffed with a velvet roller. Sandwiched films were prepared by melting the powders between two substrates at a temperature 20 °C above T_c followed by annealing 20 °C below T_c for 1 h with subsequent cooling at −10 °C/h to room temperature. The film thickness was controlled by glass fiber spacers (EM Industries) to within 4.1 ± 0.2 μm, as determined by the interference fringes from the air gap between the substrates using a UV–vis–near-IR spectrophotometer. Single-substrate films were prepared by spin-coating from a chloroform solution at 2500 rpm. Subsequent air-drying in a laminar flow hood for a few hours and vacuum-drying overnight at room temperature removed the last traces of solvent. The single-substrate film thickness was determined on a white light interferometer (Zygo New View 100).

Orientational order of the cyanobiphenyl pendant was characterized by linear dichroism using a FTIR spectrometer (Nicolet 20 SXC). Two measurements were performed with the transmission axis parallel and perpendicular to the nematic director (i.e., the buffing direction) of the sample. A UV–vis–near-IR spectrophotometer (Perkin-Elmer Lambda 9) was employed to measure light absorption and transmission (both at normal incidence) and reflection (at 15° incidence from the surface normal) at room temperature. An aluminum mirror served as a specular reflection standard, and the results were reported as percent reflectivity of incident unpolarized light. In all measurements, Fresnel reflections from the two air–glass interfaces were accounted for using a reference cell comprising an index-matching fluid sandwiched between two surface-treated substrates. Photoluminescence spectra were collected with a spectrofluorometer (Photon Technology International Quanta Master C-60SE). A liquid light guide (2 mm diameter × 1 m long, Photon Technology International) was used to direct the UV excitation source onto the center of the film through a glass filter (UG11, Schott Glass Technologies). The light guide also served as a polarization randomizer for the excitation source. In the case of circularly polarized photoluminescence (CPPL), polarization analysis was performed via a circular analyzer with maximum polarization efficiency greater than 99% at 425 nm. At 560 nm the efficiency dropped to 90%. In the case of linearly polarized photoluminescence (LPPL), two identical UV–vis linear polarizers were used for the polarization of the incident light and the analysis of the emitted light. Their efficiency was better than 99%, across a wide wavelength range, from 275 to 725 nm. All the polarized photoluminescence (both LPPL and CPPL) spectra were corrected for both the efficiency and the transmission dispersion of the analyzer. The order parameter governing the poly(*p*-phenylene) backbone was determined by the LPPL and CPPL spectra of a nematic and chiral–nematic film, respectively. In all cases, the order parameter was measured with an uncertainty of ±0.05 of the mean.

III. Results and Discussion

The molecular structures of nematic and chiral monomers, **I** and **II** as well as nematic and chiral–nematic

(15) Mourey, T. H.; Balke, S. T. *J. Appl. Polym. Sci.* **1998**, *70*, 831.

Table 1. Number- and Weight-Average Molecular Weights and Thermotropic Properties of Poly(*p*-phenylene)s

polymer	$\bar{M}_n$[a] (SEC)	$\bar{M}_w$[a] (SEC)	$\overline{DP}$[b]	$\bar{M}_w$[c] (LS)	DSC (°C)[d]
III-0.00	3380	6320	9	6760	*G* 66 *N* 165–196 *I*
III-0.07	5440	10000	13	10600	*G* 72 *Ch* 168–195 *I*
III-0.12	7050	14500	17	15200	*G* 75 *Ch* 162–192 *I*
III-0.17	3900	8100	9	8170	*G* 70 *Ch* 147–175 *I*
III-0.23	4610	10400	11	10300	*G* 73 *Ch* 153–181 *I*

[a] Number- and weight-average molecular weights, $\bar{M}_n$ and $\bar{M}_w$, calculated from the molecular weight distribution measured by SEC with universal calibration using polystyrene standards. [b] Number-average degree of polymerization, $\overline{DP} = \bar{M}_n/\bar{M}_1$, where $\bar{M}_1$ is the nominal molecular weight of a "chiral–nematic repeat unit", i.e., the molecular weights of chiral and nematic repeat units weighted with mole fraction. [c] $\bar{M}_w$ evaluated with the integrated 15° LS signal and the mass injected; agreement between SEC and LS indicating the absence of polymer aggregation. [d] Samples preheated to 200 °C with subsequent cooling to room temperature for gathering heating scans at 20 °C/min on a differential scanning calorimeter; glass transition temperature, T_g, reported as the inflection point across the step change, and clearing temperature, T_c, as the range over which nematic or cholesteric mesomorphism vanishes into an isotropic fluid.

poly(*p*-phenylene)s **III-*x*** were elucidated with analytical as well as ^{1}H NMR spectral data. The chiral mole fraction, x, was calculated from the intensities of the two sets of ^{1}H NMR signals centered around δ 6.14 and between δ 4.70 and δ 3.70 ppm. The structures of poly(*p*-phenylene)s were further elucidated with ^{13}C NMR spectra of **I**, **II**, **III-0.00**, and **III-0.23**, which are provided as Supporting Information. On the basis of the accepted Ni(0)-catalyzed polymerization mechanism[16] and reduction with hydrogen chloride as part of the workup procedure,[17] it is believed that the resultant poly(*p*-phenylene)s are terminated with hydrogen atoms. In the presence of ester linkages other than those directly attached to the backbone, the degree of regioregularity could not be assessed with ^{1}H NMR or ^{13}C NMR spectroscopy. However, a multitude of peaks between δ 166.0 and δ 168.8 in the ^{13}C NMR spectrum of nematic homopolymer **III-0.00** seems to indicate the absence of regioregularity[18] in the resultant polymers. The average molecular weight of a repeat unit in **III-*x***, $\bar{M}_1$, was calculated using the molecular weights of monomers **I** and **II** less iodine atoms. Number- and weight-average molecular weights, $\bar{M}_n$ and $\bar{M}_w$, were determined from the molecular weight distribution measured with size-exclusion chromatography (SEC) based on universal calibration using polystyrene standards. The ratio, $\bar{M}_n/\bar{M}_1$, yields the number-average degree of polymerization, $\overline{DP}$. The light scattering (LS) signal observed at 15° was employed for an independent evaluation of $\bar{M}_w$. The results are presented in Table 1. The fact that the $\bar{M}_w$ values measured by size-exclusion chromatography agree with those by light scattering to within ±5% on average suggests the absence of aggregation in solution. The depicted polymer structures are consistent with analytical data for which the calculation was performed using the chiral mole fraction determined with ^{1}H NMR spectroscopy and the number average degree of polymerization determined with size-exclusion chromatography and on the basis of the observation that hydrogen atoms represent the end groups. Also reported in Table 1 are the glass transition temperature, T_g, and the nematic-to-isotropic or cholesteric-to-isotropic transition (i.e., clearing) temperature, T_c, based on the 20 °C/min heating scans of samples preheated to 200 °C with subsequent cooling to room temperature.

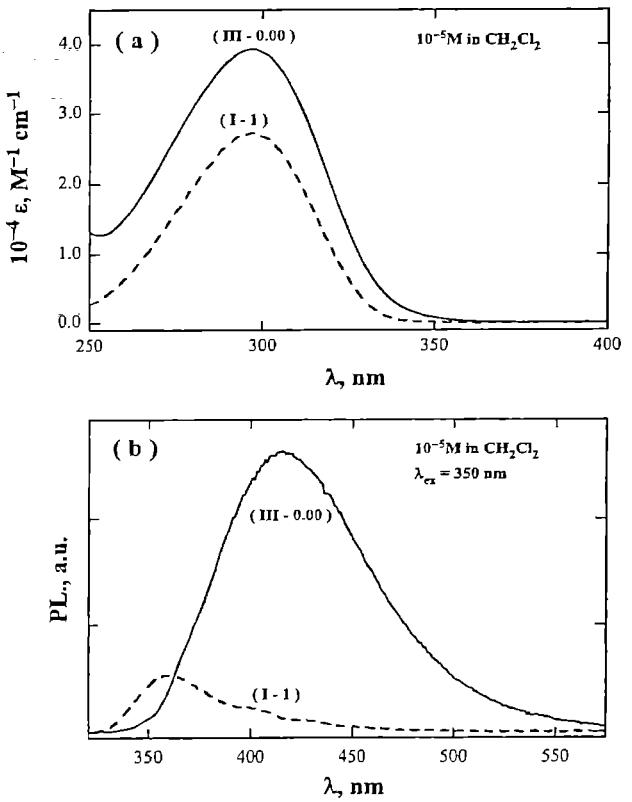

Figure 1. Absorption (a) and photoluminescence (b) spectra of nematic pendant, **I-1**, and nematic homopolymer, **III-0.00**, in methylene chloride at 10^{-5} M repeat units.

The resultant system **III-*x*** represents conjugated polymers functionalized with nematic and chiral-nematic mesogens, the latter being a mixture of the nematic and chiral pendants depicted as **I-1** and **II-6**, respectively, in Scheme 1. Through such functionalization, the conjugated segments are induced to align in a manner dictated by the pendant groups. The orientation of the pendants with respect to the backbone remains to be probed with spectroscopic techniques. The fact that the nematic and chiral pendants do not crystallize independently of the poly(*p*-phenylene) backbone suggests some extent of coupling between two structural elements through the methylenic spacer. In fact, the hybrid system **III-*x*** was found to undergo glass transition, thereby permitting the liquid crystalline order achieved in the mesomorphic melt state (viz., between T_g and T_c) to be frozen in the vitreous state upon cooling. The UV–vis absorption and photoluminescence spectra are compiled in Figure 1 for the nematic precursor depicted as **I-1** in Scheme 1 and the nematic homopolymer **III-0.00** in methylene chloride at 10^{-5} M. The chiral precursor **II-7** is not included in Figure 1 because it was found to have a UV absorption cutoff at 325 nm and to be nonfluorescent with excitation at 350 nm. Figure 1a

(16) Yamamoto, T. *Bull. Chem. Soc. Jpn.* **1999**, *72*, 621.
(17) Grob, M. G.; Feiring, A. E.; Auman, B. C.; Percec, V.; Zhao, M.; Hill, D. H. *Macromolecules* **1996**, *29*, 7284.
(18) Wang, Y.; Quirk, R. P. *Macromolecules* **1995**, *28*, 3495.

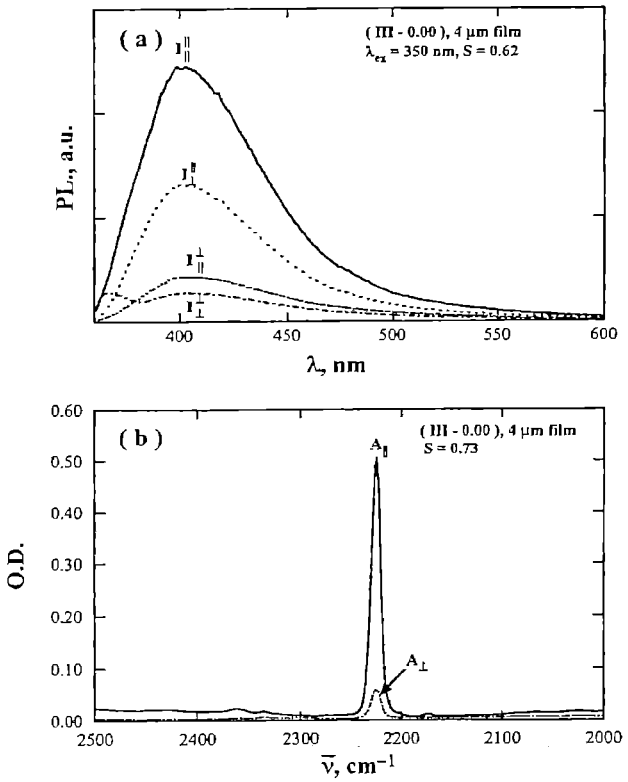

Figure 2. (a) Linearly polarized photoluminescence and (b) FTIR dichroism of a film of nematic homopolymer **III-0.00** for the evaluation of the orientational order parameter governing the conjugated backbone and the nematic pendant, respectively.

indicates that the nematic pendant is essentially nonabsorbing above 340 nm in comparison to the backbone. Excited with $\lambda_{ex} = 350$ nm, the poly(*p*-phenylene) backbone showed an emission peak at 410 nm, whereas the cyanobiphenyl group produced a minor emission peak at 360 nm, as shown in Figure 1b.

Anisotropic light absorption and emission involving an axially aligned film were characterized to independently evaluate the orientational order of the conjugated backbone and that of the nematic pendant. A 4 μm thick film was prepared with **III-0.00** between two surface-treated calcium fluoride substrates for the characterization of LPPL. One characteristic of these substrates is the direction in which the nylon alignment coating is buffed with a velvet roller. The buffing direction defines the "nematic director". All the nematic and chiral–nematic films prepared for the present work are contained between two substrates with their directors parallel to each other. The results are shown in Figure 2a, in which the emission intensity is presented with reference to the director. As an example, $I^{\parallel}_{\perp}$ denotes the emission intensity linearly polarized parallel to the director with UV excitation linearly polarized perpendicular to the director. The observed LPPL spectra indicate that the emission intensities parallel to the director are consistently higher than those perpendicular regardless of the polarization state of the excitation source. On the basis of the available data on *p*-terphenyl and other linear luminophores,[19] it is believed that the

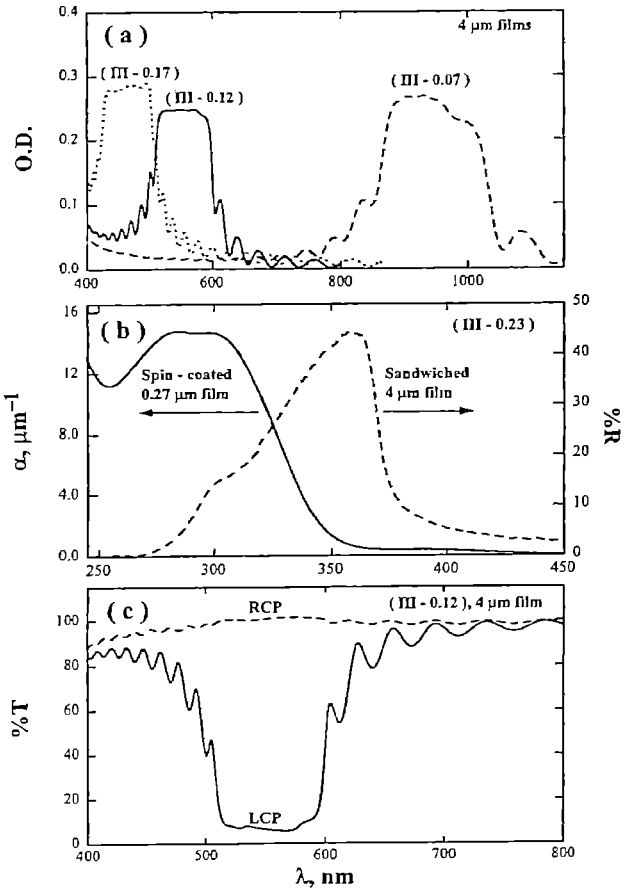

Figure 3. Optical properties of thin films prepared with chiral–nematic copolymers: (a) selective reflection spectra measured in terms of optical density for **III-0.17**, **III-0.12**, and **III-0.07**; (b) absorption coefficient, α, and reflection spectrum measured in terms of reflectivity, %*R*, for **III-0.23**; (c) transmittances of the right- and left-handed circularly polarized (RCP and LCP) light propagating through **III-0.12**.

absorption and emission transition moments of poly(*p*-phenylene) lie parallel to its long axis. It is thus concluded that the axis of poly(*p*-phenylene) lies parallel to the director. On the basis of the linearly polarized intensities observed at 410 nm, the orientational order paramenter, S, was evaluated at 0.62 using eq 39 in ref 20 based on a theory of LPPL. Orientational order of the nematic pendant was probed by FTIR dichroism involving the stretching vibration of C≡N (at 2224 cm^{-1}), as shown in Figure 2b. The absorbances parallel ($A_{\parallel}$) and perpendicular ($A_{\perp}$) to the nematic director were used to calculate the dichroic ratio, $R = A_{\parallel}/A_{\perp}$, from which the orientational order parameter emerged, $S = (R - 1)/(R + 2)$, with its transition moment lying parallel to the long molecular axis of the cyanobiphenyl group.[20] It was found that $S = 0.73$, indicating that the pendant is also oriented along the director.

To appraise the ability of **III-*x*** to form vitrified chiral–nematic films, 4 μm thick films were prepared for the characterization of selective wavelength reflection. Comprising a helical stack of quasinematic layers, a chiral–nematic film is capable of selective reflection

(19) Gryczyński, Z.; Kawski, A. *Z. Naturforsch.* **1987**, *42a*, 1396.

(20) Shi, H.; Conger, B. M.; Katsis, D.; Chen, S. H. *Liq. Cryst.* **1998**, *24*, 163.

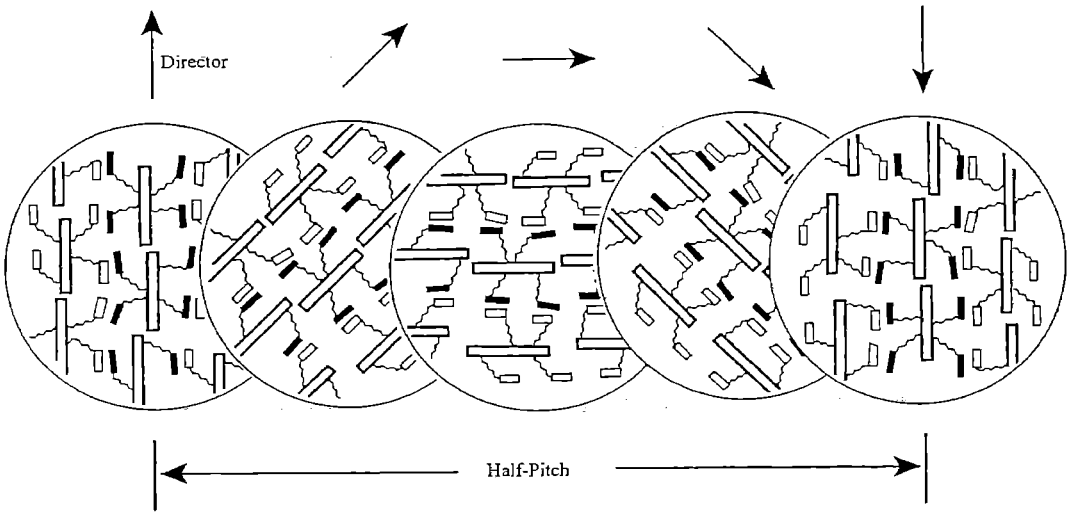

Figure 4. A schematic diagram of the supramolecular structure of a chiral–nematic film with its quasinematic director undergoing a counterclockwise rotation, as stipulated by the left-handed helical structure determined in Figure 3c. Within each layer, the backbone and the nematic pendant are oriented along the director. Note the antiparallel arrangement of nematic pendants, shown as small filled and open rectangles, from neighboring conjugated backbones. The pitch length is defined as the distance along the surface normal to quasinematic layers over which the director completes a 360° rotation.

with simultaneous circular polarization of incident unpolarized light.[10] The result is that the incident intensity is equally divided between the reflected and the transmitted components with opposite handedness in circular polarization. Thus, an optical density of 0.30 is expected of unpolarized light at normal incidence on a perfectly ordered chiral–nematic film. Polymers **III-*x*** were found not to absorb light in the visible or infrared region, where the observed attenuation of incident light can be attributed to reflection. As shown in Figure 3a, chiral–nematic films prepared with **III-*x*** were found to have an increasing selective reflection wavelength, λ_R, at a decreasing x value. At $x = 0.23$ a selective reflection band was observed in the ultraviolet region, part of which was diminished by light absorption between 300 and 350 nm, as shown in Figure 3b. Traditionally, handedness of the helical stack is defined by that of the reflected circularly polarized component.[22] Whereas handedness of a chiral–nematic film is related to the absolute configuration of the chiral pendant, no correlation between the two has been established.[23] To determine the handedness presented by films of **III-*x*** containing (*S*)-(−)-1-phenylethanol, the transmittances of both left- and right-handed circularly polarized light at normal incidence were measured, as illustrated with a film of **III-0.12** in Figure 3c. Since left-handed circularly polarized light is selectively reflected, it is concluded that the film prepared with **III-*x*** presents a left-handed, helical stack of quasinematic layers. Within each layer, both the poly(*p*-phenylene) backbone and the cyanobiphenyl pendant are oriented parallel to the director, as evidenced by LPPL of the nematic film prepared with **III-0.00**. Thus, the supramolecular structure of a chiral–nematic film is as depicted in Figure 4, with the chiral pendants (not shown) providing the rotation between adjacent quasinematic layers. The schematic diagram also reflects the lack of regioregularity and the antiparallel arrangement of cyanobiphenyl pendants from neighboring poly(*p*-phenylene) backbones.

To determine the orientational order parameter governing the helically stacked π-conjugated segments, a 4 μm thick film of **III-0.07** was prepared for the characterization of CPPL. With unpolarized excitation at 350 nm targeting the poly(*p*-phenylene) backbone, an emission peak emerged between 350 and 550 nm, which is far removed from the selective reflection band centered at 945 nm of the **III-0.07** film. At normal incidence of both excitation and emission, left- and right-handed circularly polarized emission intensities, I_L and I_R, were measured for the calculation of the degree of circular polarization, $g_e \equiv 2(I_L - I_R)/(I_L + I_R)$.

The experimental setup described previously[24] was simplified with a liquid light guide directing the excitation source directly onto the film. On the basis of the CPPL spectra, $g_e = -0.35$ was evaluated at 410 nm. The fact that a significant extent of CPPL resulted from emission outside the selective reflection band can be attributed to the circular polarization of linearly polarized emission originating in all quasinematic layers.[24] For light emission outside the selective reflection band of a chiral–nematic film, a CPPL theory has been constructed and validated with experimental observations without resorting to adjustable parameters.[20] The observed g_e value was employed to evaluate S governing the helically stacked poly(*p*-phenylene) backbones as the predominant light emitter with excitation at 350 nm, according to Figure 1b. To accomplish this, the average refractive index ($\bar{n}$) and the optical birefringence (Δn) of the quasinematic layer at both the excitation and emission wavelengths were determined a priori. The optical properties of a nematic homopolymer **III-0.00**, reported previously[9] served as the basis for parameter estimation: $\bar{n} = 1.75$ and $\Delta n = 0.30$ at 350 nm and $\bar{n} =$

(21) Khoo, I. C.; Wu, S.-T. *Optics and Nonlinear Optics of Liquid Crystals*; World Scientific: Singapore, 1993; p 64.
(22) De Gennes, P. G.; Prost, J. *The Physics of Liquid Crystals*; Clarendon Press: Oxford, 1993; p 264.
(23) Krishnamurthy, S.; Chen, S. H. *Macromolecules* **1991**, *24*, 3481.
(24) Katsis, D.; Schmid, A. W.; Chen, S. H. *Liq. Cryst.* **1999**, *26*, 181.

1.63 and $\Delta n = 0.25$ at 410 nm. In addition, the average absorbance per unit thickness reported previously[9] for the nematic homopolymer, 0.651 μm^{-1} at 350 nm, was adopted here as another input parameter. With the absorption and emission transition moments lying along the conjugated backbone, the agreement between the predicted and the observed g_e values was secured with $S = 0.67$. Thus, the orientational order characterizing quasinematic layers comprising a chiral–nematic film is consistent with that observed in a nematic film, $S = 0.62$, within an experimental uncertainty of ± 0.05.

Summary

A series of poly(*p*-phenylele)s functionalized with nematic and chiral pendants were synthesized and characterized as a novel class of multifunctional optical materials. Elemental analysis and ^1H and ^{13}C NMR spectroscopic techniques were employed to determine the lack of regioregularity with hydrogen atoms as the terminal groups to poly(*p*-phenylene)s. The degree of polymerization was found to vary from 9 to 17 by size-exclusion chromatography with universal calibration. A uniaxially aligned film was prepared with homopolymer to assess the orientation of the conjugated backbone and the nematic pendant with reference to the nematic director as defined by the direction of buffing on the substrates. With an excitation source at 350 nm, LPPL revealed the alignment of the conjugated backbone with the nematic director and an orientational order parameter, $S = 0.62$. The cyanobiphenyl pendant was found to align with the nematic director as well, as shown by FTIR dichroism of the C≡N stretching vibration observed at 2224 cm^{-1}, resulting in $S = 0.73$. At a decreasing chiral mole fraction, films prepared with chiral–nematic copolymers showed a selective reflection band in the ultraviolet to visible and infrared regions. Moreover, the chiral–nematic film was found to consist of a left-handed helical stack of quasinematic layers with (*S*)-(−)-1-phenylethanol as the chiral moiety. The supramolecular structure representing the chiral–nematic film was further characterized with CPPL. On the basis of a recent theory, the orientational order of the conjugated backbone was evaluated at $S = 0.67$. The agreement between the S values determined with the LPPL and CPPL techniques, 0.62 versus 0.67 within experimental uncertainty, validates the proposed supramolecular structure on the basis of which theories governing light absorption, emission, and propagation in structured media were constructed.

Acknowledgment. We express our gratitude for the financial support from the Army Research Office under the Multidisciplinary University Research Initiative, Grant DAAD19-99-1-0206, and the National Science Foundation under Grants CTS-9811172, CTS-9818234, and CHE-9120001. Additional support was provided by the Department of Energy Office of Inertial Confinement Fusion under Cooperative Agreement No. DE-FC03-92SF19460 with the Laboratory for Laser Energetics, and the New York State Energy Research and Development Authority.

Supporting Information Available: ^{13}C NMR spectra of **I**, **II**, **III-0.00**, and **III-0.23**. This material is available free of charge via the Internet at http://pubs.acs.org.

CM000238M